HAL
open science

Innovative liposomes with double encapsulation properties for the treatment of acute myeloid leukemia

Zhiqiang Wang

To cite this version:

Zhiqiang Wang. Innovative liposomes with double encapsulation properties for the treatment of acute myeloid leukemia. Galenic pharmacology. Université Paris Saclay (COmUE), 2019. English. NNT : 2019SACLS432 . tel-03437572

HAL Id: tel-03437572

https://theses.hal.science/tel-03437572v1

Submitted on 20 Nov 2021

HAL is a multi-disciplinary open access archive for the deposit and dissemination of scientific research documents, whether they are published or not. The documents may come from teaching and research institutions in France or abroad, or from public or private research centers.

L'archive ouverte pluridisciplinaire **HAL**, est destinée au dépôt et à la diffusion de documents scientifiques de niveau recherche, publiés ou non, émanant des établissements d'enseignement et de recherche français ou étrangers, des laboratoires publics ou privés.

université PARIS-SACLAY

UNIVERSITÉ PARIS SUD
Comprendre le monde, construire l'avenir

NNT : 2019SACLS432

Innovative liposomes with double encapsulation properties for the treatment of acute myeloid leukemia

Thèse de doctorat de l'Université Paris-Saclay
préparée à l'Université Paris-Sud

École doctorale n°569 Innovation thérapeutique : du fondamental à l'appliqué
Spécialité de doctorat : Pharmacotechnie et Biopharmacie

Thèse présentée et soutenue à Châtenay-Malabry, le 14 novembre 2019, par

Zhiqiang Wang

Composition du Jury :

Mme GEZE, Annabelle Maître de Conférences, Université de Grenoble-Alpes (DPM, UMR CNRS 5063, ICMG FR 2607)	Rapporteuse
M SAULNIER, Patrick Professeur des Universités – Praticien Hospitalier, Université d'Angers (INSERM U1066 / CNRS 6021)	Rapporteur
Mme FOURMENTIN, Sophie Professeur des Universités, Université du Littoral Côte d'Opale (UCEIV, MREI)	Examinatrice
M PONCHEL, Gilles Professeur des Universités, Université Paris–Saclay (Institut Galien Paris-Sud, UMR CNRS 8612)	Président
Mme BARRATT, Gillian Directeur de Recherches CNRS, Université Paris–Saclay (Institut Galien Paris-Sud, UMR CNRS 8612)	Directrice de thèse
M LEGRAND, François-Xavier Maître de Conférences, Université Paris–Saclay (Institut Galien Paris-Sud, UMR CNRS 8612)	Co-directeur de thèse

Thèse de doctorat

Table of contents

Table of contents i
Abbreviations v
Résumé 1
Introduction 5
Chapter 1 7
State-of-the-art 7
1.1. Acute myeloid leukemia (AML) 8
1.1.1. Leukemia 8
1.1.2. Classification of AML 9
1.1.3. Treatment of AML 11
1.1.3.1. Classical drugs 11
1.1.3.2. Standard chemotherapy 12
1.1.3.3. Antibody-drug conjugates 12
1.1.3.4. Novel agents 13
1.1.3.4.1. Clofarabine 13
1.1.3.4.2. Sorafenib 14
1.1.3.4.3. Midostaurin 15
1.1.3.4.4. Crenolanib 15
1.1.3.4.5. Quizartinib 16
1.1.4. Repurposing of CPZ for AML treatment 16
1.1.4.1. General introduction to CPZ 17
1.1.4.2. CPZ for treatment of AML 18
1.2. Liposomes 20
1.2.1. Classification of liposomes 21
1.2.2. Components of liposomes 21
1.2.2.1. Phospholipids 21
1.2.2.2. Cholesterol 24
1.2.3. Mechanism of liposome-cell interaction 25
1.2.4. Development of liposomes 27
1.2.4.1. Conventional liposomes 28
1.2.4.2. Long-circulating liposomes 28
1.2.4.3. Targeted liposomes 29
1.2.4.4. Multifunctional liposomes 31
1.2.5. Fate of liposomes after different routes of administration 33
1.2.5.1. Transdermal delivery 33
1.2.5.2. Oral delivery 34

1.2.5.3. Pulmonary delivery 35
1.2.5.4. Brain delivery 36
1.2.6. Nano-sized drug carriers for AML 38
1.2.6.1. Polymeric nanoparticles for AML 39
1.2.6.2. Liposomes for AML 39
1.2.7. Biological challenges of liposome delivery 40
1.3. Drug-cyclodextrins-liposomes (DCL) system 42
1.3.1. Cyclodextrins 42
1.3.1.1. Derivatives of CDs 43
1.3.1.2. CDs complexes 44
1.3.1.3. Effect of CDs on the photostability of associated drugs 46
1.3.1.4. Pharmaceutical applications of CDs 47
1.3.2. Drawbacks of CD-drug complexes 47
1.3.3. DCL system 48
1.3.4. Impact of CDs on DCL 49
1.3.5. Preparation methods for DCL system 50
1.3.5.1. Passive loading methods 50
1.3.5.2. Active loading methods 53
1.3.6. CPZ-encapsulated DCL for treatment of AML 54
Chapter 2 69
Cyclodextrin complexation as a tool to allow repurposing of chlorpromazine 69
2.1 Introduction 70
2.2 Materials and methods 72
2.1.1 Materials 72
2.1.2 Methods 73
2.1.2.1 ITC studies 73
2.1.2.2 NMR studies 74
2.1.2.3 Computational details 75
2.1.2.4 Molecular Dynamics Simulations 75
2.1.2.5 Ab initio calculations 76
2.1.2.6 Photodegradation studies 76
2.1.2.7 HPLC analyses 77
2.3 Results and discussion 77
2.3.1 Cyclodextrin screening 77
2.3.2 Advanced thermodynamic characterisation 83
2.3.3 Structure of the β-CD/CPZ complex 86
2.3.4 Structure of the heptakis(2,6-di-O-methyl)-β-CD/CPZ complexes 90
2.3.5 Characterisation of the γ-CD/CPZ complexes 92

2.3.6 Characterisation of the sugammadex/CPZ complexes 94
2.3.7 Impact of the presence of CDs on CPZ photodegradation 98
2.4 Conclusion 100
Chapter 3 112
Physicochemical studies of the formulation 112
3.1 Introduction 113
3.2 Materials and methods 115
3.1.1 Materials 115
3.1.2 Methods 115
3.1.1.1 Preparation of liposomes 115
3.1.1.2 Size measurements 116
3.1.1.3 Differential scanning calorimetry (DSC) 116
3.1.1.4 Micro-DSC 117
3.1.1.5 X-ray scattering 117
3.1.1.6 Turbidity measurements 118
3.3 Results and discussion 119
3.3.1 Interaction between CDs and lipid bilayers 119
3.3.1.1 Impact of CDs on the thermotropic behavior of PSPC 119
3.3.1.2 Impact of CDs on the lamellar distance of PSPC 124
3.3.1.3 Impact of CDs on the hydrocarbon chain packing of PSPC 127
3.3.2 Stability of liposomes in presence of CDs 130
3.3.2.1 Effect of CDs on the stability of SUVs with cholesterol 130
3.3.2.2 Effect of CDs on the stability of SUVs without cholesterol 135
3.3.3 Interaction between CPZ and lipid bilayers 137
3.4 Conclusion 139
Chapter 4 142
Formulation and biological evaluation of CPZ-in-CD-in-liposomes 142
4.1 Introduction 143
4.2 Materials and methods 145
4.2.1 Materials 145
4.2.2 Methods 146
4.2.2.1 SUV preparation 146
4.2.2.2 DRV preparation 146
4.2.2.3 Size measurements 148
4.2.2.4 Quantification of CPZ by HPLC 148
4.2.2.5 Determination of the encapsulation efficiency of CPZ 148
4.2.2.6 Phospholipid assay 149
4.2.2.7 Cell culture 149

4.2.2.8 Cytotoxicity evaluation 150
4.2.2.9 Flow cytometry 151
4.3 Results and discussion 151
4.3.1 DRV preparation and characterization 151
4.3.1.1 DRV prepared by the standard method 151
4.3.1.2 DRV prepared by the ammonium sulfate gradient method 153
4.3.1.3 DCL liposomal formulation 155
4.3.2 *In-vitro* evaluation of DCL 158
4.3.2.1 Cytotoxicity of CPZ 158
4.3.2.2 Cytotoxicity of empty liposomes and CDs 159
4.3.2.3 Cytotoxicity of DCL 160
4.3.2.4 Cytotoxicity evaluation of DCL on a panel of cell lines 162
4.3.2.5 Cellular uptake of the DCL system 168
4.4 Conclusion 171
General discussion 175

Abbreviations

ABC: Accelerated Blood Clearance

AML: Acute myeloid leukemia

APL: Acute promyelocytic leukemia.

BBB: Blood-brain barrier

BM: Bone marrow

CD: Cyclodextrin

CML**:** Chronic myeloid leukemia

CPZ: Chlorpromazine

CR: Complete remission

CRC: Colorectal cancer

CRYSMEB: Low methylated-β-cyclodextrin

CYP: Cytochrome P450

DCL: Drug-in-CD-in-liposomes

DIMEB: Dimethyl-β-cyclodextrin

DPPC: Dipalmitoyl phosphatidylcholine

DSC: Differential scanning calorimetry

DRV: Dried reconstituted vesicles

DSPE-PEG_{2000}:1,2-distearoyl-sn-glycero-3-phosphoethanolamine-N-[methoxy(polyethylene glycol)-2000]

EE: Encapsulation efficiency

EFS: Event-free survival

EGFR: Epidermal growth factor receptor

Fab: Antigen-binding fragments

FDA: Food and Drug Administration

FLT3: FMS-like tyrosine kinase 3

GI: Gastrointestinal

GO: Gemtuzumab ozogamicin

GUV: Giant unilamellar vesicles

HEPES: 4-(2-hydroxyethyl)-1-piperazine ethane sulfonic acid

HPLC: High-performance liquid chromatography

HP-β-CD: 2-hydroxypropyl-β-cyclodextrin

HP-γ-CD: 2-hydroxypropyl γ-cyclodextrin

IC_{50}: Half maximal inhibitory concentration

ICG: Indocyanine green

ITD: Internal tandem duplication

LUV: Large unilamellar vesicles

MPS: Mononuclear phagocyte system

MRI: Magnetic resonance imaging

NMR: Nuclear magnetic resonance

NPs: Nanoparticles

OD: Optical density

OS: Overall survival

PA: Phosphatidic acid

PC: Phosphatidylcholine

PdI**:** Polydispersity index

PE: Phosphatidylethanolamine

PEG: Polyethylene glycol

PG: Phosphatidylglycerol

PS: Phosphatidylserine

PSPC: Palmitoyl-2-stearoyl-sn-glycero-3-phosphocholine

QCM-D: Quartz crystal microbalance with dissipation monitoring

RAMEB: Randomly methylated β-cyclodextrin

Rhodamine B PE: 1,2-dioleoyl-sn-glycero-3-phosphoethanolamine-N-(lissamine rhodamine B sulfonyl)

ROESY: Rotating-frame overhauser effect spectroscopy

SAXS: Small-angle X-ray scattering

SBE-Et-β-CD: Sulfobutylether-ethyl-β-cyclodextrin

SBE-β-CD: Sulfobutylether β-cyclodextrin

SBE-γ-CD: Sulfobutylether γ-cyclodextrin

scFv: Single-chain variable fragments

SGM: Sugammadex

SUV: Small unilamellar vesicles

SVLs: Solid-supported lipid vesicle layers

TKIs: Tyrosine kinase inhibitor

Tm-onset: Onset temperature of main transition

Tp-onset: Onset temperature of pre-transition

WAXS: Wide-angle X-ray scattering

WHO: World Health Organization

Résumé

Les leucémies sont une famille des cancers issus de la prolifération maligne des cellules hématopoïétiques. La leucémie myéloïde aigue (AML) représente 30% des leucémies chez les adultes et menace surtout les personnes âgées de 64 ans et plus. Actuellement, la chimiothérapie est la méthode principale de prise en charge de l'AML, mais celle-ci comporte des effets secondaires importants ainsi qu'un risque de récidive qui freinent son développement. Le redéploiement des molécules déjà utilisées pour d'autres maladies est une stratégie émergente dans le traitement du cancer. Par exemple, la chlorpromazine (CPZ), une molécule à activité antipsychotique, démontre une activité contre les lignes cellulaires issues d'AML, mais son activité au niveau du système nerveux central entraine des effets indésirables.

Compte tenu de l'activité de CPZ contre les cellules leucémiques, nous avons mis au point un système de vectorisation de médicaments original pour le traitement d'AML. La CPZ est d'abord incluse dans une cyclodextrine (CD, molécule cage à base de glucose) et ensuite ce complexe est encapsulé dans des liposomes (vésicules à contenu aqueux délimitées par une ou plusieurs bicouches phospholipidiques). Ce système de "drug-in-CD-in-liposomes" (DCL) est conçu pour circuler longtemps dans le sang après injection intraveineuse mais ne peut pas traverser la barrière hémato-encéphalique (BHE).

Il a été nécessaire d'optimiser la formulation avec ses trois composants principaux : CPZ, CD et phospholipides. Ainsi, une évaluation physico-chimique approfondie a été entreprise dans l'objectif de mieux appréhender les interactions entre les différents partenaires, notamment pour les couples CD/CPZ, CD/lipides et CPZ/lipides. La calorimétrie de titration isotherme (ITC) a permis de déterminer la stœchiométrie et la constante d'association pour les complexes d'inclusion CD/CPZ. Des stœchiométries 1:1, 1:2 ou 1:1+1:2 ont été déterminées pour les complexes CD/CPZ. Le complexe formé avec la sugammadex (SGM), une cyclodextrine de type gamma substituée, présente uniquement une stœchiométrie de type 1:2. De plus, les associations les plus

importantes vis-à-vis de la CPZ sont obtenues en présence de sugammadex ou de la sulfobutyléther-β-CD (SBE-β-CD). Par ailleurs, la spectroscopie RMN bidimensionnelle et plus particulièrement les expériences de type ROESY ont permis de déterminer la structure des complexes d'inclusion entre les CDs et la molécule de CPZ en conjugaison avec des simulations de dynamique moléculaire.

La CPZ est une molécule photosensible, surtout sous lumière UV-C et la photodégradation suit une cinétique de premier ordre au début de la réaction. L'inclusion de la CPZ dans les CDs accélère légèrement la photodégradation, d'un degré qui dépend de la CD. Il est à noter que la plus grande accélération est observée en présence de SGM.

Avant de formuler les liposomes, nous avons étudier les interactions entre les CDs et les lipides. Dans une première étape, des liposomes multilamellaires (MLVs) préparés à partir de palmitoylstearoylphosphatidylcholine (PSPC) ont été utilisés et les interactions avec les différentes CDs ont été étudiées par calorimétrie différentielle à balayage (DSC) ainsi que par diffraction des rayons X aux petits et grands angles (SAXS/WAXS). Les résultats de DSC démontrent que la majorité des CDs n'influencent pas les transitions de phase du phospholipide, et seules des concentrations supérieures à 25 mM de sulfobutyléther-éthyle-β-CD (SBE-Et-β-CD) perturbent fortement la bicouche phospholipidique. Les analyses par diffraction de rayons X confirment les résultats obtenus par DSC. Toutefois, une augmentation de l'épaisseur des bicouches a été observée pour des fortes concentrations en CDs ioniques et pour des températures élevées. Par contre, aucune influence sur l'organisation des chaînes latérales n'a été observée, indiquant que l'interaction des CDs se faisait avec les têtes polaires.

Pour confirmer ces résultats dans des conditions plus proches de celles de l'évaluation biologique, des liposomes unilamellaires (SUV) ont étés formulés à partir d'un phospholipide d'origine naturelle, la phosphatidylcholine d'œuf hydrogénée (HEPC), avec une petite proportion d'un phospholipide porteur de poly(ethylène glycol) (DSPE-PEG_{2000}) pour assurer leur rémanence vasculaire, en présence ou non de

cholestérol, le rôle du cholestérol étant de les stabiliser davantage. Des études de suivie de la turbidité pendant l'ajout progressive de CD ont démontré que les liposomes SUV ne sont pas perturbés par la plupart des CD, que ce soit en présence ou non de cholestérol. Seulement, la SBE-Et-β-CD a provoqué un effet délétère sur les liposomes, surtout en absence de cholestérol.

Suite aux études physico-chimiques, trois cyclodextrines ont été retenues pour la formulation des DCL et les études biologiques : la sugammadex (SGM), la sulfobutyléther-β-CD (SBE-β-CD) et la 2-hydroxypropyle-γ-CD (HP-γ-CD). Les deux premières CDs démontraient des très fortes associations avec la CPZ, alors que l'HP-γ-CD a montré la plus faible association vis-à-vis de la CPZ mais est connue pour sa faible toxicité *in vivo*.

La méthode « dehydration-rehydration vesicles » (DRV) a été choisie pour la formulation de DCL car cette méthode est connue pour fournir des taux d'encapsulation élevés des molécules hydrophiles de haut poids moléculaire. Or, les premiers essais produisaient des liposomes d'une taille trop importante pour une administration intraveineuse (IV). L'addition d'une étape supplémentaire d'extrusion à permis d'en réduire la taille, mais le pourcentage de CPZ encapsulée (EE) s'avérait faible (environ 10%). Ainsi la méthode DRV combinée à l'utilisation d'un gradient de concentration de sulfate d'ammonium, afin de « piéger » la CPZ dans les liposomes sous forme insoluble, a été utilisée. Ce protocole optimisé a permis d'augmenter l'EE en CPZ à environ 30% en absence de CD et à 15-18% en présence de CD tout en gardant une taille compatible avec l'administration IV.

La cytotoxicité de ces formulations a été évaluée sur 4 lignées cellules humaines leucémiques (HL-60 - une lignée de leucémie promyélocytique et MOLM13, MV4-11 and OCI-AML issues d'AML). Pour comparaison, une lignée normale de cellules de rein de rat (NRK) a également été utilisée. Le critère d'évaluation était la réduction des composés à base de tétrazolium (MTS ou WST-1) par les enzymes mitochondriales.

Sur les lignées leucémiques, les liposomes contenant de la CPZ ont tous démontré un effet cytotoxique tandis que les liposomes vides avaient tendance à stimuler la

croissance et les CD seules étaient sans effet. Pourtant, l'activité des liposomes comportant les complexes d'inclusion CD/CPZ (DCL) était moins importante que celle des liposomes chargés en CPZ, dans l'ordre DCL-SGM/CPZ < DCL-SBE-β-CD/CPZ < DCL-HP-γ-CD/CPZ. L'activité était inversement proportionnelle à la constante d'affinité entre la CD et la CPZ, suggérant une libération retardée. Cette hypothèse a été confortée par le fait que l'activité des DCL à base de complexes d'inclusion CD/CPZ était plus importante après une exposition de 72h qu'après 24h. En effet, les DCL-SGM/CPZ ne démontrent pas d'activité après des temps d'incubation courts, mais une activité a été révélée après 72h.

Afin d'étudier la capture des DCL par les cellules, les liposomes ont été rendus fluorescents par l'insertion d'une petite proportion d'un phospholipide porteur de rhodamine (18:1 Liss Rhod PE). La préparation de liposomes fluorescents a permis une évaluation de leur association avec les cellules MOLM13 par cytométrie de flux. Toutefois, la CPZ conduit à atténuer la fluorescence de la rhodamine, ce qui a rendu l'interprétation des résultats difficile.

Par ailleurs, la cytotoxicité des formulations de CPZ vis-à-vis des cellules NRK était moins importante que celle observée avec les cellules leucémiques à 24h mais était majorée à 72h. Une expérience dans laquelle les cellules NRK ont été mises en contact avec les formulations pendant 24h, puis en milieu frais pendant 48h de plus démontraient une activité similaire à celle de l'incubation de 24h. L'ensemble de ces résultats sont prometteurs pour la mise au point de systèmes à libération contrôlée de CPZ pour le traitement d'AML, sans toxicité pour les tissus normaux.

Introduction

Leukemia is a group of cancers caused by the uncontrollable proliferation of progenitor cells in the bone marrow (BM). Accounting for 30% of all leukemias in adults, acute myeloid leukemia (AML) is especially a threat for older people with a median age of 64 years old. Presently, chemotherapy, the standard "7+3 regimen" for example, is the main therapeutic strategy for AML, but severe side-effects and possibility of relapse have hampered its development.

Chlorpromazine (CPZ), a typical antipsychotic, has attracted attention since it was reported to show cytotoxic activity towards human promyelocytic leukemic granulocytes (HL-60) (Hait et al. 1985). To the best of our knowledge, no published work refers to the AML-treating properties of CPZ. Therefore, it is a new strategy and only limited information could be obtained from the literature, making it necessary to perform fundamental investigations on the feasibility of using CPZ for AML treatment.

To repurpose CPZ as a novel therapeutic strategy for AML, the first problem to be overcome is its passage through the blood-brain barrier (BBB), an essential property for an antipsychotic but undesirable in other applications. Considering the 'solid' capillary walls formed by polarized endothelial cells in BBB, liposomes would be suitable drug carrier, because they could be excluded from the central nervous system due to their larger diameter. Furthermore, polyethylene glycol (PEG), a hydrophilic polymer, will be grafted to the surface of liposomes to reduce their recognition by serum components and render them "stealth" in the blood stream (Klibanov et al. 1990). The long-circulating property of PEGylated liposomes can significantly alter the pharmacokinetics of the formulation after intravenous administration.

However, an important fact is that CPZ is an amphiphilic molecule, which may lead to drug leakage or even destruction of the nanocarriers in the harsh physiological environment of circulating system. Therefore, cyclodextrins (CDs), a group of cyclic oligosaccharides, were considered. Due to the hydrophilic outer rim and hydrophobic internal cavity, CDs can entrap various hydrophobic or amphiphilic molecules to form inclusion complexes, leading to the alteration of guest molecule's

physicochemical behavior. In our case, the affinity of CPZ for lipids could be weakened by association with CDs, and hypothetically, drug leakage would be avoided.

Therefore, a versatile drug delivery strategy, the drug-in-CDs-in-liposomes (DCL) system was envisaged. This concept was first reported by McCormack and Gregoriadis, by encapsulating the CD/drug inclusion complexes within liposomes (McCormack and Gregoriadis 1994). Based on the potential of CPZ in AML treatment, we designed a similar DCL system, which involves 3 interrelated ingredients: CPZ, CDs, and phospholipids. To get a better insight into the properties of the liposomal formulation and select the most appropriate CD candidate for the DCL system, we performed comprehensive investigations on the interactions between CD/CPZ, CD/lipid and CPZ/lipid.

This thesis is divided into 4 chapters.

Chapter 1 details the current status and the possibility of repurposing CPZ in AML treatment. It also addresses the development of liposomes and the role of CDs in DCL system.

Chapter 2 focuses on interaction between CD/CPZ. It describes the formation and spatial structure of the CD/CPZ inclusion complexes, and the photodegradation of CPZ in presence of CDs.

Chapter 3 concentrates on the interaction between CD/lipid and CPZ/lipid. It reports the impact of CDs on the phase transition, lamellar distance and hydrocarbon chain packing of phospholipids, the destructing effect of CDs on liposomes, and the optimal CPZ concentration to prepare the liposomal formulation.

Chapter 4 is dedicated to the preparation of the liposomal formulation, the cytotoxic evaluation of the formulation and its ingredients against leukemia cell lines, and the cellular uptake of the formulation by AML cells.

Chapter 1

State-of-the-art

1.1. Acute myeloid leukemia (AML)

1.1.1. Leukemia

Leukemia is a group of cancers caused by malignant clonal proliferation of hematopoietic stem cells. The uncontrollable expansion and growth of progenitor cells in the bone marrow (BM) leads to a reduction of normal hemopoiesis and an accumulation of immature leukemic cells that spread to other organs of the body, such as liver, spleen and lymph nodes (Fig. 1). Therefore, various severe consequences follow, the most common of which are haemorrhage, anemia and secondary infections. These complications increase the risk of death so the mortality associated with leukemia cannot be ignored. According to a systematic analysis for the Global Burden of Disease, leukemia was present in 2.4 million people and led to 518,500 deaths throughout the world in 2017, with increase of 25.1% compared with 2007 (James et al. 2018).

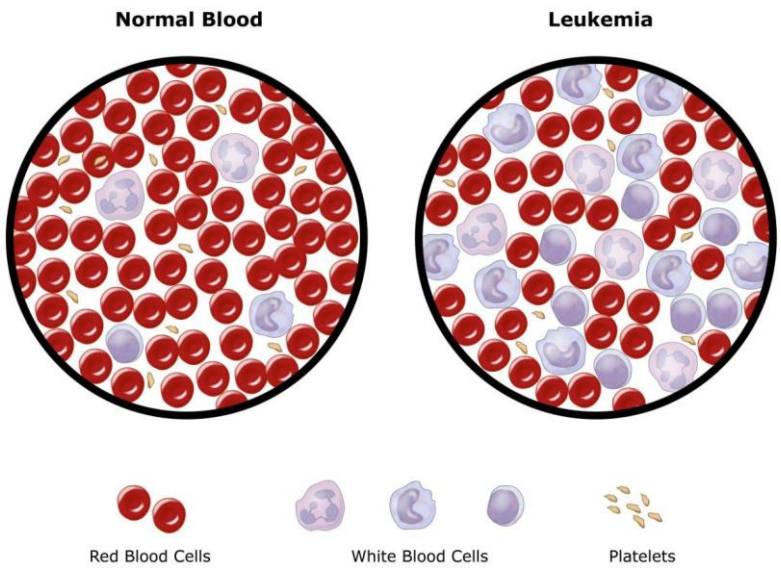

Fig. 1. Malignant clonal proliferation of hematopoietic stem cells in leukemia*
* From *healthwan.com*, May, 2019

Generally, leukemia can be classified as acute and chronic according to disease onset and course, and myeloid and lymphocytic based on differentiation (Kohlschütter et al. 2008). Compared with chronic leukemia, acute leukemia has a much shorter

disease course and may deteriorate or even cause life-threatening consequences within a few weeks without therapy.

Accounting for 30% of all leukemias in adults, acute myeloid leukemia (AML) is an especial threat for older people with a median age of 64 years for presentation (Bordoni and Zucca 2007). According to an investigation from the UK, AML mortality is closely related to age (Fig. 2). The age-specific mortality rate shows a clear increase for people older than 60 years and reaches the highest point in the 85-89 age group, for both males and females.

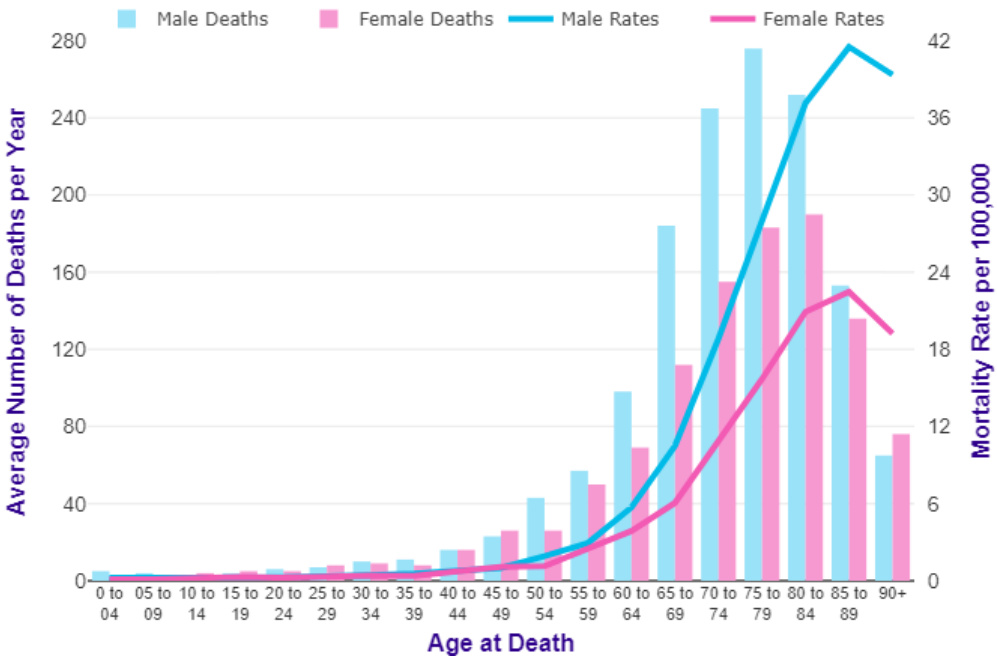

Fig. 2. Average number of deaths per year and age-specific mortality rates, UK*

* From: *cruk.org/cancerstats*, May, 2019

1.1.2. Classification of AML

Careful diagnosis of AML is essential to ensure better treatment. For instance, "preleukemic" cases, different from AML, should be given distinct treatment. Therefore, a comprehensive classification of AML is both necessary and clinically useful.

The first classification system for AML was called “French-American-British” strategy, which divided AML into 8 subtypes (M0 to M7). The World Health

Organization (WHO) produced a new classification in 2008 and an updated version in 2016, based on cytogenetic alterations and genetic abnormalities (Table 1).

Table 1 Acute myeloid leukemia (AML) and related neoplasms (Niederwieser and Deininger 2002;Arber et al. 2016)

Type	Genetic abnormalities
AML with recurrent genetic abnormalities	AML with t(8:21)(q22;q22); RUNX1-RUNX1T1
	AML with inv(16)(p13.1q22) or t(16;16)(p13.1;q22); CBFB-MYH11
	APL with PML-RARA
	AML with t(9;11)(p21.3;q23.3); MLLT3-KMT2A
	AML with t(6;9)(p23;q34.1); DEK-NUP214
	AML with inv(3)(q21.3q26.2) or t(3;3)(q21.3;q26.2); GATA2, MECOM
	AML (megakaryoblastic) with t(1;22)(p13.3;q13.3); RBM15-MKL1
	AML with BCR-ABL1 (provisional entity)
	AML with mutated NPM1
	AML with biallelic mutations of CEBPA
	AML with mutated RUNX1 (provisional entity)
AML with myelodysplasia-related changes	
Therapy-related myeloid neoplasms	
AML not otherwise specified	AML with minimal differentiation
	AML without maturation
	AML with maturation
	Acute myelomonocytic leukemia
	Acute monoblastic/monocytic leukemia
	Acute erythroid leukemia
	Pure erythroid leukemia
	Acute megakaryoblastic leukemia
	Acute basophilic leukemia
	Acute panmyelosis with myelofibrosi
Myeloid sarcoma	
Myeloid proliferations related to Down syndrome	Transient abnormal myelopoiesis
	Myeloid leukemia associated with Down syndrome

Abbreviations: AML, acute myeloid leukemia; APL, acute promyelocytic leukemia.

1.1.3. Treatment of AML

1.1.3.1. Classical drugs

The chemotherapeutic strategy for AML treatment has been based on a combination of two classical cytostatic drugs: anthracyclines and cytarabine (Fig. 3).

Anthracyclines are a class of anticancer drugs that were first extracted from *Streptomyces bacterium* in 1960s (Fujiwara et al. 2008). These antibiotics consist of a tetracycline ring with a sugar moiety connected via a glycosidic bond. Based on their particular chemical structure, these drugs intercalate with DNA when they have been taken up by cells and induce breakage of the DNA double-strand. During the past decades, numerous anthracyclines have been developed and one of these, daunorubicin (DNR) (Fig. 3), has become the most commonly used agent for AML treatment. Nevertheless, the cardiotoxic side effects of current anthracyclines have stimulated the interest in the development of novel related analogs.

Cytarabine (Ara-C) (Fig. 3), also known as cytosine arabinoside, is a cell-phase-specific cytotoxic drug widely used in chemotherapy for treatment of leukemia, including AML (Murphy and Yee 2017). It was first synthesized in 1959 and approved by FDA in 1969. Cytarabine is a nucleoside analog and when it has entered the cell, it incorporated into DNA and impedes its replication. Due to the cell-phase specificity, cytarabine exerts its effects mainly on cells undergoing rapid DNA synthesis such as cancer cells. It is intravenously administered and high doses are required to offset the drawback of its short half-life (Phillips et al. 1991).

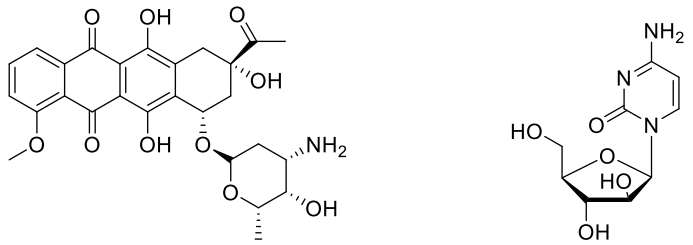

Daunorubicin Cytarabine

Fig. 3. Chemical structure of daunorubicin and cytarabine

1.1.3.2. Standard chemotherapy

The common clinical chemotherapy used in AML is the so-called '7+3 regimen', which consists of a continuous infusion of cytarabine (100-200 mg/m^2) for 7 days with daunorubicin (60-90 mg/m^2) or idarubicin (12 mg/m^2) infusion on the first 3 days (Briot et al. 2018). This induction therapy remains largely as it was at its first clinical application in 1970s, despite a variety of schemes that were designed and assessed in the following years, such as changing the dose of the two components or adding extra agents. Benefiting from this strategy, 60-80% of younger patients can achieve a complete remission, while the percentage for older patients is 45-65% (Desroches and Rosenbaum 2010; Short et al. 2018).

However, chemotherapy always carries the risk of side effects. For example, anthracyclines can lead to damage to the heart, especially in long-term treatment. Coordination problems may be caused by high doses of cytarabine because of its effects on the brain of patients. Moreover, chemotherapeutic drugs can reduce the renewal of blood cells, inducing a higher risk from infections or bleeding. Considering the side effects caused by current chemotherapy, novel agents need to be developed.

1.1.3.3. Antibody-drug conjugates

Receptor-targeted drug delivery is a promising solution in cancer therapy to increase specificity and efficacy. With the targeting function of ligands, antibody-drug conjugates can be directed to the target site after systemic administration, resulting in increased therapeutic efficiency and fewer side effects.

CD33 is a membrane receptor specifically expressed by myeloid blasts in AML but not by healthy hematopoietic stem cells. To exploit this difference, gemtuzumab ozogamicin (GO) was developed and approved by FDA as the first receptor-targeted drug for AML treatment (Briot et al. 2018). GO is an anti-CD33 antibody conjugated to the cytostatic drug calicheamicin, which would lead to DNA double-strand fractures (Kohlschütter et al. 2008). However, life-threatening side effects of GO, for example

anaphylactic reactions, have been reported and the increase in therapy-related mortality slowed down the final approval by FDA until 2017. With a trade name of Mylotarg®, GO is presently used to treat adults with newly diagnosed CD33-positive AML.

FMS-like tyrosine kinase 3 (FLT3) is another membrane receptor mainly expressed by AML cells (approximately 30% of all AML cases) and its most common mutation is internal tandem duplication (ITD, approximately 25% of all AML cases) (Daver et al. 2019). Several tyrosine kinase inhibitors (TKIs), such as sorafenib, midostaurin and lestaurtinib, show potential activity against FLT3 and some of them will be discussed below. Although some FLT3 inhibitors are undergoing evaluation in patients with FLTS-ITD-mutated AML, their lack of specificity seems to be an unavoidable hurdle for further application.

1.1.3.4. Novel agents

Although the standard chemotherapy strategy ('7+3' regimen) has achieved high remission rates in AML, its severe side effects and limited solution for older patients have stimulated exploration for novel therapeutic agents for AML treatment. Several small molecules have been developed with the aim of blocking or damaging the intracellular signaling cascades and thereby inducing cell death.

1.1.3.4.1. Clofarabine

As a purine nucleoside antimetabolite, clofarabine is approved by the FDA for treating relapsed or refractory acute lymphoblastic leukemia in children (Fig. 4). In recent years, it has shown potential in AML therapy. A phase II trial of clofarabine, idarubicin, and cytarabine as a frontline therapy was conducted in younger patients under 60 years old with newly diagnosed AML. 74% of complete remission (CR) was achieved and the median event-free survival (EFS) was 13.5 months (Nazha et al. 2013). Clofarabine played a promising role in this study in prolonging overall survival (OS) and EFS compared to historical patients treated with idarubicin and cytarabine only. The standard intensive chemotherapy always provokes severe side effects in older

adults with AML and thus a less toxic regimen is needed for this population. Kadia et al developed a novel strategy for patients with newly diagnosed AML in a Phase 2 trial (Kadia et al. 2015). After receiving clofarabine and low-dose cytarabine alternating with decitabine, the patients achieved 60% of CR rate, with 11.1 months' median OS and 14.1 months' median EFS. Moreover, the low mortality rates revealed that the regimen was well tolerated.

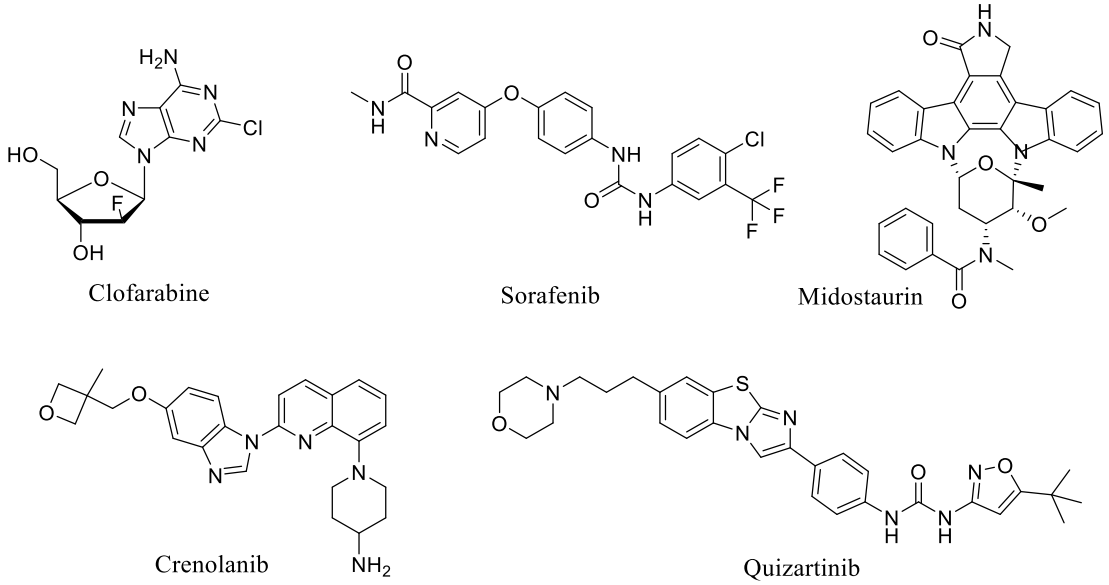

Fig. 4. Chemical structure of novel therapeutic agents for AML treatment: clofarabine, sorafenib, midostaurin, crenolanib and quizartinib.

1.1.3.4.2. Sorafenib

Sorafenib is a TKI, approved for treatment for renal cell carcinoma, hepatocellular carcinoma and thyroid carcinoma (De Kouchkovsky and Abdul-Hay 2016) (Fig. 4). In recent years, clinical trials in patients with FLT3-ITD-positive AML indicate that sorafenib can induce growth arrest and apoptosis of leukemic cells or even complete remissions. A phase I study showed that 5 (10%) of FLT3-ITD-positive patients achieved CR after following treatment schedules of sorafenib, with an additional 17 (34%) of the responses being found reduction of leukemic cells in bone marrow and/or peripheral blood blasts (Borthakur et al. 2011). Moreover, the combination of sorafenib

with other agents was reported to have a higher therapeutic index and this further improved the status of sorafenib in AML therapy (Al-Kali et al. 2011; Ravandi et al. 2014). Nevertheless, Serve et al carried out a placebo-controlled trial in 201 older patients newly diagnosed with AML and finally found that the sorafenib-chemotherapy protocol was not a benefit for elderly patients (Serve et al. 2013).

1.1.3.4.3. Midostaurin

Midostaurin is another multi-kinase inhibitor that targets FLT3 (wild type and mutated) (Wang et al. 2008) (Fig. 4). The role of midostaurin in combination with the 7+3 regimen and high-dose cytarabine consolidation chemotherapy was evaluated by Stone et al in a randomized, placebo-controlled phase 3 trial of 717 patients with FLT3-mutated (ITD or TKD) AML (Stone et al. 2017). Patients randomized to the midostaurin group had significantly prolonged overall and EFS compared to the placebo group, although there is no difference in the rate of severe adverse events (AEs) between the two groups. AEs were often observed during AML treatment with midostaurin, including infection, febrile neutropenia and lymphopenia (Stone et al. 2017). Another phase I/II trial conducted by Strati et al demonstrated that the combination of midostaurin and azacytidine is an effective and safe regimen in patients with AML and high-risk myelodysplastic syndrome (Strati et al. 2015).

1.1.3.4.4. Crenolanib

Crenolanib is a second generation FLT3 TKI , showing potent inhibiting activity against FLT3-ITD and FLT3-TKD mutations (Chen et al. 2017) (Fig. 4). This extensive inhibiting property makes crenolanib a promising molecule, justifying its inclusion in multiple clinical trials. In a phase II study in relapsed/refractory AML patients with FLT3 mutations, crenolanib was administered orally continuously for 28-day cycles. The median EFS was 8 weeks and the OS was 19 weeks (Randhawa et al. 2014). More clinical studies evaluating crenolanib in AML patients are ongoing, including combination with “7+3” regimen (Wang et al. 2016).

1.1.3.4.5. Quizartinib

As a specifically designed second generation FLT3 inhibitor, quizartinib is highly potent and selective, and is therefore a promising drug for clinical use (Fig. 4). In a large phase 2 trial of 333 patients with relapsed/refractory AML, quizartinib showed high activity and good tolerability, with 56% of FLT3-ITD-positive patients achieving composite complete remission in cohort 1 (157 patients who were older than 60 with AML within 1 year after first-line therapy) and 46% in cohort 2 (176 patients who were older than 18 with AML following salvage chemotherapy or haemopoietic stem cell transplantation) (Cortes et al. 2018). The findings confirm the clinical potential of quizartinib as a single-agent strategy in FLT3-ITD mutated patients and opened the way for a phase 3 trial, in which the efficiency of quizartinib monotherapy and its combination with standard chemotherapy was evaluated (*clinicaltrials.gov/ NCT02668653*).

1.1.4. Repurposing of CPZ for AML treatment

Although several strategies have been developed for AML treatment, including the standard regimen and various agents being evaluated in clinical trials, it is still necessary to search for new directions in therapy. Chlorpromazine (CPZ), a commonly used antipsychotic, was reported to have inhibiting effect on AML cell lines and this finding leads to its repurposing in the field of AML treatment (Table 2).

Table 2 Chemical information of CPZ

Name	Molecular formula	Molecular weight	Chemical structure	pKa
chlorpromazine	$C_{17}H_{19}ClN_2S$	318.86	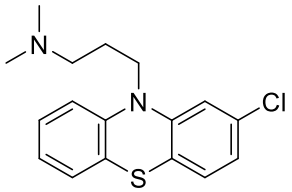	9.3

1.1.4.1. General introduction to CPZ

CPZ is a well-known first-generation antipsychotic and has been regarded as the "gold standard" for almost 70 years for the treatment of psychological disorders, despite the appearance of several second-generation antipsychotics (Fig. 5). CPZ was first synthesized in 1951 by Paul Charpentier in a French pharmaceutical company (Rhône-Poulenc) and underwent clinical investigation in 1952 (Ban 2007). Subsequently in 1957, CPZ was approved by FDA and entered the USA market under the brand name Thorazine®. With the improvement of clinical treatment of schizophrenia, the field developed considerably.

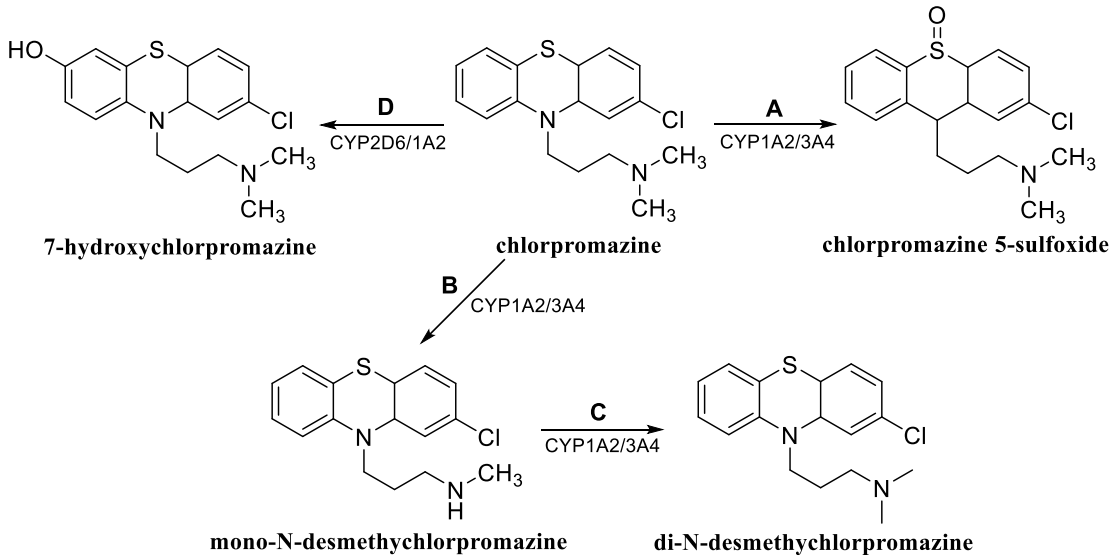

Fig. 5. Primary metabolites of CPZ catalyzed by P450 isozymes: (A) 5-sulfoxidation, (B) mono-N-demethylation, (C) di-N-demethylation, and (D) 7-hydroxylation. Copyright (Boyd-Kimball et al. 2018)

As a typical antipsychotic, CPZ acts by antagonizing dopamine receptors, especially the dopamine D_2 receptor. CPZ can be administrated either orally or intravenously, leading to different types of metabolism. When administered by the oral route, CPZ undergoes extensive first-pass metabolism, whereas in the case of intravenous administration, this first-pass metabolism is circumvented, thereby obtaining a longer half-life. Hepatic cytochrome P450 (CYP) isozymes play a major

role in catalyzing the metabolism of CPZ, producing four main metabolites: mono-N-demethylchlorpromazine, di-N-demethylchlorpromazine, chlorpromazine 5-sulfoxide and 7-hydroxy- chlorpromazine (Robinson 1963; Boksa and Daniel 2010; Boyd-Kimball et al. 2018) (Fig. 5).

1.1.4.2. CPZ for treatment of AML

Phenothiazine and its derivatives are highly bioactive and possess a broad range of medical applications, such as antibacterial, anti-inflammatory, anticonvulsant, etc. (Pluta and Morak-m 2011). Several different phenothiazines were reported to show promising biological activity in inducing cell death via internucleosomal DNA fragmentation in human myelogenous leukemic cell lines (Sakagami et al. 1995). As a commonly used phenothiazine derivative, CPZ was used as adjuvant in anticancer treatment for reducing vomiting (Davis and Hallerberg 2010). All this information indicates the possibility of CPZ acting as an antitumor candidate.

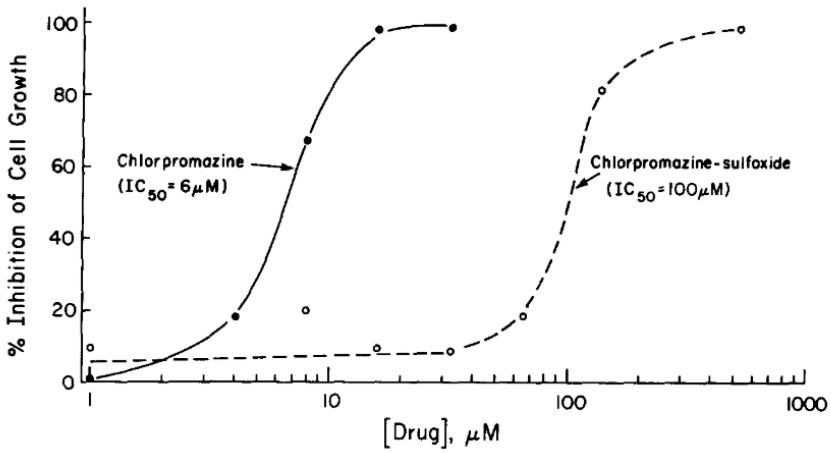

Fig. 6. Inhibiting effect of chlorpromazine and chlorpromazine sulfoxide on the growth of L1210 murine leukemic lymphocytes. Copyright (Hait et al. 1985)

To the best of our knowledge, the application of CPZ in treatment of leukemia is still an unknown field, since only a limited number of published works refer to this topic. A noteworthy study is from Hait (Hait et al. 1985), who investigated the effect of CPZ and chlorpromazine-sulfoxide on the growth of murine leukemic lymphocytes

(L1210 and L5178Y) and human promyelocytic leukemia granulocytes (HL-60). CPZ showed significantly stronger inhibiting efficiency than chlorpromazine-sulfoxide and their IC50 values for the HL-60 cell line were 8 μM and 100 μM, respectively (Fig. 6). This finding provides strong evidence that CPZ has the therapeutic potential against human leukemia.

In addition, Mello et al demonstrated the cytotoxicity of CPZ against chronic myeloid leukemia (CML) tumor cells (Mello et al. 2016). When encapsulated in a poloxamer-based nanostructured system, the antitumor activity of CPZ was enhanced and the selectivity against CML tumor cells was increased.

Despite limited study indicating the therapeutic potential of CPZ against leukemia related tumor, we evaluated the cytotoxicity of CPZ with human AML cell lines in preliminary experiments. It was observed that CPZ exerts obvious cytotoxicity, encouraging the repurposing of CPZ as a novel agent for treatment of AML. However, as mentioned above, CPZ is a typical antipsychotic, which indicates its capability to pass through the BBB and tendency to accumulate in the central nervous system. Adverse effects at this level are an unavoidable obstacle and new strategies that could block the central nervous system action of the drug are needed. Additionally, when administrated by intravenous route, CPZ undergoes high but quickly decaying peak levels in the plasma and this relatively short half-life is not enough for transportation to and uptake by the target tissue. During the past decades, liposomes as an efficient nanometric drug delivery system won the favor of researchers due to multiple advantages. In our case, a liposomal formulation could effectively prevent crossing the BBB and prolong the circulation time of CPZ by altering its pharmacokinetics. Meanwhile, targeting to tumor site, bone marrow for instance, could be also achieved by modifying the surface of liposome with appropriate monoclonal antibodies or fragments. Therefore, liposomes could be an efficient tool to encapsulate CPZ for AML treatment.

1.2. Liposomes

It is generally believed that liposomes were first observed as phospholipid vesicles by Bangham and his colleagues in 1965 (Bangham et al. 1965), who found that a phospholipid membrane could maintain a concentration gradient of cations. In 1964, Bangham had already identified a lamellar structure formed by lecithin in the electron microscope with a negative-staining technique (Bangham and Horne 1964). The definition "liposomes", phospholipid spherules consisting of a series of lipid bilayers, was first put forward by Weissmann in 1968 in a review and subsequently liposomes were recognized as a promising nanometric drug delivery system (Sessa and Weissmann 1968).

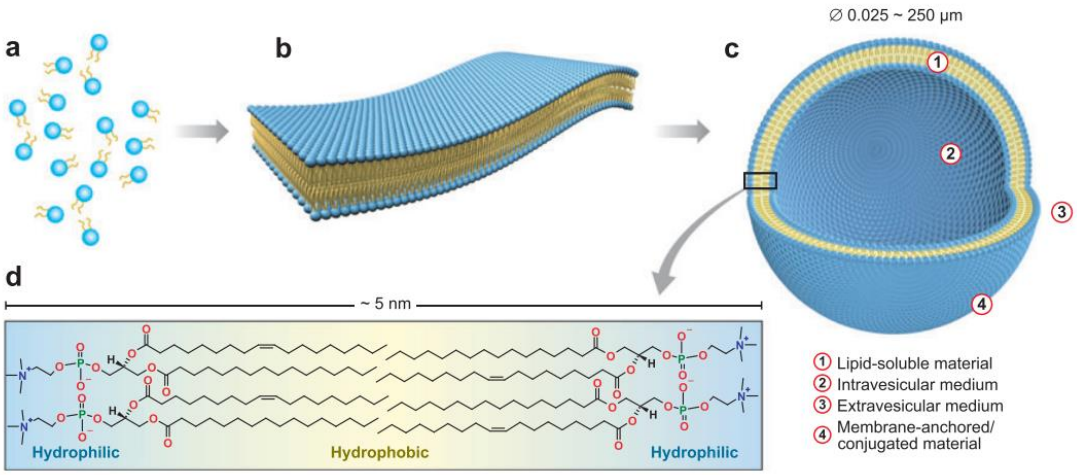

Fig. 7. Illustration of the self-assembly process of liposomes, from free phospholipid molecules (a) to bilayer membrane (b) and the formation of liposomes (c). The thickness of single bilayer is 5 nm, with orderly arrangement of lipid molecules (d). Copyright (Jesorka and Orwar 2008)

It is worth mentioning that in 1971, Gregoriadis et al innovatively entrapped *Aspergillus niger* amyloglucosidase and ^{13I}I-labelled albumin within liposomes. After intravenous administration to rats, most of radioactivity was found in liver and spleen, which indicated that liposomes have the potential to be a carriers for bioactive substances (Gregoriadis and Ryman. 1971).

1.2.1. Classification of liposomes

The formation of liposomes involves a self-assembly process, with individual lipid molecules forming a bilayer membrane (Fig. 7). Generally, liposomes can be classified by their number of membrane bilayers and size. Base on the lamellarity, they can be categorized as unilamellar (single bilayer) or multilamellar (multiple bilayers separated by a aqueous phase) (Pattni et al. 2015). Different sizes of unilamellar vesicles have been clearly identified: small unilamellar vesicles (SUV), large unilamellar vesicles (LUV), and giant unilamellar vesicles (GUV) (Fig. 8) (Jesorka and Orwar 2008).

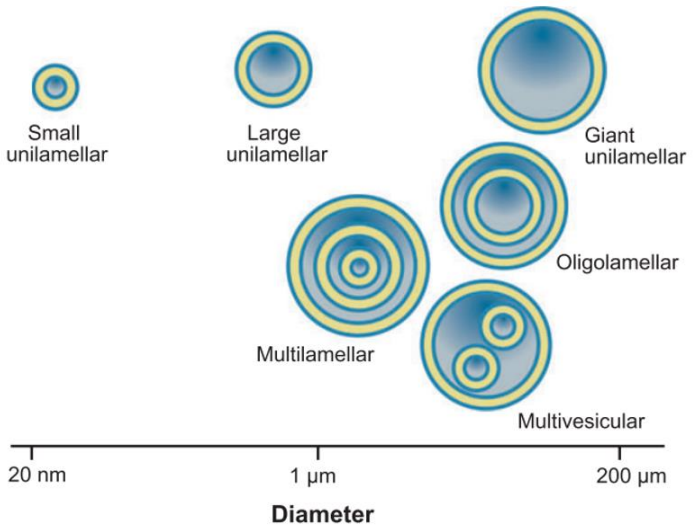

Fig. 8. General classification of liposomes by size and number of membrane bilayers. Small unilamellar vesicles (< 200 nm, SUVs), large unilamellar vesicles (200 nm~1000 nm, LUVs), and giant unilamellar vesicles (>1000 nm, GUVs) are three commonly used unilamellar vesicles. Copyright (Jesorka and Orwar 2008)

1.2.2. Components of liposomes

1.2.2.1. Phospholipids

As the major components of biological membranes, phospholipids are commonly used in liposomal preparation. Due to the wide distribution in nature, phospholipids can be isolated from animals and plants at a relatively low cost, from egg yolk and soybean for example. Nevertheless, such a natural source means a mixture of phospholipids, both in head group and acyl chains, which can lead to instability of liposomal

formulations during formulation storage and use. Another source is from chemical synthesis. Synthetic phospholipids have defined structure and stable physicochemical properties, whereas their high production cost is a drawback for extensive application.

The chemical structure of these amphipathic molecules consists of a hydrophilic head group and a pair of aliphatic side chains, linked by a glycerol bridge. The nature of the polar group determines the type of phospholipid: such as phosphatidylglycerol (PG), phosphatidylcholine (PC), phosphatidylethanolamine (PE), phosphatidylserine (PS), and phosphatidic acid (PA) (Li et al. 2014). Within each type, phospholipids can be further classified by the length and saturation of the fatty acids. The assembly of phosphate head group and polar moieties creates a variety of phospholipids with diverse physicochemical properties. One of these that deserves to be mentioned is the phase transition temperature: the temperature at which the phospholipids change from a gel to liquid crystalline state, since it correlates closely with the pharmacokinetics of the liposomal formulation.

The lipid phase transition can be influenced by a variety of factors, such as temperature, water content and lipid composition (Koynova and Tenchov 2013). Generally, the lipid forms a crystalline phase (L_c) at low temperature, in which the hydrocarbon tails are highly ordered (Fig. 9). In some situations, the lipid could form more than one type of L_c in replacement of other subgel phases (Kulkarni 2012). The crystalline phase would transform to gel phase (L_β) on heating, in which the acyl chains exhibit all-trans configuration and still have high order. In the L_β phase, the hydrocarbon chains are ordered parallel to the bilayer normal, but a tilted form ($L_{\beta'}$) would be observed once the area of head group expands. With increasing temperature, the gel phase transforms to liquid crystalline or fluid phase (L_α), where the tails are completely disordered and the bilayer shows high lipid mobility. This fluid phase is the most common state in biology which has been widely investigated with various techniques. Between the L_α and L_β phase, there exists a rippled configuration called $P_{\beta'}$ phase, which is caused by the periodic modulation of the lipid lamellar (Khakbaz and Klauda 2018). However, not all species of lipids show a $P_{\beta'}$ state.

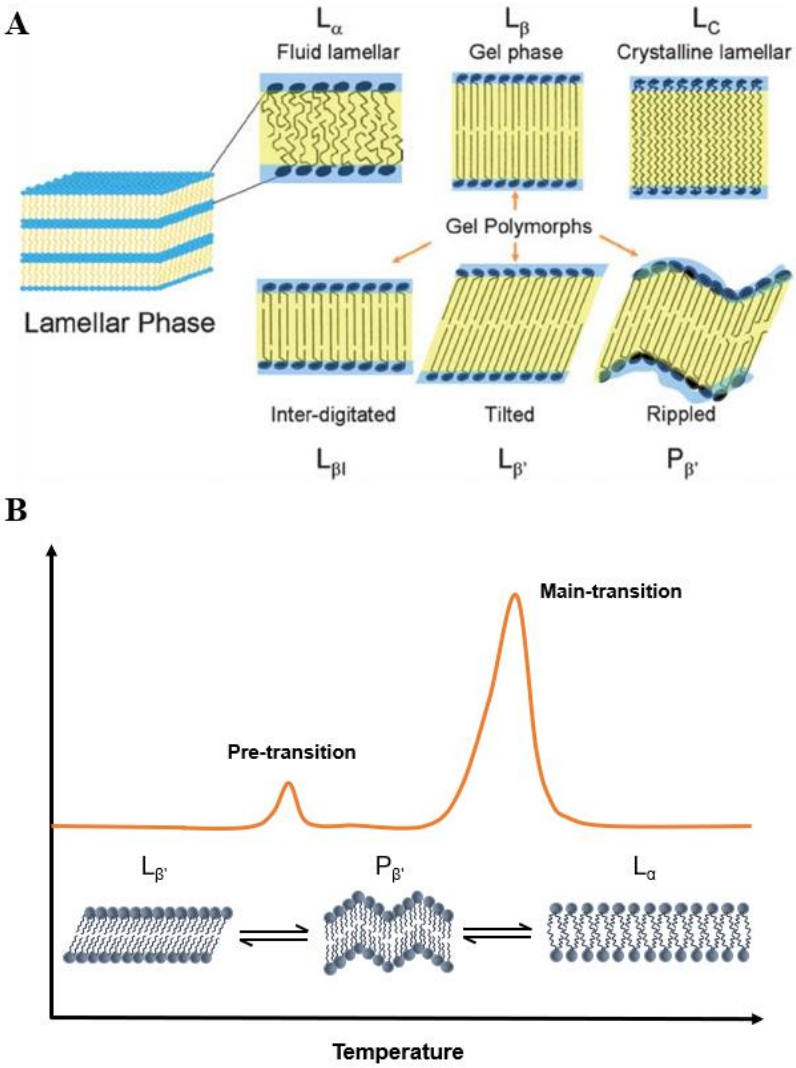

Fig. 9. Lipid phase transition from crystalline, gel and liquid crystalline state (A), copyright from (Kulkarni 2012); and DSC investigation on the thermotropic behavior of pre-transition and main-transition (B), reproduced from (Pignatello et al. 2011).

Differential scanning calorimetry (DSC) is a frequently used technique to study the thermotropic behavior of lipid membranes, whether they are composed of pure lipid or incorporating other substances (Bastos 2016). Most studies focus on the main transition, which is a reversible transition from L_β to L_α, with high transition enthalpies. However, a pre transition can also be measured in lipids like phosphatidylcholines from L_β' to P_β', with small enthalpies at lower temperatures than the main transition. It should be noted that the pre-transition peak can be easily influenced by the scan rate.

Table 3 Phase transition temperature of selected phospholipids (Li et al. 2014)

Phospholipid	Abbreviation	Tc (°C)
Soybean phosphatidylcholine	SPC	-20 to -30
Hydrogenated soybean phosphatidylcholine	HSPC	52
Egg phosphatidylcholine	EPC	-5 to -15
Dimyristoyl phosphatidylcholine	DMPC	23
Dipalmitoyl phosphatidylcholine	DPPC	41
Dioleoyl phosphatidylcholine	DOPC	-22
Dimyristoyl phosphatidylglycerol	DMPG	23
Dipalmitoyl phosphatidylglycerol	DPPG	41
Dioleoyl phosphatidylglycerol	DOPG	-18
Dimyristoyl phosphatidylethanolamine	DMPE	50
Dipalmitoyl phosphatidylethanolamine	DPPE	60
Dioleoyl phosphatidylethanolamine	DOPE	-16

1.2.2.2. Cholesterol

The membrane composition of liposomes has a critical effect on their organization and dynamics (Oliveira et al. 2014). In some cases, poor physical stability of the lipid bilayer can lead to undesired leakage of encapsulated drugs. To circumvent this problem, cholesterol, a common component of mammalian cell membranes, is added to the composition (Fig. 10). Cholesterol plays an important role in altering the fluidity and polarity of lipid membranes, which results in decrease of liposome permeability and drug leakage. The incorporation of cholesterol into the lipid bilayers can be investigated by DSC, with the change of thermotropic profile. For instance, at 30 mol% of cholesterol incorporation, the phase transition of diacylphospholipids is eliminated and the lipid bilayer is brought into a more stable state (Kohli et al. 2015). Furthermore, similar disappearance of the main transition peak induced on the addition of cholesterol

was detected by another technique, quartz crystal microbalance with dissipation monitoring (QCM-D). When adding 32.5 mol% cholesterol to solid-supported lipid vesicle layers (SVLs), no transition was observed, implying a homogeneous liquid ordered phase in this situation (Neupane et al. 2018).

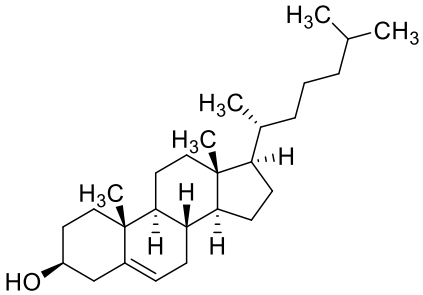

Fig. 10. Chemical structure of cholesterol.

Although the advantage of cholesterol has been proved in many cases, it is not an ideal membrane component in some situations. For example, liposomes containing cholesterol was found to exert a strong tendency to retain cisplatin inside and prevent its release to achieve efficient cytotoxicity (Zamboni et al. 2004). Thus, cholesterol is not necessarily an advantage in the formulation and its presence and its concentration have to be considered in each case.

1.2.3. Mechanism of liposome-cell interaction

There are several ways of interaction between liposomes and the targeted cells. Liposomes can be adsorbed onto the cell membrane specifically or non specifically and lead to different modes of drug release, as extensively described by Torchilin (Torchilin 2005) and Bozzuto (Bozzuto 2015) (Fig. 11). Concretely, when contacting with cells, liposomes can be degraded by enzymes or certain cell membrane components and release the drug directly into the extracellular matrix, followed by the diffusion through cell membrane. This process depends on the hydrophobic property of the encapsulated drug. Another route is the fusion of liposomes with the cell membrane, inducing the discharge of drug into the cell cytoplasm. The most common way for the liposome-cell interaction is endocytosis, in which the liposomes can either be delivered to lysosome

by endosome, or encounter destruction during the transport process.

The mechanism of the interaction is significantly affected by the state of targeted cells and physicochemical properties of the liposomes, such as the size, shape and surface charge. For example, smaller liposomes (diameter <150 nm) are more likely to be absorbed via receptor-mediated endocytosis, and positively charged liposomes are more easily taken up due to the negative charge on the cell membrane (Nogueira et al. 2015). Neutral liposomes show less interaction with cells, increasing the tendency of drug release in the extracellular fluid. Additionally, a lack of surface charge would result in aggregation of liposomes during storage (Bozzuto 2015).

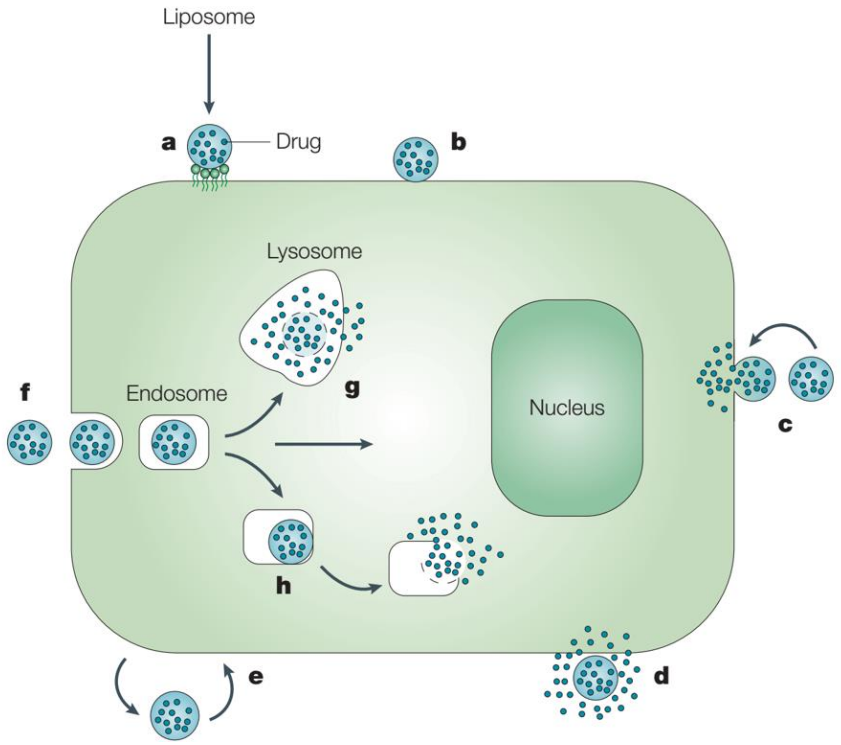

Fig. 11. Liposome-cell interaction. liposome entrapped with drug bind to the cell surface specifically (a) and nonspecifically (b). Lipid nanocarriers can also fuse with cell membrane and followed by drug release into the cell (c), or the liposomal structure is dismantled during the interaction with cell (d). Component exchange of the lipid bilayer with cell membrane also occurs under certain conditions (e). For endocytosis (f), liposome can either be transported to lysosome via endosome (g), or undergo destruction during the transport process (h). Copyright (Torchilin 2005)

1.2.4. Development of liposomes

Since the investigation of clinical application of traditional liposomes in the 1980s (Dagan et al. 1982), some breakthroughs in liposome research have accelerated the development of pharmaceutical liposomal delivery. In 1990, lipid-based amphotericin B (AmBisome®) was put on the European market as the first liposomal drug to treat a broad range of fungal infections (Hann and Prentice 2001). Subsequently, the anticancer drug Doxil was approved by FDA in 1995 (Allen and Cullis 2013). Considering the development history of liposomes in the past several decades, four typical generations can be summarized for the liposomal delivery system (Fig. 12).

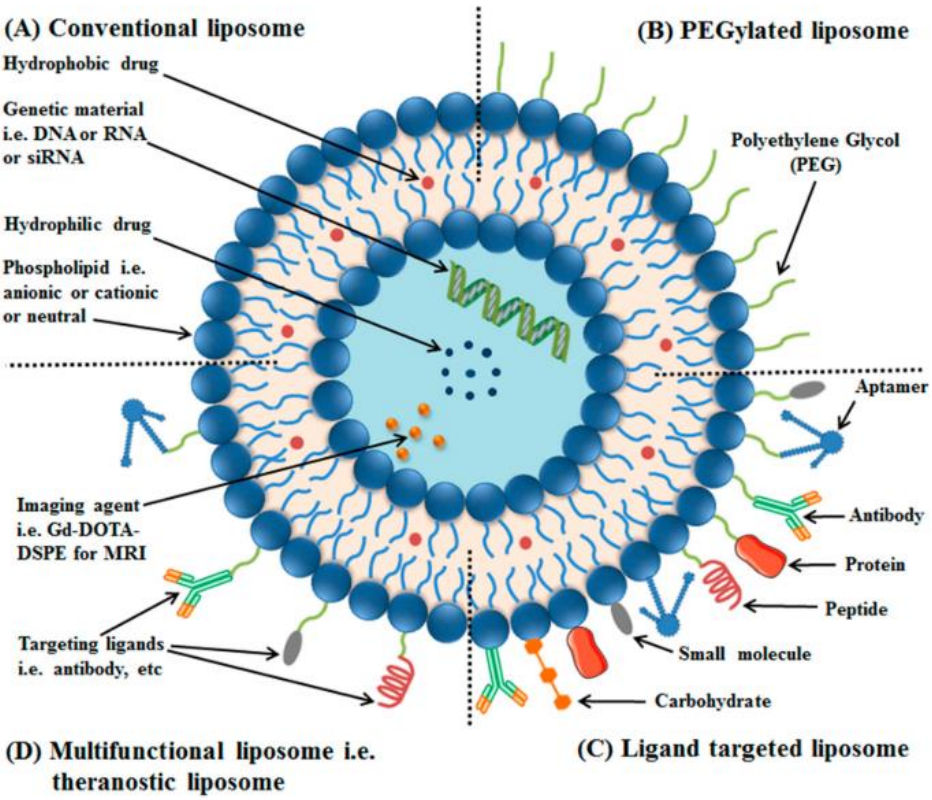

Fig. 12. Typical generations liposomes: Traditional plain liposomes consisting of phospholipids (A); long-circulation liposomes coated with a layer of polyethylene glycol (PEG) (B); targeted liposomes containing a specific targeting ligand (C); and multifunctional liposomes loaded with imaging agents (D). Copyright (Riaz et al. 2018)

1.2.4.1. Conventional liposomes

Consisting of phospholipid bilayers, conventional liposomes can alter the biodistribution and pharmacokinetics of the encapsulated drug *in-vivo*, thus reducing the toxicity to normal tissue and increasing drug delivery to disease site (Sercombe et al. 2015). However, this kind of liposomes will be subject to opsonization with serum components and taken up by the mononuclear phagocyte system (MPS), especially in the liver, leading to elimination from the bloodstream and a resulting short circulation time (Hua and Wu 2013).

Liposomes composed of PC with saturated fatty acyl chains have a longer half-life in the blood compared with those containing unsaturated fatty acyl chains, and larger-size liposomes are more easily eliminated from the blood than smaller ones (Senior and Gregoriadis 1982). Senior has also demonstrated that positively charged liposomes can be cleared rapidly (Senior 1987). Therefore, the efficacy of the drug is reduced. This led to the development of "stealth" or long-circulating liposomes that can avoid rapid uptake by the MPS.

1.2.4.2. Long-circulating liposomes

Long-circulating liposomes are obtained by coating with hydrophilic polymer, polyethylene glycol (PEG) for example, to reduce their recognition by serum components and render them "stealth" in the bloodstream (Klibanov et al. 1990). PEGylated liposomes (also called sterically stabilized liposomes) can significantly alter the pharmacokinetics of the formulation and enhance drug accumulation at the target site. The half-life of PEGylated doxorubicin liposomes in humans is as high as 45 hours (A Gabizon et al. 1994). The first long-circulating liposome formulation approved by the FDA was PEGylated liposomal doxorubicin (PLD) (Doxil®/Caelyx®), which was used to treat Kaposi's sarcoma in 1995, to treat ovarian cancer in 1999 and to treat multiple myeloma in 2007 (Olusanya et al. 2018).

Probable mechanisms to explain the longevity of sterically stabilized liposomes have been critically evaluated by Moghimi and Szebeni (Moghimi and Szebeni 2003) and they have indicated that PEG cannot completely prevent the activation of complement system and that macrophages also play a key role. Moreover, although liposomes grafted with PEG have a longer circulating time, the coating attenuates the interaction between liposomes and the targeted site to some extent and finally reduces the therapeutic efficacy (Ulrich 2002).

Although PEG was regarded as the gold standard for long-circulating liposomes and deemed to be harmless from a physical perspective, some evidence indicates that PEGylated liposomes can lead to side effects by activating the complement system (Moghimi and Szebeni 2003). Another strategy involves a removable PEG coating of liposomes to improve the recognition and uptake by cells. With the accumulation of PEGylated liposome at requisite site, the PEG moiety detaches due to the special physiological environment, lower pH for instance, thereby increasing the drug capture (Maeda et al. 2001).

1.2.4.3. Targeted liposomes

Targeted liposomes were developed so as to increase drug accumulation at the intended site and reduce toxicity towards healthy tissues, via coupling with various available ligands, such as antibodies and their fragments, peptides, carbohydrates and small molecules (Sapra and Allen 2003; Medina et al. 2004) Among the multiple targeting moieties, monoclonal antibodies are preferable due to their better stability and higher coupling avidity (Immordino et al. 2006). Furthermore, specific antibody fragments such as antigen-binding fragments (Fab), single-chain variable fragments (scFv) and dimers of antigen-binding fragments ($F(ab')_2$) are also commonly used as active targeting ligands with higher safety in the plasma due to their reduced non-specific binding, although their stability is lower when compared with the whole structure (Peer et al. 2007).

To obtain targeted liposomes, a variety of chemical coupling methods can be employed. Considering the diverse conjugation strategies, three kinds of basic reactions can be identified: between thiols and maleimide derivatives, between amino groups and carboxyl groups and between thiols and pyridyldithiols (Torchilin 2005). Among them, thiolation of antibodies with Traut's reagent (2-iminothiolane) has become a frequently used method in recent years, through the ring-opening reaction of 2-imidothioester's cyclic group (Eloy et al. 2017) (Fig. 13).

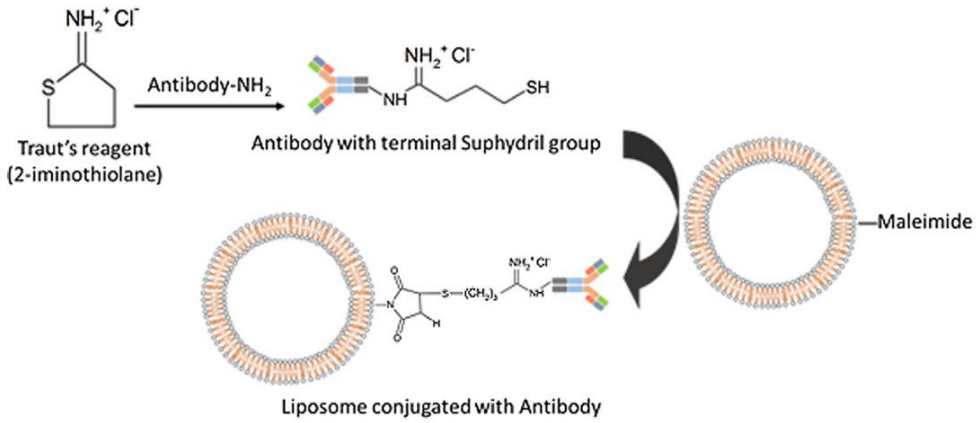

Fig. 13. Immunoliposome formation through the post-insertion method. Copyright (Eloy et al. 2017)

Early long-circulating immunoliposomes were prepared by decorating the surface of liposomes with PEG and antibody separately, which could lead to steric hindrances of the targeting ligand by the PEG chains (Torchilin 1992). Subsequently, with advances in liposomal technology, the targeting moiety could be linked to the distal end of the PEG arm so as to achieve specific delivery and long circulation at the same time. Using plasminogen as a homing device, Blume et al (Blume et al. 1993) found that PEGylated liposomes with Glu-plasminogen attached to DSPE-PEG 3500-COOH-terminus has longer circulation time in the blood and higher target binding capability than "ordinary" ones. Another kind of antibody-coating liposomes, cytoskeleton-targeting liposomes, exhibit advantages to specifically targeting to hypoxic cells with secretion of myosin to the extracellular matrix caused by membrane damage, especially in the case of experimental myocardial infarction (Khaw et al. 1984; Torchilin et al. 1992).

As far as liposomes targeted with monoclonal antibodies or fragments are concerned, some positive results have been achieved and most of the work has focused on cancer targeting. HER2, a member of the human epidermal growth factor receptor family, plays a significant role in the development of breast cancer, since 20-25% of breast cancer patients exhibit upregulation of HER2 (Eloy et al. 2017). Therefore, anti-HER2 immunoliposomes have been constructed. Fab' fragments of recombinant humanized monoclonal antibody rhuMAbHER2 were conjugated to doxorubicin (dox)-loaded liposomes, which showed significantly increased antitumor cytotoxicity and less systemic toxicity compared with free dox in multiple HER2-overexpressing human breast tumor xenograft models (Parka et al. 1997).

EGFR is another critical receptor that is closely associated with different types of cancers. Zalba et al prepared EGFR-targeted immunoliposomes with cetuximab (CTX, a monoclonal antibody) and its Fab′ fragments for the treatment of colorectal cancer (CRC). In the CRC xenograft model, drug delivery was significantly improved with targeted liposomes. Interestingly, liposomes coated with CTX-Fab′ fragments showed outstanding drug accumulation in tumor tissue compared with CTX liposomes or non-targeted liposomes (Zalba et al. 2015). Furthermore, transferrin receptors and folate receptors have also been targeted with interest because, similarly, they are highly expressed in a variety of tumor types.

1.2.4.4. Multifunctional liposomes

To meet the different requirements for current drug delivery system, multifunctional liposomes have emerged carrying a combination of several modifications in a single formulation. Currently, various versatile liposome formulations have been reported (Riaz et al. 2018), such as liposomes with dual-targeting (peptide T7 and DA7R) and co-delivery (doxorubicin and vincristine) abilities for treatment of glioma (Zhang et al. 2017), liposomes simultaneously coated with the near-infrared fluorescent molecule indocyanine green (ICG) and the cetuximab monoclonal antibody directed towards the epidermal growth factor receptor (EGFR)

(Portnoy et al. 2011) and liposomes carrying a combination of therapeutic and imaging agents (Li et al. 2012), etc.

Although the applications of liposomes for drug delivery have been described widely, their role as theranostics nanocarriers deserves to be presented, especially in the molecular imaging area. The use of liposomes to monitor treatment progression has several advantages, such as the possibility of combining a variety of imaging agents, targeting to the desired site with a specific ligand and the enhancement of imaging signal (Immordino et al. 2006). Faced with the short half-life of imaging agents, stealth liposomes decorated with PEG with prolonged circulation time in the body after administration can provide higher accumulation in the targeted tissue and a stronger signal. Fluorescence imaging is the most commonly used theranostic strategy. Quantum-dot functionalized liposomes (f-QD-L) hybrid nanoparticles have been formulated by Al-Jamal et al, demonstrating improved targeting and internalizing capability in tumor-cell monolayer cultures. Subsequently, extensive fluorescent staining of tumor cells was demonstrated after injecting f-QD-L intratumorally into solid tumor models, compared with f-QD alone. Taken together, this work indicates that f-QD-L is an efficient imaging tool both *in-vitro* and *in-vivo* (Al-Jamal et al. 2008).

As well as fluorescence imaging, magnetic resonance imaging (MRI) is attracting significant attention as a non-invasive technique. Due to the versatile properties of liposomes, multiple MRI contrast agents, paramagnetic Gd^{3+} for example, can be incorporated into one liposomal formulation, obtaining efficient delivery and enhanced imaging (Xing et al. 2016). Furthermore, the combination of MRI and an active drug allows real-time monitoring and therapeutic intervention at the same time. Tagami et al reported a multifunctional thermosensitive liposome with co-incorporation of Gd-DTPA (an MRI agent) and doxorubicin. The success of simultaneous drug release and molecular imaging in heated tumors in this study confirms the potential of liposomes as nanocarriers for theranostic applications (Tagami et al. 2011).

1.2.5. Fate of liposomes after different routes of administration

Liposomes are widely studied for treatment of many kinds of diseases, such as cancer, infection and multiple sclerosis (Palazzo et al. 2019). In order to obtain satisfactory therapeutic effects, several routes of administration have been studied, including intravenous delivery, transdermal delivery, oral delivery and pulmonary delivery. Depending on the route of administration, liposomes will be submitted to different physiological conditions that will affect their stability and distribution and, ultimately, their therapeutic efficiency.

As the most commonly used delivery route for liposome, intravenous administration possesses several advantages. For example, the systemic delivery liposomes can avoid toxicity to normal tissue compared to free drug by changing its distribution, as well as increasing the circulation time of the drug in the plasma by PEGylation. Since extensive information about liposomes for systemic administration has been provided above, “Stealth” and targeted liposomes for example, the sections below will concentrate on other routes of liposomal delivery.

1.2.5.1. Transdermal delivery

Skin drug delivery generally includes dermal (deliver to the skin) and transdermal (deliver across the skin) delivery (Fig. 14). As a more attractive alternative compared with oral or parenteral administration, transdermal delivery has various advantages, such as avoiding first-pass metabolism, achieving controlled release and reducing side effects (Sala et al. 2018). To permeate the skin barrier which is constituted mainly by the stratum corneum and improve drug delivery efficiency, researchers have tried different strategies and transferosomes were developed with enhanced permeation capacity across the skin due to their “gel state” property resulted from special additives (Cevc and Blume 1992). For example, elastic liposomes were reported to show effective treatment for deep dermal infection with delivery of neomycin sulphate (Darwhekar et al. 2012). Transfenac, a transfersomes formulation of diclofenac, was

shown to be superior to the marketed diclofenac hydrogel by different kinds of animal experiments (Cevc and Blume 2001).

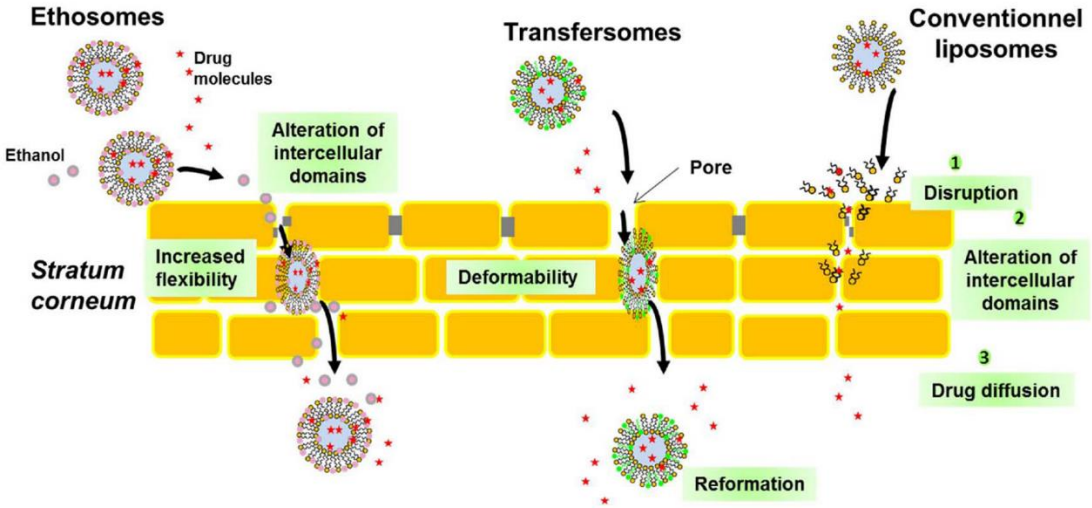

Fig. 14. Schematic representation of the main permeation mechanisms of lipid-based vesicles. Copyright (Sala et al. 2018)

Another kind of liposomes designed to improve the penetration efficiency, ethosomes, has been developed relying on ethanol's penetrating properties (Fig. 17). They were first reported in 1999 (Godin and Touitou 1999) and subsequently numerous investigations have demonstrated their potential for clinical applications (Zylberberg and Matosevic 2016).

1.2.5.2. Oral delivery

Oral administration is a major route for drug delivery. However, the extreme physiological conditions in the gastrointestinal (GI) tract presents stringent requirements for orally delivered liposomes, such as stability at low pH and in the presence of digestive enzymes (Nguyen et al. 2016), and the ability to penetrate through the intestinal wall into the blood (Torchilin 2005). Many attempts have been made to improve the bioavailability of drugs delivered by oral liposomes, for example, chitosan-coated liposomes have been reported to have enhanced mucoadhesive properties and to allow increased bioavailability of alendronate in rats (Han et al. 2012). An insulin-loaded liposomal drug delivery system has also been developed for diabetes mellitus

(Hanato et al. 2009) and Wong et al (Wong et al. 2018) have given a detailed review. To induce a better mucosal immune response in mice, PEGylated liposomes encapsulating ovalbumin have been studied (Minato et al. 2003), as an example for the development of oral vaccines. Moreover, for better oral drug delivery, surface modification (surfactants, anionic polymers, etc.) of liposomes has been substantially investigated to provide improved stability, increased solubility, controlled release and enhanced adherence (Nguyen et al. 2016).

Although liposomes for oral administration have undergone extensive development in the past decades, critical advances are still needed to make these nanocarriers suitable for clinical use and for commercialization. For clinical applications, the main hurdle is to develop a full-featured liposomal delivery system of the combines the desired stability, solubility and distribution *in-vivo*. The harsh physiological environment of the GI tract is an unavoidable challenge and only liposomes that have been carefully designed can survive. Additionally, these clinical requirements demand a higher level of manufacturing technology in order to go on the market, such as the quality control and storage conditions (Zhang et al. 2013).

1.2.5.3. Pulmonary delivery

Owing to the large absorption surface and easy solute permeation, the lungs are regarded as a promising route for drug delivery (Sung et al. 2007). Nanoparticles loaded with therapeutic drugs can be non-invasively delivered to the lungs for either local or systemic applications. Local pulmonary delivery for treatment of lung-related diseases requires a lower overall dose, thereby reducing the accompanying side effects. In the case of systemic delivery via the lungs, the thinness of the epithelial cell layer plays a major role in the absorption of drug and this route allows hepatic first-pass metabolism to be avoided (Sung et al. 2007).

Advances in nanotechnology, especially in aerosol formulation, have accelerated the development of liposomal drug delivery to lungs, which shows various promising features such as sustained release, localization within lungs and lower systemic toxicity (Misra et al. 2009). Liposomes containing procaterol hydrochloride were developed for

asthma treatment by the pulmonary route and an extended pharmacological effect was observed for 120 min in a guinea pig model (Tahara et al. 2016). Transferrin-conjugated liposomes were assessed *in-vitro*, showing the potential for treatment of lung cancer as a result of receptor-mediated internalisation (Anabousi et al. 2006). Pulmonary delivery of peptides and proteins is always problematic but insulin within liposomes was developed as an aerosol pulmonary drug with specific lung targeting and induced a reduction of the plasma glucose level (Huang and Wang 2006). Therapy of tuberculosis infection can also be achieved by improved delivery of rifampicin with aerosolized liposomes (Vyas et al. 2004). Despite numerous investigations of the pulmonary delivery of liposomal aerosols, further studies need to be carried out to better understand the interaction between nanocarriers and the physiological structure of lung. The absorption mechanism and biodistribution *in-vivo* are critical factors determining the final therapeutic effect of pulmonary liposomes.

1.2.5.4. Brain delivery

The blood-brain barrier (BBB) is composed of polarized endothelial cells with tight junctions that form the capillary walls in the central nervous system, which leads to an extreme limitation of the drugs available for cerebral diseases. More than 98% of small molecule compounds and nearly 100% of high molecular-weight drugs cannot cross the BBB (Pardridge 2003). To maintain the normal physiological functions of the body, circulating compounds need to be transported across the BBB and this occurs by several routes, including the paracellular pathway (small water-soluble molecules), transcellular diffusion (lipophilic molecules), carrier-mediated transport (glucose, amino acids, nucleosides, cyclosporin, etc.), adsorptive-mediated transcytosis (plasma proteins) and receptor-mediated transport (insulin, transferrin) (Vieira and Gamarra 2016; Ramos-Cabrer and Campos 2012).

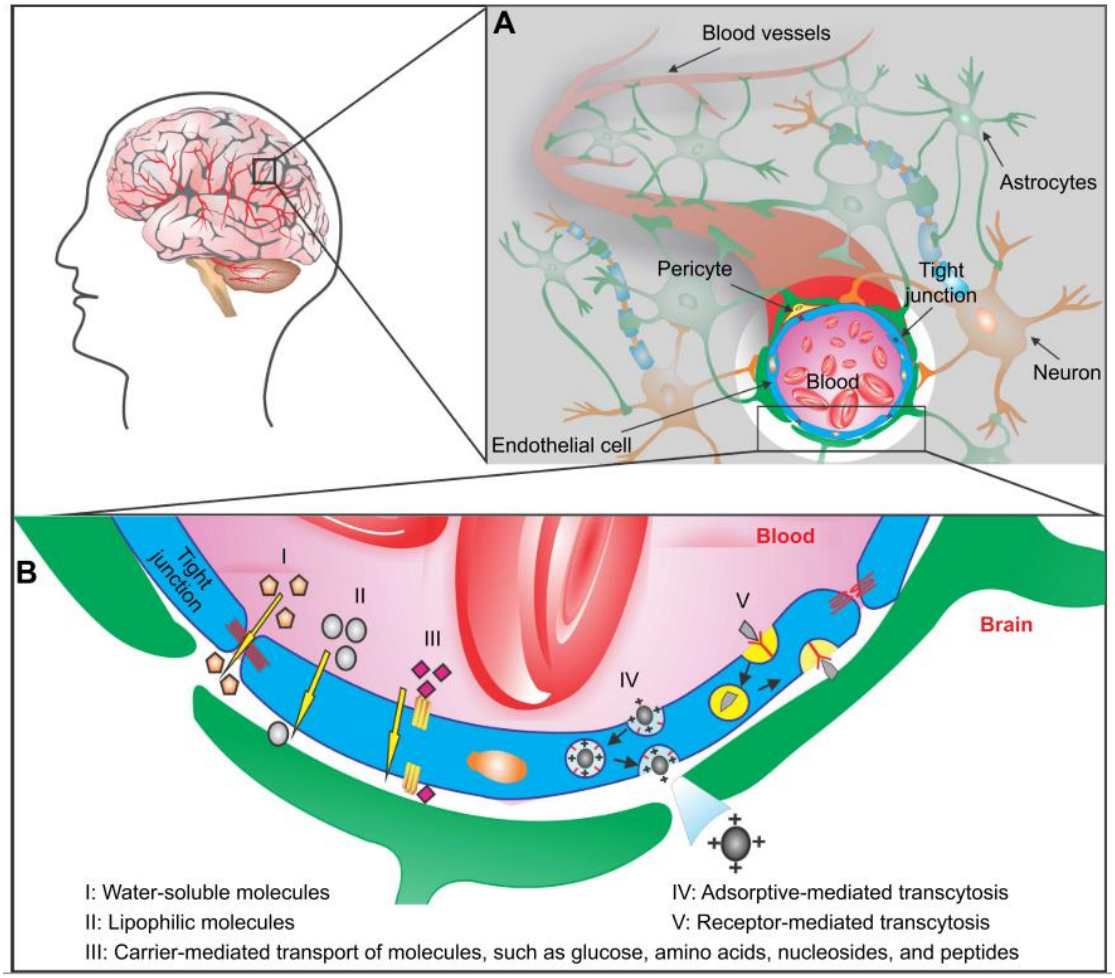

Fig. 15. Pathways for crossing the blood–brain barrier (BBB). (A) Cross-section of a cerebral capillary, showing the structure of the BBB. (B) Different mechanisms for drug delivery across the BBB. Copyright (Vieira and Gamarra 2016)

However, for systemically administered drugs that need to reach the brain, the BBB is effective in excluded these potentially toxic substances. In order to circumvent this barrier, several strategies have been studied and liposomes were chosen as an ideal drug delivery system due to their good biocompatibility and controlled release, and especially their targeting capacity when coated with peptides or antibodies. Strictly speaking, brain delivery of liposomes is not a general route of administration but a specific targeting mode that belongs to intravenous administration. Based on different transport mechanisms through the BBB, corresponding liposomal delivery systems have been developed, such as liposomes that undergo adsorption-mediated transcytosis (Helm and Fricker 2015) and receptor-mediated endocytosis (Salvati et al. 2013) (Fig. 15). Moreover, preclinical investigations have been carried out for treatment of

neurological diseases. Rivastigmine liposomes showed better memory regain function and improvement of metabolic disturbances in a rat model of Alzheimer's disease (Ismail et al. 2013). Chlorotoxin-coated liposomes encapsulating levodopa also showed their potential to cure Parkinson's disease in the methyl-phenyl-tetrahydropyridine (MPTP)-induced PD mice model (Xiang et al. 2012).

As one of the most challenging tasks in drug delivery area, liposomes for brain delivery still face a number of problems before they reach commercial application. Apart from similar hurdles to other routes of administration mentioned above, stability for example, brain-targeting liposomes must meet a higher level of biocompatibility and biodegradability, since any accumulation of non-biodegradable substances in the brain could cause unpredictable consequences. The latent side effects of brain-targeting nanocarriers are still unknown. Therefore, further study, either in animal models or in the clinic, should pay attention to this aspect, in order to facilitate the application of liposomes for treatment of neurodegenerative diseases (Poovaiah et al. 2018).

1.2.6. Nano-sized drug carriers for AML

In AML treatment, drugs are generally given by intravenous route, which not only results in rapid elimination but also leads to adverse effects due to the lack of specific targeting. Nanoparticulate systems with long circulating properties and passive targeting capability to the malignant cells in the bone marrow represent a promising strategy. Several nano-sized formulations for the treatment of AML are already available on the international market. Among them, Vyxeos, a liposomal formulation with encapsulation of daunorubicin and cytarabine, was approved by FDA in 2017 for AML therapies. Briot et al summarized the drug-loaded nanocarriers involved in clinical trials for treatment of AML in December 2017 (Briot et al. 2018). Based on their review, the updated list of liposomal formations under clinical trials for treatment of AML in May 2019 is presented in Table 4.

Table 4 Liposomes under clinical trials for treatment of AML in May 2019* (Briot et al. 2018)

Encapsulated drug	Clinical trial phase	Clinical trial ID
Annamycin	1	NCT00430443
	1-2	NCT03388749
Vincristine	1	NCT01159028
	2	NCT02337478
Grb2 Antisense Oligonucleotide	2	NCT02781883
Daunorubicin	2	NCT02286726
Daunorubicin-Cytarabine	1	NCT03878927
	1-2	NCT02642965
	2	NCT03629171/NCT03226418/NCT03226418
		NCT02269579/NCT02238925/NCT00788892
	3	NCT01696084

* From *clinicaltrials.gov*, May 2019.

1.2.6.1. Polymeric nanoparticles for AML

Polymeric NPs composed of synthetic or natural polymers are one of the different systems used in nanomedicine to entrap hydrophobic or hydrophilic agents in different treatment strategies. In terms of AML, a number of preclinical evaluations are ongoing and one has already been enrolled for clinical trial. The clinical candidate drug AZD2811, an Aurora B kinase inhibitor, was encapsulated as polymeric nanoparticles with an ion-pairing approach (Ashton et al. 2016). Two kind of block copolymers (poly-D,L-lactide (PLA) and poly (ethylene glycol) (PEG) were used and in-situ ion pairing was developed to increase the encapsulation efficiency and decrease the release rate of AZD2811. Investigations on a HL-60-xenografted mouse model demonstrated high antitumor activity of these nanoparticles. Improved tumor regression and a more sustained response were also observed in combination with cytarabine (Floc'h et al. 2017).

1.2.6.2. Liposomes for AML

As mentioned above, a liposomal formulation for treatment of AML, Vyxeos, with

co-encapsulation of cytarabine and daunorubicin, was approved by FDA in 2017 for treatment of adults with newly diagnosed therapy-related AML (t-AML) or AML with myelodysplasia-related changes (AML-MRC). Before it was released onto the market, Vyxeos underwent a number of preclinical and clinical trials under the code name of CPX-351. A phase 2 trial of CPX-351 was conducted in 126 older patients with newly diagnosed AML in comparison with the standard 7+3 regimen (JE et al. 2014). Higher response rates were achieved as well as a prolongation of EFS and OS among the secondary AML subgroup, which stimulated the clinical progress and an upgraded version was investigated in a phase 3 trial. In this study, a total of 309 patients aged 60-75 years were randomized (153 to CPX-351 + 156 to 7+3 regimen) and the former arm showed a significantly higher overall survival, event free survival, and response (Lancet et al. 2016).

Apart from these FDA-approved liposomes, several other liposomal formulations are undergoing investigation. To minimize the adverse effects of extensive chemotherapy in AML, Myhren et al formulated PEGylated liposomes encapsulating both the anthracycline daunorubicin (DNR) and emetine, a protein synthesis inhibitor that reduces the production of survival proteins. Furthermore, the surface of liposomes was coated with folate for more specific uptake by AML cells and this multi-functional liposomal formulation showed the potential to be a candidate for AML treatment (Myhren et al. 2014). Safingol, a member of the sphingolipid family with anti-leukemic property, was formulated in liposomes to overcome its low water solubility and dose-limiting hemolysis. Liposomal safingol was found to be effective on a variety of AML subtypes and can prolong the median survival time of SCID mice bearing a human leukemia xenograft from 23 days (with free drug) to 31 days (Tan et al. 2012).

1.2.7. Biological challenges of liposome delivery

As discussed above, liposomal formulations for treatment of AML are undergoing investigations at different stages (*in-vitro*, *in-vivo* and clinical trials) (Briot et al. 2018). In contrast to standard chemotherapy, drugs entrapped within liposomes have

advantages for patients, reducing side effects and the emergence of drug resistance. Targeted liposomes decorated with specific antibody or fragments against AML cell lines seem to have a promising future. However, there is always a large gap between academic research and the final commercial application of drug development. In the case of liposomes, numerous obstacles lie in their way, one of which is the biological challenge. Once administrated into the circulation system of the body, liposomes have to resist physiological defense systems like any other exogenous substances. To achieve the desired therapeutic effect, the first hurdle to be taken into consideration is the mononuclear phagocyte system (MPS), which is able to take up liposomes mainly by phagocytic cells in the liver and spleen. Fortunately, the development of PEGylated liposomes that significantly circumvent the clearance by MPS has confirmed the status of liposomes in the nanocarrier drug delivery area.

Generally, sterically stabilized liposomes were supposed to have no or limited immunogenicity in the body, until a discovery by Dams et al in 2000 (Dams et al. 2000). PEGylated liposomes were found to have significant effects on the biodistribution and pharmacokinetics of the subsequent injections of PEGylated liposomes, both in rats and rhesus monkey. Specifically, the blood content of 99mTc-PEG liposomes declined dramatically after the second dose, accompanied by an obvious increased uptake in the liver and spleen. This finding is named “Accelerated Blood Clearance” (ABC) phenomenon and it significantly impairs the long-circulation advantage of PEGylated liposomes if repeated doses are given. More seriously, severe adverse reactions could be caused by the alteration of pharmacokinetics.

After a number of investigations, Ishida et al found that the magnitude of ABC phenomenon is correlated with the lipid dose, the time interval between injections, the PEG-surface density and the drug encapsulation (Ishida and Kiwada 2008). Meanwhile, a novel modified pH-sensitive liposome with a cleavable double smart PEG-lipid derivative was reported, for which no ABC phenomenon was induced by repeated injection. Another strategy is the replacement of PEG with another hydrophilic polymer. Romberg et al used a PEG alternative, PHEA (poly (amino acid) poly (hydroxyethyl-

L-asparagine) (PHEA)), to modify liposomes and demonstrated that PHEA-liposomes had longer blood circulation times than PEG-liposomes (Romberg et al. 2007). Despite the multiple solutions that have been proposed, the mechanism of the ABC phenomenon remains unclear and deserves more attention.

1.3. Drug-cyclodextrins-liposomes (DCL) system

Liposomes have been proved to be a versatile tool for drug delivery. However, the liposomal formulation may undergo leakage or rapid release when encapsulating hydrophobic or amphipathic molecules within the membrane, which largely impairs the therapeutic efficiency. To obtain stable drug delivery system, a new approach was developed in 1994 and named as "drug-in-cyclodextrins(CDs)-in-liposomes" (DCL) system (Mccormack and Gregoriadis 1994). By entrapping the CD-drug inclusion complexes into liposomes, the DCL system ingeniously takes advantage of both CDs and liposomes.

1.3.1. Cyclodextrins

Cyclodextrins (CDs) are a group of cyclic oligosaccharides (Jambhekar and Breen 2016). Since the first discovery in 1891 (Villiers 1891), CDs have been widely investigated and used in various fields. The most common members of the CD family are α-CD, β-CD and γ-CD, composed by 6, 7 and 8 glucose units and with cavity sizes of 0.5, 0.6 and 0.8 nm, respectively (Fig. 16) (Zhang and Ma 2013; Sharma and Sharma 2001).

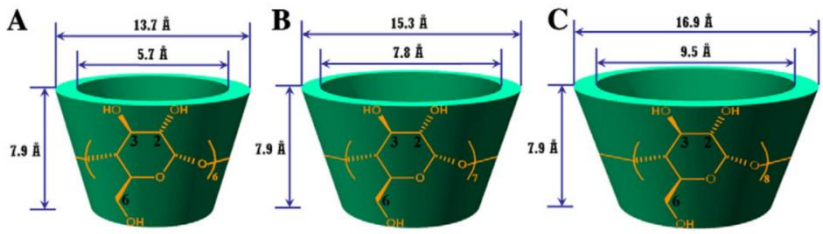

Fig. 16. Molecular structures and dimensions of CDs: A, α-CD; B, β-CD; and C, γ-CD. Copyright (Zhang and Ma 2013)

Due to the special configuration of hydroxyl groups, CDs form a cask-like three-dimensional structure with a hydrophilic outer rim and a hydrophobic internal cavity, which can incorporate various hydrophobic molecules as inclusion complexes (Fig. 17). The host-guest inclusion complexes can significantly change the guest molecule's physicochemical behavior, for example, improving apparent drug solubility (Brewster and Loftsson 2007), protecting it from photodegradation (Mielcarek and Daczkowska 1999) and promoting controlled release (Hirayama and Uekama 1999).

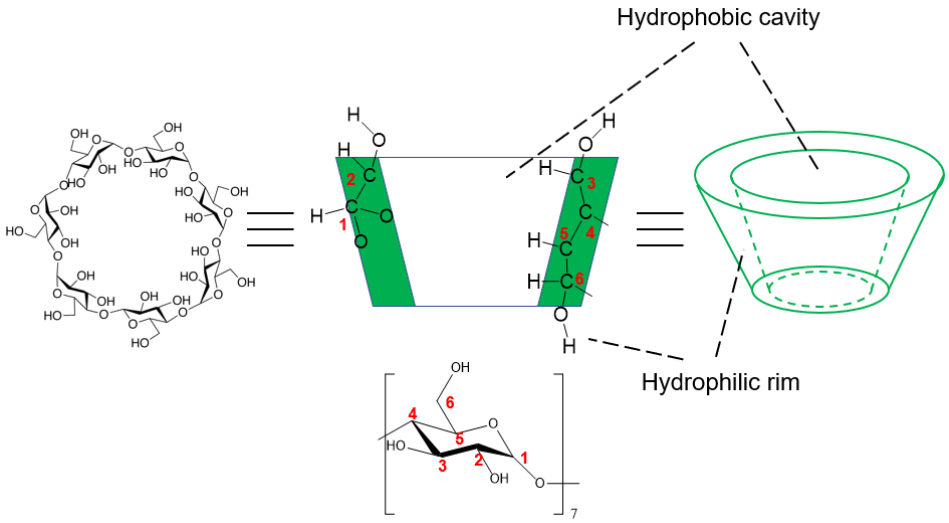

Fig. 17. Cask-like structure of β-CD with hydrophilic rim and hydrophobic cavity.

1.3.1.1. Derivatives of CDs

To satisfy the different requirements of CDs for pharmaceutical applications, a variety of derivatives have been synthesized, including derivatives with higher aqueous solubility (Szente and Szejtli 1999) or with an enhanced hydrophobic cavity (Del Valle 2004) (Fig. 18). For example, the water solubility of β-CD can be increased from 1.8% (w/w) to 60% or more by hydroxypropylation (Qi and Sikorski 1999). Chemical derivatives of β-CD, including the hydroxypropyl derivatives, sulfobutylether derivatives and randomly methylated derivatives, have been comprehensively described (Davis and Brewster 2004).

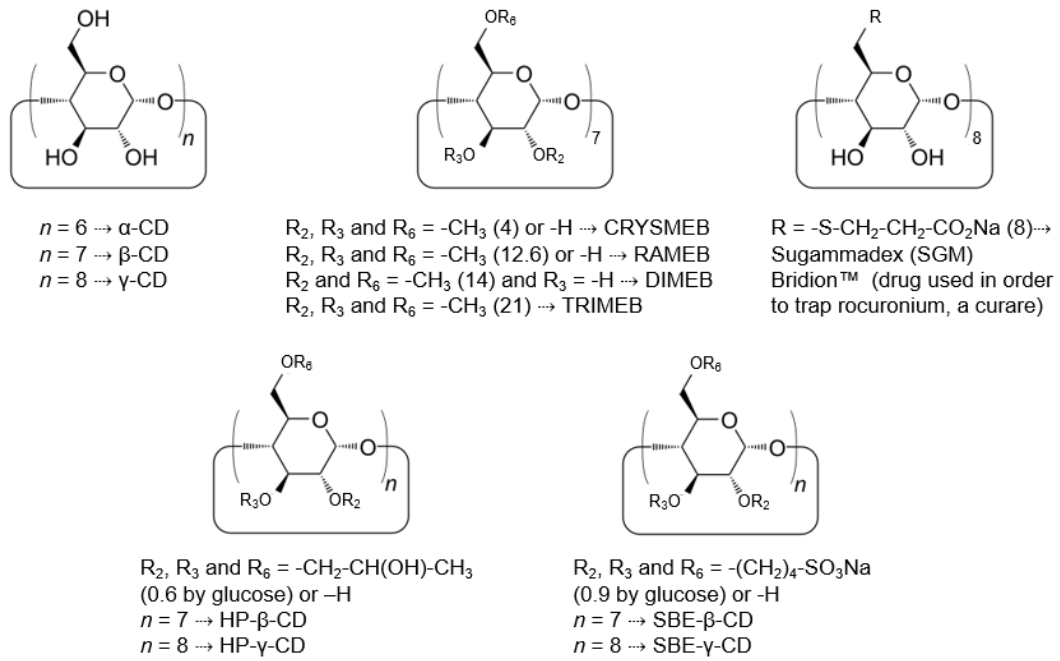

Fig. 18. Structural formulae of cyclodextrins and their chemical derivatives.

Sugammadex (SGM) is a modified γ-cyclodextrin with the addition of eight carboxyl thio ether groups. These modifications not only increase the encapsulation capability of the cyclodextrin by expanding the cavity size, but also increase its aqueous solubility. As the first selective relaxant binding agent, SGM is used to reverse neuromuscular blockade induced by rocuronium or vecuronium, by forming a concentration gradient of the drug between neuromuscular junction and the plasma (Naguib 2007). Extensive investigations have confirmed the safety and tolerance of SGM, and its biological inertness further extends its suitability for nanometric drug delivery systems.

1.3.1.2. CDs complexes

When mixed together in the solution, a dynamic equilibrium forms between the water-soluble inclusion complexes and free molecules of CD and drug. Different association models can be described according to the size of cavity and the hydrophobic properties of CD and guest molecules, with a balance of several driving forces, such as van der Waals interactions, hydrophobic interactions and electrostatic interactions

(Jambhekar and Breen 2016). Usually, the association ratio of CD/drug inclusion complexes is 1:1 or 2:1. Additionally, it should be noted that CD can form inclusion complexes with just a part of the guest molecule in some cases (Davis and Brewster 2004) (Fig. 19).

The physicochemical properties of the free molecules of cyclodextrin and drug are modified by their association, which allows a number of physicochemical methods to be used to monitor the formation process. Thus, spectroscopic methods such as fluorescence spectroscopy, UV/VIS spectroscopy and nuclear magnetic resonance (NMR) spectroscopy can be used to investigate the CD/drug inclusion complexes (Jansook et al. 2018). Moreover, techniques that detect changes in the aqueous medium are also commonly utilized, such as calorimetric titration and pH-potentiometric titration.

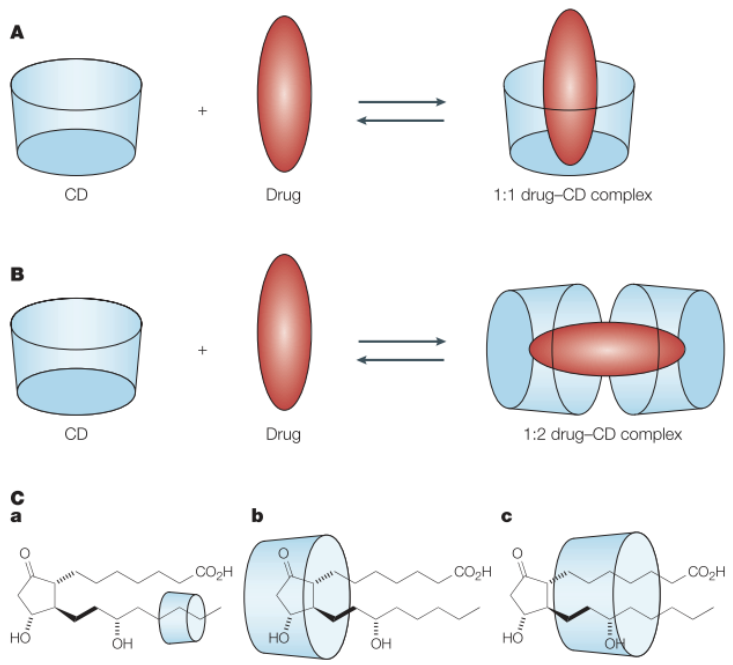

Fig. 19. Schematic illustration of the association of free cyclodextrin (CD) and drug to form drug–CD complexes. A | 1:1 drug–CD complex. B | 1:2 drug–CD complex. C | Proposed models of inclusion complexes between prostaglandin E2 and (a) α-CD, (b) β-CD and (c) γ-CD. Copyright (Davis and Brewster 2004)

1.3.1.3. Effect of CDs on the photostability of associated drugs

In addition to the well-known property of increasing solubility of the guest molecule, CD also has the capability to protect the drugs from photodegradation. Tretinoin, also known as all-trans retinoic acid, is highly sensitive to light and its photodegradation could be reduced by CD incorporation. In a comparative study of ten different CD molecules, tretinoin underwent minimal degradation after 48 hours with the CD's protection, especially in complex formation with SBE-β-CD (Semenova et al. 2003).

Another frequently used antihypertensive agent, 1,4-dihydropyridine, is also photosensitive and this characteristic was studied for the drug and a series of its derivatives. By forming inclusion complexes with β-CD, the ortho isomer showed a 200 times slower degradation rate than when it was in its crystal phase. In contrast, a 4-fold increase in the photodegradation rate was observed in the case of halogeno and cyano derivatives. The reason behind this phenomenon lies in the different position of $-NO_2$ group in the phenyl ring (Mielcarek 1997).

To investigate the effect of CD on the photostability of nicardipine, an agent used for treatment of treat high blood pressure and angina, a variety of inclusion complexes with CD were obtained. Consequently, either a photoprotective or an accelerating effect was observed. Furthermore, stereoselective photodegradation was observed in the case of β-CD complex, indicating two distinct photodegradation profiles with two different kinetic constants (Pomponio et al. 2004).

Despite the fact that numerous studies have demonstrated the protective effect of CDs on the photostability of guest molecules, Kamiya and Nakamura found the protective effect depends on the CDs. They investigated the function of several CDs during the photodegradation of parathion and paraoxon and revealed that some kinds of CD show an inhibiting effect, while others the opposite. The phenomenon can be explained by the difference in distance between the catalytic sites of the host cavities and the reaction centers of the included pesticide molecules (Kamiya and Nakamura 1995).

1.3.1.4. Pharmaceutical applications of CDs

Due to the promising physicochemical and biological properties, CDs and their derivatives have been widely used in pharmaceutical applications, such as drug delivery (Loftsson et al. 2005), medical imaging (Zhang and Ma 2013) and other applications that have been extensively reviewed (Davis and Brewster 2004; Jansook et al. 2018; Manakker et al. 2009). Despite its low aqueous solubility, β-CD occupies more than half of the medical market of CDs. The reason lies in its low cost of production (Fig. 20).

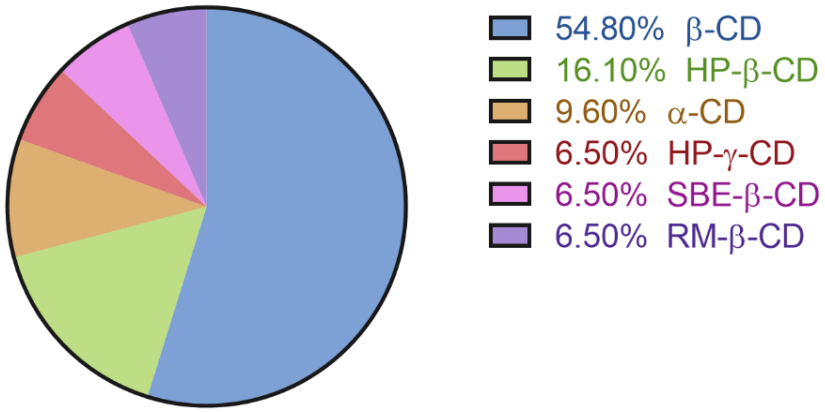

Fig. 20. Relative distribution of cyclodextrins used in marketed medicines. Reproduced from (Kurkov and Loftsson 2013)

1.3.2. Drawbacks of CD-drug complexes

Despite of the comprehensive application in pharmaceutical field, CDs and their derivatives have to face several obstacles before their usage can expand. One of the problems is the weak intermolecular forces in the host-guest inclusion complexes, which can lead to easy dissociation of the drug in plasma followed by its rapid elimination as a free molecule (Chen et al. 2014). Thus, the circulation time would be reduced and it further results in lower efficiency. Another more serious problem is the well-known phenomenon of incorporation of cholesterol and membrane lipids by CDs, especially the derivatives of β-CD. Kiss et al carried out a systematic investigation with 15 different β-CD derivatives to investigate the mechanism of CD's cytotoxic effects

on Caco-2 cells. The cytotoxicity of β-CD derivatives was found to have a correlation with their cholesterol extraction capacity, which depends on the number and position of the methyl groups and the presence of ionic groups. Thus, the cholesterol-solubilizing properties can be a predictive factor for CD's cytotoxicity and hemolytic activity (Kiss et al. 2010).

1.3.3. DCL system

Liposomes have been proved to be a useful drug delivery system both for hydrophilic and hydrophobic drugs and several products have come onto the market based on this. However, the direct encapsulation of a drug on the liposomal formulation could cause instability of the drug delivery system and even rapid release after *in vivo* administration because of incorporation of the hydrophobic drugs within lipid bilayers (Maestrelli et al. 2005). After encapsulation, hydrophobic molecules locate in the lipid bilayer rather than the aqueous core of liposomes. The limited space among lipid bilayer will not only restrict the amount of drug that can be entrapped but also increase the probability of leakage or release. Therefore, a novel strategy is needed to overcome these weaknesses. To circumvent the drawbacks of drug-CD and drug-liposome delivery systems, McCormack et al (McCormack and Gregoriadis 1994) proposed a novel concept, namely DCL system. By encapsulating the CD/drug inclusion complexes within liposomes, this strategy takes advantage of the properties of both CDs and liposomes, preventing destruction of lipid bilayers by the drug and rapid release by including it in CDs and increasing the retention time in plasma by entrapping the inclusion complexes in liposomes. This attracted the interest of researchers and numerous hydrophobic or amphipathic molecules have been entrapped in DCL systems for further application.

Temoporfin, a highly potent second-generation photosensitizer, was encapsulated within liposomes in the form of β-CD inclusion complexes. The resulting temoporfin-in-CD-in-liposome system was stable during 90 days storage and *in vitro* evaluation demonstrated a homogenous accumulation of temoporfin throughout tumor cell

spheroids (Yakavets et al. 2018) (Fig. 21). Lapenda et al reported a DCL system based on trans-dehydrocrotonin (t-DCTN) and the evaluation on its antitumor activity indicated that the liposomal formulations containing HP-β-CD/t-DCTN are a promising strategy for its application in therapy (Lapenda et al. 2013). More applications of DCL system are addressed in a comprehensive review (Gharib et al. 2015).

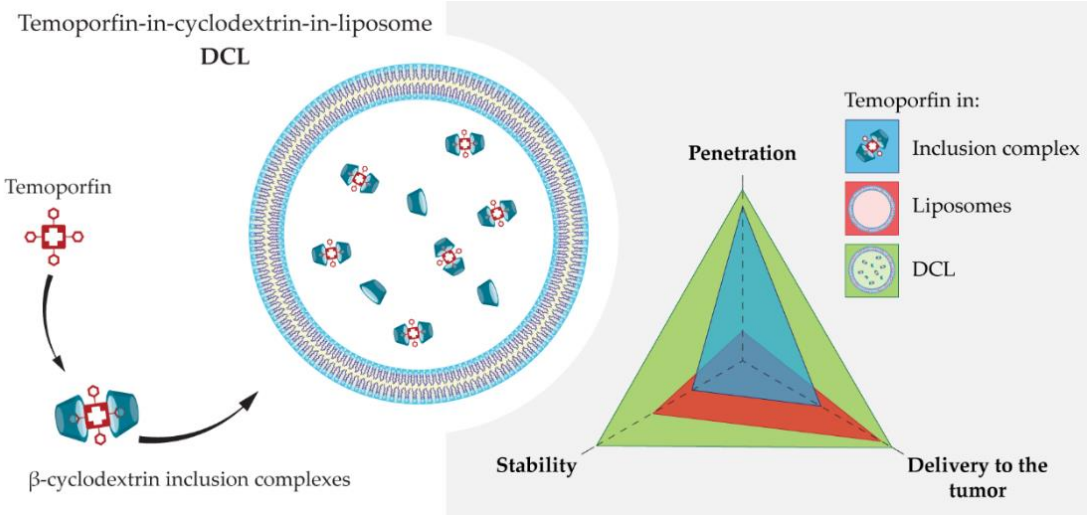

Fig. 21. Representative scheme of DCL nanoconstruct and the comparison of inclusion complex, liposomes and DCL in penetration, stability and delivery activity. Copyright (Yakavets et al. 2018)

1.3.4. Impact of CDs on DCL

Under certain conditions, the stability of DCL system can be undermined by some kinds of CDs, which are capable of extracting lipid molecules from bilayers into their hydrophobic cavities. Consequently, the exchange of drug and lipid molecules will destabilize the structural integrity of the system. Thus, the role of CD is important and the interaction between phospholipids and CDs has to be made clear.

The properties of CDs depend on the type. The cavity size and lipophilicity of CDs are two key factors that influence the interaction with phospholipids. According to Puskas, the destabilization ability of CDs on DPPC bilayers is closely related to the amount of CDs bound to the bilayer. Above a certain CD/DPPC ratio, any excess cyclodextrin would act to destroy the vesicles. Studies conducted at the same CD/DPPC ratio revealed that the destabilization ability is in the order: α-CD>β-CD>γ-CD

(Chellam and Mandal 2013). Considering that the cavity size is the smallest in α-CD, the results above indicate that the hydrophobicity of CDs, which can determine their affinity for lipids, seems to be the main cause of the destruction. To clarify this, Piel et al carried out a systematic evaluation of the affinity of the most commonly used CD for the two lipid components of liposomes, cholesterol and soybean phosphatidylcholine, confirming that the effect of CDs on the integrity of liposomes is directly related to their affinity (Piel et al. 2007).

In the DCL system, the situation becomes more complicated due to the participation of drug molecule. The affinity competition between encapsulated agents and lipid components will decide the extent of the destabilization effect of CD. A significant expansion of particle size in HP-β-CD/*trans*-dehydrocrotonin loaded liposomes was observed during long-term storage, while liposomes without HP-β-CD show higher stability. The difference could be explained by the stronger affinity between CD and the lipid component compared with the drug molecule (Lapenda et al. 2013). However, if CD has higher binding force with the active ingredient, as was the case for betamethasone for example, liposomes can remain intact even loaded with a high concentration of complexes (Piel et al. 2006).

1.3.5. Preparation methods for DCL system

In general, the methods available to prepare the DCL system can be divided into two categories: passive loading and active loading. The encapsulation efficiency of passive loading methods, such as thin-film hydration and ethanol injection, depends heavily on the physicochemical properties of the lipid, CDs and drug. On the other hand, in the case of active loading strategy, including pH gradient and ammonium gradient method, amphiphilic molecules can be encapsulated with high drug/lipid ratios.

1.3.5.1. Passive loading methods

- Thin-film hydration

Thin-film hydration is a commonly used strategy (Fig. 22), in which a thin film of

lipid is first obtained by dissolving the lipid with organic solvent, followed by solvent-removing step under reduced pressure. Subsequently, an aqueous mixture of CD/drug complexes is added to hydrate the film (Piel et al. 2007; Gharib et al. 2015).

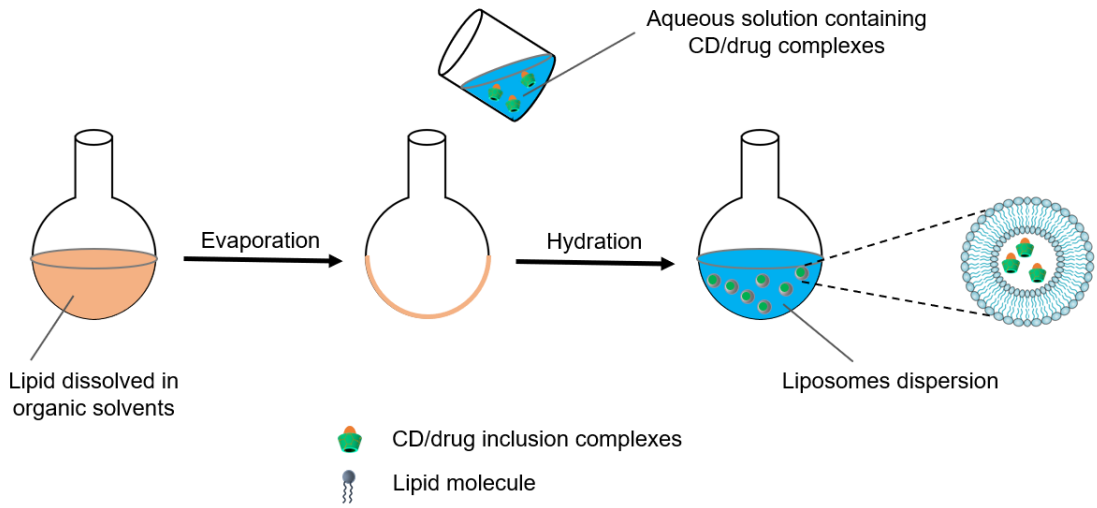

Fig. 22. Preparation of liposomes by the thin-film method. Reproduce from (Gharib et al. 2015)

The thin-film hydration is one of simplest ways of preparing a DCL system and has been widely used in the literature. For example, Dhule et al prepared HP-γ-CD/curcumin liposomes as delivery vehicles for osteosarcoma by the thin-film hydration method, with promising anticancer potential both *in vitro* and *in vivo* against KHOS osteosarcoma cell line and MCF-7 breast cancer cell line (Dhule et al. 2016). Furthermore, liposomes containing CD/indomethacin inclusion complexes obtained by the same method showed higher encapsulation efficiency and slower drug release compared with conventional liposomes (Chen et al. 2007).

- Ethanol injection

Another frequently used method is ethanol injection. The lipid components are dissolved in ethanol, after which the solution is injected in an aqueous mixture containing CD/drug complexes stepwise under stirring. The ethanol is finally eliminated under reduced pressure (Skalko et al. 1996; Gharib et al. 2015) (Fig. 23). Based on this method, Skalko et al obtained HP-β-CD/nifedipine loaded liposomes with

higher EE (77.7%) and higher stability in the plasma compared with liposomes containing nifedipine (Skalko 1996). Both the phospholipid and the cholesterol concentration were found to have effect on the size of liposomes (Shaker et al. 2017).

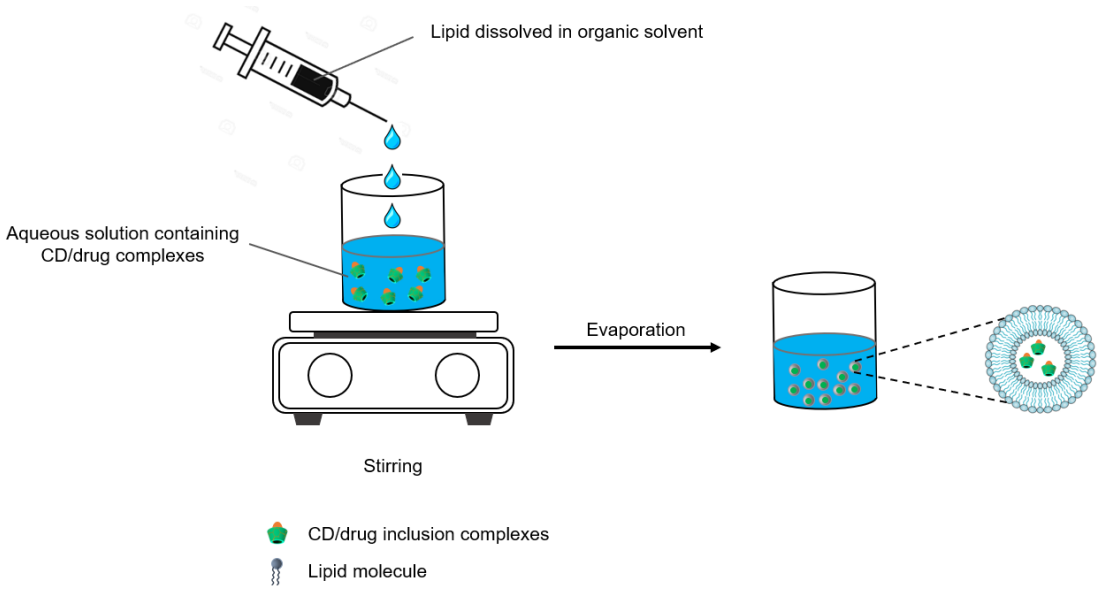

Fig. 23. Preparation of liposomes by the ethanol injection method. Reproduce from (Gharib et al. 2015)

- Dehydration-rehydration

The dehydration-rehydration method, yielding liposomes named dried reconstituted vesicles (DRV), was first developed by Kirby and Gregoriadis in 1984 (Kirby and Gregoriadis 1984). To prepare DRV, empty SUVs are first obtained, followed by mixing with same volume of aqueous solution containing CD/drug complexes. After overnight lyophilization, the freeze-dried powder is rehydrated with appropriate buffer and MLVs are obtained with relatively higher EE, due to the close contact of drug molecules with phospholipids in the freeze-drying state (Fig. 24). The DRV method has been widely used to prepare liposomal formulations containing various substances, such as low molecular weight drug molecules (Mugabe et al. 2006), proteins (Rodriguez-Nogales et al. 2004) and DNA (Pupo et al. 2005). The EE of DRV is significantly influenced by the diameter of the empty SUVs, the properties of the rehydration buffer and the experimental conditions applied during the whole workflow.

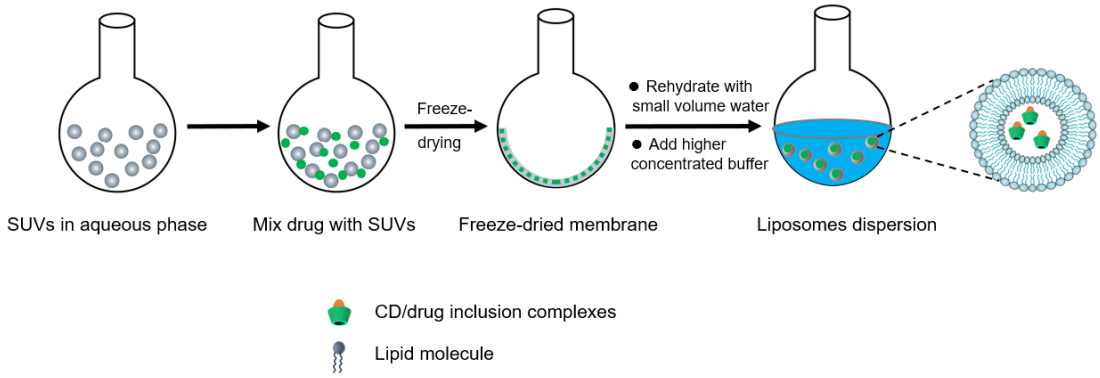

Fig. 24. Preparation of liposomes by the dehydration-rehydration method

1.3.5.2. Active loading methods

In contrast to passive loading methods, an active loading strategy applied in liposomal formulations is more effective for encapsulating weak base drugs to a high EE. Nichols and Deamer first reported the pH gradient method to prepare catecholamine-loaded liposomes, after which the technique was widely introduced (Nichols and Deamer 1976). In active loading, the drug molecules are driven into the internal aqueous phase by a transmembrane pH gradient. Specifically, the unionized form of drug can cross the lipid membrane easily, while it undergoes ionization in the intraliposomal medium due to the lower pH and becomes “locked” inside. In 1989, an evolutive form of the pH gradient method, ammonium sulfate gradient method, was proposed by Gabizon (Gabizon et al. 1989). In this method, the active pumping force originates from a transmembrane gradient of ammonium sulfate. Due to its efficient loading capability, the ammonium sulfate gradient method has been used to encapsulate various amphipathic drugs, for example, doxorubicin (Fig. 25).

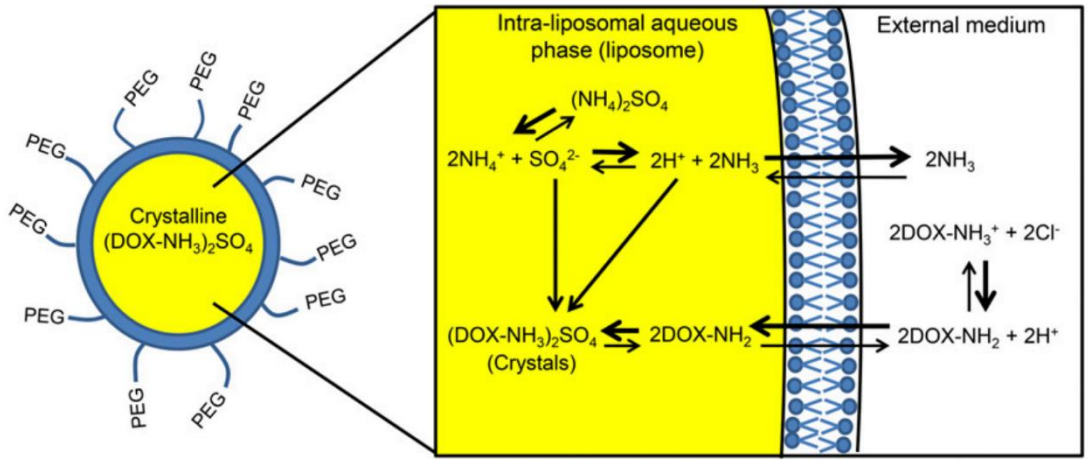

Fig. 25. Illustration of the mechanism of the ammonium sulfate gradient method. Copyright (Yingchoncharoen et al. 2016)

As the pH or ammonium sulfate gradient method depends on the weak base property of the drug, a poor EE would be achieved for nonionizable molecules even by the active loading. Sur et al synthesized cyclodextrins with multiple weakly basic functional groups to transport nonionizable drugs across the liposomal membrane, in the form of inclusion complexes (Sur et al. 2014). Consequently, the drugs were actively loaded into liposomes and greater efficacy was observed in *in-vivo* evaluation compared with free drugs.

1.3.6. CPZ-encapsulated DCL for treatment of AML

In order to take advantage of the capacity of CPZ to inhibit the growth of leukemic cell lines, we aim to design and develop a novel nanometric drug delivery system for treatment of AML (Fig. 26). As discussed above, liposomes could be an ideal choice for this application, with several advantages including the ability to prevent CPZ from passing through the BBB and prolong its circulation time in the plasma. However, the direct encapsulation of CPZ within the liposomes could compromise their integrity, considering the amphiphilic property of CPZ. Unlike the aqueous phase distribution of hydrophilic drugs, hydrophobic molecules are inclined to locate in the lipid bilayer and such incorporation would cause leakage during the storage or even rapid release when

administrated intravenously. Therefore, the CPZ-encapsulated DCL system could provide a promising solution. By entrapping CPZ molecules within its hydrophobic internal cavity and forming inclusion complexes, CD could efficiently confine the majority of CPZ within the aqueous core of liposomes, which contributes not only to the systematic stability but also the controlled release. Another well-known property of CPZ is its photosensitivity. As mentioned above, CDs show a protective effect on the photostability of guest molecules in most cases, indicating that CPZ may remain stable in the DCL system.

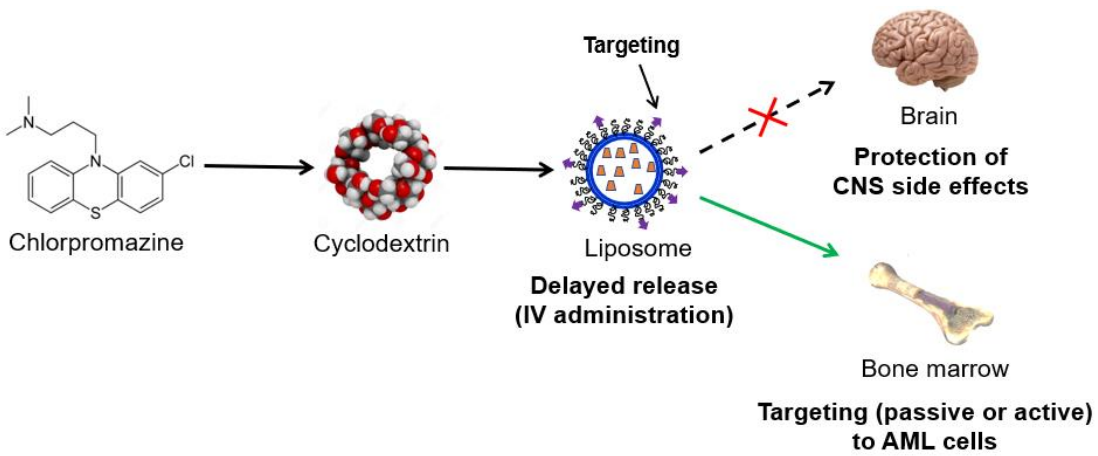

Fig. 26. CPZ-encapsulated DCL for treatment of AML

The DCL system is a sophisticated and complicated strategy, considering the three relatively independent and interrelated ingredients: CD, CPZ and phospholipids. Since any subtle change, ratio or type of component, has an effect on the physicochemical properties of liposomal formulations, it is critical to perform a comprehensive investigation in order to have an overall understanding of the interaction between CD/CPZ, CD/lipid and CPZ/lipid.

References

Al-Jamal, W. T., Al-Jamal, K. T., Bomans, P. H., Frederik, P. M., & Kostarelos, K. (2008). Functionalized-quantum-dot–liposome hybrids as multimodal nanoparticles for cancer. Small, 4(9), 1406-1415.

Al-Kali, Aref, Jorge Cortes, Stefan Faderl, Dan Jones, Caroline Abril, Sherry Pierce, Mark Brandt, Hagop Kantarjian, and Farhad Ravandi. 2011. "Patterns of Molecular Response to and Relapse after Combination of Sorafenib, Idarubicin, and Cytarabine in Patients with FLT3 Mutant Acute Myeloid Leukemia." Clinical Lymphoma, Myeloma and Leukemia 11 (4): 361–66.

Allen, Theresa M., and Pieter R. Cullis. 2013. "Liposomal Drug Delivery Systems: From Concept to Clinical Applications." Advanced Drug Delivery Reviews 65 (1): 36–48.

Anabousi, Samah, Udo Bakowsky, Marc Schneider, Hanno Huwer, Claus Michael Lehr, and Carsten Ehrhardt. 2006. "In Vitro Assessment of Transferrin-Conjugated Liposomes as Drug Delivery Systems for Inhalation Therapy of Lung Cancer." European Journal of Pharmaceutical Sciences 29 (5): 367–74.

Arber, D. A., Orazi, A., Hasserjian, R., Thiele, J., Borowitz, M. J., Le Beau, M. M., ... & Vardiman, J. W. (2016). The 2016 revision to the World Health Organization classification of myeloid neoplasms and acute leukemia. Blood, 127(20), 2391-2405.

Ashton, S., Song, Y. H., Nolan, J., Cadogan, E., Murray, J., Odedra, R., ... & Ellston, R. (2016). Aurora kinase inhibitor nanoparticles target tumors with favorable therapeutic index in vivo. Science Translational Medicine, 8(325), p325ra17.

Ban, T. A. (2007). Fifty years chlorpromazine: a historical perspective. Neuropsychiatric Disease and Treatment, 3(4), 495.

Bangham, A. D., M. M. Standish, and J. C. Watkins. 1965. "Diffusion of Univalent Ions across the Lamellae of Swollen Phospholipids." Journal of Molecular Biology 13 (1): 238-52.

Bangham, A. D., & Horne, R. W. (1964). Negative staining of phospholipids and their structural modification by surface-active agents as observed in the electron microscope. Journal of molecular biology, 8(5), 660-68.

Blume, G., Cevc, G., Crommelin, M. D. J. A., Bakker-Woudenberg, I. A. J. M., Kluft, C., & Storm, G. (1993). Specific targeting with poly (ethylene glycol)-modified liposomes: coupling of homing devices to the ends of the polymeric chains combines effective target binding with long circulation times. Biochimica et Biophysica Acta (BBA)-Biomembranes, 1149(1), 180-184.

Boksa, Jan, and Władysława A Daniel. 2010. "Main Contribution of the Cytochrome P450 Isoenzyme 1A2 (CYP1A2) to N-Demethylation and 5-Sulfoxidation of the Phenothiazine Neuroleptic Chlorpromazine in Human Liver — A Comparison with Other Phenothiazines" 80: 1252–59.

Bordoni, A, and E Zucca. 2007. "Epidemiology of Hematological Malignancies".

Epidemiology of Hematological Malignancies, 18 (Supplement 1): 3–8.

Borthakur, G., Kantarjian, H., Ravandi, F., Zhang, W., Konopleva, M., Wright, J. J., ... & Cortes, J. E. (2011). Phase I study of sorafenib in patients with refractory or relapsed acute leukemias. Haematologica, 96(1), 62-68.

Boyd-Kimball, Debra, Katelyn Gonczy, Benjamin Lewis, Thomas Mason, Nicole Siliko, and Jacob Wolfe. 2018. "Classics in Chemical Neuroscience: Chlorpromazine." Review-article. ACS Chemical Neuroscience 10 (Scheme 2): 79–88.

Bozzuto, Giuseppina. 2015. "Liposomes as Nanomedical Devices," 975–99.

Brewster, Marcus E., and Thorsteinn Loftsson. 2007. "Cyclodextrins as Pharmaceutical Solubilizers." Advanced Drug Delivery Reviews 59 (7): 645–66.

Briot, Thomas, Emilie Roger, Sylvain Thépot, and Frederic Lagarce. 2018. "Advances in Treatment Formulations for Acute Myeloid Leukemia." Drug Discovery Today 23 (12): 1936–49.

Cevc, G., and G. Blume. 1992. "Lipid Vesicles Penetrate into Intact Skin Owing to the Transdermal Osmotic Gradients and Hydration Force." BBA - Biomembranes 1104 (1): 226–32.

Cevc, Gregor, and Gabriele Blume. 2001. "New, Highly Efficient Formulation of Diclofenac for the Topical, Transdermal Administration in Ultradeformable Drug Carriers, Transfersomes." Biochimica et Biophysica Acta - Biomembranes 1514 (2): 191–205.

Chellam, Jaynthy, and Asit Baran Mandal. 2013. "Influence of Cyclodextrins on the Physical Properties of Collagen." International Journal of Pharma and Bio Sciences 4 (4): 795–806.

Chen, Hailiang, Jianqing Gao, Fei Wang, and Wenquan Liang. 2007. "Preparation, Characterization and Pharmacokinetics of Liposomes- Encapsulated Cyclodextrins Inclusion Complexes for Hydrophobic Drugs." Drug Delivery 14 (4): 201–8.

Chen, J., Lu, W. L., Gu, W., Lu, S. S., Chen, Z. P., Cai, B. C., & Yang, X. X. (2014). Drug-in-cyclodextrin-in-liposomes: a promising delivery system for hydrophobic drugs. Expert Opinion on Drug Delivery, 11(4), 565-577.

Chen, Yun, Yihang Pan, Yao Guo, Wanke Zhao, Wanting Tina Ho, Jianlong Wang, Mingjiang Xu, Feng-Chun Yang, and Zhizhuang Joe Zhao. 2017. "Tyrosine Kinase Inhibitors Targeting FLT3 in the Treatment of Acute Myeloid Leukemia." Stem Cell Investigation 4 (6): 48–48.

Cortes, J., Perl, A. E., Döhner, H., Kantarjian, H., Martinelli, G., Kovacsovics, T., ... & Strickland, S. (2018). Quizartinib, an FLT3 inhibitor, as monotherapy in patients with relapsed or refractory acute myeloid leukaemia: an open-label, multicentre, single-arm, phase 2 trial. The Lancet Oncology, 19(7), 889-903.

Dagan, A., Y. Barenholz, and Z. Fuks. 1982. "Liposomes as in Vivo Carriers of Adriamycin: Reduced Cardiac Uptake and Preserved Antitumor Activity in Mice." Cancer Research 42 (11): 4734–39.

Dams, E. T., Laverman, P., Oyen, W. J., Storm, G., Scherphof, G. L., Van der Meer, J. W., ... & Boerman, O. C. (2000). Accelerated blood clearance and altered biodistribution of repeated injections of sterically stabilized liposomes. Journal of Pharmacology and Experimental Therapeutics, 292(3), 1071-1079.

Darwhekar, Gajanan, Dinesh Kumar Jain, and Aashish Choudhary. 2012. "Elastic Liposomes for Delivery of Neomycin Sulphate in Deep Skin Infection." Asian Journal of Pharmaceutical Sciences 7 (4): 236–41.

Daver, N., Schlenk, R. F., Russell, N. H., & Levis, M. J. (2019). Targeting FLT3 mutations in AML: review of current knowledge and evidence. Leukemia, p1.

Davis, Mark E., and Marcus E. Brewster. 2004. "Cyclodextrin-Based Pharmaceutics: Past, Present and Future." Nature Reviews Drug Discovery 3 (12): 1023–35.

Davis, Mellar P, and Gretchen Hallerberg. 2010. "A Systematic Review of the Treatment of Nausea and / or Vomiting in Cancer Unrelated to Chemotherapy or Radiation." Journal of Pain and Symptom Management 39 (4): 756–67.

Desroches, Catherine M, and Sara J Rosenbaum. 2010. "Jectives of the Office of the National Coordinator for Health Information Technology . The Regional Extension Centers Funded by This Organization Should Play an Important Role in This Area ." Health (San Francisco), 2010–2010.

Dhule, Santosh S, Patrice Penfornis, Trivia Frazier, Ryan Walker, Joshua Feldman, Grace Tan, Jibao He, et al. 2016. "Curcumin-Loaded γ-Cyclodextrin Liposomal Nanoparticles as Delivery Vehicles for Osteosarcoma". Nanomedicine: Nanotechnology, Biology and Medicine, 8 (4): 440–51.

Eloy, Josimar O, Raquel Petrilli, Lucas Noboru, Fatori Trevizan, and Marlus Chorilli. 2017. "Immunoliposomes : A Review on Functionalization Strategies and Targets for Drug Delivery." Colloids and Surfaces B: Biointerfaces 159: 454–67.

F., Ravandi, Alattar M.L., Grunwald M.R., Rudek M.A., Rajkhowa T., Richie M.A., Pierce S., et al. 2014. "Phase 2 Study of Azacytidine plus Sorafenib in Patients with Acute Myeloid Leukemia and FLT-3 Internal Tandem Duplication Mutation." Blood 121 (23): 4655–62.

Floc'h, Nicolas, Susan Ashton, Paula Taylor, Dawn Trueman, Emily Harris, Rajesh Odedra, Kim Maratea, et al. 2017. "Optimizing Therapeutic Effect of Aurora B Inhibition in Acute Myeloid Leukemia with AZD2811 Nanoparticles." Molecular Cancer Therapeutics 16 (6): 1031–40.

Frank van de Manakker, Tina Vermonden, Cornelus F. van Nostrum, and Wim E. Hennink. 2009. "Cyclodextrin-Based Polymeric Materials: Synthesis, Properties, and Pharmaceutical/Biomedical Applications." FEBS Letters 170 (2): 343–49.

Fujiwara, Akiko, Tatsuo Hoshino, and John W. Westley. 2008. Anthracycline Antibiotics. Crit. Rev. Biotech. Vol. 3.

Gabizon, A, R Catane, B Uziely, B Kaufman, T Safra, R Cohen, F Martin, A Huang, and Y

Barenholz. 1994. “Prolonged Circulation Time and Enhanced Accumulation in Malignant Exudates of Doxorubicin Encapsulated in Polyethylene-Glycol Coated Liposomes.” Cancer Research 54: 987–92.

Gabizon, Alberto, Renee Shioia, and Demetrios Papahadjopoulos. 1989. “Pharmacokinetics and Tissue Distribution of Doxorubicin Encapsulated in Stable Liposomes With Long Circulation Times.” Journal of the National Cancer Institute, 81(19), 1484-1488.

Gharib, Riham, Hélène Greige-Gerges, Sophie Fourmentin, Catherine Charcosset, and Lizette Auezova. 2015. “Liposomes Incorporating Cyclodextrin-Drug Inclusion Complexes: Current State of Knowledge.” Carbohydrate Polymers 129: 175–86.

Godin, Biana, and Elka Touitou. 2003. “Ethosomes: New Prospects in Transdermal Delivery.” Critical Reviews in Therapeutic Drug Carrier Systems 20 (1): 63–102.

Gregoriadis, G., And Brenda E. Ryman. 1971. “Liposomes as Carriers of Enzymes or Drugs: A New Approach to the Treatment of Storage Diseases.” Proceedings of The Biochemical Society, 1971.

Hait, William N, Linda Grais, Constance Benz, and Ed C Cadman. 1985. “Inhibition of Growth of Leukemic Cells by Inhibitors of Calmodulin : Phenothiazines and Melittin I00 Mellitin,” 202–5.

Han, Hyo Kyung, Hyun Jae Shin, and Dong Hoon Ha. 2012. “Improved Oral Bioavailability of Alendronate via the Mucoadhesive Liposomal Delivery System.” European Journal of Pharmaceutical Sciences 46 (5): 500–507.

Hanato, Junko, Kazuki Kuriyama, Takahiro Mizumoto, Kazuhiro Debari, Junya Hatanaka, Satomi Onoue, and Shizuo Yamada. 2009. “Liposomal Formulations of Glucagon-like Peptide-1: Improved Bioavailability and Anti-Diabetic Effect.” International Journal of Pharmaceutics 382 (1–2): 111–16.

Hann, Ian M, and H Grant Prentice. 2001. “Lipid-Based Amphotericin B : A Review of the Last 10 Years of Use” International Journal of Antimicrobial Agents, 17(3), 161-169.

Helm, Frieder, and Gert Fricker. 2015. “Liposomal Conjugates for Drug Delivery to the Central Nervous System.” Pharmaceutics 7 (2): 27–42.

Hirayama, F., and K. Uekama. 1999. “Cyclodextrin-Based Controlled Drug Release System.” Advanced Drug Delivery Reviews 36 (1): 125–41.

Hua, S., & Wu, S. Y. (2013). The use of lipid-based nanocarriers for targeted pain therapies. Frontiers in Pharmacology, 4, 143.

Huang, Yi Y., and Ching H. Wang. 2006. “Pulmonary Delivery of Insulin by Liposomal Carriers.” Journal of Controlled Release 113 (1): 9–14.

Immordino, Dosio, and Cattel. 2006. “Stealth Liposomes: Review of the Basic Science, Rationale, and Clinical Applications, Existing and Potential,” International Journal of Nanomedicine, 1(3), 297.

Ishida, Tatsuhiro, and Hiroshi Kiwada. 2008. "Accelerated Blood Clearance (ABC) Phenomenon upon Repeated Injection of PEGylated Liposomes" International Journal of Pharmaceutics, 354(1-2), 56-62.

Ismail, Manal Fouad, Aliaa Nabil Elmeshad, and Neveen Abdel Hameed Salem. 2013. "Potential Therapeutic Effect of Nanobased Formulation of Rivastigmine on Rat Model of Alzheimer's Disease." International Journal of Nanomedicine 8: 393–406.

Jambhekar, Sunil S., and Philip Breen. 2016. "Cyclodextrins in Pharmaceutical Formulations I: Structure and Physicochemical Properties, Formation of Complexes, and Types of Complex." Drug Discovery Today 21 (2): 356–62.

James, Spencer L., Degu Abate, Kalkidan Hassen Abate, Solomon M. Abay, Cristiana Abbafati, Nooshin Abbasi, Hedayat Abbastabar, et al. 2018. "Global, Regional, and National Incidence, Prevalence, and Years Lived with Disability for 354 Diseases and Injuries for 195 Countries and Territories, 1990–2017: A Systematic Analysis for the Global Burden of Disease Study 2017." The Lancet 392 (10159): 1789–1858.

Jansook, Phatsawee, Noriko Ogawa, and Thorsteinn Loftsson. 2018. "Cyclodextrins: Structure, Physicochemical Properties and Pharmaceutical Applications." International Journal of Pharmaceutics 535 (1–2): 272–84.

Lancet, J.E., Cortes, J.E., Hogge, D.E., Tallman, M.S., Kovacsovics, T.J., Damon, L.E., Komrokji, R., Solomon, S.R., Kolitz, J.E., Cooper, M. and Yeager, A.M. 2014. "Phase 2 Trial of CPX-351, a Fixed 5: 1 Molar Ratio of Cytarabine/Daunorubicin, vs Cytarabine/Daunorubicin in Older Adults with Untreated AML." Blood 123 (21): 3239–46.

Jesorka, Aldo, and Owe Orwar. 2008. "Liposomes: Technologies and Analytical Applications." Annual Review of Analytical Chemistry 1 (1): 801–32.

Kadia, Tapan M., Stefan Faderl, Farhad Ravandi, Elias Jabbour, Guillermo Garcia-Manero, Gautam Borthakur, Alessandra Ferrajoli, et al. 2015. "Final Results of a Phase 2 Trial of Clofarabine and Low-Dose Cytarabine Alternating with Decitabine in Older Patients with Newly Diagnosed Acute Myeloid Leukemia." Cancer 121 (14): 2375–82. https://doi.org/10.1002/cncr.29367.

Kamiya, Mamoru, and Kaori Nakamura. 1995. "Cyclodextrin Inclusion Effects on Photodegradation Rates of Organophosphorus Pesticides." Environment International 21 (3): 299–304.

Khakbaz, Pouyan, and Jeffery B. Klauda. 2018. "Investigation of Phase Transitions of Saturated Phosphocholine Lipid Bilayers via Molecular Dynamics Simulations." Biochimica et Biophysica Acta - Biomembranes 1860 (8): 1489–1501.

Khaw, Ban-an, Jeffrey A Mattis, Gwen Melincoff, H William Strauss, Herman K Gold, And Edgar HabeR. 1984. "Monoclonal Antibody to Cardiac Myosin: Imaging of Experimental Myocardial Infarction." Hybridoma 3 (1): 11–23.

Kirby, Christopher, and Gregory Gregoriadis. 1984. "Dehydration-Rehydration Vesicles: A Simple Method for High Yield Drug Entrapment in Liposomes." Nature Biotechnology, 2(11),

979.

Kiss, T, F Fenyvesi, I Bácskay, J Váradi, É Fenyvesi, R Iványi, L Szente, Á Tósaki, and M Vecsernyés. 2010. "Evaluation of the Cytotoxicity of β-Cyclodextrin Derivatives: Evidence for the Role of Cholesterol Extraction." European Journal of Pharmaceutical Sciences 40: 376–80.

Klibanov, Alexander L., Kazuo Maruyama, Vladimir P. Torchilin, and Leaf Huang. 1990. "Amphipathic Polyethyleneglycols Effectively Prolong the Circulation Time of Liposomes." FEBS Letters 268 (1): 235–37.

Kohli, Aditya G., Paul H. Kierstead, Vincent J. Venditto, Colin L. Walsh1, and Francis C. Szoka. 2015. "Designer Lipids for Drug Delivery : From Heads to Tails," Journal of controlled release, 190, 274-287.

Kohlschütter, Johannes, Stefan Michelfelder, and Martin Trepel. 2008. "Drug Delivery in Acute Myeloid Leukemia." Expert Opinion on Drug Delivery 5 (6): 653–63.

Kouchkovsky, I. De, and M. Abdul-Hay. 2016. "'Acute Myeloid Leukemia: A Comprehensive Review and 2016 Update.'" Blood Cancer Journal 6 (7).

Koynova, R, and B Tenchov. 2013. "Transitions between Lamellar and Nonlamellar Phases in Membrane Lipids and Their Physiological Roles." OA Biochemistry 1 (1): 1–9.

Kulkarni, Chandrashekhar V. 2012. "Lipid Crystallization: From Self-Assembly to Hierarchical and Biological Ordering." Nanoscale 4 (19): 5779–91.

Kurkov, Sergey V., and Thorsteinn Loftsson. 2013. "Cyclodextrins." International Journal of Pharmaceutics 453 (1): 167–80.

Lancet, Jeffrey E, Geoffrey L Uy, Jorge E Cortes, Laura F Newell, Tara L Lin, Ellen K Ritchie, Robert K Stuart, Stephen Anthony Strickland, Donna Hogge, and Scott R Solomon. 2016. "Final Results of a Phase III Randomized Trial of CPX-351 versus 7+ 3 in Older Patients with Newly Diagnosed High Risk (Secondary) AML." American Society of Clinical Oncology.

Lapenda, T. L.S., W. A. Morais, F. J.F. Almeida, M. S. Ferraz, M. C.B. Lira, N. P.S. Santos, M. A.M. MacIel, and N. S. Santos-Magalhães. 2013. "Encapsulation of Trans-Dehydrocrotonin in Liposomes: An Enhancement of the Antitumor Activity." Journal of Biomedical Nanotechnology 9 (3): 499–510.

Li, Jing, Xuling Wang, Ting Zhang, Chunling Wang, Zhenjun Huang, Xiang Luo, and Yihui Deng. 2014. "A Review on Phospholipids and Their Main Applications in Drug Delivery Systems." Asian Journal of Pharmaceutical Sciences 10 (2): 81–98.

Li, Shihong, Beth Goins, Lujun Zhang, and Ande Bao. 2012. "Novel Multifunctional Theranostic Liposome Drug Delivery System: Construction, Characterization, and Multimodality MR, near-Infrared Fluorescent, and Nuclear Imaging." Bioconjugate Chemistry 23 (6): 1322–32.

Loftsson, T., Jarho, P., Masson, M., & Järvinen, T. (2005). Cyclodextrins in drug delivery. Expert Opinion on Drug Delivery, 2(2), 335-351.

Maeda, H., Sawa, T., & Konno, T. (2001). Mechanism of tumor-targeted delivery of macromolecular drugs, including the EPR effect in solid tumor and clinical overview of the prototype polymeric drug SMANCS. Journal of controlled release, 74(1-3), 47-61.

Maestrelli, Francesca, Maria Luísa González-Rodríguez, Antonio Maria Rabasco, and Paola Mura. 2005. "Preparation and Characterisation of Liposomes Encapsulating Ketoprofen-Cyclodextrin Complexes for Transdermal Drug Delivery." International Journal of Pharmaceutics 298 (1): 55–67.

McCormack, Brenda, and Gregory Gregoriadis. 1994. "Drugs-in-Cyclodextrins-in Liposomes: A Novel Concept in Drug Delivery" International Journal of Pharmaceutics, 112(3), 249-258.112: 249–58.

Medina, Zhu, and Kairemo. 2004. "Targeted Liposomal Drug Delivery in Cancer." Current Pharmaceutical Design 10 (24): 2981–89.

Mello, Joyce C De, Vivian Wr, Carolina M Watashi, C Deyse, Leide P Cavalcanti, Margareth Kkd, Fabiano Yokaichiya, and Daniele R De Araujo. 2016. "Enhancement of Chlorpromazine Antitumor Activity by Pluronics F127 / L81 Nanostructured System against Human Multidrug Resistant Leukemia." Pharmacological Research 111: 102–12.

Mielcarek, Jadwiga. 1997. "Photochemical Stability of the Inclusion Complexes Formed by Modified 1 , 4-Dihydropyridine Derivatives with Fl-Cyclodextrin 1." Journal of Pharmaceutical and Biomedical Analysis 15: 681–86.

Mielcarek, Jadwiga, and Ewa Daczkowska. 1999. "Photodegradation of Inclusion Complexes of Isradipine with Methyl-β- Cyclodextrin." Journal of Pharmaceutical and Biomedical Analysis 21 (2): 393–98.

Minato, Seiichiro, Kazunori Iwanaga, Masawo Kakemi, Shinji Yamashita, and Naoto Oku. 2003. "Application of Polyethyleneglycol (PEG)-Modified Liposomes for Oral Vaccine: Effect of Lipid Dose on Systemic and Mucosal Immunity." Journal of Controlled Release 89 (2): 189–97.

Misra, Ambikanandan, Kaustubh Jinturkar, Deepa Patel, Jigar Lalani, and Mahavir Chougule. 2009. "Recent Advances in Liposomal Dry Powder Formulations: Preparation and Evaluation." Expert Opinion on Drug Delivery 6 (1): 71–89.

Moghimi, S. M., and J. Szebeni. 2003. "Stealth Liposomes and Long Circulating Nanoparticles: Critical Issues in Pharmacokinetics, Opsonization and Protein-Binding Properties." Progress in Lipid Research 42 (6): 463–78.

Mugabe, Clement, Ali O. Azghani, and Abdelwahab Omri. 2006. "Preparation and Characterization of Dehydration-Rehydration Vesicles Loaded with Aminoglycoside and Macrolide Antibiotics." International Journal of Pharmaceutics 307 (2): 244–50.

Murphy, Tracy, and Karen W.L. Yee. 2017. "Cytarabine and Daunorubicin for the Treatment of Acute Myeloid Leukemia." Expert Opinion on Pharmacotherapy 18 (16): 1765–80.

Myhren, Lene, Ida Mostrøm Nilssen, Valérie Nicolas, Stein Ove Døskeland, Gillian Barratt,

and Lars Herfindal. 2014. “Efficacy of Multi-Functional Liposomes Containing Daunorubicin and Emetine for Treatment of Acute Myeloid Leukaemia.” European Journal of Pharmaceutics and Biopharmaceutics 88 (1): 186–93.

Naguib, Mohamed. 2007. “Sugammadex: Another Milestone in Clinical Neuromuscular Pharmacology.” Anesthesia and Analgesia 104 (3): 575–81.

Nazha, Aziz, Hagop Kantarjian, Farhad Ravandi, Xuelin Huang, Sangbum Choi, Guillermo Garcia-Manero, Elias Jabbour, et al. 2013. “Clofarabine, Idarubicin, and Cytarabine (CIA) as Frontline Therapy for Patients ≤60 Years with Newly Diagnosed Acute Myeloid Leukemia.” American Journal of Hematology 88 (11): 961–66.

Neupane, Shova, Yana De Smet, Frank U. Renner, and Patricia Losada-Pérez. 2018. “Quartz Crystal Microbalance With Dissipation Monitoring: A Versatile Tool to Monitor Phase Transitions in Biomimetic Membranes.” Frontiers in Materials 5 (August): 1–8.

Nguyen, T. X., Huang, L., Gauthier, M., Yang, G., & Wang, Q. (2016). Recent advances in liposome surface modification for oral drug delivery. Nanomedicine, 11(9), 1169-1185.

Nguyen, Thanh Xuan, Lin Huang, Mario Gauthier, Guang Yang, and Qun Wang. 2016. “Recent Advances in Liposome Surface Modification for Oral Drug Delivery.” Nanomedicine 11 (9): 1169–85.

Nichols, J. Wylie, and David W. Deamer. 1976. “Catecholamine Uptake and Concentration by Liposomes Maintaining PH Gradients.” BBA - Biomembranes 455 (1): 269–71.

Niederwieser, Dietger, and Michael W N Deininger. 2002. “To the Editor :” 100 (3): 1092–93.

Nogueira, Eugénia, Andreia C Gomes, Ana Preto, and Artur Cavaco-paulo. 2015. “Design of Liposomal Formulations for Cell Targeting” Colloids and Surfaces B: Biointerfaces, 136, 514-526.

Eloy, J. O., de Souza, M. C., Petrilli, R., Barcellos, J. P. A., Lee, R. J., & Marchetti, J. M. (2014). Liposomes as carriers of hydrophilic small molecule drugs: strategies to enhance encapsulation and delivery. Colloids and surfaces B: Biointerfaces, 123, 345-363.

Olusanya, Temidayo O.B., Rita Rushdi Haj Ahmad, Daniel M. Ibegbu, James R. Smith, and Amal Ali Elkordy. 2018. “Liposomal Drug Delivery Systems and Anticancer Drugs.” Molecules 23 (4): 1–17.

Palazzo, Claudio, Julie Laloy, Anne-sophie Delvigne, Gwenael Nys, Marianne Fillet, Jean-michel Dogne, Christel Pequeux, Jean-michel Foidart, Brigitte Evrard, and Geraldine Piel. 2019. “European Journal of Pharmaceutical Sciences Development of Injectable Liposomes and Drug-in-Cyclodextrin-in-Liposome Formulations Encapsulating Estetrol to Prevent Cerebral Ischemia of Premature Babies.” European Journal of Pharmaceutical Sciences 127 (June 2018): 52–59.

Pardridge, W. M. (2003). Blood-brain barrier drug targeting: the future of brain drug development. Molecular interventions, 3(2), 90.

Parka, John W, Keelung Hongb, Dmitri B Kirpotinb, Olivier Meye, Demetrios

Papahadjopoulosb, and Christopher C Benza. 1997. “Cancer” 118: 153–60.

Pattni, Bhushan S., Vladimir V. Chupin, and Vladimir P. Torchilin. 2015. “New Developments in Liposomal Drug Delivery.” Chemical Reviews 115 (19): 10938–66.

Peer, Dan, Jeffrey M Karp, Seungpyo Hong, Omid C Farokhzad, Rimona Margalit, and Robert Langer. 2007. “Nanocarriers as an Emerging Platform for Cancer Therapy,” Nature nanotechnology, 2(12), 751.

Phillips, G L, D E Reece, J D Shepherd, M J Barnett, R A Brown, D A Frei-Lahr, H G Klingemann, B J Bolwell, J J Spinelli, and R H Herzig. 1991. “High-Dose Cytarabine and Daunorubicin Induction and Postremission Chemotherapy for the Treatment of Acute Myelogenous Leukemia in Adults.” Blood 77 (7): 1429–35.

Piel, G., M. Piette, V. Barillaro, D. Castagne, B. Evrard, and L. Delattre. 2007. “Study of the Relationship between Lipid Binding Properties of Cyclodextrins and Their Effect on the Integrity of Liposomes.” International Journal of Pharmaceutics 338 (1–2): 35–42.

Piel, Géraldine, Marie Piette, Valery Barillaro, Delphine Castagne, Brigitte Evrard, and Luc Delattre. 2006. “Betamethasone-in-Cyclodextrin-in-Liposome: The Effect of Cyclodextrins on Encapsulation Efficiency and Release Kinetics.” International Journal of Pharmaceutics 312 (1–2): 75–82.

Pignatello, R, T Musumeci, L Basile, C Carbone, and G Puglisi. 2011. “Biomembrane Models and Drug-Biomembrane Interaction Studies: Involvement in Drug Design and Development.” Journal of Pharmacy and Bioallied Sciences 3 (1): 4.

Pluta, K., Morak-Młodawska, B., & Jeleń, M. (2011). Recent progress in biological activities of synthesized phenothiazines. European journal of medicinal chemistry, 46(8), 3179-3189.

Pomponio, R., R. Gotti, J. Fiori, V. Cavrini, P. Mura, M. Cirri, and F. Maestrelli. 2004. “Photostability Studies on Nicardipine-Cyclodextrin Complexes by Capillary Electrophoresis.” Journal of Pharmaceutical and Biomedical Analysis 35 (2): 267–75.

Poovaiah, Nitya, Zahra Davoudi, Haisheng Peng, Benjamin Schlichtmann, Surya K Mallapragada, Balaji Narasimhan, and Qun Wang. 2018. “Treatment of Neurodegenerative Disorders through the Blood-Brain Barrier Using Nanocarriers.” Nanoscale, 10(36), 16962-16983.

Portnoy, Emma, Shimon Lecht, Philip Lazarovici, Dganit Danino, and Shlomo Magdassi. 2011. “Cetuximab-Labeled Liposomes Containing near-Infrared Probe for in Vivo Imaging.” Nanomedicine: Nanotechnology, Biology, and Medicine 7 (4): 480–88.

Pupo, Elder, Amalis Padrón, Enrique Santana, Jorge Sotolongo, Diógenes Quintana, Santiago Dueñas, Carlos Duarte, Maria C. De La Rosa, and Eugenio Hardy. 2005. “Preparation of Plasmid DNA-Containing Liposomes Using a High-Pressure Homogenization-Extrusion Technique.” Journal of Controlled Release 104 (2): 379–96.

Qi, Z Helena, and Christopher T Sikorski. 1999. “Controlled Delivery Using Cyclodextrin Technology.” Intelligent Materials for Controlled Release 728: 113–30.

Ramos-Cabrer, Pedro, and Francisco Campos. 2012. "Liposomes and Nanotechnology in Drug Development : Focus on Oncotargets," International journal of nanomedicine, 8, 951.

Randhawa, Jasleen K, Hagop M Kantarjian, Gautam Borthakur, Philip Alastair Thompson, Maria Konopleva, Naval Daver, Naveen Pemmaraju, Elias Jabbour, Tapan M Kadia, and Zeev Estrov. 2014. "Results of a Phase II Study of Crenolanib in Relapsed/Refractory Acute Myeloid Leukemia Patients (Pts) with Activating FLT3 Mutations." Am Soc Hematology.

Riaz, Muhammad Kashif, Muhammad Adil Riaz, Xue Zhang, Congcong Lin, Ka Hong Wong, Xiaoyu Chen, Ge Zhang, Aiping Lu, and Zhijun Yang. 2018. "Surface Functionalization and Targeting Strategies of Liposomes in Solid Tumor Therapy: A Review." International Journal of Molecular Sciences 19 (1).

Beckett, A. H., Beaven, M. A., & Robinson, A. E. (1963). Metabolism of chlorpromazine in humans. Biochemical Pharmacology, 12(8), 779-794.

Rodriguez-Nogales, José Manuel, Manuel Pérez-Mateos, and Ma Dolores Busto. 2004. "Application of Experimental Design to the Formulation of Glucose Oxidase Encapsulation by Liposomes." Journal of Chemical Technology and Biotechnology 79 (7): 700–705.

Romberg, Birgit, Christien Oussoren, Cor J Snel, Myrra G Carstens, Wim E Hennink, and Gert Storm. 2007. "Pharmacokinetics of Poly (Hydroxyethyl- L -Asparagine) -Coated Liposomes Is Superior over That of PEG-Coated Liposomes at Low Lipid Dose and upon Repeated Administration" Biochimica et Biophysica Acta (BBA)-Biomembranes, 1768(3), 737-743.

Sakagami, H, H Takahashi, H Yoshida, M Yamamura, K Fukuchi, K Gomi, N Motohashi, and M Takeda. 1995. "Induction of DNA Fragmentation in Human Myelogenous Leukaemic Cell Lines by Phenothiazine-Related Compounds." Anticancer Research 15 (6B): 2533–40.

Sala, M., R. Diab, A. Elaissari, and H. Fessi. 2018. "Lipid Nanocarriers as Skin Drug Delivery Systems: Properties, Mechanisms of Skin Interactions and Medical Applications." International Journal of Pharmaceutics 535 (1–2): 1–17.

Salvati, Elisa, Francesca Re, Silvia Sesana, Ilaria Cambianica, Giulio Sancini, Massimo Masserini, and Maria Gregori. 2013. "Liposomes Functionalized to Overcome the Blood-Brain Barrier and to Target Amyloid-β Peptide: The Chemical Design Affects the Permeability across an in Vitro Model." International Journal of Nanomedicine 8: 1749–58.

Sapra, P., and T. M. Allen. 2003. "Ligand-Targeted Liposomal Anticancer Drugs." Progress in Lipid Research 42 (5): 439–62.

Semenova, Ekaterina M, Alan Cooper, Clive G Wilson, and A Carolyn. 2003. "Stabilization of All- Trans -Retinol by Cyclodextrins : A Comparative Study Using HPLC and Fluorescence Spectroscopy," Journal of inclusion phenomena and macrocyclic chemistry, 44(1-4), 155-158.

Senior, J H. 1987. "Fate and Behavior of Liposomes in Vivo: A Review of Controlling Factors." Critical Reviews in Therapeutic Drug Carrier Systems 3 (2): 123–93.

Senior, Judith, and Gregory Gregoriadis. 1982. "Is Half-Life of Circulating Liposomes Determined by Changes in Their Permeability?" FEBS Letters 145 (1): 109–14.

Sercombe, Lisa, Tejaswi Veerati, Fatemeh Moheimani, Sherry Y. Wu, Anil K. Sood, and Susan Hua. 2015. "Advances and Challenges of Liposome Assisted Drug Delivery." Frontiers in Pharmacology 6 (DEC): 1–13.

Serve, Hubert, Uta Brunnberg, Oliver Ottmann, Christian Brandts, Björn Steffen, Utz Krug, Ruth Wagner, et al. 2013. "Sorafenib in Combination with Intensive Chemotherapy in Elderly Patients with Acute Myeloid Leukemia: Results from a Randomized, Placebo-Controlled Trial." Journal of Clinical Oncology 31 (25): 3110–18.

Sessa, Grazia, and Gerald Weissmann. 1968. "Phospholipid Spherules (Liposomes) as a Model for Biological Membranes" Journal of lipid research, 9(3), 310-318..

Shaker, Sherif, Ahmed Gardouh, and Mamdouh Ghorab. 2017. "Factors Affecting Liposomes Particle Size Prepared by Ethanol Injection Method." Research in Pharmaceutical Sciences 12 (5): 346–52.

Sharma, Loretta, and Ajit Sharma. 2001. "Influence of Cyclodextrin Ring Substituents on Folding-Related Aggregation of Bovine Carbonic Anhydrase." European Journal of Biochemistry 268 (8): 2456–63.

Short, Nicholas J., Michael E. Rytting, and Jorge E. Cortes. 2018. "Acute Myeloid Leukaemia." The Lancet 392 (10147): 593–606.

Skalko. 1996. "Liposomes with Nifedipine and Nifedipine-Cyclodextrin Complex: Calorimetrical and Plasma Stability Comparison" European journal of pharmaceutical sciences, 4(6), 359-366.

Stone, Richard M., Sumithra J. Mandrekar, Ben L. Sanford, Kristina Laumann, Susan Geyer, Clara D. Bloomfield, Christian Thiede, et al. 2017. "Midostaurin plus Chemotherapy for Acute Myeloid Leukemia with a FLT3 Mutation." New England Journal of Medicine 377 (5): 454–64.

Strati, Paolo, Hagop Kantarjian, Farhad Ravandi, Aziz Nazha, Gautam Borthakur, Naval Daver, Tapan Kadia, et al. 2015. "Phase I/II Trial of the Combination of Midostaurin (PKC412) and 5-Azacytidine for Patients with Acute Myeloid Leukemia and Myelodysplastic Syndrome." American Journal of Hematology 90 (4): 276–81.

Sung, Jean C., Brian L. Pulliam, and David A. Edwards. 2007. "Nanoparticles for Drug Delivery to the Lungs." Trends in Biotechnology 25 (12): 563–70.

Sur, Surojit, Anja C. Fries, Kenneth W. Kinzler, Shibin Zhou, and Bert Vogelstein. 2014. "Remote Loading of Preencapsulated Drugs into Stealth Liposomes." Proceedings of the National Academy of Sciences 111 (6): 2283–88.

Szente, Lajos, and Jozsef Szejtli. 1999. "Highly Soluble Cyclodextrin Derivatives: Chemistry, Properties, and Trends in Development." Cancer 54 (7): 1461–65.

Tagami, Tatsuaki, Warren D Foltz, Mark J Ernsting, Carol M Lee, Ian F Tannock, Jonathan P May, and Shyh-dar Li. 2011. "Biomaterials MRI Monitoring of Intratumoral Drug Delivery and Prediction of the Therapeutic Effect with a Multifunctional Thermosensitive Liposome."

Biomaterials 32 (27): 6570–78.

Tahara, Kohei, Hiromasa Tomida, Yousuke Ito, Suguru Tachikawa, Risako Onodera, Hiroyuki Tanaka, Yuichi Tozuka, and Hirofumi Takeuchi. 2016. “Pulmonary Liposomal Formulations Encapsulated Procaterol Hydrochloride by a Remote Loading Method Achieve Sustained Release and Extended Pharmacological Effects.” International Journal of Pharmaceutics 505 (1–2): 139–46.

Tan, Kuan Boone, Leong Uung Ling, Ralph M. Bunte, Wee Joo Chng, and Gigi N C Chiu. 2012. “In Vivo Efficacy of a Novel Liposomal Formulation of Safingol in the Treatment of Acute Myeloid Leukemia.” Journal of Controlled Release 160 (2): 290–98.

Torchilin, V. P., Klibanov, A. L., Huang, L., O'Donnell, S., Nossiff, N. D., & Khaw, B. A. (1992). Targeted accumulation of polyethylene glycol-coated immunoliposomes in infarcted rabbit myocardium. The FASEB journal, 6(9), 2716-2719.

Torchilin, V P, A L Klibanov, L Huang, S O’Donnell, N D Nossiff, and B A Khaw. 1992. “Targeted Accumulation of Polyethylene Glycol-Coated Immunoliposomes in Infarcted Rabbit Myocardium.” The FASEB Journal 6 (9): 2716–19.

Torchilin, V. P. (2005). Recent advances with liposomes as pharmaceutical carriers. Nature Reviews Drug Discovery, 4(2), 145.

Torchilin, V. P. (2005). Recent advances with liposomes as pharmaceutical carriers. Nature Reviews Drug Discovery, 4(2), 145.

Ulrich, Anne S. 2002. “Biophysical Aspects of Using Liposomes as Delivery Vehicles.” Bioscience Reports 22 (2): 129–50.

Del Valle, E. M. (2004). Cyclodextrins and their uses: a review. Process biochemistry, 39(9), 1033-1046.

Vieira, Débora B., and Lionel F. Gamarra. 2016. “Getting into the Brain: Liposome-Based Strategies for Effective Drug Delivery across the Blood–Brain Barrier.” International Journal of Nanomedicine 11: 5381–5414.

Villiers, A. 1891. “Sur La Fermentation de La Fécule Par l’action Du Ferment Butyrique.” Compt. Rend. Acad. Sci 112: 536–38.

Vyas, S. P., M. E. Kannan, Sanyog Jain, V. Mishra, and Paramjit Singh. 2004. “Design of Liposomal Aerosols for Improved Delivery of Rifampicin to Alveolar Macrophages.” International Journal of Pharmaceutics 269 (1): 37–49.

Wang, Eunice S, Richard M Stone, Martin S Tallman, Roland B Walter, John R Eckardt, and Robert Collins. 2016. “Crenolanib, a Type I FLT3 TKI, Can Be Safely Combined with Cytarabine and Anthracycline Induction Chemotherapy and Results in High Response Rates in Patients with Newly Diagnosed FLT3 Mutant Acute Myeloid Leukemia (AML).” Blood, 128 (22): 1071.

Wang, Yanfeng, Ophelia Q.P. Yin, Peter Graf, James C. Kisicki, Horst Schran, Green, and Kane. 2008. “Dose- and Time-Dependent Pharmacokinetics of Midostaurin in Patients with

Diabetes Mellitus." Journal of Clinical Pharmacology 48 (6): 763–75.

Wong, Chun Y., Hani Al-Salami, and Crispin R. Dass. 2018. "Recent Advancements in Oral Administration of Insulin-Loaded Liposomal Drug Delivery Systems for Diabetes Mellitus." International Journal of Pharmaceutics 549 (1–2): 201–17.

Xiang, Y., Qian Wu, Liang Liang, Xueqing Wang, Jiancheng Wang, Xuan Zhang, Xiaoping Pu, and Qiang Zhang. 2012. "Chlorotoxin-Modified Stealth Liposomes Encapsulating Levodopa for the Targeting Delivery against the Parkinson's Disease in the MPTP-Induced Mice Model." Journal of Drug Targeting 20 (1): 67–75.

Xing, H., Hwang, K., & Lu, Y. (2016). Recent developments of liposomes as nanocarriers for theranostic applications. Theranostics, 6(9), 1336.

Yakavets, Ilya, Henri-Pierre Lassalle, Dietrich Scheglmann, Arno Wiehe, Vladimir Zorin, and Lina Bezdetnaya. 2018. "Temoporfin-in-Cyclodextrin-in-Liposome—A New Approach for Anticancer Drug Delivery: The Optimization of Composition." Nanomaterials 8 (10): 847.

Yingchoncharoen, P., D. S. Kalinowski, and D. R. Richardson. 2016. "Lipid-Based Drug Delivery Systems in Cancer Therapy: What Is Available and What Is Yet to Come." Pharmacological Reviews 68 (3): 701–87.

Zalba, Sara, Ana M Contreras, Azadeh Haeri, L M Timo, Iñigo Navarro, Gerben Koning, and María J Garrido. 2015. "Cetuximab-Oxaliplatin-Liposomes for Epidermal Growth Factor Receptor Targeted Chemotherapy of Colorectal Cancer." Journal of Controlled Release 210: 26–38.

Zamboni, William C, Æ Anne C Gervais, Merrill J Egorin, Æ Jan H M Schellens, Elleanor G Zuhowski, Æ Dick Pluim, Æ Erin Joseph, et al. 2004. "Systemic and Tumor Disposition of Platinum after Administration of Cisplatin or STEALTH Liposomal-Cisplatin Formulations (SPI-077 and SPI-077 B103) in a Preclinical Tumor Model of Melanoma," Cancer chemotherapy and pharmacology, 53(4), 329-336.

Zhang, Lin, Shuli Wang, Manhong Zhang, and Jie Sun. 2013. "Nanocarriers for Oral Drug Delivery." Journal of Drug Targeting 21 (6): 515–27.

Zhang, and Peter X. Ma. 2013. "Cyclodextrin-Based Supramolecular Systems for Drug Delivery: Recent Progress and Future Perspective." Advanced Drug Delivery Reviews 65 (9): 1215–33.

Zhang, Yue, Meifang Zhai, Zhijiang Chen, Xiaoyang Han, Fanglin Yu, Zhiping Li, Xiangyang Xie, et al. 2017. "Dual-Modified Liposome Codelivery of Doxorubicin and Vincristine Improve Targeting and Therapeutic Efficacy of Glioma." Drug Delivery 24 (1): 1045–55.

Zylberberg, Claudia, and Sandro Matosevic. 2016. "Pharmaceutical Liposomal Drug Delivery: A Review of New Delivery Systems and a Look at the Regulatory Landscape." Drug Delivery 23 (9): 3319–29.

Chapter 2

Cyclodextrin complexation as a tool to allow repurposing of chlorpromazine

Cyclodextrin complexation as a tool to allow repurposing of chlorpromazine

Zhiqiang Wang,[a] David Landy,[b] Christina Sizun,[c] Christine Cézard,[d] Rosa Calderón Jacinto,[a] Cédric Przybylski,[e] Luc de Chaisemartin,[fg] Lars Herfindal,[h] Gillian Barratt,[a] and François-Xavier Legrand*[a]

2.1 Introduction

Acute myeloid leukemia (AML) is an aggressive leukemia that usually results in death after two months if untreated and even when treatment is successful, the relapse rate is high. In particular, leukemic stem cells in the bone marrow appear to survive chemotherapy. In younger patients, the outcome can be improved by allogenic bone marrow transfer, but this option is not available for older patients who, furthermore, tolerate intensive chemotherapy poorly. Therefore, there is a need to find new drugs to add to the current arsenal, which is headed by a combination of cytarabine and daunorubicin (Juliusson et al. 2009)(Döhner et al. 2010)(Lichtman 2013).

A recent development in cancer chemotherapy is “re-purposing” – the application of molecules already in use for other pathologies to cancer. An example of this is the observation that phenothiazines, a class of drugs active on the central nervous system, have anti-proliferative and pro-apoptopic effects in leukemia cells lines (Zhelev et al. 2004). This phenomenon may be mediated in part by an effect on mitochondrial

[a.] Institut Galien Paris-Sud, CNRS UMR 8612, Univ. Paris-Sud, Universite Paris-Saclay, 92290 Chatenay-Malabry, France.

[b.] Unité de Chimie Environnementale et Interactions sur le Vivant (UCEIV, EA 4492), SFR Condorcet FR CNRS 3417, Université du Littoral Côte d'Opale, 59140 Dunkerque, France.

[c.] Institut de Chimie des Substances Naturelles, CNRS UPR 2301, Université Paris Saclay, 91190 Gif-sur-Yvette, France.

[d.] Laboratoire de Glycochimie, des Antimicrobiens et des Agroressources, CNRS UMR 7378, Université de Picardie Jules Verne, 80000 Amiens, France.

[e.] Institut Parisien de Chimie Moléculaire, CNRS UMR 8232, Sorbonne Université, 75005 Paris, France.

[f.] Service d'Immuno-hématologie, Hôpital Bichat-Claude-Bernard, Assistance Publique-Hôpitaux de Paris, 75018 Paris, France.

[g.] Unité « Inflammation, Chimiokines et Immunopathologie », INSERM UMR 996, Univ. Paris-Sud, Universite Paris-Saclay, 92290 Chatenay-Malabry, France.

[h.] Department of Clinical Science, University of Bergen, Jonas Lies Vei 87, 5009 Bergen, Norway.

membranes, since the ATP content of the cells was observed to be reduced. Inhibition of calmodulin and protein kinases, as well as the P-glycoprotein involved in multi-drug resistance, have also been implicated (Jaszczyszyn et al. 2012). One molecule from this series, chlorpromazine (CPZ), was found as early as 1998 to inhibit vincristine transport in multi-drug resistant leukemia cells (Syed et al. 1998), again suggesting a membrane-associated mechanism. CPZ and other phenothiazines are photosensitive and the thiazine dyes methylene blue and toluidine blue can be used for photodynamic therapy of tumors (O'Connor et al. 2009).

More recently, Rai et al (Rai et al. 2014) observed that CPZ inhibited the growth of human AML cell lines in vitro and in mouse xenografts in vivo. While recent studies have been directed towards developing new phenothiazine derivatives with increased activity against leukemia (Brem et al. 2017), a true repurposing strategy would use a molecule already in clinical use, such as CPZ. However, to avoid undesirable side-effects in the central nervous system, it is necessary to control the distribution of the drug to prevent its passage across the blood-brain barrier and allow its accumulation in the bone marrow that harbors the AML cells. Therefore, in this work, we have investigated the possibility of associating CPZ with cyclodextrins (CD) to modify its biodistribution to render it suitable for use in AML.

CDs are cyclic oligomers of 6, 7 or 8 glucose units (α, β and γCD respectively), providing a central cavity that can accommodate hydrophobic guest molecules. A wide range of pharmaceutical molecules have been formulated as inclusion complexes in order to increase their apparent solubility in aqueous media, improve their bioavailability and stability and reduce their toxicity. Several studies have focussed on the interactions of CDs with the blood-brain barrier in terms of toxicity and their ability to modulate the activity of pharmacological agents. The cytotoxicity of a range of CDs was studied on an in-vitro co-culture model (Monnaert et al. 2004). Based on the passage of sucrose through the barrier, native CDs (α, β and γ) were the most toxic and in general, substitution reduced toxicity. The effect of CDs on membrane integrity has been linked to their ability to extract lipids from the bilayer. In particular, β-CD is able

to complex and remove cholesterol from the membrane. The permeability of CD across a brain endothelial cell monolayer has also been investigated. β-CD showed the highest passage, but this was reduced by methylation or hydroxypropylation (Monnaert et al, 2004). However, the permeability constants were much lower than those for small molecules. Numerous studies, reviewed in (Vecsernyés et al. 2014), have examined the influence of cyclodextrin on the passage and activity of drug molecules in the brain. In general, CDs can improve the efficacy of the drug without added toxicity. Interestingly, this is not necessarily correlated with the presence of a drug in the CD, since a therapeutic effect of hydroxypropyl-β-CD was observed in Niemann-Pick type C1 disease, due to its ability to redistribute cholesterol (Calias 2017).

Some studies of the complexation of CPZ with CDs have already been performed. Most of these studies employed β-CD, sometimes modified with hydrophobic chains, and was observed that these complexes have 1:1 stoichiometry. Complexation with CD resulted in a decrease in the haemolytic and photosensitizing side effects of CPZ, without changing its activity in the central nervous system (Uekama et al. 1981)(Irie et al.1985)(Hoshino et al. 1989).

Therefore, in this work, we have undertaken a systematic study of the inclusion of CPZ in a range of CDs, focussing on native CDs and derivatives that are already authorized for pharmaceutical applications. We have used physico-chemical techniques, and in particular isothermal titration calorimetry (ITC) to thoroughly characterize the nature of the complexes formed with each CD. This information will be essential for designing formulations using CD to control the distribution and biological activity of CPZ.

2.2 Materials and methods

2.1.1 Materials

HP-β-CD (Cavasol® W7HP Pharma) and HP-γ-CD (Cavasol® W8HP Pharma) were gifts from Ashland Global Specialty Chemicals Inc. SBE-β-CD (Captisol®), SBE-

γ-CD and SBE-Et-β-CD were gifts from Ligand Pharmaceuticals Inc. Sugammadex (Bridion®) was kindly provided Dr. Luc de Chaisemartin from Bichat Hospital. Chlorpromazine hydrochloride, sodium chloride and HEPES were purchased from Sigma-Aldrich. Milli-Q water was obtained by a Millipore® purification system (Millipore, Germany).

2.1.2 Methods

2.1.2.1 ITC studies

Formation constants and inclusion enthalpies were determined simultaneously for each CD/CPZ system using an isothermal calorimeter (ITC_{200}, MicroCal Inc., USA). CPZ and CD solutions were prepared in phosphate buffer solution (pH 7.0). The sample cell and syringe were filled with a 0.4 mM degassed CPZ solution (V_0 = 202.8 μL) and a 4 mM CD solution (40 μL), respectively. After addition of an initial aliquot of 0.2 μL, 10 aliquots of 3.7 μL of the syringe solution were delivered over 7 s for each injection. This number of ten injections was chosen according to Tellinghuisen's recommendation (Tellinghuisen 2005). The time interval between two consecutive injections was 90 s, which proved to be sufficient for a systematic and complete return to baseline. The agitation speed was set to 1000 rpm. The resulting heat flow was recorded as a function of time. All measurements were performed in triplicate. Prior to data analysis, blank titrations were carried out under the same experimental conditions by injecting individual species into buffer, and/or buffer into species and buffer into buffer in order to determine the heat of dilution. These values were subtracted from the measured heats in the presence of CPZ and CD. The peak area following each injection was obtained by integration of the resulting signal and was expressed as the heat effect per injection. The binding constants (K_B) and inclusion enthalpies ($\Delta_b H°$) were determined by

nonlinear regression analysis of the binding isotherms by the means of an in-house program developed by Bertaut and Landy (Bertaut & Landy. 2014).

2.1.2.2 NMR studies

One-dimensional ^{1}H and two-dimensional off-resonance ROESY spectra were recorded for β-CD, γ-CD and DIMEB on a Bruker Avance III spectrometer at a magnetic field of 16.4 T (ν(^{1}H) = 699.42 MHz) with a PATXI probe equipped with Z gradients, at a temperature of 298 K. An improved version of 2D off-resonance ROESY was used (Desvaux et al. 1995) with a continuous wave (cw) spin-lock of 9.6 kHz and 300 ms mixing time.

1D ^{1}H and off-resonance ROESY spectra of the SGM/CPZ system were obtained on a Bruker Avance III spectrometer at a magnetic field of 22.3 T (ν(^{1}H) = 950.13 MHz) with a cryogenic TCI probe equipped with Z gradients, at a temperature of 318 K. 40 ms Gaussian pulses were used for selective excitation in 1D ROESY experiments. 1D and 2D ROESY spectra were performed with a 4.5 kHz cw spin-lock and 200 ms mixing time.

1D ^{1}H spectra with 3-9-19 water suppression and 2D COSY experiments were acquired at different SGM:CPZ ratios on a Bruker Avance III spectrometer at a magnetic field of 14.1 T (ν(^{1}H) = 600.13 MHz) equipped with a cryogenic Z-gradient TCI probe and a SampleJet sample changer at two temperatures: 298 K and 318 K. Data were analysed by tracing Jobplots. Diffusion ordered spectroscopy (DOSY, (Johnson et al. 1999)) was performed under the same conditions with a stimulated echo pulse sequence using 2.0-3 ms bipolar sine gradients, with a power level linearly ramped from 2 to 98 % in 16 steps, and a diffusion time of 100 ms. The water signal was suppressed by excitation sculpting. DOSY data were analysed with an exponential model in Dynamics Center software (Bruker) to extract diffusion coefficients, D ($m^2.s^{-1}$).

2.1.2.3 Computational details

Initial geometries of native β- and γ-CD and DIME-β-CD studied in this work were built using the LEaP program from the AmberTools16 distribution(Case et al. 2015). The sugammadex structure was obtained from the Cambridge Structural Database under reference number AWEZIN (Xu et al. 2016). The fragments needed to build the native and DIMEB CD were taken from the R.E.DD.B. database (Dupradeau et al. 2008) under project F-85 (http://q4md-forcefieldtools.org/REDDB/) and the fragments needed to construct the sugammadex and the CPZ ligand were parameterized and defined according to the strategy developed previously (Cézard et al. 2011).

2.1.2.4 Molecular Dynamics Simulations

The SANDER module of the AmberTools16 program suite was used to perform MD simulations on all the cyclodextrin-CPZ complexes (Case et al. 2015). The systems were solvated in a truncated octahedral box with a buffer distance of 10.0 Å along with sodium or chlorine counter-ions to neutralize the system's net charge. The q4md-CD force field parameters were used to model the cyclodextrin systems (Cézard et al. 2011) and the GAFF force field (Wang et al. 2004) was used for the CPZ ligand. The parameters used for water were taken from the TIP3P model (Jorgensen et al. 1983). After minimization, the systems were brought to target temperature by ramping up the temperature over periods of 25 ps followed by a run of 200 ps to relax and equilibrate the system. Classical MD simulations of 50 ns were then performed using the NPT ensemble at a pressure of 1 atm and a temperature of 300 K. The weak coupling algorithm (Jorgensen et al. 1983) was used to regulate the temperature and pressure. The temperature was maintained close to the intended value by weak coupling to an external temperature bath with a relaxation time of 2 ps and the pressure to an external pressure bath of 1 atm with a coupling constant of 2 ps. The shake

algorithm (Ryckaert et al. 1977) was used to constrain C-H bonds, and a time step of 2 fs was used to integrate the equations of motion. Periodic boundary conditions were imposed during simulation. The distance cutoff of 9.0 Å was applied to non-bonded interactions and the PME method (Essmann et al. 1995) was used to compute long-range interactions. Configurations of the systems were stored at intervals of 1 ps. Analyses of the trajectories were performed using the Cpptraj module (Roe & Cheatham 2013) available in the AmberTools distribution.

2.1.2.5 Ab initio calculations

The conformational space explored using molecular dynamics simulations was clustered with Cpptraj (Roe & Cheatham 2013) and powered by the hierarchical agglomerative approach. A representative structure of each system was obtained by clustering the conformations sampled in the corresponding trajectories into ten representative classes, whose central conformations were further minimized *ab initio*; the most stable structure among these was retained. All *ab initio* quantum chemical calculations were performed with the Gaussian09 program at the M06 level of theory (Zhao & Truhlar 2008) using the 6-31G* basis set. To estimate the influence of solvation, SCRF continuum calculations were made in water (ε = 78.3553).

2.1.2.6 Photodegradation studies

A CPZ solution was prepared immediately before use at a concentration of 1.4 mM with buffer (50 mM KH_2PO_4, 30 mM NaOH, pH 7). Subsequently, 3 mL of 13.5 mM β-CD, 1.93 mM SBE-β-CD, 2.17 mM DIME-β-CD, 2.92 mM γ-CD, 6.3 mM SBE-γ-CD and 0.7 mM sugammadex solutions were prepared by dissolving the CD powder in the CPZ solution above and added into quartz cuvettes. Photodegradation was investigated by placing the cuvettes at a distance of 2.5 cm from a UV lamp (VL-6.C, 6W-254 nm Tube, power :12 W in a dark room. 100 µL from each cuvette was collected

at 0, 10, 20, 30, 60, 120, 180, 240 min and mixed with 400 µL HPLC mobile phase (acetonitrile/water/0.1 mM ammonium bicarbonate pH 7, 7:2:1, v:v:v). The initial rate constant and half-time of the reaction ($t_{1/2}$) was calculated according to the first-order reaction kinetics.

2.1.2.7 HPLC analyses

HPLC analysis of the concentration of intact CPZ was performed using a Waters 717 Plus Autosampler HPLC system equipped with Waters 2487 Dual λ Absorbance Detector at wavelength of 254 nm and 309 nm. A C18 chromatographic column (Waters XTerra®, 5µm, 3.0×150 mm) was used for separation. The mobile phase was comprised of a mixture of acetonitrile, water and 0.1 mM ammonium bicarbonate pH 7 (7:2:1, v:v:v) and flow rate was set at 0.7 mL/min. The injection volume was 10 µL. A calibration curve was prepared using CPZ in mobile phase at concentrations between 5 µg/mL and 100 µg/mL.

2.3 Results and discussion

2.3.1 Cyclodextrin screening

ITC is a very sensitive technique for determining the stoichiometry, binding constant, enthalpy, and entropy of complex formation in a single experiment. Firstly, we observed that complexation of CPZ with the smallest cyclodextrin, α-CD (Fig. 1), displays a very weak constant at 25°C (see table 1, entry 1). Indeed, from the fit of the binding isotherm, a stoichiometry, an association constant K_B and a binding enthalpy change $\Delta_b H°$ of 1:1, 1.84×10^2 M^{-1} and -12.9 $kJ.mol^{-1}$ were found respectively, leading to an entropic term $- T \times \Delta_b S°$ equal to 0 $kJ.mol^{-1}$, indicating that the binding is solely enthalpy-driven. The association constant determined in this study is identical to the value found by Uekama et al. at 25°C and at pH 7.0 by UV-visible spectroscopy (Uekama et al. 1978).

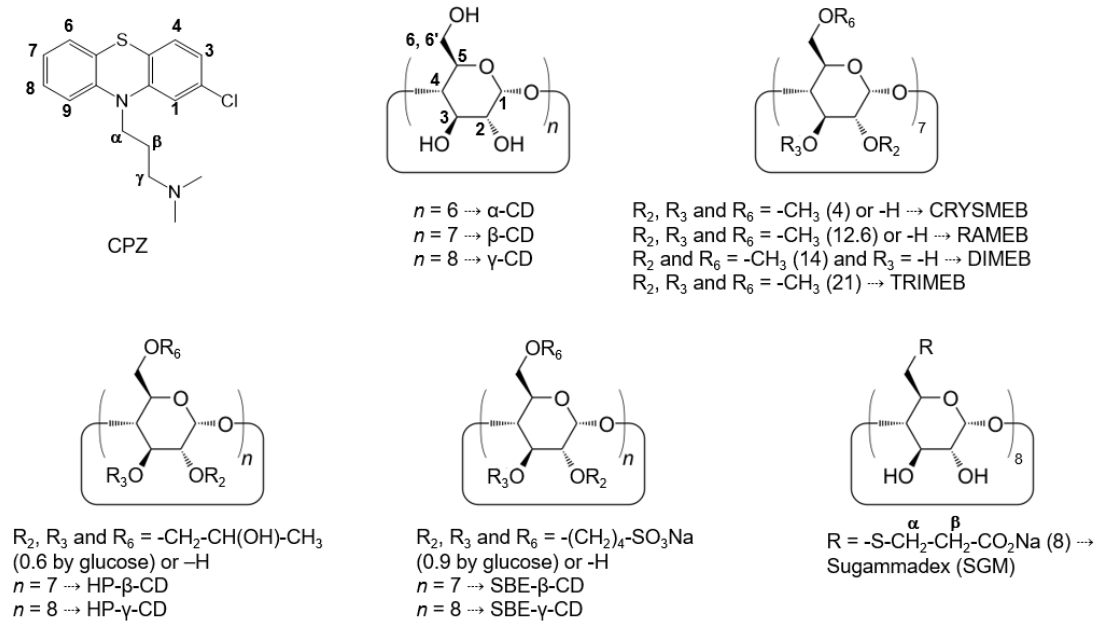

Fig. 1. Structural formulae of CPZ and the CDs used in this study

When the cavity size of CD was enlarged to β-CD, a higher association constant and a lower binding enthalpy with CPZ were obtained (see table 1, entry 2). The association constant of about 1.18×10^4 M^{-1} is very close to the value found by Otagiri et al. At 25°C and at pH 7.0 by UV-visible spectroscopy (Otagiri et al. 1975) of 1.20×10^4 M^{-1}, to the value found by Kitamura and Imayoshi at 25°C and at pH 7.0 by UV-visible spectroscopy (Kitamura & Imayoshi at al. 1992) of 1.05×10^4 M^{-1} and to the value determined by Hardee et al. by ITC of 8.32×10^3 M^{-1} (Hardee et al. 1978). Moreover, a binding enthalpy change $\Delta_b H°$ AND an entropic term - T × $\Delta_b S°$ equal to -29.9 $kJ.mol^{-1}$ and 6.7 $kJ.mol^{-1}$ respectively were found, showing that the inclusion of CPZ in the CD cavity was completely enthalpy-driven. Hardee et al. were the first to report thermodynamic parameters for the 1:1 β-CD/CPZ complexes with $\Delta_b H°$ = -26.8 $kJ.mol^{-1}$ AND - T × $\Delta_b S°$ = 4.5 $kJ.mol^{-1}$ and the values obtained in our study are very close to their values (Hardee et al. 1978). Shiotani et al. found similar values for the thermodynamic parameters at 25°C, ie. $\Delta_b H°$ = -28.4 $kJ.mol^{-1}$ and - T × $\Delta_b S°$ = 5.8 $kJ.mol^{-1}$ (Shiotani et al. 1994). The negative entropy change could be mainly

attributed to the tight binding of guest molecules in the CD cavity, resulting in the loss of freedom of both CD and guest molecules.

The use of methylated β-CD derivatives led to very different results, depending on the derivative used. The low and randomly 2-*O*-methylated-β-CD, i.e. CRYSME-β-CD, gave similar results to the β-CD (see table 1, entry 3). In contrast, RAME-β-CD, a randomly methylated β-CD (12.6 OH group on average replaced by OMe at positions 2, 3 and 6), showed a decrease in the association by a factor of two (see table 1, entry 4). Moreover, in the case of RAME-β-CD, the entropic contribution is not negligible and contributes about 20% of the Gibbs energy change. In order to understand the impact of methylation better, two well-defined methylated β-CD were used. On one hand, heptakis(2,6-di-*O*-methyl)-β-CD, or DIME-β-CD provided an increase in the association constant by a factor of about two (see table 1, entry 5). On the other hand, the tri-methylated heptakis(2,3,6-tri-*O*-methyl)-β-CD was not able to form an inclusion complex with CPZ (data not shown). We can therefore conclude that: 1) methylation of position 2 of the β-CD does not modify the inclusion properties of the cyclodextrin; 2) methylation of position 6 increases the inclusion capacity, probably by increasing the volume of the cavity and 3) methylation of position 3 has a detrimental effect on the complexation by inducing a steric hindrance on the secondary side. It should be noted that Uekama's group has reported an association constant for the DIME-β-CD/CPZ complex (Ishida et al. 1988). However, the value of the constant (8800 M^{-1}) suggests that the study was performed with a DIME-β-CD that contained over-methylated CD.

Table 1. Binding constants KB for association of chlorpromazine with different CDs and related thermodynamic parameters at T = 25°C.

Entry	Cyclodextrin	Stoichiometry	K_B [1]	$\Delta_b H^{o}$ [2]	$-T \times \Delta_b S^{o}$ [2]	$\Delta_b G^{o}$ [2]
1	α-CD	1:1	$(1.84 \pm 0.35) \times 10^2$	- 12.9 ± 2.0	0 ± 2.4	- 12.9 ± 0.5
2	β-CD	1:1	$(1.18 \pm 0.02) \times 10^4$	- 29.9 ± 0.2	6.7 ± 0.2	- 23.2 ± 0.1
3	CRYSME-β-CD	1:1	$(1.29 \pm 0.09) \times 10^4$	- 25.9 ± 0.3	2.4 ± 0.5	- 23.5 ± 0.2
4	RAME-β-CD	1:1	$(6.05 \pm 0.42) \times 10^3$	- 17.2 ± 0.7	- 4.4 ± 0.9	- 21.6 ± 0.2
5	DIME-β-CD	1:1	$(2.61 \pm 0.09) \times 10^4$	- 23.7 ± 0.1	- 1.5 ± 0.2	- 25.2 ± 0.1
6	HP-β-CD	1:1	$(5.43 \pm 0.72) \times 10^3$	- 17.7 ± 0.3	- 3.6 ± 0.6	- 21.3 ± 0.3
7	SBE-β-CD	1:1	$(1.99 \pm 0.02) \times 10^4$	- 15.8 ± 0.2	- 8.7 ± 0.2	- 24.5 ± 0.1
		1:2	$(2.09 \pm 0.20) \times 10^3$	- 2.9 ± 0.5	- 16.1 ± 0.8	- 18.9 ± 0.2
8	γ-CD	1:1	$(5.34 \pm 1.01) \times 10^2$	- 6.8 ± 2.2	- 8.7 ± 2.7	- 15.6 ± 0.5
		1:2	$(5.71 \pm 1.10) \times 10^3$	- 63.5 ± 4.3	42.0 ± 4.8	- 21.4 ± 0.5
9	HP-γ-CD	1:1	$(4.57 \pm 0.84) \times 10^2$	- 8.3 ± 0.9	- 6.9 ± 1.4	- 15.2 ± 0.5
		1:2	$(1.07 \pm 0.41) \times 10^3$	- 42.7 ± 7.2	25.4 ± 8.2	- 17.3 ± 1.0
10	SBE-γ-CD	1:1	$(1.66 \pm 0.17) \times 10^3$	- 3.0 ± 1.0	- 15.4 ± 1.2	- 18.4 ± 0.2
		1:2	$(7.38 \pm 0.72) \times 10^3$	- 46.6 ± 2.0	24.6 ± 2.2	- 22.1 ± 0.2
11	sugammadex	1:2	$(6.37 \pm 0.25) \times 10^9$	- 73.2 ± 0.3	17.2 ± 0.4	- 55.9 ± 0.1

1 expressed in M^{-1}, except the entry 11, which is expressed in M^{-2}.

2 expressed in $kJ.mol^{-1}$.

The complexation of CPZ with HP-β-CD, which is generally recognized as safe and is approved as a pharmaceutical additive, was studied. An association constant and thermodynamic parameters similar to those of RAME-β-CD were obtained (see table 1, entry 6). Moreover, the value of the association constant is intermediate between the value found by Okimoto et al. from the phase solubility diagram ($K_f = 7.01 \times 10^3\ M^{-1}$; (Okimoto et al. 1999) and that found by Piñero et al. by UV-visible spectroscopy ($K_f = 3.27 \times 10^3\ M^{-1}$; (Piñero et al. 2012) and is close to that reported by Ishida et al. ($K_f = 4.40 \times 10^3\ M^{-1}$; (Ishida et al. 1988).

Next, a second safe and approved modified β-CD was studied: the well-known sulfobutylated-β-CD (SBE-β-CD). The isotherm obtained during the titration of CPZ by SBE-β-CD was analysed using a two-site binding model involved within a sequential process (see table 1, entry 7). The binding constant measured for the 1:1 complex ($K_{1:1} = 1.99 \times 10^4$ M^{-1}) was one order of magnitude higher than that measured for the 1:2 complex ($K_{1:2} = 2.09 \times 10^3$ M^{-1}). This difference could arise from a more difficult access of the second CPZ molecule into the CD cavity. Okimoto et al. studied the SBE-β-CD/CPZ complex by means of a phase solubility diagram and found a higher association constant of 3.21×10^4 M^{-1} (Okimoto et al. 1999). This difference is the result of the complexation model used by Okimoto et al., which was a 1:1 model. The thermodynamic parameters reveal that the 1:1 process is enthalpy- and entropy-driven while the entropic component is the main driving force for the following 1:2 step. This favourable entropy change is probably due to the displacement of ordered water molecules around (or inside) the cavity. The formation of a 1:2 complex can be understood from the enlarged cavity generated by chemical modification.

Finally, with γ-CD and its derivatives, the formation of a 1:2 complex is always observed and is the only type of complex formed in the case of sugammadex. For γ-CD (see table 1, entry 8), the 1:2 binding constant was one order of magnitude higher than that measured for the 1:1 complex. In 1978, Uekama et al. found an association constant close to 1000 M^{-1} for a 1: 1 complex (Uekama et al. 1978). This stoichiometry is not in agreement with the mixture of stoichiometries found in the present study. On the other hand, using potentiometry, Takisawa et al. found similar behaviour to that observed in our study with the same magnitude of difference between the two constants (Takisawa et al. 1993). Moreover, these authors explain the great stability of the 1:2 complex by the stacking of the aromatic rings in the large cavity of γ-CD's. From a thermodynamic point of view, the Gibbs energy change of the 1:1 complex is distributed approximately equally between enthalpy and entropy changes, whereas in the case of the 1:2 complex, the complexation is entropically unfavourable

(- T × $\Delta_b S°$ = 42.0 kJ.mol^{-1}) but this is counterbalanced by a strong and negative complexation enthalpy change value ($\Delta_b H°$ = -63.5 kJ.mol^{-1}) which is the result of van der Waals interactions, π-π stacking and possibly also hydrogen bonding. The high and positive complexation entropy change is probably derived from the loss of translational and rotational degrees of freedom upon complexation.

In the same way as for HP-β-CD, the complexation of CPZ with HP-γ-CD is less efficient than with the corresponding native CD (see table 1, entry 9) and the 1:2 binding constant value is about twice the 1:1 complexation constant. The thermodynamic parameters show that the 1:1 process is enthalpy- and entropy-driven while, as for the 1:2 step with γ-CD, the complexation is entropically unfavourable but enthalpically favourable.

In the case of SBE-γ-CD, as for SBE-β-CD, the binding constants are higher, indicating that the complexation is more effective with sulfobutyl ether CDs (see table 1, entry 10). The binding constant measured for the 1:2 complex ($K_{1:2}$ = 7.38 × 10^3 M^{-1}) was four times higher than that measured for the 1:1 complex ($K_{1:1}$ = 1.66 × 10^3 M^{-1}). Moreover, the thermodynamic parameters for SBE-γ-CD follow the same trend as for γ-CD with a preponderant entropic component for the 1:1 process. For the subsequent 1:2 step, as for γ-CD, complexation is entropically unfavourable, but the high negative enthalpy change value allows to have a negative Gibbs energy change.

Finally, the use of sugammadex (the octasodium salt of octakis(6-deoxy-6-S-(2-carboxyethyl)-6-thio)cyclomaltooctaose) led to an unexpected result. Indeed, the fit of the isotherm obtained during the titration of CPZ by sugammadex reveals a stoichiometry equal to the ratio of 1:2 (the existence of a complex with a 1:1 stoichiometry could not be excluded but the amount is probably negligible) and an association constant very close to 6.37 × 10^9 M^{-2}. Hirai et al. were the first to report the formation of pure 1:2 γ-CD/guest complexes and determined high association constants for these complexes (Hirai et al.1981). It should be noted

that the association constant of the 1:2 sugammadex/CPZ complex is the second strongest constant reported in the literature to our knowledge. Indeed, an association constant equal to 9.0×10^{10} M^{-2} was reported by the group of S.F. Lincoln for the 1:2 γ-CD/roccellin complex (Clarke et al. 1986). Finally, the thermodynamic parameters of the 1:2 sugammadex/CPZ complex follow the same trend as the other 1:2 complexes; that is, a very negative value for the binding enthalpy change and an unfavourable entropy change.

2.3.2 Advanced thermodynamic characterization

In order to obtain a deeper insight into the thermodynamic behaviour of the complexes, the binding heat capacity changes were determined for the most promising complexes. The heat capacity change $\Delta_b C_p°$ is defined as the first derivative of binding enthalpy change with temperature at constant pressure. The magnitude and sign of $\Delta_b C_p°$ is directly related to modifications of the well-ordered solvent molecules present around hydrophobic or polar groups of the host and guest molecules. From the temperature dependencies of the binding enthalpy changes, a heat capacity change $\Delta_b C_p° = - 272.5 \pm 0.1$ $J.mol^{-1}.K^{-1}$ was found for the interaction of CPZ with β-CD. Thus, the large negative values of the $\Delta_b C_p°$ reported in this work are to a large extent due to the dehydration of the apolar part of the CD and the guest molecule. In the case of DIME-β-CD, an higher heat capacity change $\Delta_b C_p° = - 365.7 \pm 0.1$ $J.mol^{-1}.K^{-1}$ was found, which could be explained by a higher degree of dehydration of the hydrophobic area of the host and the guest. Moreover, the favourable entropic contribution encourages the release of water molecules during the inclusion process. The complexation of CPZ towards SBE-β-CD leads to a surprising result. For the 1:1 complex, a negative heat capacity change $\Delta_b C_p° = - 486.9 \pm 0.1$ $J.mol^{-1}.K^{-1}$ was determined while a positive heat capacity change $\Delta_b C_p° = 309.2 \pm 0.1$ $J.mol^{-1}.K^{-1}$ was found for the 1:2 complex. We can hypothesize that the longer sulfobutyl substituents could entrap a larger part of the first included CPZ molecule, leading

to an expulsion of more water molecules. For the second encapsulated CPZ molecule, the positive heat capacity change reflects a conformational change of the CD during the inclusion process (Brocos et al. 2011). This conformational rearrangement corresponds to the passage from a flexible CD molecule to a tight one. So, during the inclusion of the second CPZ molecule, the disordered sulfobutyl arms must be rearranged to encapsulate the second molecule, since the β-CD macrocycle is unable to bind two CPZ molecules.

For the γ-CD/CPZ system, heat capacity changes $\Delta_b C_p° = - 513.3 \pm 0.1$ and $- 385.1 \pm 0.1$ J.mol^{-1}.K^{-1} were found for the inclusion complexes 1:1 and 1:2 respectively. The more negative value for the 1:1 complex compared with the β-CD/CPZ complex is the reflection of a larger number of water molecules involved during the inclusion process. Moreover, the less negative value for the 1:2 complex compared with the 1:1 complex could indicate a number of water molecules involved during the complexation is smaller, but a concomitant conformational rearrangement of the γ-CD macrocycle cannot be excluded.

Similar behaviour was observed for the SBE-γ-CD/CPZ system ($\Delta_b C_p° = - 608.3 \pm 3.7$ and $- 150.2 \pm 7.9$ J.mol^{-1}.K^{-1} for the inclusion complexes 1:1 and 1:2 respectively). The lower heat capacity change value obtained for the 1:1 complex in the case of the SBE-γ-CD compared with the γ-CD could be explained in the same way as the 1:1 SBE-β-CD/CPZ system. Furthermore, the less negative value obtained for the 1:2 SBE-γ-CD/CPZ inclusion complex compared with the 1:2 γ-CD/CPZ is probably the result of the rearrangement of sulfobutyl arms as for the 1:2 SBE-β-CD/CPZ. Finally, the heat capacity change obtained for the 1:2 sugammadex/CPZ complex ($\Delta_b C_p° = - 619.2 \pm 0.1$ J.mol^{-1}.K^{-1}) is of the same order of magnitude as the 1:1 SBE-γ-CD/CPZ system and can be explained by the fact that sugammadex can encapsulate two CPZ molecules with or without a small amount of conformational rearrangement.

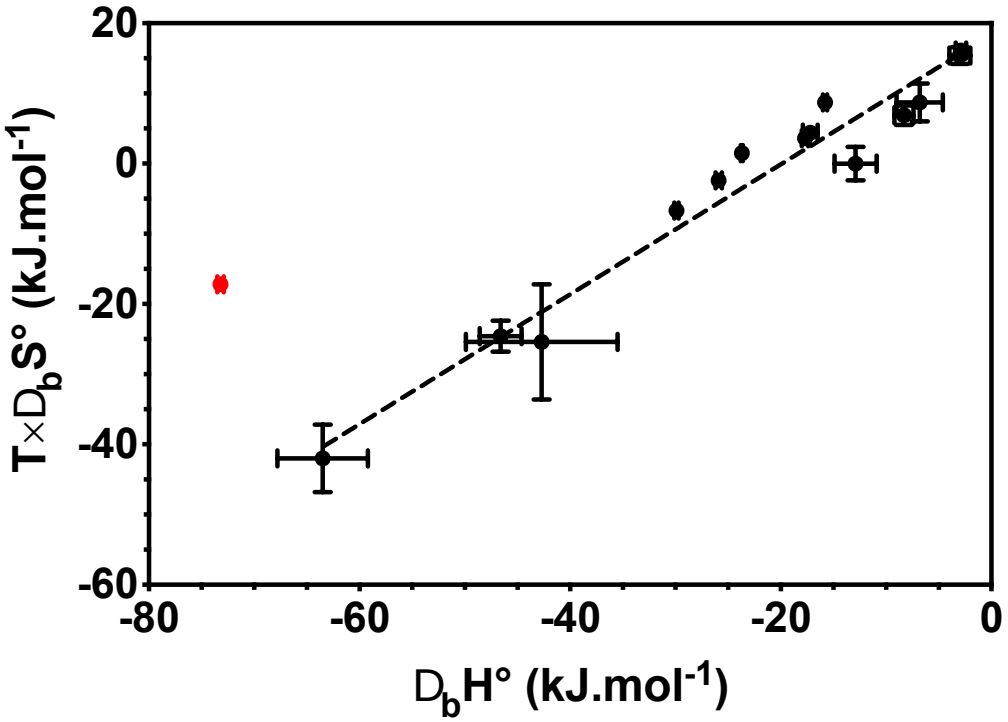

Fig. 2. Enthalpy-entropy compensation plot for the inclusion complexation of CPZ with various CDs obtained in the present work in an aqueous buffer solution at 25°C.

Enthalpy-entropy compensation has often been observed empirically for inclusion processes in the supramolecular chemistry field (Rekharsky & Inoue. 1998). This relationship between the enthalpy and entropy of binding suggest that the enthalpic changes are offset by the entropic changes. The observed linear relationship in enthalpy-entropy compensation plots follows from $T \times \Delta_b S° = \alpha \times \Delta_b H° + T \times \Delta_b S°_0$ implying that the changes in entropy of binding are dependent on enthalpy of binding with a slope α and an intercept $T \times \Delta_b S°_0$. The slope α and intercept $T \times \Delta_b S°_0$ of the $T \times \Delta_b S°$ *vs.* $\Delta_b H°$ plot have been proposed as quantitative measurements of the conformational change and the extent of desolvation upon complex formation, respectively. In accordance with this, the $T \times \Delta_b S°$ are plotted against the $\Delta_b H°$ to obtain a good straight line with a correlation coefficient r = 0.978 but the point corresponding to the sugammadex/CPZ complex falls outside the correlation (Fig. 2). The slope α =

0.93 ± 0.06, comprised between the values reported by Rekharsky and Inoue for natural and modified CD, indicates a rearrangement of the peripheral hydrogen bond network and the accompanying skeletal conformational changes, while the intercept ($T \times \Delta_b S°_0$ = 18.4 ± 1.6 kJ.mol^{-1}), very close to the value reported by Rekharsky and Inoue for modified CD, means fairly extensive dehydration occurs upon inclusion.

2.3.3 Structure of the β-CD/CPZ complex

As only few publications report the 1D NMR spectrum of the β-CD/CPZ complex (Takamura et al. 1983), the ^{1}H NMR spectrum of an equimolar mixture of β-CD and CPZ was recorded in deuterium oxide at 25°C. A comparison of ^{1}H NMR spectrum of β-CD (1 mM in D_2O) in the presence and absence of CPZ was performed to highlight chemical shift variations on the H_3 and H_5 protons located inside the β-CD cavity and on the H_6 protons located on the periphery of the cavity (Fig. 3). The addition of CPZ to β-CD led to an upfield chemical shift variation on H_3, H_5 and $H_6/H_{6'}$, consistent with the formation of an inclusion complex. Moreover, the H_1, H_2 and H_4 protons located outside the β-CD cavity were also affected during the inclusion process, as an upfield chemical shift variation was observed for the H_1 and H_4 protons while the H_2 protons led to a small downfield chemical shift variation. In the case of CPZ, it should be noted that all protons (except the methyl protons) were affected during the complexation (Fig. 4). With the exception of the H_1 proton of the CPZ, the formation of an inclusion complex causes downfield shifts in the plane of the aromatic rings. Moreover, upfield shifts of all methylene protons as a result of the addition of the β-CD were also found. A splitting of the three methylene peaks was observed to result from the formation of an inclusion complex. This effect was most pronounced with the H_α methylene protons, whereas the H_β protons were less affected.

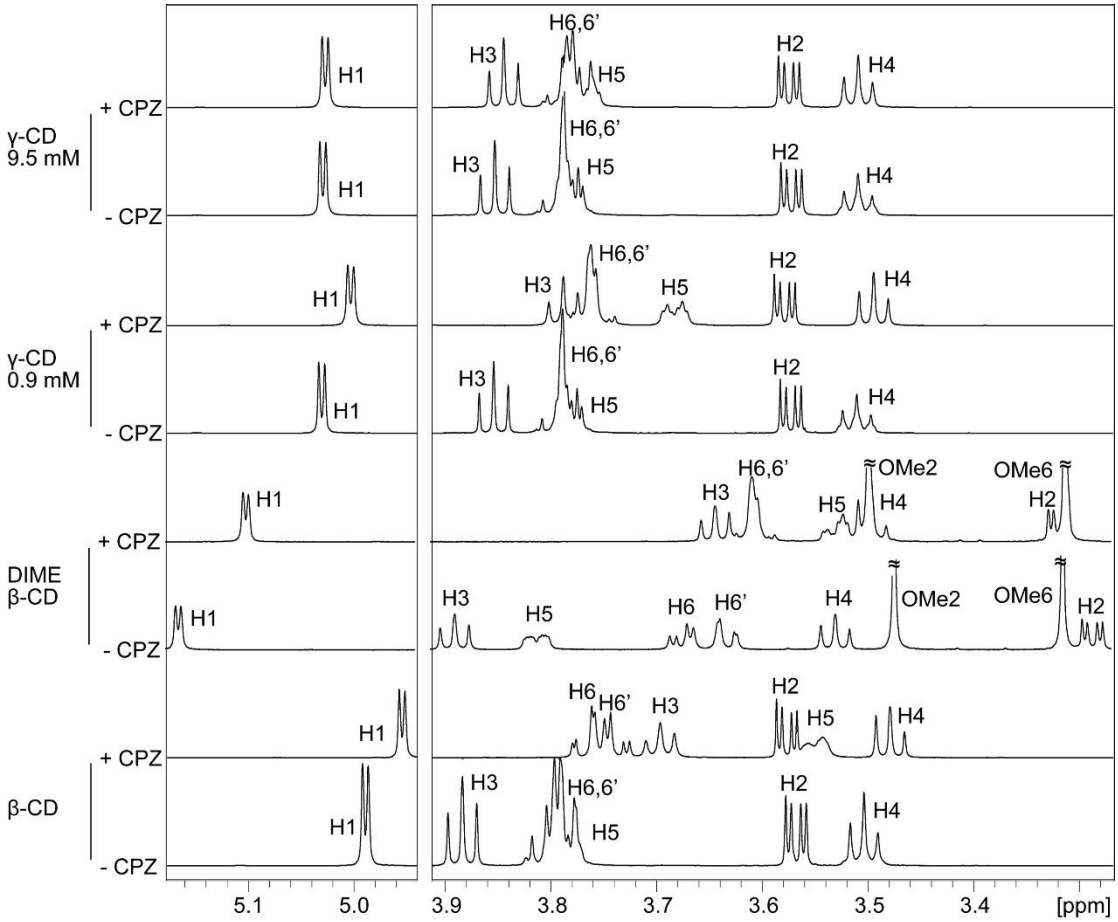

Fig. 3. ^{1}H NMR spectra of 1 mM of β-CD, 1 mM of DIME-β-CD, 0.9 mM of γ-CD or 9.5 mM of γ-CD in D_2O with or without 1 mM of CPZ (T = 25°C, 700 MHz).

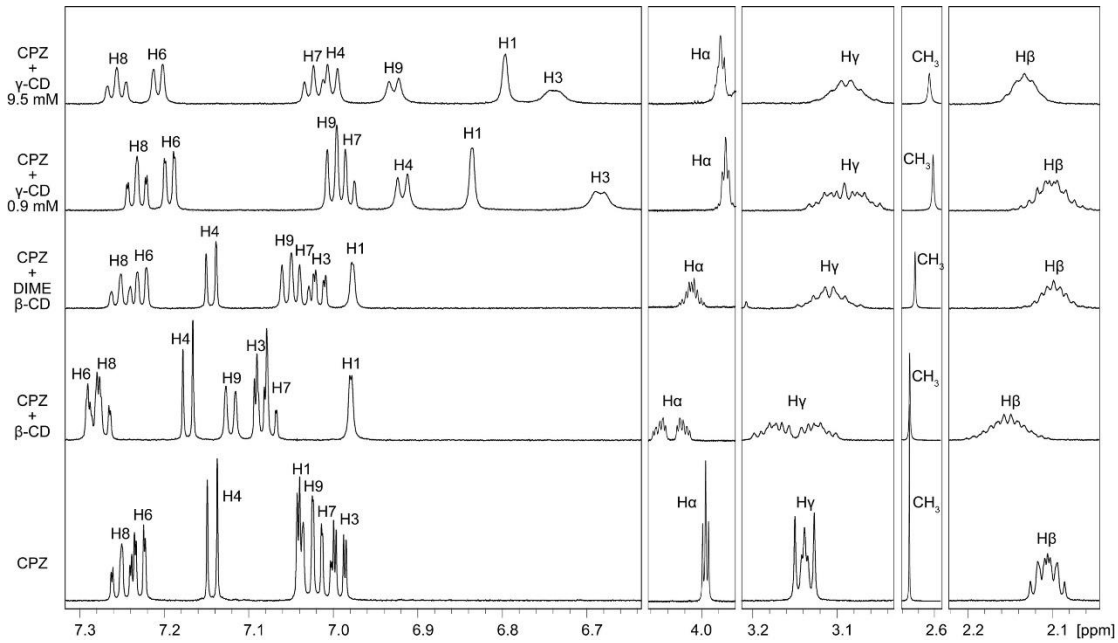

Fig. 4. ^{1}H NMR spectra of 1 mM of CPZ in D_2O and in the presence of 1 mM of β-CD, 1 mM of DIME-β-CD, 0.9 mM of γ-CD or 9.5 mM of γ-CD (T = 25°C, 700 MHz).

In order to have a better insight into the three-dimensional structure of the inclusion complex, an off-resonance ROESY experiment was performed on the same β-CD/CPZ mixture (Fig. 5). This revealed dipolar contacts between CPZ and CD cavity protons. Strong interactions between the H_3 protons of β-CD and the H_1, H_4, H_6 and H_9 protons of the aromatic moiety of CPZ were observed as well as between the H_5 protons of β-CD and the H_1, H_3, H_4, H_6 and H_9 protons of CPZ. Other interactions involving the protons $H_6/H_{6'}$ of the β-CD and the protons H_3 and H_4 of CPZ (weak interactions) were also detected. No interaction between the protons H_7 and H_8 of the aromatic part of CPZ and the protons H_3 and H_5 located inside the β-CD were observed, indicating that a part of the aromatic ring was outside the CD cavity. Moreover, for the aliphatic part of CPZ, a strong interaction with the protons H_α and a weaker one with the protons H_β were detected with the protons H_3 of the β-CD. All this information suggests that CPZ enters the β-CD by the wider side of the rim and the chlorinated aromatic part of the CPZ is deeply included within the β-CD cavity. It should be noted that Piñero et al. showed that the same inclusion mechanism led to the lowest energy during a computational study of the interaction of CPZ with HP-β-CD (Pinero et al. 2012).

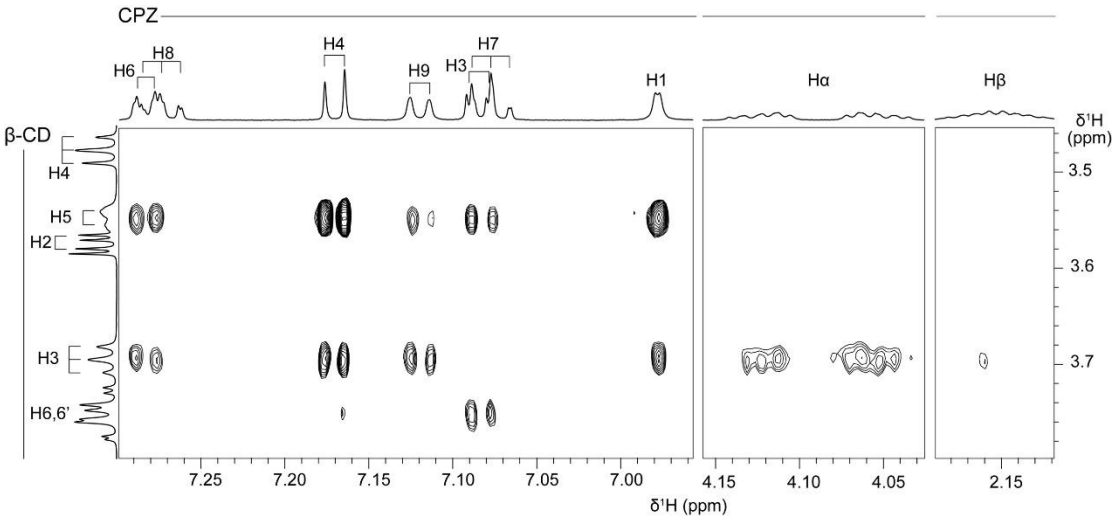

Fig. 5. Partial contour plots of an off-resonance ROESY experiment (25°C, 700 MHz, D_2O, effective angle: 54.7°, mixing time: 300 ms) recorded on a mixture of β-CD (1 mM) and CPZ (1 mM).

Finally, molecular dynamic simulation of the complex was undertaken in an attempt to have a better representation of the β-CD/CPZ complex. Taking into account the results of ^{1}H NMR spectroscopy, molecular dynamic simulation was undertaken, and all the snapshots were clustered into 10 structures to provide a reliable ensemble of representative conformations. The best representative structure, compatible with 2D NMR spectroscopy, was further minimized by DFT calculations (Fig. 6). This structure totally explains the 2D NMR spectroscopy results, especially the lack of cross-correlation between the protons H_7 and H_8 of CPZ and the protons H_3 of the β-CD, since the mean distances H_7-H_3 and H_8-H_3 (considering only the 3 closest H_3 protons) were equal to 5.2 and 6.0 Å for the H_7 and H_8 protons respectively. Moreover, the mean distances H_3-H_6/$H_{6'}$ (considering the 2 nearest H_6 or $H_{6'}$ protons) and H_4-H_6/$H_{6'}$ (considering the 3 closest H_6 or $H_{6'}$ protons) were equal to 3.6 and 4.3 Å for the H_3 and H_4 protons respectively, corroborating a strongest cross-correlation spot for the proton H_3 with the protons H_6 or $H_{6'}$ of the β-CD. As far as the aliphatic protons of the CPZ chain were concerned, the mean distances H_α-H_3 and H_β-H_3 (considering the 3 closest H_3 protons) were equal to 2.8 and 4.3 Å and were in accordance with the strong and weak cross-correlation spots observed for the H_α and H_β protons of the CPZ molecule toward the H_3 protons of the β-CD.

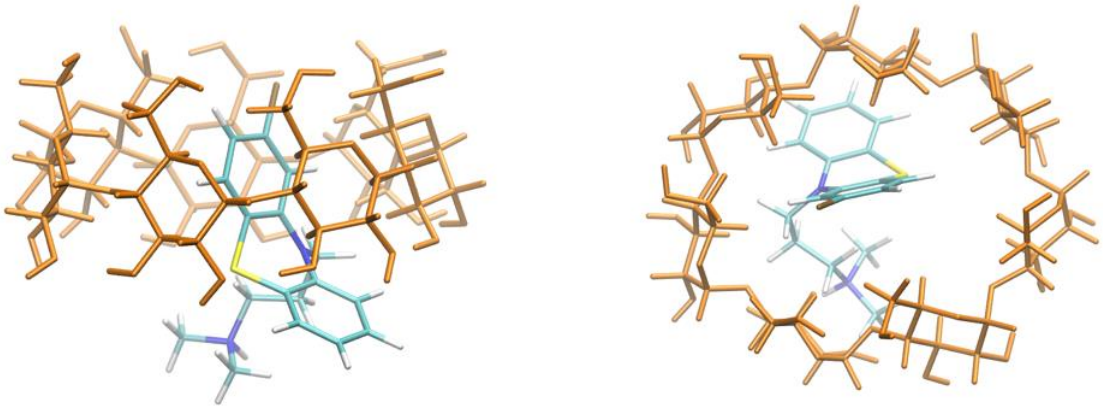

Fig 6. Molecular dynamic simulation of the β-CD/CPZ complex.

2.3.4 Structure of the heptakis(2,6-di-*O*-methyl)-β-CD/CPZ complexes

As the heptakis(2,6-di-*O*-methyl)-β-CD, more often called DIME-β-CD, is a well-defined cyclodextrin and gives a pure 1:1 complex, a precise structural characterization was carried out using ^{1}H NMR spectroscopy. As for β-CD, the addition of CPZ to DIME-β-CD led to an upfield chemical shift variation on the internal protons H_3 and H_5, on the peripheral protons $H_6/H_{6'}$ and on the external protons H_1 and H_4 and to a downfield chemical shift variation on the external protons H_2. Moreover, the protons of the two methoxy groups located on the periphery of the CD cavity were also affected during the inclusion process, as a small upfield chemical shift variation was observed for the O_6-CH_3 protons while the O_2-CH_3 protons led to a downfield chemical shift variation. For the CPZ protons, the ^{1}H NMR spectra led to a more complex situation as a broadening of the majority of the protons was observed. Unlike the β-CD/CPZ complex, the chemical shift of the H_8 proton of the CPZ remains unchanged but a broadening was observed. As for the β-CD/CPZ complex, an upfield chemical shift variation was observed for the H_1 proton of the CPZ but a small upfield chemical shift variation was observed for the H_6 proton unlike the β-CD/CPZ complex. Moreover, the formation of an inclusion complex caused downfield shifts of the other protons (H_3, H_4, H_7 and H_9) of the two aromatic rings. Considering the aliphatic chain of the CPZ, an upfield chemical shift variation was observed for all protons (included the N-CH_3 protons) except for the H_α protons for which an increase in the chemical shift was noticed. Furthermore, unlike the β-CD/CPZ complex, no clear splitting was observed for the methylene protons.

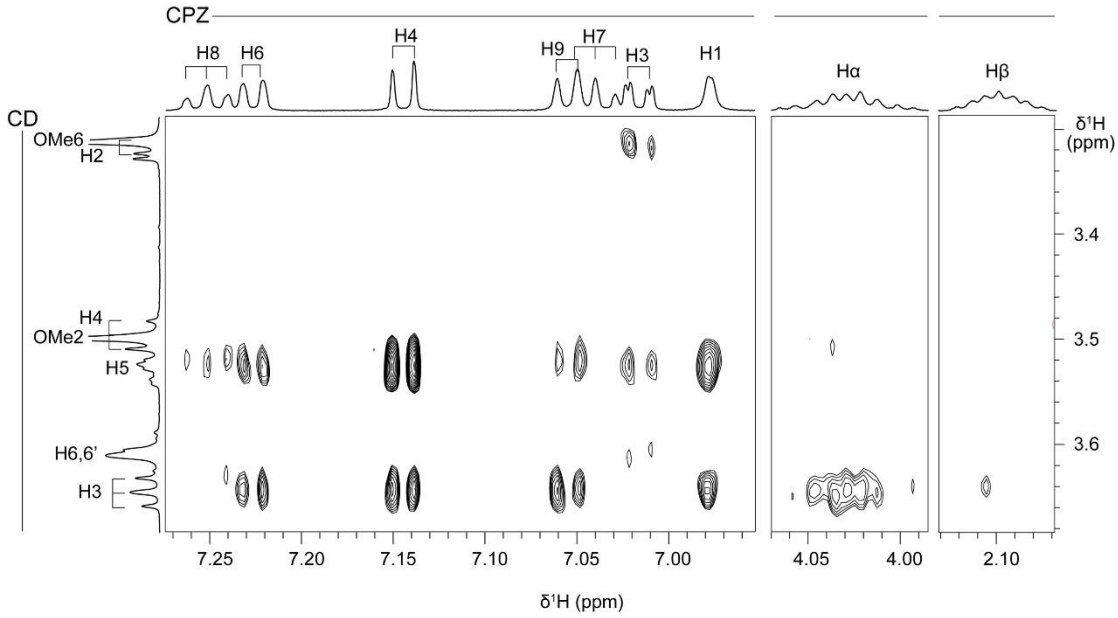

Fig. 7. Partial contour plots from an off-resonance ROESY experiment (25°C, 700 MHz, D_2O, effective angle: 54.7°, mixing time: 300 ms) recorded on a mixture of DIME-β-CD (1 mM) and CPZ (1 mM).

In order to obtain information about the spatial proximity of CPZ protons towards CD protons, a 2D off-resonance ROESY spectrum was recorded (Fig. 7). In contrast to the β-CD/CPZ complex, a weak and a very weak interaction between the proton H_8 of the aromatic part of CPZ and the protons H_3 and H_5 of the DIME-β-CD respectively were detected but, as for the β-CD/CPZ complex, no interaction of the internal CD proton towards the H_7 proton of CPZ was observed, indicating that a smaller part of the aromatic ring was outside the CD cavity. The same interactions were observed for the cross-correlation spots between the other aromatic protons of CPZ and the internal protons H_3 and H_5 of DIME-β-CD. Moreover, a very weak interaction involving the protons $H_6/H_{6'}$ of the DIME-β-CD and the proton H_3 of CPZ (weak interactions) were detected and a weak interaction between the same CPZ proton towards the methoxy protons O_6-CH_3 was observed, suggesting that the mechanism of inclusion was not perturbed by the methylation of the β-CD macrocycle. Finally, the same interactions as in the β-CD/CPZ complex were detected between the methylene protons of CPZ and the internal protons of the CD but a very weak interaction

between with the protons H_α and the methoxy protons O_2-CH_3 was observed. With these structural data, a molecular dynamic simulation combined with DFT calculations was carried out and the geometry of the DIME-β-CD/CPZ complex was obtained (Fig. 8). The three-dimensional structure of the DIME-β-CD/CPZ complex is very close to that of the β-CD/CPZ complex.

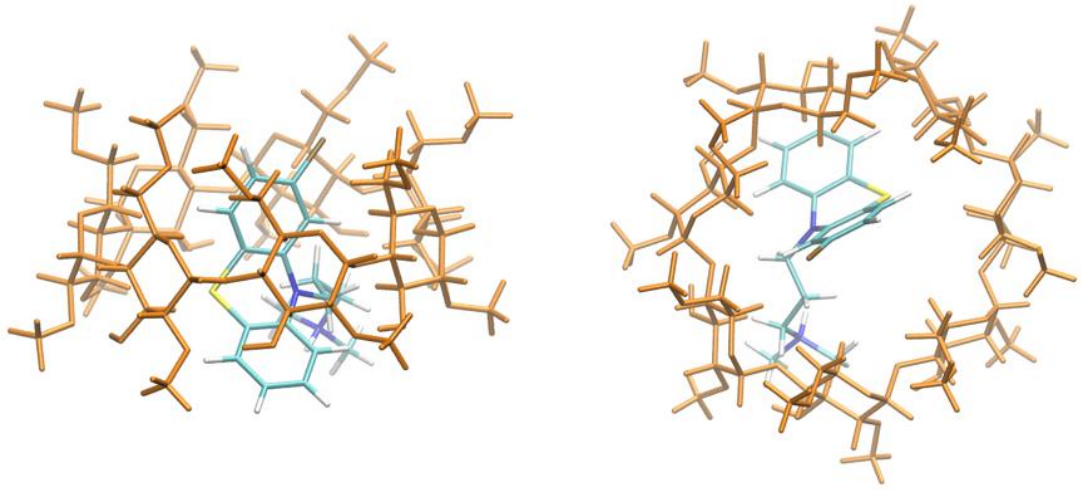

Fig. 8. Molecular dynamic simulation of the DIME-β-CD/CPZ complex.

2.3.5 Characterisation of the γ-CD/CPZ complexes

Only one report in the literature describes the ^{1}H NMR spectrum of the γ-CD/CPZ complex (Takamura et al. 1983)**.** However, these authors described the γ-CD/CPZ complex as a 1:2 complex. In our hands, since two γ-CD/CPZ complexes, with 1:1 and 1:2 stoichemistry, coexist in solution, the γ-CD concentration was optimised in order to maximise the amount of each complex. The use of a low concentration of γ-CD gave the maximum yield of the γ-CD/CPZ_2 complex. In particular, the use of a γ-CD concentration equal to 0.87 mM led to a mixture containing 40% of free CPZ, 11% of the γ-CD/CPZ complex and 49% of the γ-CD/CPZ_2 complex in terms of CPZ concentration. On the other hand, if a γ-CD concentration of 9.5 mM of γ-CD was used, the mixture contained 9% of free CPZ, 44% of the γ-CD/CPZ complex and 47% of the γ-

CD/CPZ$_2$ complex, corresponding to the highest γ-CD/CPZ concentration. Firstly, the ^{1}H NMR spectrum of a mixture of 0.87 mM of γ-CD and 1 mM of CPZ was recorded. Results similar to those recorded for the β-CD/CPZ complex were obtained, but the phenomenon was less marked. Upfield chemical shift variations on H_1, H_3, H_4, H_5 and H_6/$H_{6'}$ protons of γ-CD were observed, together with a small downfield chemical shift variation for the H_2 protons.

However, as far as the aromatic protons of CPZ were concerned, the situation was totally different, because upfield chemical shift variations of all the aromatic protons were detected, and this was more pronounced for the protons of the chlorinated aromatic cycle with a significant broadening of the protons H_3 and H_4 of CPZ. Moreover, considering the aliphatic protons of CPZ, upfield chemical shift variations were also observed for all methylene protons as well as with the methyl protons. In order to obtain a better description of the γ-CD/CPZ complex, 2D off-resonance ROESY spectroscopy was attempted, but this was impossible due to the weak overlap of the signals related to H_3 and H_6/$H_{6'}$ protons of the γ-CD and the coexistence of the γ-CD/CPZ and γ-CD/CPZ$_2$ complexes. It should be noted that no cross-correlation peak was detected for the H_3 and H_7 protons of CPZ towards the internal protons of the γ-CD, probably as a result of the broadening of the peak of the H_3 proton of CPZ and the proton H_7 being located outside the cyclodextrin, which was likely because only a weak cross-correlation peak was detected for the H_8 proton of CPZ towards the internal protons of the γ-CD. A measurement at a lower temperature was performed with the intent of separating the signal emanating from the free form and the complexed form for the H_3 and H_4 protons of CPZ; however, this led to a larger broadening of these protons and a splitting of the methylene protons of the aliphatic chain of CPZ.

Finally, the ^{1}H NMR spectrum of the γ-CD/CPZ mixture containing a higher concentration of γ-CD was recorded. In this case, the ^{1}H NMR spectrum of the γ-CD/CPZ mixture was very close to that of the γ-CD, which could easily be

explained by the presence of 93% of free γ-CD. However, upfield chemical shift variations on the internal H_3, H_5 and $H_6/H_{6'}$ protons of γ-CD were observed, confirming the formation of an inclusion complex. Concerning the aromatic protons of the CPZ, some differences compared to the low γ-CD concentration spectrum have been identified. A downfield chemical shift variation was observed for the H_7 and H_8 protons of the CPZ while a smaller upfield chemical shift variation was noticed for the H_3 and H_4 protons of the CPZ. On the contrary, a larger upfield chemical shift variation was detected for the H_1 and H_9 protons of the CPZ. These differences in phenomena can be explained by a larger proportion of 1: 1 complex in solution.

Finally, our attempt to obtain additional data from a 2D off-resonance ROESY spectrum was inconclusive for the same reasons as stated above. As for the low γ-CD concentration, no cross-correlation peak was detected for the H_3 and H_7 protons of CPZ towards the internal protons of the γ-CD, again for similar reasons, but with a high concentration of γ-CD a weak cross-correlation peak was detected for the H_8 proton of CPZ towards the H_5 and $H_6/H_{6'}$ protons of the γ-CD. Unfortunately, no three-dimensional structure could be determined in the presence of the γ-CD.

2.3.6 Characterization of the sugammadex/CPZ complexes

As for the other complexes, the ^{1}H spectrum of a mixture of sugammadex and CPZ in a molar ratio 1:2 was recorded at 25°C in order to compare it to the ^{1}H spectra of the compounds taken separately (Fig. 9). A broadening of the aromatic protons of CPZ in presence of sugammadex was observed; in particular a large broadening of the H_6 and H_8 protons of the CPZ. An even more extensive broadening of the H_3 and H_7 protons of the CPZ was also noed, since these two protons could not be observed on the spectrum. So, in order to recover the signals of these protons, the temperature was increased in order to restore a better dynamic. At 45°C, all the protons of CPZ could be observed on the ^{1}H spectrum

of the sugammadex/CPZ mixture. In particular, the H_3 and H_7 protons of the CPZ can be observed, despite considerable broadening, and the other aromatic protons are much less broadened. So, a temperature of 45°C was chosen for later experiments unless otherwise stated. An upfield chemical shift variation of all protons of sugammadex was noticed except for the H_2 protons for which a downfield chemical shift variation was observed. As far as the protons of CPZ were concerned, an upfield chemical shift variation of all aromatic protons was observed as well as for the methylene H_γ and methyl CH_3 protons while the methylene H_α and H_β protons were subject to a downfield chemical shift variation. With the exceptions of some differences at the level of the aliphatic chain, the same observations as for the γ-CD/CPZ mixture containing a low concentration of γ-CD were made.

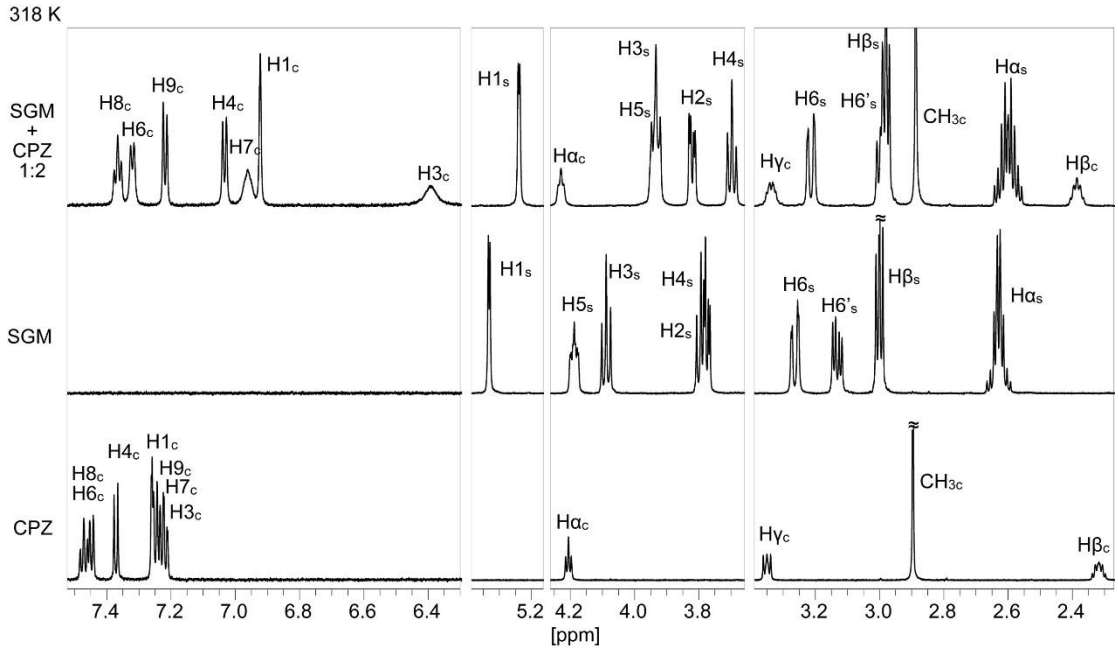

Fig. 9. ^{1}H NMR spectra of 1 mM of CPZ, 0.5 mM of sugammadex and a mixture of 0.5 mM of sugammadex and 1 mM of CPZ in D_2O (T = 45°C, 700 MHz).

In order to confirm the formation of a unique 1:2 sugammadex/CPZ complex unambiguously, the continuous variation's method, known as "Job's method", based on ^{1}H NMR titration experiments was used (See S5-8). This method required that the total concentration of sugammadex and CPZ was kept constant (1 mM) with the ratio r_i being varied from zero to one (with i = CPZ or sugammadex). Plots of the observed $\Delta\delta_i \times [i]$ as a function of r_i led to Job plots. Taking into account the H3 and H_5 protons of sugammadex, the Job plots showed a minimum at $r_{sugammadex} = 0.35$. As for the protons H_1, H_3, H_4 and H_7 of CPZ, the minimum was found for $r_{CPZ} = 0.65$. These values are consistent with a 1:2 stoichiometry for the complex, confirming the obtained result by ITC. This result was confirmed by DOSY measurements at 25°C and 45°C. Indeed, at 25°C, the diffusion coefficient for sugammadex, with or without CPZ, was equal to $D_{sugammadex} = (1.81 \pm 0.06) \times 10^{-10}$ M^2.s^{-1} whatever the CPZ concentration. For CPZ, a diffusion coefficient of CPZ $D_{complexed\ CPZ} = (1.80 \pm 0.03) \times 10^{-10}$ M^2.s^{-1} was determined for $r_{CPZ} < 0.6$ and an increase in the amount of CPZ led to an increase in the diffusion coefficient to reach the value of the diffusion coefficient of pure CPZ ($D_{free\ CPZ} = 4.68 \times 10^{-10}$ M^2.s^{-1}). Similar behaviour was observed at 45°C with the following values: $D_{sugammadex} = (3.89 \pm 0.32) \times 10^{-10}$ M^2.s^{-1}, $D_{complexed\ CPZ} = (4.02 \pm 0.26) \times 10^{-10}$ M^2.s^{-1} (for $r_{CPZ} < 0.6$) and $D_{free\ CPZ} = 8.57 \times 10^{-10}$ M^2.s^{-1}.

Finally, in order to obtain the three-dimensional structure of the sugammadex/CPZ complex, a 2D off-resonance ROESY spectrum was recorded and numerous cross-correlation peaks were observed on the 2D spectrum (Fig. 10). Firstly, due to the large broadening of the H_3 and H_7 protons of CPZ, no cross-correlation peak was detected. One cross-correlation peak was observed between the H_8 proton of CPZ and the H_5 protons of sugammadex and an another between the H_6 proton of CPZ and the H_3 protons of sugammadex. For this last CPZ proton, weak cross-correlation peaks were also observed towards the H_6 and H_β protons of sugammadex. For the other CPZ aromatic protons (H_1, H_4 and H_9),

strong cross-correlation peaks were noticed with the H_3 and H_5 protons of sugammadex and weaker ones were observed towards the H_6 and H_β protons of sugammadex. In the case of the methylene protons of the aliphatic chain of CPZ, a strong cross-correlation peak was observed between the H_α proton of CPZ and the H_3 and H_5 protons of sugammadex while the two others methylene protons H_β and H_γ showed weak cross-correlation peaks towards the H_3 and H_5 protons of sugammadex. Weak cross-correlation peaks were observed for the H_α and H_γ protons of CPZ towards the H_β protons of sugammadex and a weaker one was detected between the H_α protons of CPZ and the H_6 protons of sugammadex. It should be pointed out that $H_{6'}$ and H_α of sugammadex did not show any cross-correlation peak with the protons of CPZ.

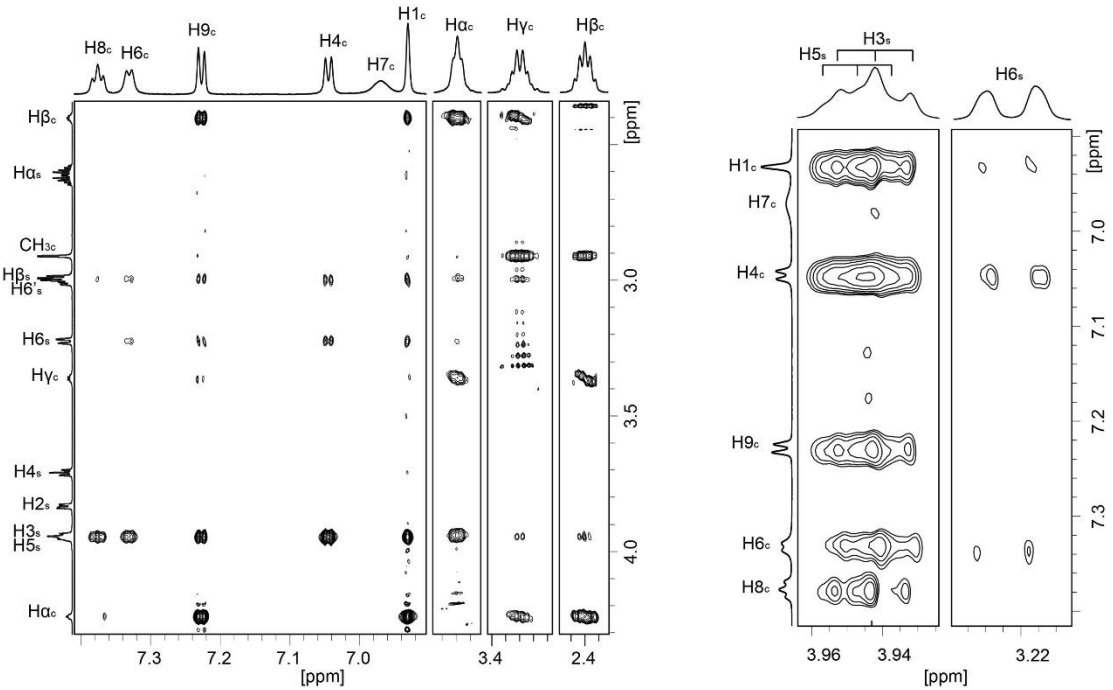

Fig. 10. Partial contour plots from an off-resonance ROESY experiment (45°C, 950 MHz, D_2O, effective angle: 54.7°, mixing time: 200 ms) recorded on a mixture of sugammadex (0.5 mM) and CPZ (1 mM).

In order to obtain further data, a 2D off-resonance ROESY spectrum was recorded on a 1:1 mixture but unfortunately no new information could be

deduced from this spectrum. 1D selective ROESY spectra were recorded on the 1:2 mixture of sugammadex and CPZ in the place of the 2D off-resonance ROESY spectrum. From these spectra, it could be seen that the H_6 and H_8 protons of CPZ were located near the H_3 and H_5 protons of sugammadex. Moreover, selective excitation of the H_α of the aliphatic chain of CPZ allows us to conclude that these protons are close to the H_3 protons of sugammadex. Taking account of all these structural data, several three-dimensional models have been considered. The two aliphatic chains are probably orientated in opposite directions, the first being in the side-chains on the primary side of the sugammadex and the second located at the secondary side of the sugammadex. Moreover, the first CPZ is probably located in the extra cavity defined by the side-chains and more precisely the chlorinated ring. Considering the second CPZ molecule, π-π stacking interactions must be involved between the unchlorinated cycle of the CPZ molecule that is deeply anchored within the cyclodextrin and the chlorinated cycle of the second CPZ molecule. However, molecular modelling was not able to confirm our hypothesis as the choice of the initial conditions strongly influences the results obtained.

2.3.7 Impact of the presence of CDs on CPZ photodegradation

As CPZ is photosensitive, we investigated the photodegradation of CPZ in presence of a series of CDs (β-CD, γ-CD, DIME-β-CD, SBE-β-CD, SBE-γ-CD and sugammadex). Based on the different complexation capability, different concentration of CDs was used to mix with 1.4 mM of CPZ, to obtain the same percentage (95%) of CPZ that could form complexes. As shown in Fig. 11, 77% of CPZ was degraded in absence of CDs after 240 min, confirming the low photostability of CPZ. To simplify the comparison, 240 min of UV exposure was used in the following discussion. The photodegradation was enhanced in presence of all the CDs studied (see the photodegradation profile in S11). For example, only 8% of CPZ was remained when β-CD was added, while this value decreased to 1% in presence of sugammadex, although

it has the highest complexation constant with CPZ. In addition, according to the residual CPZ concentration as a function of time, we found the degradation of CPZ (with or without CD) follows first-order reaction kinetics. The initial rate constant and corresponding $t_{1/2}$was listed in Table 2.

Table 2 Parameters of CPZ solution with CDs.

	-	β-CD	DIMEB	SBE-β	γ-CD	SBE-γ	SGM
CPZ concentration (mM)	1.4	1.4	1.4	1.4	1.4	1.4	1.4
CD concentration (mM)	-	2.9	2.2	1.9	13.5	6.3	0.7
Initial rate constant (min^{-1})	0.0213	0.0175	0.0159	0.0185	0.0211	0.0197	0.0243
$t_{1/2}$ (min)	32.5	39.6	43.6	37.5	32.9	35.2	28.5
Residual CPZ after 240 min (%)	23	8	7	5	4	2	1

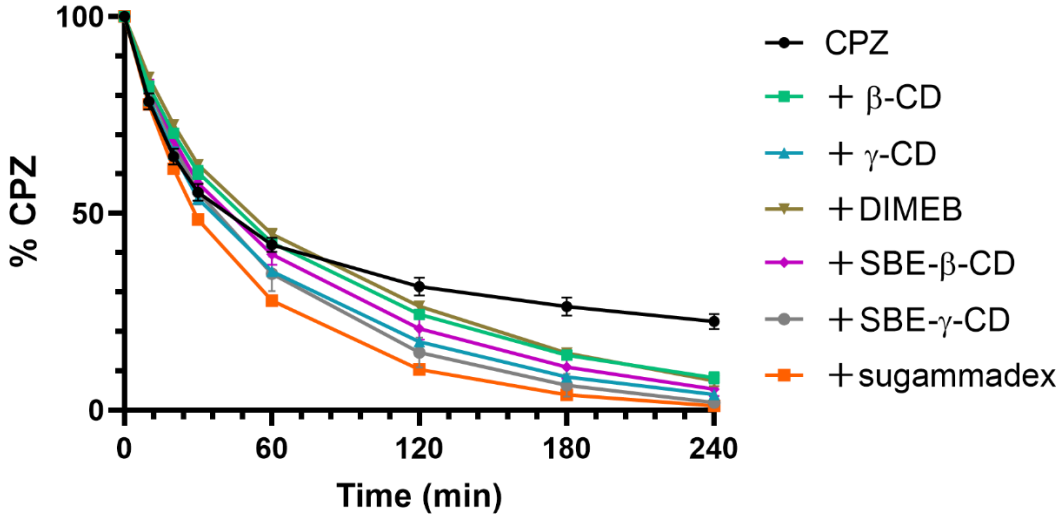

Fig. 11. Photodegradation of CPZ in presence of CDs. The results are mean ± SD of three replicate experiments.

In fact, CDs exhibit act as a photo-stabilizer in numerous cases. For example, the photostability of Rhein, an anthraquinonic drug, was significantly improved by forming inclusion complexes with β-CD and HP-β-CD (Petralito et al. 2009). HP-β-CD also showed a protective effect on the photostability of cilnidipine (Hu et al. 2012). However,

CDs may play a different role under some conditions. A systematic investigation on the photostability of nicardipine was carried out by Pomponio et al, using a range of CDs and either a protective or an accelerating effect was observed depending on the CD (Pomponio et al. 2004). The mechanism by which CDs accelerate CPZ has not yet been determined. A hypothesis could be that CD may act as a catalyst during the photodegradation, thus further study on the degradation products would help to elucidate the mechanism.

2.4 Conclusion

ITC experiments showed that it was possible to form inclusion complexes between CPZ complexes and different kinds of CDs. The stoichiometry of the complexes obtained varied (1:1, 1:2 or mixture of 1:1 and 1:2), and sugammadex gave the highest complexation constant. The association process was either enthalpy-driven or entropy-driven, depending on the cavity size and the chemical modification on the CDs. Structural investigation (1D NMR spectrum and 2D ROESY spectrum) of the inclusion complexes, backed up by molecular dynamic simulation in some cases, revealed that different regions or orientations of the CPZ molecule was included by different CDs. However, all the CDs studied accelerated the photodegradation of CPZ. These results indicate that cyclodextrin complexation of CPZ could play a part in a repurposing strategy but that further formulation steps will be necessary to avoid photodegradation.

Supplement

Figure S1. Temperature dependence of the ^{1}H NMR spectrum of a mixture of 0.87 mM of γ-CD and 1 mM of CPZ (700 MHz).

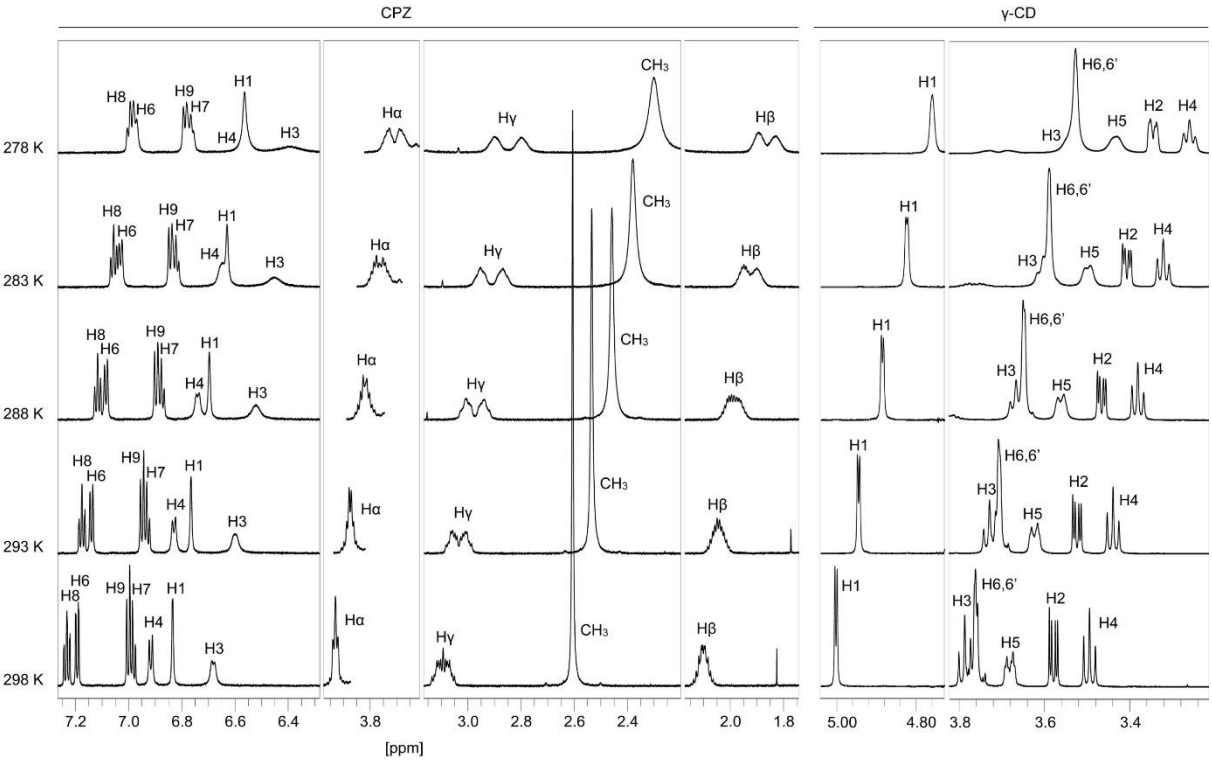

Figure S2. Partial contour plot from an off-resonance ROESY experiment (25°C, 700 MHz, D_2O, effective angle: 54.7°, mixing time: 300 ms) recorded on a mixture of γ-CD (0.87 mM) and CPZ (1 mM).

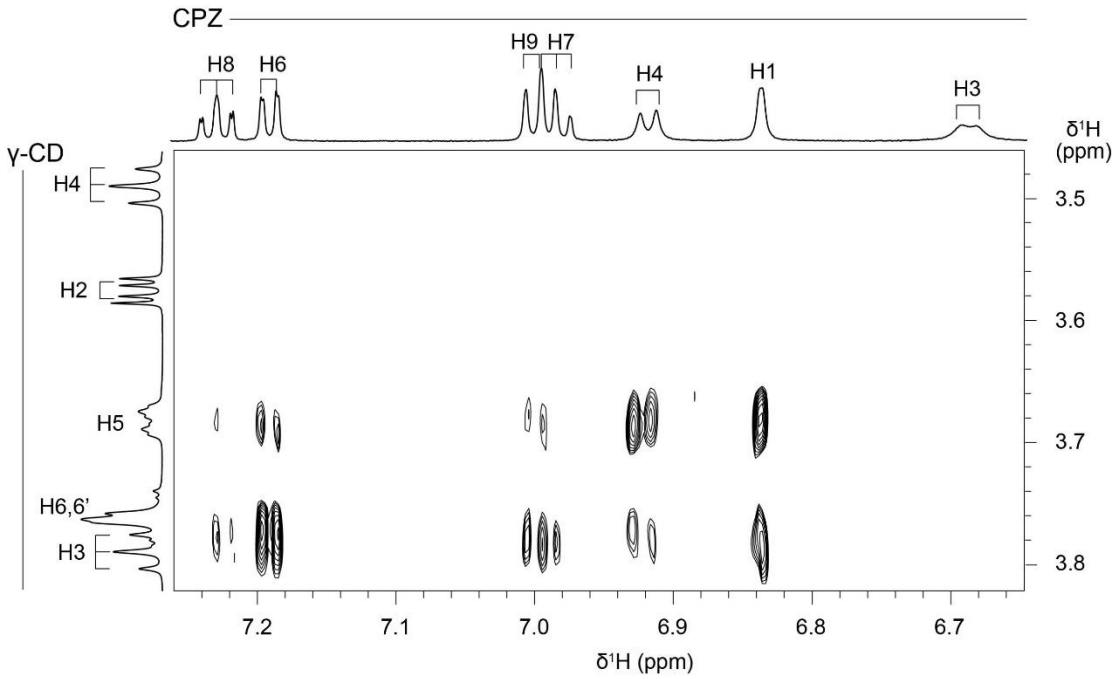

Figure S3. Partial contour plot from an off-resonance ROESY experiment (25°C, 700 MHz, D_2O, effective angle: 54.7°, mixing time: 300 ms) recorded on a mixture of γ-CD (9.5 mM) and CPZ (1 mM).

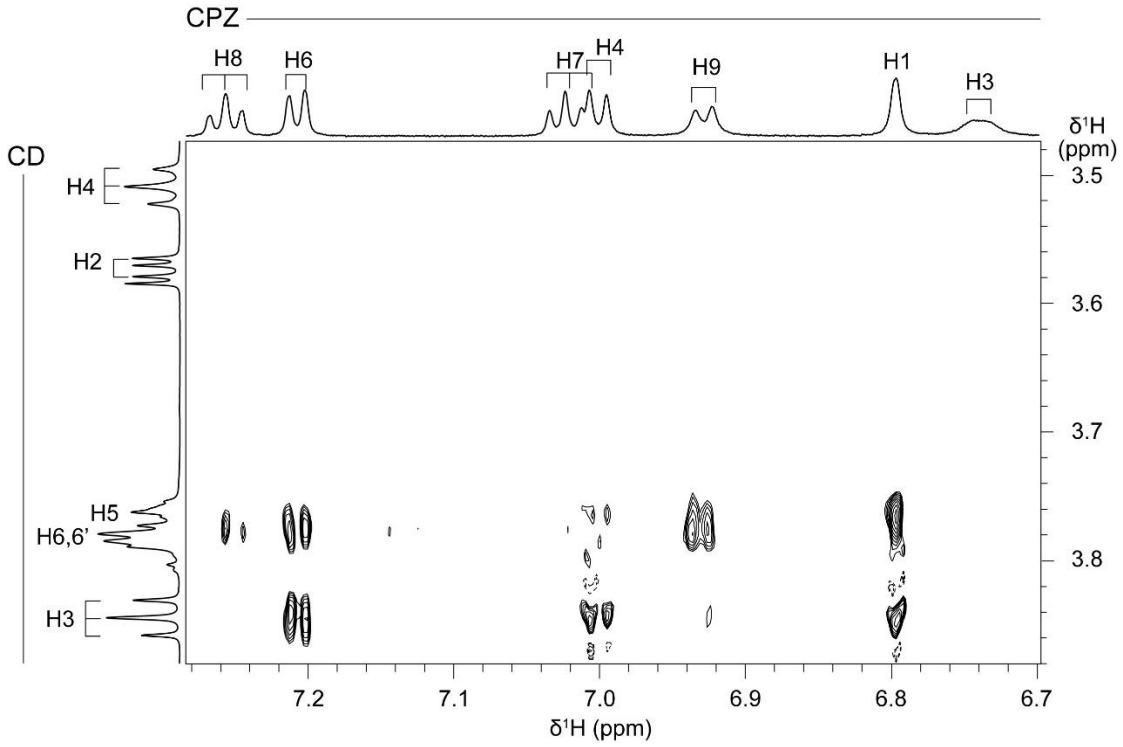

Figure S4. ^{1}H NMR spectra of 1 mM of CPZ, 0.5 mM of sugammadex and a mixture of 0.5 mM of sugammadex and 1 mM of CPZ in D_2O (T = 25°C, 700 MHz).

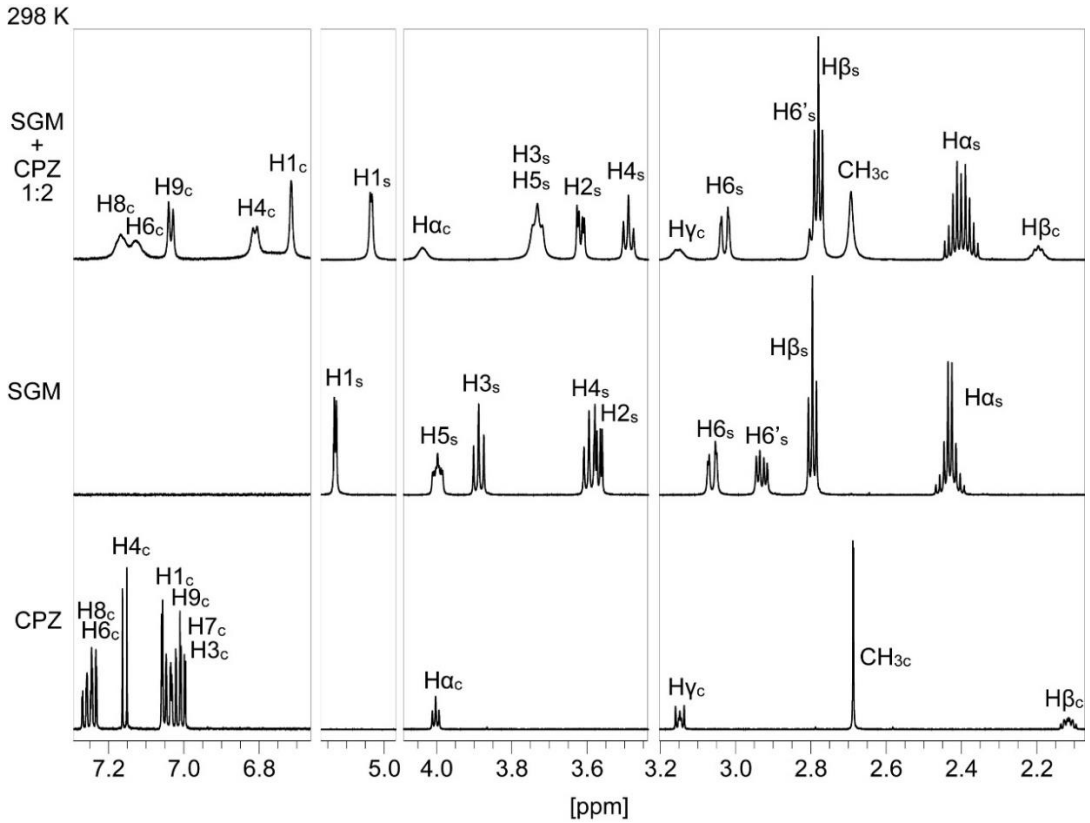

Figure S5. Continuous variation plot (Job Plot) for the H_3 (•) and H_5 (•) protons of sugammadex (600 MHz, D_2O, 45°C).

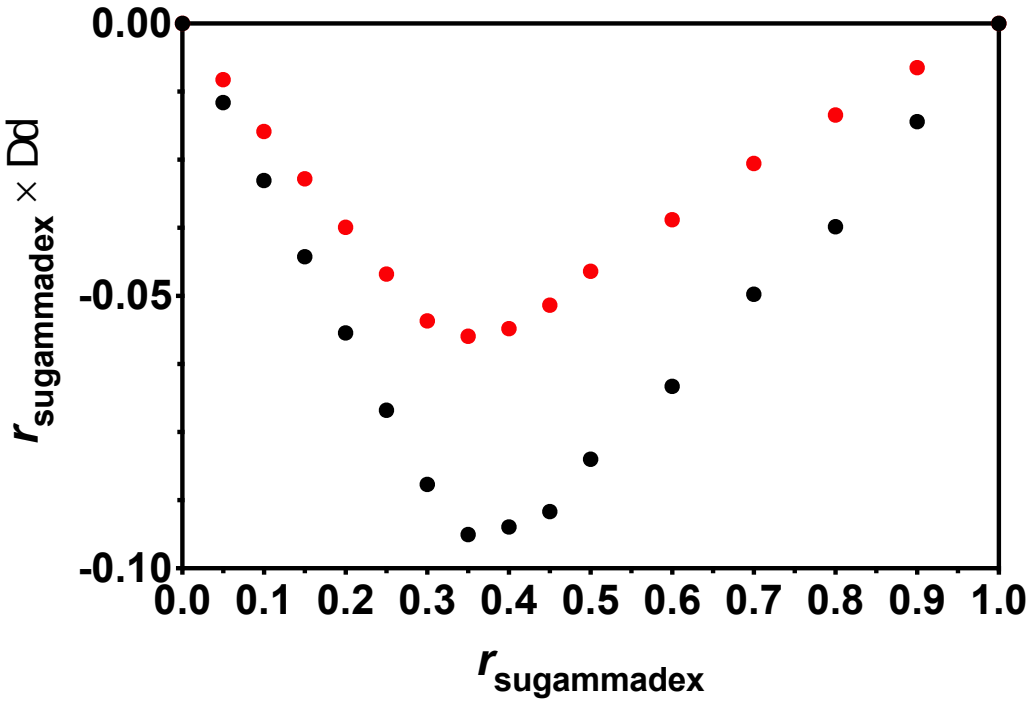

Figure S6. Continuous variation plot (Job Plot) for the H_1 (•), H_3 (•), H_4 (•) and H_7 (•) protons of chlorpromazine (600 MHz, D_2O, 45°C).

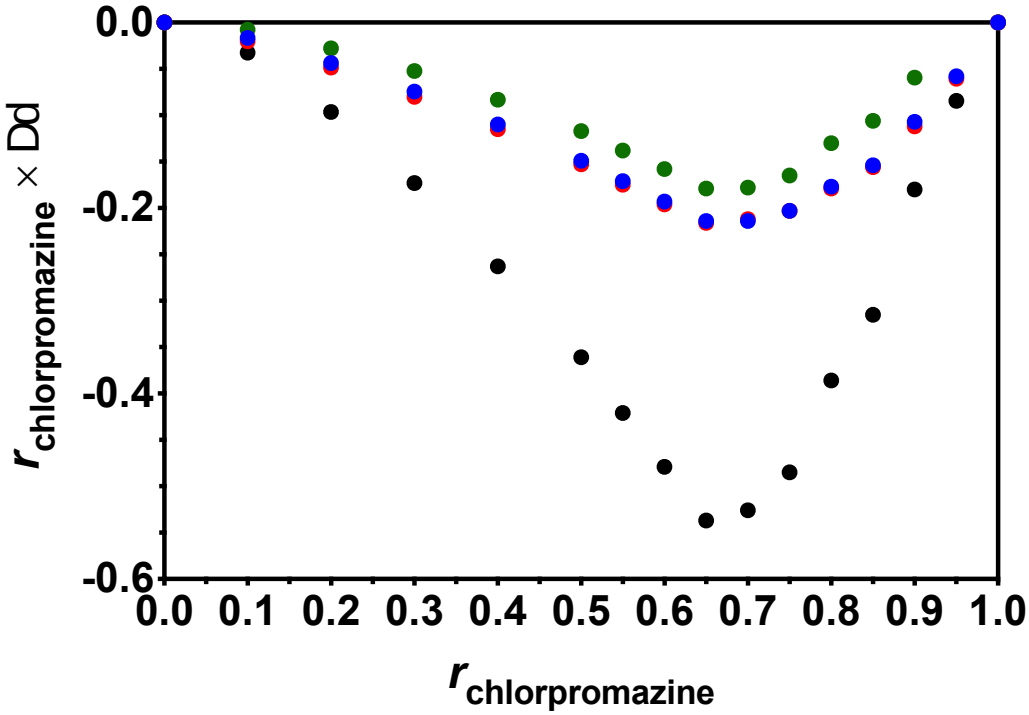

Figure S7. Evolution of the diffusion coefficients of sugammadex (•) and chlorpromazine (•) as a function of r_{CPZ} (600 MHz, D_2O, 25°C).

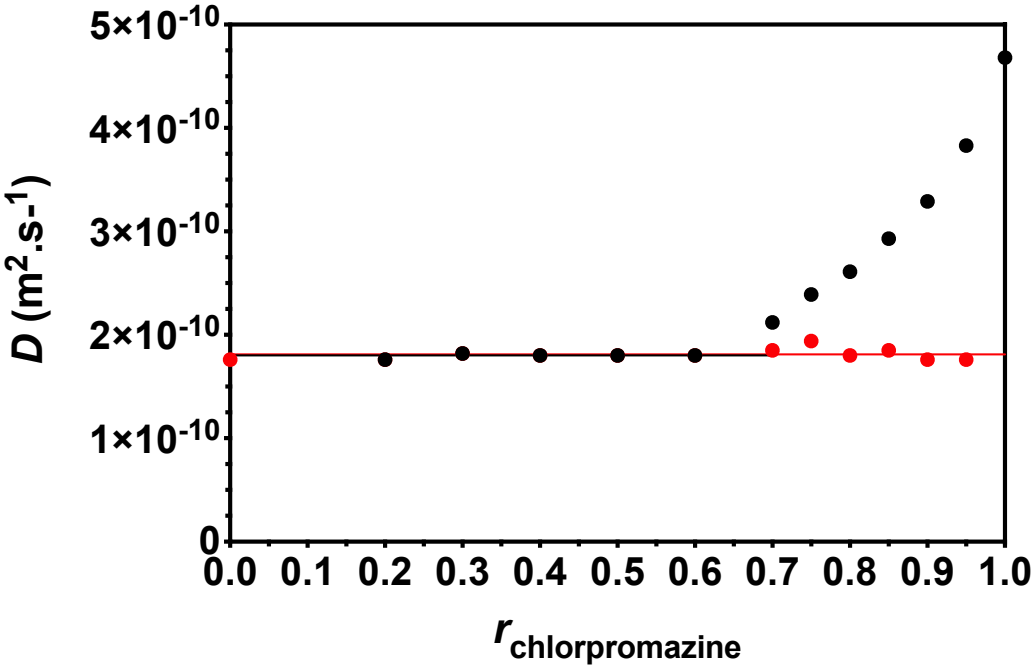

Figure S8. Evolution of the diffusion coefficients of sugammadex (•) and chlorpromazine (•) as a function of r_{CPZ} (600 MHz, D_2O, 45°C).

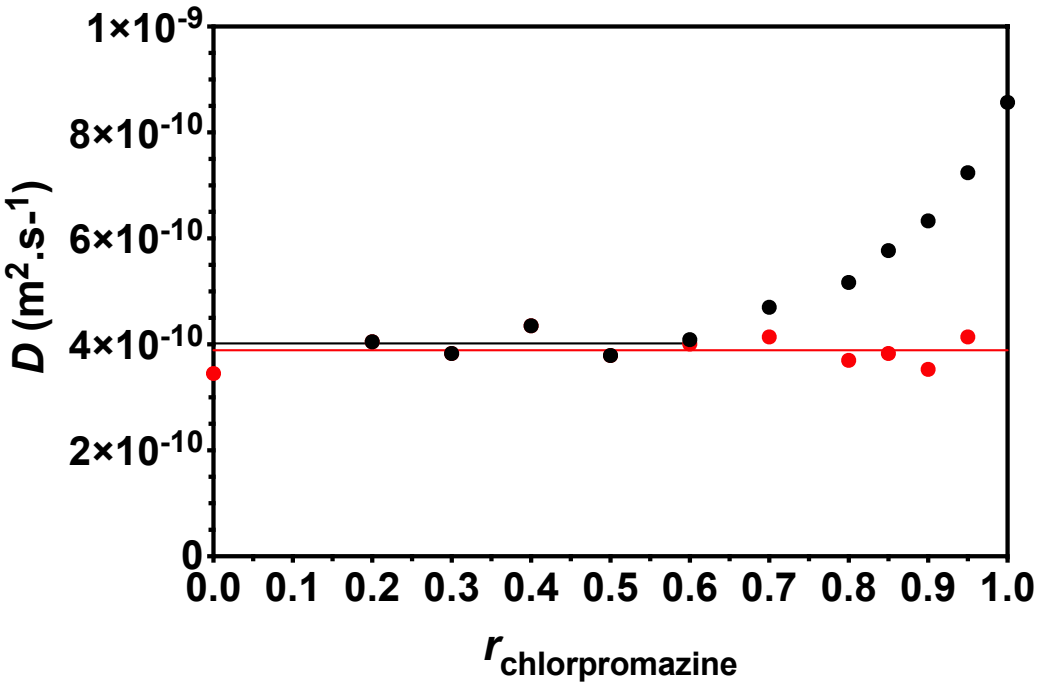

Figure S9. Partial contour plots from an off-resonance ROESY experiment (45°C, 950 MHz, D_2O, effective angle: 54.7°, mixing time: 200 ms) recorded on a mixture of sugammadex (0.5 mM) and CPZ (0.5 mM).

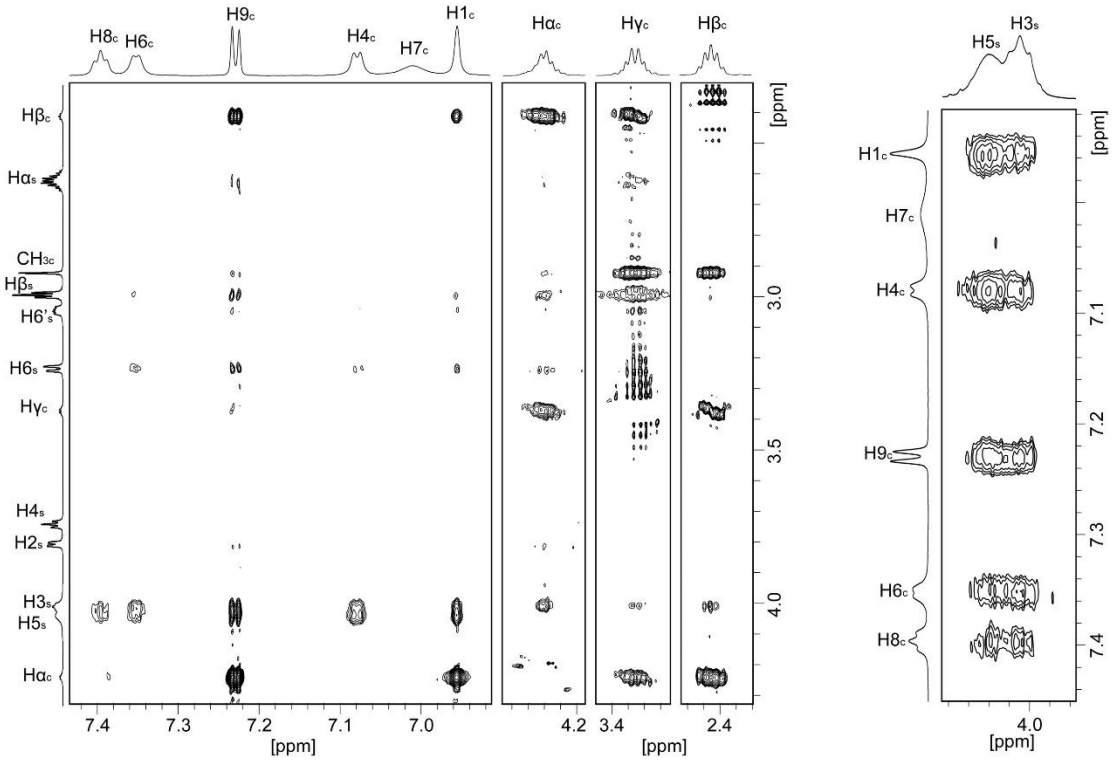

Figure S10. Spectra of a mixture of 0.5 mM of sugammadex and 1 mM of chlorpromazine in D_2O at 45°C. From bottom to top: 1D proton spectrum and 1D-ROESY proton spectra with selective excitation of protons H_1, H_4, H_6, H_8, H_9 of chlorpromazine, H_6 of sugammadex and H_α of chlorpromazine, respectively.

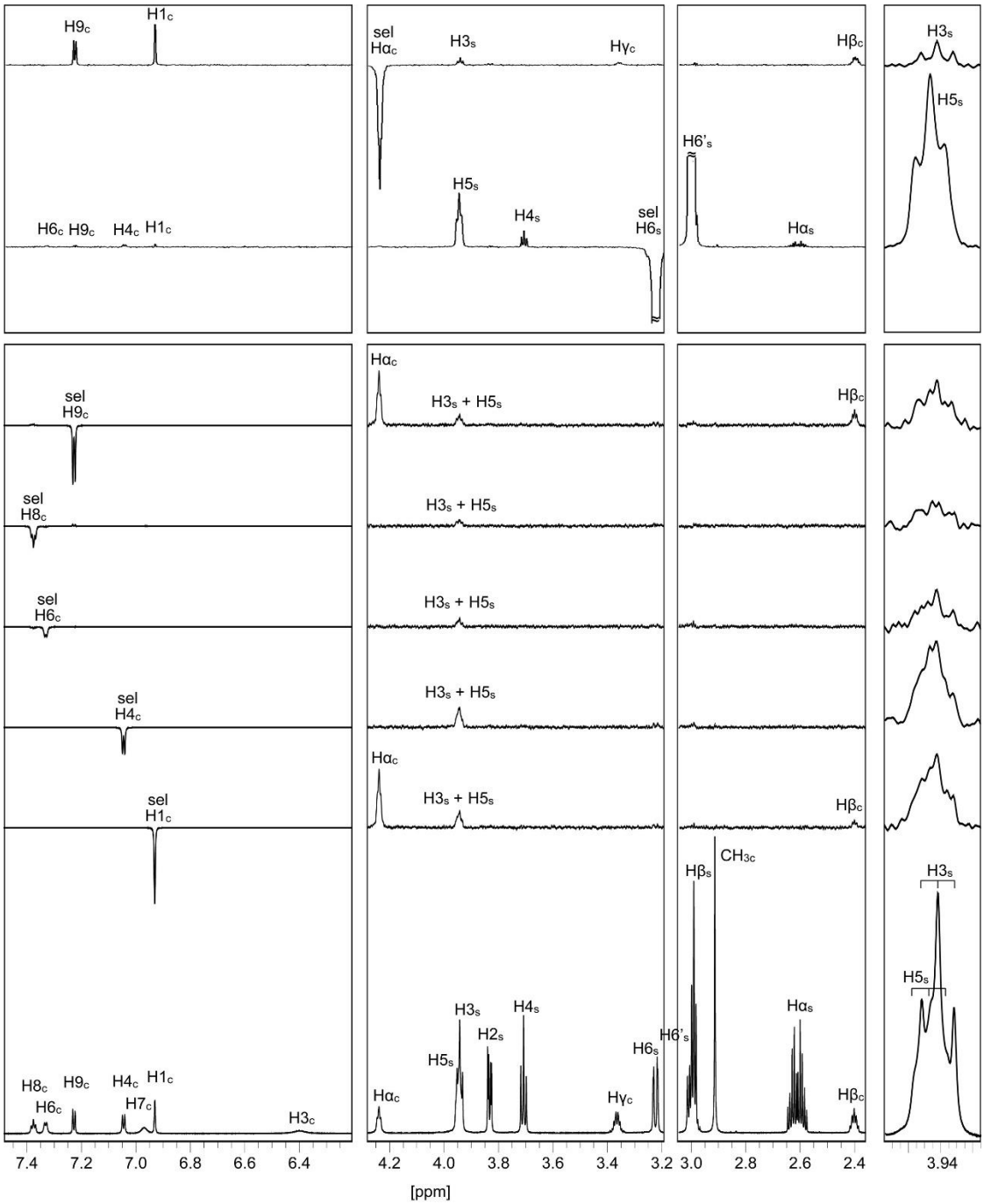

Figure S11. Photodegradation profile of CPZ in presence of CDs.

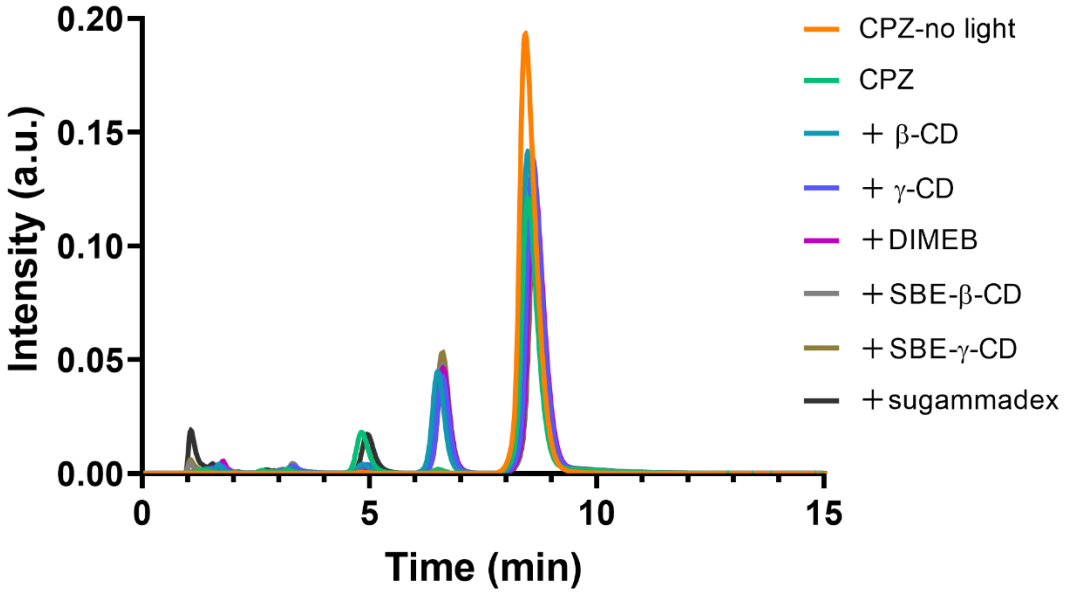

References

Berendsen HJ, Postma JV, van Gunsteren WF, DiNola AR, Haak JR. Molecular dynamics with coupling to an external bath. The Journal of Chemical Physics. 1984 81(8):3684-90.

Bertaut E, Landy D. Improving ITC studies of cyclodextrin inclusion compounds by global analysis of conventional and non-conventional experiments. Beilstein Journal of Organic Chemistry. 2014 10(1):2630-41.

Brem, B., Gal, E., Găină, L., Silaghi-Dumitrescu, L., Fischer-Fodor, E., Tomuleasa, C.I., Grozav, A., Zaharia, V., Filip, L. and Cristea, C., 2017. Novel thiazolo [5, 4-b] phenothiazine derivatives: synthesis, structural characterization, and in vitro evaluation of antiproliferative activity against human leukaemia. International Journal of Molecular Sciences, 18(7), 1365.

Brocos P, Banquy X, Díaz-Vergara N, Pérez-Casas S, Pineiro Á, Costas M. A critical approach to the thermodynamic characterization of inclusion complexes: multiple-temperature isothermal titration calorimetric studies of native cyclodextrins with sodium dodecyl sulfate. The Journal of Physical Chemistry B. 2011 115(49):14381-96.

Calias P. 2-Hydroxypropyl-β-cyclodextrins and the Blood-Brain Barrier: Considerations for Niemann-Pick Disease Type C1. Current Pharmaceutical Design. 2017 23(40):6231-8.

Case DA, JTB R, Betz DS, Cerutti III TE, Cheatham III TA, Darden RE. Duke, TJ Giese, H. Gohlke, AW Goetz, N. Homeyer, S. Izadi, P. Janowski, J. Kaus, A. Kovalenko, TS Lee, S. LeGrand, P. Li, T. Luchko, R. Luo, B. Madej, KM Merz, G. Monard, P. Needham, H. Nguyen, HT Nguyen, I. Omelyan, A. Onufriev, DR Roe, A. Roitberg, R. Salomon-Ferrer, CL Simmerling, W. Smith, J. Swails, RC Walker, J. Wang, RM Wolf, X. Wu, DM York and PA Kollman Amber. 2015.

Cézard C, Trivelli X, Aubry F, Djedaïni-Pilard F, Dupradeau FY. Molecular dynamics studies of native and substituted cyclodextrins in different media: 1. Charge derivation and force field performances. Physical Chemistry Chemical Physics. 2011 13(33):15103-21.

Clarke RJ, Coates JH, Lincoln SF. Complexation of roccellin by β-and γ-cyclodextrin. Journal of the Chemical Society, Faraday Transactions 1: Physical Chemistry in Condensed Phases. 1986 82(8):2333-43.

Döhner H, Estey EH, Amadori S, Appelbaum FR, Büchner T, Burnett AK, Dombret H, Fenaux P, Grimwade D, Larson RA, Lo-Coco F. Diagnosis and management of acute myeloid leukemia in adults: recommendations from an international expert panel, on behalf of the European LeukemiaNet. Blood. 2010 115(3):453-74.

Dupradeau FY, Cezard C, Lelong R, Stanislawiak E, Pêcher J, Delepine JC, Cieplak P. RE DD. B.: a database for RESP and ESP atomic charges, and force field libraries.

Nucleic Acids Research. 2007 36:D360-7.

Essmann U, Perera L, Berkowitz ML, Darden T, Lee H, Pedersen LG. A smooth particle mesh Ewald method. The Journal of Chemical Physics. 1995 Nov 15;103(19):8577-93.

Frisch MJ, Trucks GW, Schlegel HB, Scuseria GE, Robb M, Cheeseman JR, Scalmani G, Barone V, Mennucci B, Petersson GA, Nakatsuji H. Gaussian 09, Revision D. 01, Gaussian. Inc.: Wallingford, CT. 2009.

Hardee GE, Otagiri M, Perrin JH. Microcalorimetric investigations of pharmaceutical complexes. I. Drugs and beta-cyclodextrin. Acta pharmaceutica Suecica. 1978 15(3):188.

Hirai H, Toshima N, Uenoyama S. Inclusion complex formation of cyclodextrin with large dye molecule. Polymer Journal. 1981 13(6):607.

Hoshino T, Ishida K, Irie T, Uekama K, Ono T. An attempt to reduce the photosensitizing potential of chlorpromazine with the simultaneous use of β-and dimethyl-β-cyclodextrins in guinea pigs. Archives of Dermatological Research. 1989 281(1):60-5.

Hu L, Zhang H, Song W, Gu D, Hu Q. Investigation of inclusion complex of cilnidipine with hydroxypropyl-β-cyclodextrin. Carbohydrate Polymers. 2012 90(4):1719-24.

Irie T, Uekama K. Protection against the photosensitized skin irritancy of chlorpromazine by cyclodextrin complexation. Journal of Pharmacobio-dynamics. 1985 8(9):788-91.

Ishida K, Hoshino T, Irie T, Uekama K. Alleviation of chlorpromazine-photosensitized contact dermatitis by β-cyclodextrin derivatives and their possible mechanisms. Drug Metabolism and Pharmacokinetics. 1988 3(4):377-86.

Jaszczyszyn A, Gąsiorowski K, Świątek P, Malinka W, Cieślik-Boczula K, Petrus J, Czarnik-Matusewicz B. Chemical structure of phenothiazines and their biological activity. Pharmacological Reports. 2012 64(1):16-23.

Johnson Jr CS. Diffusion ordered nuclear magnetic resonance spectroscopy: principles and applications. Progress in Nuclear Magnetic Resonance Spectroscopy. 1999 34(3-4):203-56.

Jorgensen WL, Chandrasekhar J, Madura JD, Impey RW, Klein ML. Comparison of simple potential functions for simulating liquid water. The Journal of Chemical Physics. 1983 79(2):926-35.

Juliusson G, Antunovic P, Derolf Å, Lehmann S, Möllgård L, Stockelberg D, Tidefelt U, Wahlin A, Höglund M. Age and acute myeloid leukemia: real world data on decision to treat and outcomes from the Swedish Acute Leukemia Registry. Blood. 2009 113(18):4179-87.

KITAMURA K, IMAYOSHI N. Second-derivative spectrophotometric determination of the binding constant between chlorpromazine and β-cyclodextrin in aqueous

solutions. Analytical Sciences. 1992 8(4):497-501.

Lichtman MA. A historical perspective on the development of the cytarabine (7 days) and daunorubicin (3 days) treatment regimen for acute myelogenous leukemia: 2013 the 40th anniversary of 7+ 3. Blood Cells, Molecules, and Diseases. 2013 50(2):119-30.

Monnaert V, Tilloy S, Bricout H, Fenart L, Cecchelli R, Monflier E. Behavior of α-, β-, and γ-cyclodextrins and their derivatives on an in vitro model of blood-brain barrier. Journal of Pharmacology and Experimental Therapeutics. 2004 310(2):745-51.

O'Connor AE, Gallagher WM, Byrne AT. Porphyrin and nonporphyrin photosensitizers in oncology: preclinical and clinical advances in photodynamic therapy. Photochemistry and Photobiology. 2009 85(5):1053-74.

Okimoto K, Miyake M, Ohnishi N, Rajewski RA, Stella VJ, Irie T, Uekama K. Design and evaluation of an osmotic pump tablet (OPT) for prednisolone, a poorly water soluble drug, using (SBE) 7m-β-CD. Pharmaceutical Research. 1998 15(10):1562-8.

Otagiri M, Uekama K, Ikeda K. Inclusion complexes of β-cyclodextrin with tranquilizing drugs phenothiazines in aqueous solution. Chemical and Pharmaceutical Bulletin. 1975 23(1):188-95.

Petralito S, Zanardi I, Memoli A, Annesini MC, Travagli V. Solubility, spectroscopic properties and photostability of Rhein/cyclodextrin inclusion complex. Spectrochimica Acta Part A: Molecular and Biomolecular Spectroscopy. 2009 74(5):1254-9.

Pinero LE, Lebrón I, Correa J, Díaz J, Viera L, Arce R, García C, Oyola R. The effect of 2-hydroxypropyl-β-cyclodextrin on the excited triplet state of promazine and chlorpromazine. Journal of Photochemistry and Photobiology A: Chemistry. 2012 228(1):44-50.

Pomponio R, Gotti R, Fiori J, Cavrini V, Mura P, Cirri M, Maestrelli F. Photostability studies on nicardipine–cyclodextrin complexes by capillary electrophoresis. Journal of pharmaceutical and biomedical analysis. 2004 35(2):267-75.

Rai S, Tanaka H, Suzuki M, Tanimura A, Matsui K, Watanabe T, Kanakura Y, Matsumura I. Chlorpromazine, an Inhibitor of Intracellular Trafficking of FLT3-ITD and KIT D816V, Shows Prominent Anti-Leukemic Activities Against AML Cells and AML Stem Cells in Vitro and in Vivo. Matsumura Blood 2014 124:269

Rekharsky MV, Inoue Y. Complexation thermodynamics of cyclodextrins. Chemical reviews. 1998 98(5):1875-918.

Roe DR, Cheatham III TE. Ptraj and Cpptraj: software for processing and analysis of molecular dynamics trajectory data. Journal of Chemical Theory and Computation. 2013 9(7):3084-95.

Ryckaert JP, Ciccotti G, Berendsen HJ. Numerical integration of the cartesian equations of motion of a system with constraints: molecular dynamics of n-alkanes. Journal of

Computational Physics. 1977 23(3):327-41.

Shiotani k, Uehata k, Irie T, Hirayama F, Uekama K. Characterization of the Inclusion Mode of β-Cyclodextrin Sulfate and Its Effect on the Chlorpromazine-Induced Hemolysis of Rabbit Erighrocytes. Chemical and Pharmaceutical Bulletin. 1994 42(11):2332-7.

Syed SK, Christopherson RI, Roufogalis BD. Reversal of vinblastine transport by chlorpromazine in membrane vesicles from multidrug-resistant human CCRF-CEM leukaemia cells. British Journal of Cancer. 1998 78(3):321.

Takamura K, Inoue S, Kusu F. Two-guest inclusion complex of cyclodextrin with chlorpromazine. Chemistry Letters. 1983 12(2):233-6.

Takisawa N, Shirahama K, Tanaka I. Interactions of amphiphilic drugs withα-, β-, and γ-cyclodextrins. Colloid and Polymer Science. 1993 271(5):499-506.

Tellinghuisen J. Optimizing experimental parameters in isothermal titration calorimetry. The Journal of Physical Chemistry B. 2005 109(42):20027-35.

Uekama K, Irie T, Sunada M, Otagiri M, Iwasaki K, Okano Y, Miyata T, Kase Y. Effects of cyclodextrins on chlorpromazine-induced haemolysis and central nervous system responses. Journal of Pharmacy and Pharmacology. 1981 33(1):707-10.

Uekama K, Irie T, Hirayama F. Participation of cyclodextrin inclusion catalysis in photolysis of chlorpromazine to give promazine in aqueous solution. Chemistry Letters. 1978 7(10):1109-12.

Vecsernyés M, Fenyvesi F, Bácskay I, Deli MA, Szente L, Fenyvesi É. Cyclodextrins, blood–brain barrier, and treatment of neurological diseases. Archives of Medical Research. 2014 45(8):711-29.

Wang J, Wolf RM, Caldwell JW, Kollman PA, Case DA. Development and testing of a general amber force field. Journal of Computational Chemistry. 2004 25(9):1157-74.

Xu H, Rodríguez-Hermida S, Pérez-Carvajal J, Juanhuix J, Imaz I, Maspoch D. A First Cyclodextrin-Transition Metal Coordination Polymer. Crystal Growth & Design. 2016 16(10):5598-602.

Zhao Y, Truhlar DG. The M06 suite of density functionals for main group thermochemistry, thermochemical kinetics, noncovalent interactions, excited states, and transition elements: two new functionals and systematic testing of four M06-class functionals and 12 other functionals. Theoretical Chemistry Accounts. 2008 120(1-3):215-41.

Chapter 3

Physicochemical studies of the formulation

3.1 Introduction

CPZ is a well-known first-generation antipsychotic and has been regarded as the "gold standard" for almost 70 years for the treatment of psychological disorders. In 1985, Hait et al reported that CPZ and chlorpromazine-sulfoxide showed significant inhibiting effect on the growth of murine leukemic lymphocytes (L1210 and L5178Y) and human promyelocytic leukemic granulocytes (HL-60) (Hait et al. 1985). This finding indicates the therapeutic potential of CPZ for AML treatment but a suitable drug delivery system is essential to help CPZ to circumvent the BBB and target the bone marrow.

As explained in the introduction above, the drug-in-CD-in-liposomes (DCL) system could provide a promising solution for the delivery of CPZ, by first entrapping CPZ in the hydrophobic cavity of CD and encapsulating the CD/CPZ inclusion complexes into liposomes afterwards. In order to optimize this system, the resulting interactions between CD, CPZ and phospholipids need to be investigated and clarified. In the previous chapter, the CD/CPZ inclusion complexes were systematically studied, including the formation constant, complex structure and photodegradation of CPZ in presence of a variety of CDs. Another property that needs to be investigated is the lipid-extracting capability of CDs, due to the hydrophobic nature of their internal cavity. It was found that CD (α-, β- and γ-CD) could cause a definite destruction of the phospholipid bilayers above a CD/DPPC ratio (Chellam and Mandal 2013). Additionally, Piel reported that the destructive capacity of CDs was closely related to their affinity for lipid components (Piel et al. 2007).

To better understand the effect of CDs or CPZ on phospholipids, a critical physicochemical property, lipid phase, should be addressed. Generally, there are several bilayer phases for fully saturated phosphatidylcholine derivatives (Fig. 1). The lipid can form a crystalline phase (L_c) when kept at low temperature for a long period, in which the hydrocarbon tails are highly ordered on an orthorhombic lattice. The crystalline phase can be transformed to a gel phase by heating, resulting in a tilted form

($L_{\beta'}$) with the expansion of acyl chains, which packed on a quasi-hexagonal lattice. With increasing temperature (after the pre-transition), a ripple phase ($P_{\beta'}$) would form due to the periodic modulation of the lipid bilayer. A liquid crystalline phase (L_{α}) can be observed at higher temperature (after the main-transition) in which the tails are completely disordered (Cunningham et al. 1998 ; Ruocco and Shipley 1982).

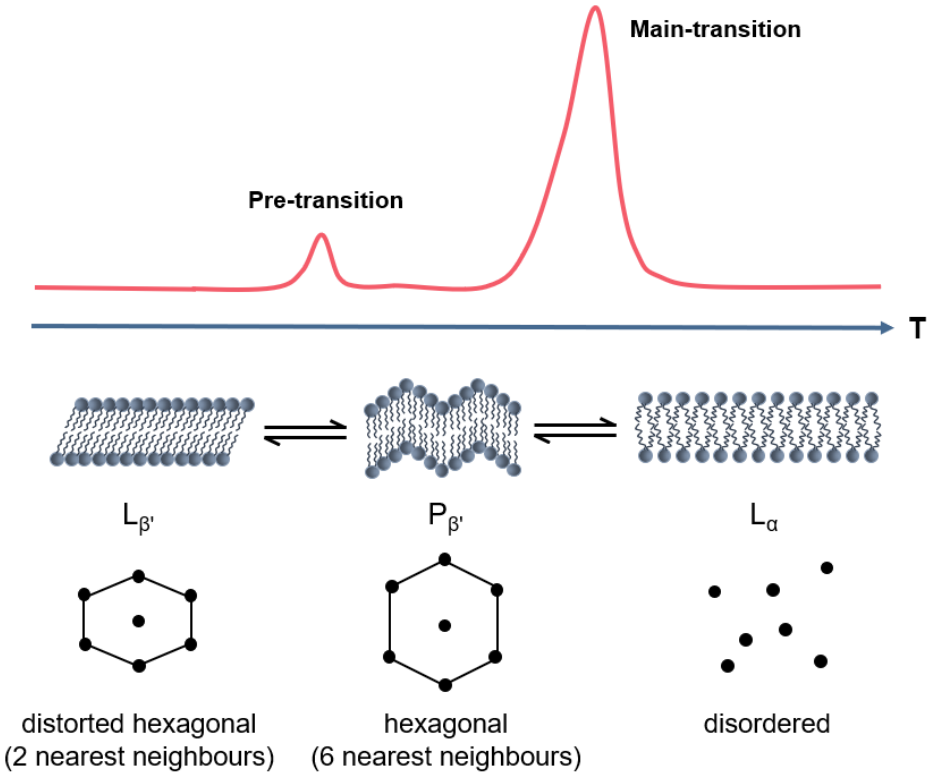

Fig. 1. Characteristics of lipid at different phases, reproduced from (Pignatello et al. 2011).

Based on its phase transition behavior, the impact of CDs on the thermotropic behavior of PSPC was first studied by differential scanning calorimetry (DSC), a frequently used thermo analytical technique. Subsequently, small-angle X-ray scattering (SAXS) was performed to obtain the bilayer thickness while wide-angle X-ray scattering (WAXS) was used to determine hydrocarbon chain packing. Turbidimetry experiments were carried out to investigate the destruction or solubilization of HEPC SUVs after the addition of CDs. Furthermore, an appropriate CPZ concentration to prepare the DCL system was determined by DSC.

3.2 Materials and methods

3.1.1 Materials

HP-β-CD (Cavasol® W7HP Pharma) and HP-γ-CD (Cavasol® W8HP Pharma) were gifts from Ashland Global Specialty Chemicals Inc. SBE-β-CD (Captisol®), SBE-γ-CD and SBE-Et-β-CD were gifts from Ligand Pharmaceuticals Inc. Sugammadex (Bridion®) was kindly provided Dr. Luc de Chaisemartin from Bichat Hospital. Chlorpromazine hydrochloride, sodium chloride and HEPES were purchased from Sigma-Aldrich. Milli-Q water was obtained by a Millipore® purification system (Millipore, Germany).

Hydrogenated Egg L-α-phosphatidylcholine (HEPC), 1-palmitoyl-2-stearoyl-sn-glycero-3-phosphocholine (PSPC), cholesterol (ovine wool) and 1,2-distearoyl-sn-glycero-3-phosphoethanolamine-N-[methoxy(polyethylene glycol)-2000] ammonium salt (DSPE-PEG_{2000}) were all supplied by Avanti Polar Lipids, Inc. (Albaster, AL, USA).

3.1.2 Methods

3.1.1.1 Preparation of liposomes

Liposomes were obtained by the film hydration method. Specifically, the components were dissolved in a mixture of chloroform and methanol (2:1, v/v), then organic solvents were evaporated at room temperature under a gentle stream of nitrogen, followed by drying under a vacuum overnight in order to completely remove residual organic solvents. An appropriate volume of filtered buffer (10 mM HEPES, 145 mM sodium chloride, pH 7.4) was added to the film to obtain a total lipid concentration of 30 mM. The lipid suspension subsequently underwent 10 repeats of 1 min heating at 62°C and 1 min vortexing. SUVs were obtained by extrusion (Lipex™, Northern Lipids, Canada) through polycarbonate membranes (1×0.4 μm, 2×0.2 μm, 10× 0.1 μm) at 62°C.

3.1.1.2 Size measurements

Mean hydrodynamic diameters of the liposomes were obtained by dynamic light scattering using a Zetasizer Nano ZS90 (Malvern Instruments Corp., Worcestershire, UK). 40 μL sample was diluted in 1.8 mL buffer (10 mM HEPES, 145 mM sodium chloride, pH 7.4) for the measurements at 25°C. Size distributions by intensity were recorded and the polydispersity index (PDI) was also acquired as an indication of the size distribution.

3.1.1.3 Differential scanning calorimetry (DSC)

DSC measurements were done with a DSC Diamond calorimeter (Perkin Elmer). CD solutions at different concentrations (range from 1 to 50 mM) were prepared with 10 mM HEPES (containing 145 mM sodium chloride, pH 7.4) and 90 mg of CD solution was mixed with 10 mg of PSPC to obtain 10% PSPC (w/w). After heating at 62°C, 15 mg of the mixture was introduced into aluminum capsules. Samples were subjected to repeated heating/cooling procedures in the temperature range of 20-65°C (Table 1). Onset temperature and enthalpy variations (ΔH) of pre-transition peak and main-transition peak were calculated.

Table 1. DSC procedure setting for PSPC investigation

Step	Temperature (°C)	Speed (°C/min)
1	25°C for 10 min	-
2	25-20	5
3	20-65	5
4	65-20	5
5	20-65	5
6	65-20	5
7	20-65	4
8	65-20	5
9	20-65	3
10	65-20	5
11	20-65	2
12	65-20	5
13	20-65	5

3.1.1.4 Micro-DSC

Micro-DSC measurements were carried out using a MicroCal Automated PEAQ-DSC calorimeter (Malvern Instruments). To remove the thermal history of the sample, a first heating scan was recorded between 25 and 80°C at a scan rate of 60°C/h followed by a cooling scan back to the initial temperature at the same rate. Then, a heating scan was recorded at a scan rate of 30°C/h between the same temperatures. The samples used for the micro-DSC measurements were prepared as 10 mg/mL lipid suspensions in HEPES buffer. Each measurement was preceded by a baseline scan with the buffer. The heat capacity of the buffer was subtracted from that of the lipid sample before analysis.

3.1.1.5 X-ray scattering

X-ray scattering experiments were performed on the Austrian SAXS beamline at ELETTRA Synchrotron Light Laboratory (Trieste, Italy). The energy and wavelength of the incident X-ray beam were 8 keV and 1.54 Å respectively. The samples were thermostated in the laboratory-made sample holder, Microcalix, allowing both sample temperature control and simultaneous differential scanning calorimetry analysis. Simultaneous small-angle (SAXS) and wide-angle (WAXS) X-ray scattering patterns were recorded using a Pilatus3 1M detector for the SAXS signal, and a Pilatus 100k detector for the WAXS range. After 2D-image treatment in the SAXS experiments, the scattered intensity was reported as a function of the scattering vector $q = 4\pi\sin\theta/\lambda = 2\pi/d$, where 2θ is the scattering angle, λ is the wavelength and d is the repeat distance between two reticular plans. The calibration of the SAXS and WAXS detectors were achieved using silver behenate and 4-bromobenzoic acid, respectively. The samples were prepared as described in the DSC part (2.2.3) and then loaded into quartz capillaries (Quarzkapillaren, Germany) with an external diameter of 1.5 ± 0.1 mm and a wall thickness of 0.01 mm. All data were analyzed with the IGOR Pro software (WaveMetrics, Inc. USA).

Equidistant peaks can be obtained by SAXS in the lamellar phase of lipid, resulting q_1, q_2, q_3… The repeated distance of the bilayer can be calculated with Bragg law (equation 1):

$$d = n \times 2\pi/q_n \quad (1)$$

The average distance between phospholipids can be deduced from Bragg law as well as using the WAXS data.

3.1.1.6 Turbidity measurements

Turbidity measurements were carried out by continuous addition of CD solution into a quartz cuvette containing SUVs as described in the literature (Boulmedarat et al. 2005; Andrieux et al. 2009; Ramaldes et al. 1996) (Fig. 2). The optical density (OD) was assayed at 350 nm at 25°C by a Perkin-Elmer Lambda 2 double beam spectrophotometer (Perkin-Elmer, Courtaboeuf, France) and recorded by computer. A 1mL precision syringe (Hamilton, Switzerland) on a syringe pump (Braun Perfusor VI, Roucaire, France) was used to gradually inject CD solution into the liposome dispersion at 27.8 µL/min. The raw data, recorded in the form "OD at 350 nm as function of time" were converted to "OD at 350 nm as function of CD concentration" with the following equation:

$$[CD]_{tot}=([CD]_0vt)/(V_0+vt) \quad (2)$$

where $[CD]_{tot}$ is the total concentration of CD in the cuvette at time t, $[CD]_0$ is the initial concentration of CD solution, v is the injection speed of CD solution converted by the rate of syringe pump and V_0 is the starting volume of SUV dispersion. Meanwhile, the lipid concentration ($[Lip]_{tot}$) decreased with the addition of CD solution and it could be calculated with equation 2:

$$[Lip]_{tot}=([Lip]_0V_0)/(V_0+vt) \quad (3)$$

Where $[Lip]_0$ is the initial lipid concentration in the cuvette.

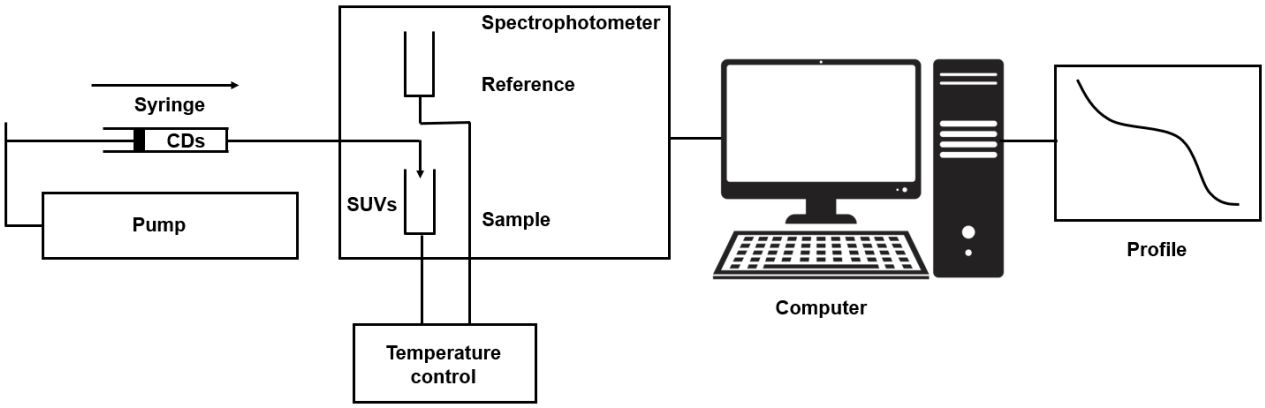

Fig. 2. Work flow of turbidity measurement. Reproduced from (Ramaldes et al, 1996)

3.3 Results and discussion

3.3.1 Interaction between CDs and lipid bilayers

3.3.1.1 Impact of CDs on the thermotropic behavior of PSPC

As a key factor in the DCL system, the interaction between CD and phospholipid bilayers needs in-depth understanding. The thermotropic properties of phospholipid in presence of CD were investigated by DSC. PSPC was as the phospholipid for this study since HEPC is naturally occurring phospholipid with a mixture of fatty acids and PSPC is the main species present in HEPC. Cholesterol was not included in the evaluation because it would significantly attenuate the phase transition of the phospholipids (Ohvo-rekila et al. 2002).

Saturated phospholipids can exhibit several thermotropic phase transitions, such as the main-transition and pre-transition, which have been extensively studied. For long-chain saturated PC lipid bilayers, a low-temperature chain packing transition, sub-main transition can be observed between the pre-transition and main-transition with a low enthalpy (Jørgensen 1995; Pressl et al. 1997; Trandum et al. 1999). As this phenomenon has never been described in the literature for PSPC and to have an insight into it, we carried out micro-DSC investigations on PSPC. Fig. 3 shows the thermogram of pure PSPC, with a clear main transition peak (Tm-onset = 48.7°C) (Fig. 3). In

addition, the enlarged inset demonstrates the peaks of the pre-transition and sub-main transitions, with T-onset of 35.3°C and 47.0°C, respectively. Jørgensen et al also reported the occurrence of the highly cooperative low-enthalpy transition close to the main transition of DCPC vesicles (Trandum et al. 1999). For the thermal experiments with cyclodextrins, only pre-transition and main transition will be considered, as the sub-main transition phenomenon is highly dependent on parameters such as ionic strength, cooling rate and low temperature storage.

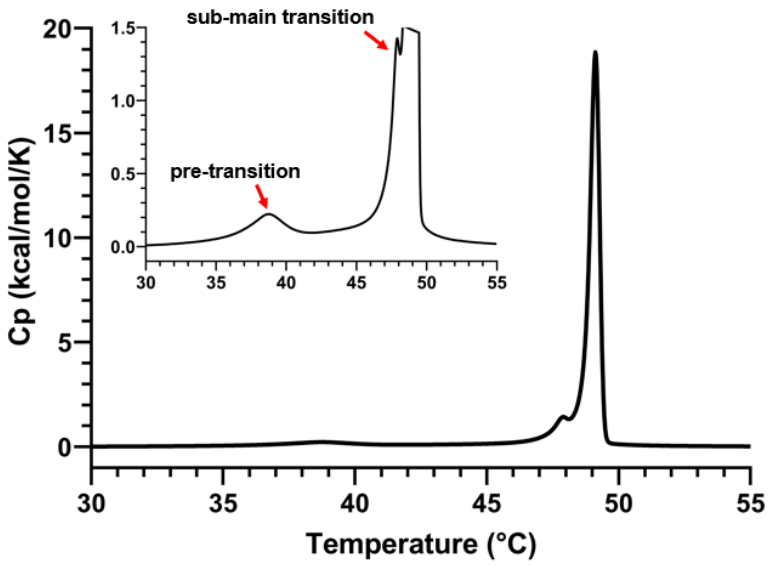

Fig. 3. Micro-DSC thermogram for PSPC.

In the case of PSPC with HP-β-CD, a range of concentrations of HP-β-CD was prepared, from 1 mM to 50 mM (Fig. 4). The thermogram of pure PSPC (0.14 mM) obviously demonstrated 2 transition peaks, a main transition peak (Tm-onset = 50.2°C and ΔH = 53.8 J/g) and a weak pre-transition peak (Tp-onset = 38.7°C and ΔH = 2.61 J/g). These values are in accordance with the literature (Mattai et al. 1987; Chen and Sturtevant 1981; Stumpel et al. 1983; Lin et al. 1990; Goto et al. 2008). Indeed, in the case of pre-transition, temperatures between 37.5 and 40.6°C were found with transition enthalpies of between 1.05 and 3.02 J/g. For the main transition, the temperature and enthalpy ranges were between 48.2 and 52.0°C and between 45.8 and 56.6 J/g,

respectively. With the increase of HP-β-CD concentration, a slight decrease of the T-onset and T-endset of the main transition was observed but the whole thermotropic variation was not significant, indicating that the molecule of HP-β-CD has no interaction with PSPC even at 50 mM. This could be explained by the strong hydrophilicity of HP-β-CD which remains in the aqueous phase of the lipid bilayer. Nishijo et al also reported that the thermotropic behavior of DPPC was barely influenced by β-CD, γ-CD and HP-β-CD, while in the presence of heptakis (2,3,6-tri-*O*-methyl)-β-cyclodextrin (TOM-β-CD), a decreasing Tm was observed in a concentration-dependent manner. The hydrophobic character of TOM-β-CD was regarded as the reason, assuming that it included the acyl chain of DPPC molecule (Nishijo et al 1998).

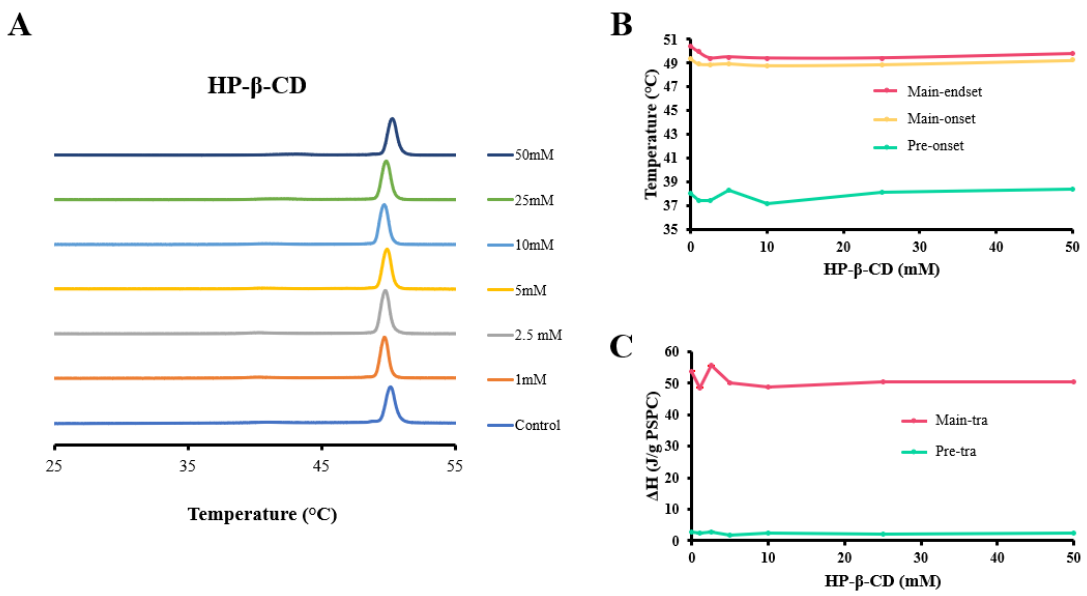

Fig. 4. DSC thermograms (A), transition onset (B) and enthalpy (C) for PSPC with HP-β-CD. The enthalpy was normalized with respect to the mass of phospholipids.

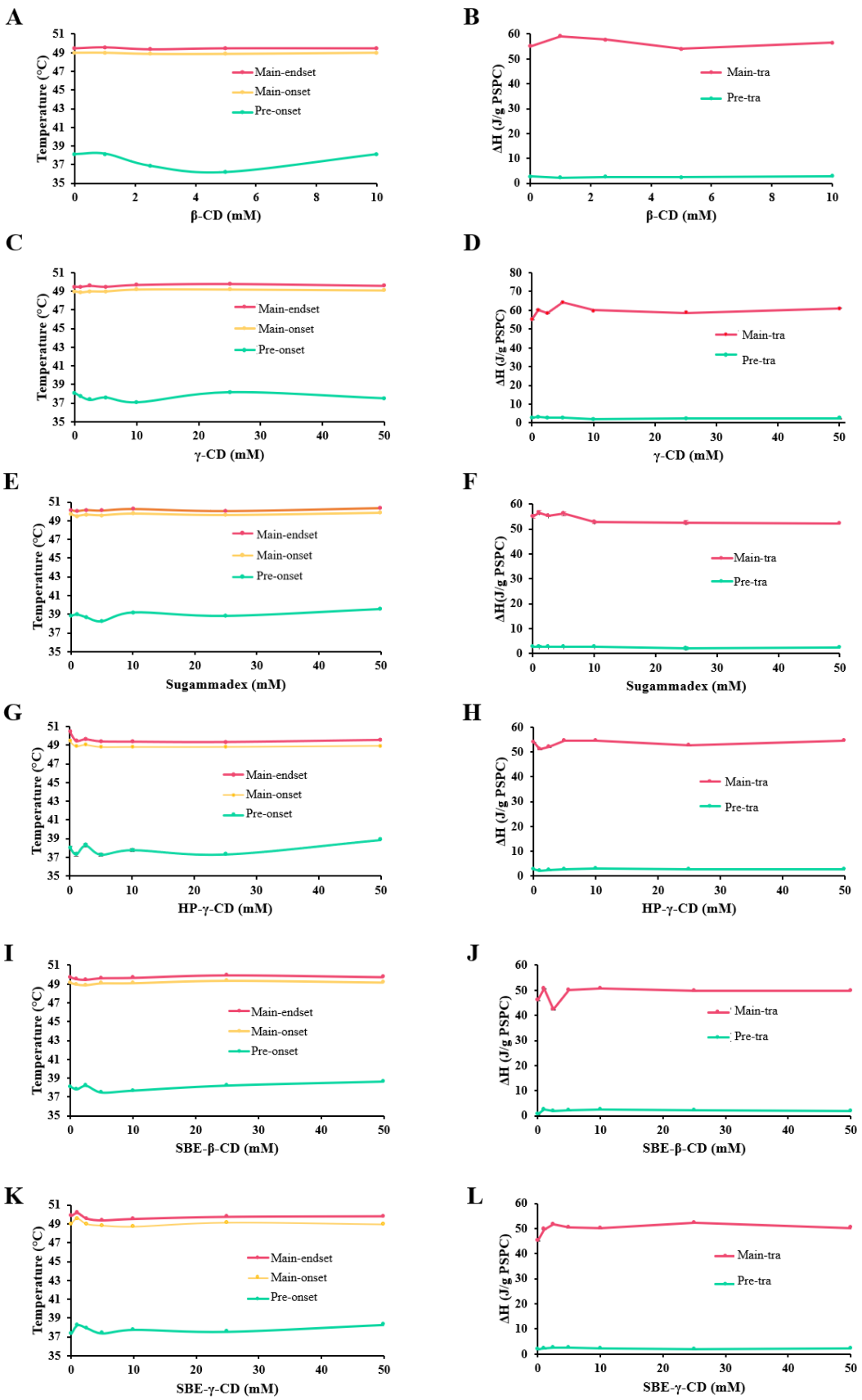

Fig. 5. Transition onset and enthalpy for PSPC with β-CD (A, B), γ-CD (C, D)，sugammadex (E, F), HP-γ-CD (G, H), SBE-β-CD (I, J) and SBE-γ-CD (K, L).

Similar results were obtained in the case of β-CD, γ-CD, sugammadex, HP-γ-CD and SBE-β-CD. None of the CDs mentioned above showed any interaction with PSPC, in terms of Tm, Tp and ΔH (Fig. 5). However, for SBE-γ-CD, the evolution of ΔH revealed a slight interaction with PSPC.

When higher concentration of SBE-Et-β-CD, 25 mM or above, were added, the thermogram of PSPC exhibited significant deformation (Fig. 6). Concretely, the onset of Tm showed slight increase but the ΔH decreased sharply in presence of 25 mM of SBE-Et-β-CD, while the main transition peak was completely suppressed when 50 mM was added. Although the detailed mechanism of the interaction between SBE-Et-β-CD and PSPC was difficult to discern, the disappearance of the main transition peak clearly reveals that the molecule of SBE-Et-β-CD penetrates into the phospholipid bilayer in some way, indicating that the integrity of PSPC MLVs could be undermined in the presence of SBE-Et-β-CD. As a consequence, SBE-Et-β-CD was rejected as a candidate for liposomal formulation preparation.

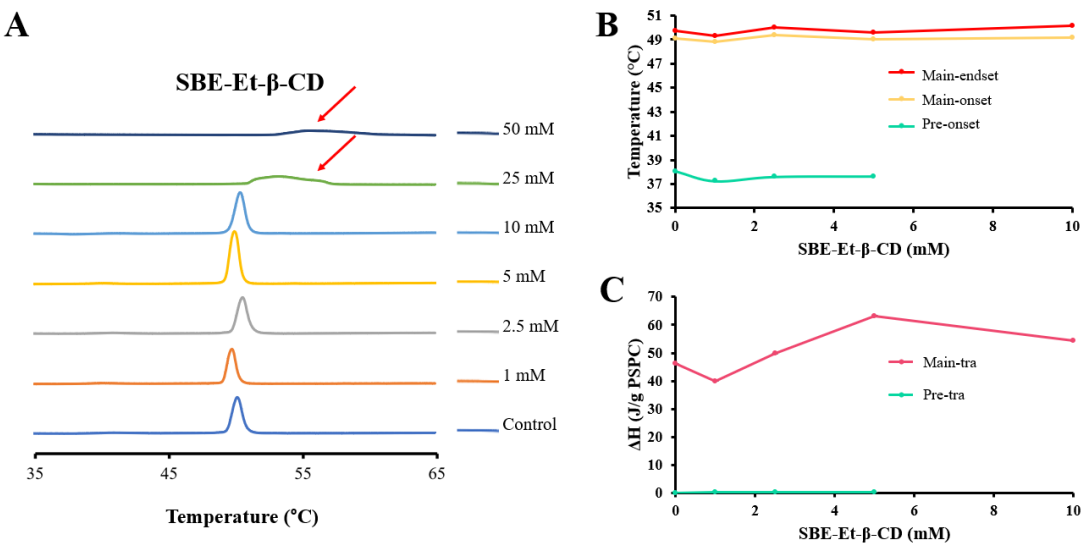

Fig. 6. DSC thermograms (A), transition onset (B) and enthalpy (C) for PSPC with SBE-Et-β-CD. The enthalpy was normalized with respect to the mass of phospholipids.

Several factors could influence the interactions between CDs and phospholipids, including the length of the fatty acid chains of the phospholipid and the hydrophobicity and cavity size of CDs (Nishijo and Shiota 2000). According to Huang and London, an increasing concentration of methyl-β-cyclodextrin (from 10 to 60 mM) is needed to solubilize the PC MLVs as the acyl chain length increases (from di C14:1 PC to di C22:1 PC), possibly due to the unfavorable free energy when acyl chains are in contact with water (Huang and London 2013).

3.3.1.2 Impact of CDs on the lamellar distance of PSPC

To understand the effect of CDs on the lipid bilayers of PSPC in different phases, SAXS was carried out. As mentioned above, SAXS can reveal the lamellar distance of the multilamellar structure. Fig. 7A shows the SAXS pattern of pure PSPC hydrated in 10 mM HEPES buffer (10%, w/w). Two sharp peaks centered at 0.91 nm^{-1} and 1.84 nm^{-1} were observed when PSPC is in liquid crystalline state at 55℃, consistent with the equidistant-peak feature of lamellar phase of lipid. Here, to compare the transformation of the lipid bilayer in different phases, an average lamellar distance (d) was used according to the q value at the different orders. Hence, according to Bragg law, the lamellar distance is 6.87 nm at 55℃, which remains unchanged when the temperature is 50℃. The results were slightly higher than those obtained by Cunningham et al (6.70 nm) for the same phase for a sample hydrated in water (Cunningham et al. 1998). However, for the $P_{\beta'}$ phase at 45℃, the pattern underwent broadening and the first order peak shifted to 0.84 nm^{-1}, with a significant increase of the distance (7.49 nm). The expansion could be explained by the periodic modulation of the lipid lamellar in the rippled state. The peak centered at 0.57 nm^{-1} demonstrated the corresponding periodicity of the ondulation was 11.1 nm.

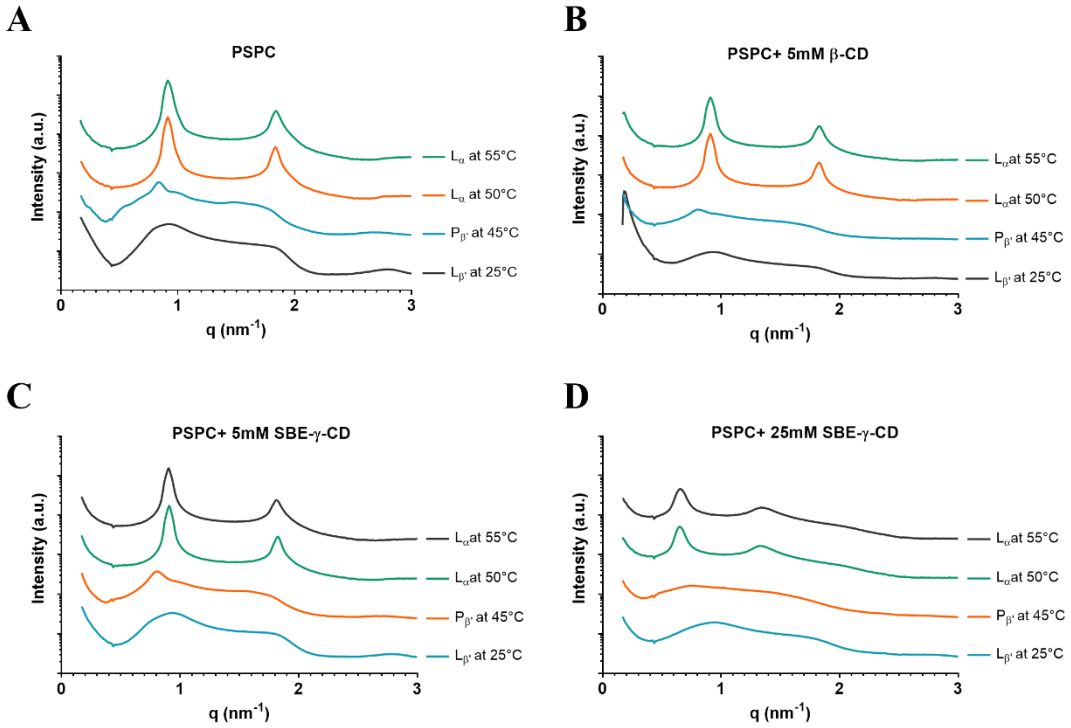

Fig. 7. SAXS patterns for pure PSPC (A), PSPC with 5 mM β-CD (B), PSPC with 5 mM SBE-γ-CD (C) and PSPC with 25 mM SBE-γ-CD (D).

A similar increase of the lamellar distance of PSPC from L_α phase to $P_{\beta'}$ phase was also found by Mattai et al, who reported the d was 6.65 nm at L_α phase but 7.14 nm at $P_{\beta'}$ phase (Mattai et al. 1987). When the temperature was decreased to 25°C, PSPC formed a gel phase ($L_{\beta'}$) and the diffraction peaks became broadened, due to the enlargement of the distribution of lamellar distances. The corresponding distance is 6.77 nm, which is in good agreement with the value (6.76 nm) obtained by Cunningham et al (Cunningham et al. 1998).

When PSPC was in presence of 5 mM of β-CD, no obvious difference was observed at the $L_{\beta'}$ and L_α phase, with a slight increase of the lamellar distance by 0.03 nm and 0.05 nm, respectively. However, for the $P_{\beta'}$ phase, the distance increased significantly to 7.80 nm compared with pure PSPC (7.49 nm), implying an influence of β-CD on the PSPC bilayer at $P_{\beta'}$ phase. It is noteworthy that the periodicity of the ripple phase could not be determined for all the cases, since the corresponding peak was

broadened due to an enlargement of the distribution of the periodicity or a modification of the electronic contrast.

Table 2 SAXS investigation of PSPC in presence of CDs at 25°C, 45°C, 50°C and 55°C.

CD	Conc. (mM)	Lamellar distance (nm)			
		25 °C ($L_{\beta'}$)	45 °C ($P_{\beta'}$)	50 °C (L_{α})	55 °C (L_{α})
-	0	6.70 ± 0.97	7.49	6.87 ± 0.09	6.87 ± 0.27
β-CD	5	6.73 ± 1.28	7.80	6.92 ± 0.28	6.92 ± 0.28
γ-CD	5	6.67 ± 1.24	7.80	6.87 ± 0.09	6.87 ± 0.09
	25	6.66 ± 1.12	7.74	6.92 ± 0.28	6.92 ± 0.09
HP-β-CD	5	6.65 ± 0.97	7.80	6.87 ± 0.45	6.82 ± 0.27
	25	6.68 ± 1.38	7.49	6.53 ± 0.19	6.48 ± 0.31
HP-γ-CD	5	6.69 ± 1.15	7.61	6.82 ± 0.27	6.82 ± 0.44
	25	6.69 ± 1.17	7.42	6.43 ± 0.34	6.39 ± 0.51
SBE-β-CD	5	6.68 ± 1.23	7.87	7.03 ± 0.09	7.19 ± 0.49
	25	6.73 ± 1.63	9.03	8.86 ± 0.57	8.98 ± 0.96
SBE-γ-CD	5	6.65 ± 1.04	7.80	6.92 ± 0.28	6.97 ± 0.28
	25	6.54 ± 0.12	8.45	9.70 ± 1.60	9.60 ± 1.56
SGM	5	6.66 ± 1.12	7.67	6.72 ± 0.42	6.77 ± 0.44
	25	6.67 ± 1.90	7.87	9.70 ± 1.60	9.50 ± 0.86
SBE-Et-β-CD	5	6.67 ± 1.14	7.80	6.92 ± 0.46	6.92 ± 0.09
	25	6.67	8.08	9.80 ± 0.89	9.91 ± 2.02
	50	6.38 ± 2.31	10.25	9.70 ± 0.90	9.81 ± 1.98

Similar results to those obtained with 5 mM of β-CD were observed when mixing PSPC with 5 mM of SBE-γ-CD. The lamellar distance was 6.65 nm at 25℃, 7.80 nm at 45℃, 6.92 nm at 50℃ and 6.97 nm at 55℃. However, when the concentration of

SBE-γ-CD was increased to 25 mM, a significant effect was observed. Concretely, the lamellar distance increased by 0.96 nm at 45℃, 2.83 nm at 50℃ and 2.73 nm at 55℃, respectively, while a slight decrease of 0.16 nm was observed at 25℃. The expansion of the lamellar in the $P_{\beta'}$ phase, especially in the L_{α} phase, implied that the molecule of SBE-γ-CD began to penetrate into the lipid bilayer of PSPC MLVs at higher concentration. Moreover, this kind of penetration didn't occur at lower temperature, $L_{\beta'}$ phase for example, probably due to the relatively high packing of the hydrocarbon tails. Lamellar thickening was also observed when higher concentrations of SBE-β-CD, SGM and SBE-Et-β-CD were added, while for γ-CD, HP-β-CD and HP-γ-CD, such kind of influence was limited. The obvious lamellar expansion induced by SBE-Et-β-CD at 25 mM or 50 mM confirmed the interaction that had been revealed by DSC.

3.3.1.3 Impact of CDs on the hydrocarbon chain packing of PSPC

Typical WAXS diffraction patterns for PSPC with different concentrations of CDs are shown in Fig 8. For pure PSPC hydrated in water (10%, w/w), the pattern revealed a sharp peak centered at 14.74 nm^{-1} with a shoulder at 14.96 nm^{-1} at 25℃, which is characteristic of the $L_{\beta'}$ phase and indicates that acyl chains are tilted and packed in a quasi-hexagonal lattice (Cunningham et al. 1998). The corresponding lattice parameters (0.426 nm and 0.420 nm) are a bit lower than those obtained by Mattai et al at 22℃, with 0.441 nm and 0.427 nm (Mattai et al. 1987). For the $P_{\beta'}$ phase, the WAXS pattern consists of a single peak at 14.77 nm^{-1} (d' = 0.425 nm at 45℃), which is in good agreement with the value reported by Mattai at 37℃ (0.422 nm) and 42℃ (0.426 nm) (Mattai et al. 1987). Additionally, according to Cunningham et al, the symmetry of the peak in $P_{\beta'}$ phase implied that the acyl chains were ordered in a hexagonal lattice (Cunningham et al. 1998). The pattern of liquid crystalline state at 50℃ showed a broad peak centered at 13.93 nm^{-1} (d' = 0.451 nm), which can be explained by the loosely packed hydrocarbon chains (Sun et al. 2017). Thereafter, the distance remained unchanged on increasing the temperature to 55℃.

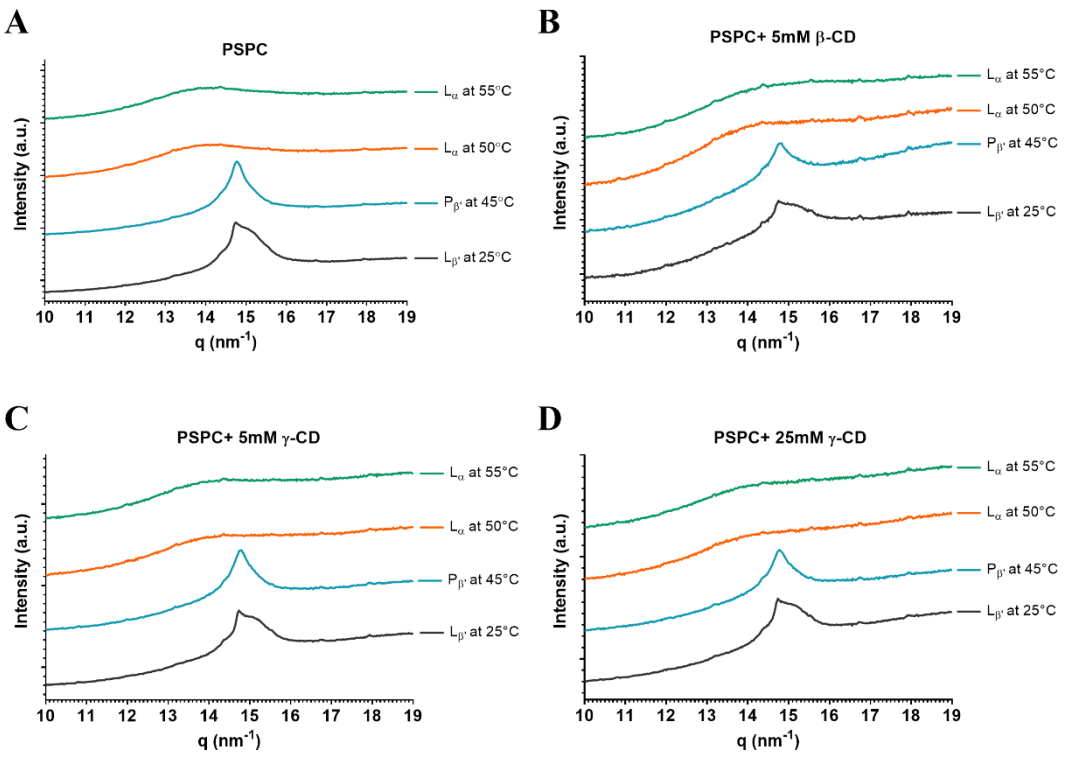

Fig. 8. WAXS patterns for PSPC (A), PSPC with 5 mM β-CD (B), PSPC with 5 mM γ-CD (C) and PSPC with 25 mM γ-CD (D).

For PSPC with 5 mM of β-CD, the WAXS pattern of the $L_{\beta'}$ phase and $P_{\beta'}$ phase showed no distinct difference compared to PSPC alone. For example, the lattice parameter remained unchanged at 0.425 nm in the $P_{\beta'}$ phase. However, in the L_{α} state at 50°C, the distance (0.442 nm) was obviously lower than that obtained for PSPC alone (0.451 nm), implying that β-CD influenced the acyl chain packing of PSPC in the liquid crystalline phase.

In the case of PSPC with 5 mM of γ-CD, similar patterns were revealed in the $L_{\beta'}$ phase (q_1=14.73 nm^{-1}, q_2=14.97 nm^{-1}) and $P_{\beta'}$ phase (q=14.79 nm^{-1}). Nevertheless, the space underwent a small decrease in the L_{α} state, with 0.445 nm at 50°C and 0.447 nm at 55°C, respectively. To further investigate the effect of γ-CD at higher concentration, 25 mM of γ-CD was added and similar patterns were observed, suggesting that γ-CD had limited impact on the acyl chain order of PSPC even at 25 mM. Moreover, no significant effect was found with the addition of different concentrations (5 mM and 25

mM) of HP-β-CD, HP-γ-CD, SBE-β-CD, SBE-γ-CD and SGM. For SBE-Et-β-CD, a higher concentration was used (50 mM), resulting in a pattern similar to those in presence of lower concentrations. Although the SAXS results revealed an obvious impact of SBE-Et-β-CD on the lamellar distance of PSPC, the limited disturbance in the hydrocarbon chain packing indicated that the interaction between SBE-Et-β-CD and PSPC occurred mainly near the polar group but not in the alkyl chain region of the lipid lamellae.

Table 3 WAXS investigation of PSPC in presence of CDs at 25°C, 45°C, 50°C and 60°C.

CD	**Conc.(mM)**	**Lattice parameter d' (nm)**				
		25 °C ($L_{\beta'}$)		**45 °C ($P_{\beta'}$)**	**50 °C (L_{α})**	**55 °C (L_{α})**
		d_1'	**d_2'**			
-	0	0.426	0.420	0.425	0.451	0.452
β-CD	5	0.426	0.419	0.425	0.442	0.428
γ-CD	5	0.426	0.420	0.425	0.445	0.447
	25	0.426	0.420	0.425	0.443	0.443
HP-β-CD	5	0.425	0.420	0.425	0.436	0.435
	25	0.426	0.420	0.425	0.446	0.446
HP-γ-CD	5	0.426	0.420	0.425	0.445	0.445
	25	0.426	0.420	0.425	0.446	0.446
SBE-β-CD	5	0.426	0.420	0.425	0.442	0.439
	25	0.426	0.420	0.425	0.440	0.443
SBE-γ-CD	5	0.426	0.420	0.426	0.448	0.448
	25	0.426	0.420	0.425	0.443	0.442
SGM	5	0.426	0.420	0.425	0.448	0.448
	25	0.424	0.419	0.425	0.429	0.436
SBE-Et-β-CD	5	0.426	0.420	0.425	0.436	0.431
	25	0.424	0.419	0.425	0.442	0.445
	50	0.424	0.419	0.425	0.439	0.441

3.3.2 Stability of liposomes in presence of CDs

3.3.2.1 Effect of CDs on the stability of SUVs with cholesterol

To evaluate the effect of CD on the stability of SUVs, turbidity experiments were performed. Turbidimetry has been widely used as a simple but effective technique to investigate various properties of liposomes, such as permeability (Cohen and Bangham 1972) and dissolution (Wang et al. 2013). Wang et al gave a simplified schematic diagram to illustrate this technique (Wang et al. 2018) (Fig. 9). By measuring the intensity of light that is transmitted through the liposomal dispersion, turbidity can be regarded as a key indicator that reveals changes in physicochemical properties. In the present experiments, by adding CD solution into the SUV dispersion at a defined speed, the concentration of CD increases gradually until it is high enough to destroy or solubilize the phospholipid bilayers, resulting in an increase in the amount of light that reaches the detector.

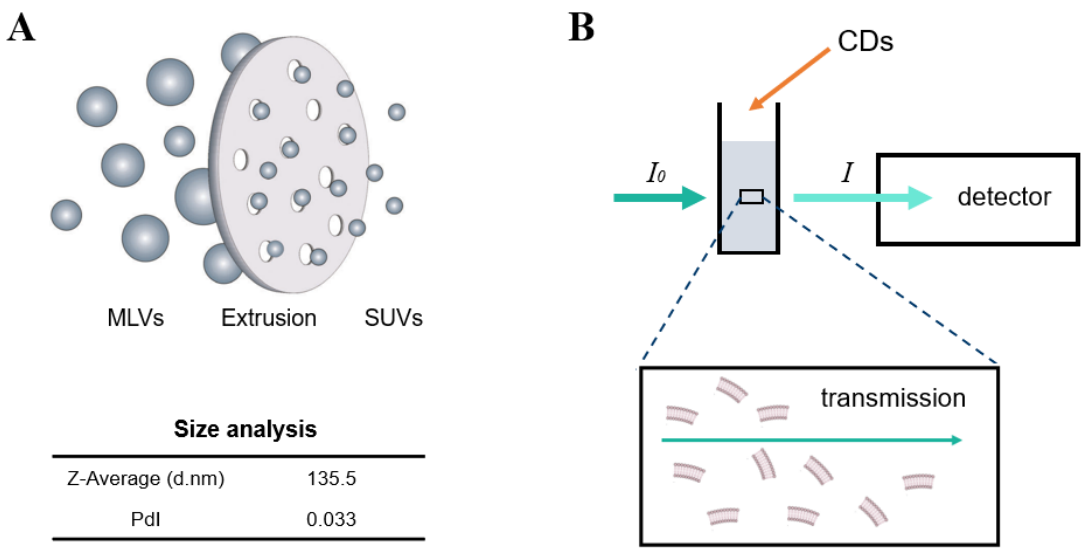

Fig. 9. Illustration for SUVs obtained by extrusion (A) and turbidimetry (B), reproduced from (Wang et al. 2018)

According to previous studies, a typical profile can be used to demonstrate the process of solubilization of liposomes (Boulmedarat et al. 2005; Andrieux et al. 2009) (Fig. 10). Generally, the liposomes would undergo a vesicle-micelle transition, along with aggregation of the vesicles induced by the addition of substances such as calcium ions (Fatouros et al. 2005). Characteristic points are obtained by drawing tangents on the curve, which represent different stages of the solubilization process. In phase A, the turbidity decreases stepwise linearly because of the dilution of the initial liposomes. A slight but longer period of decrease then follows, namely phase B, indicating the onset of solubilization and destruction of vesicles. Subsequently, the turbidity drops sharply as a majority of liposomes start to become micelles at this stage (C). Finally, all the liposomes are solubilized and the suspension becomes transparent. Only a limited OD decrease can be observed in stage D. This typical profile allows turbidity experiments to be analyzed in more detail, but it should be noted that the solubilization process varies under different condition, depending on the physicochemical properties of the liposomes and additives.

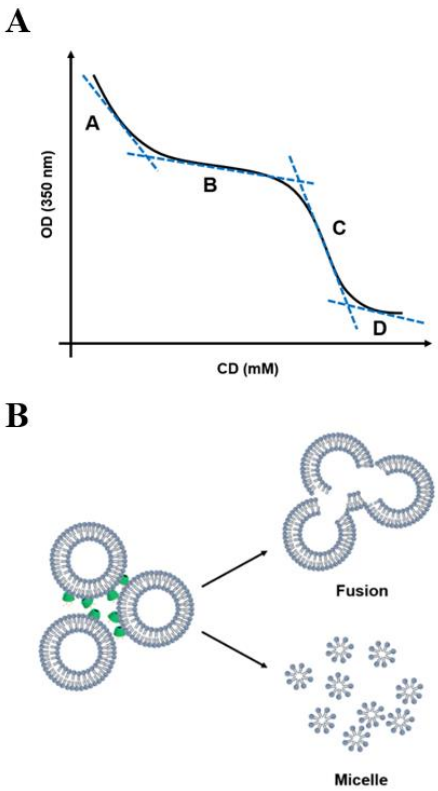

Fig. 10. Typical profile for the solubilization process of liposomes (A), and illustration for the aggregation and micelle formation (B).

Firstly, to test our method and assess the accuracy of the turbidity measurements, HEPES buffer without CD was injected into a 1 mM liposomal suspension, so that the liposomes were gradually diluted. Fig. 11 shows the concentration of lipids and corresponding OD as a function of time, revealing a close correlation. An excellent linear relationship was obtained between the two parameters, confirming the feasibility and precision of the method.

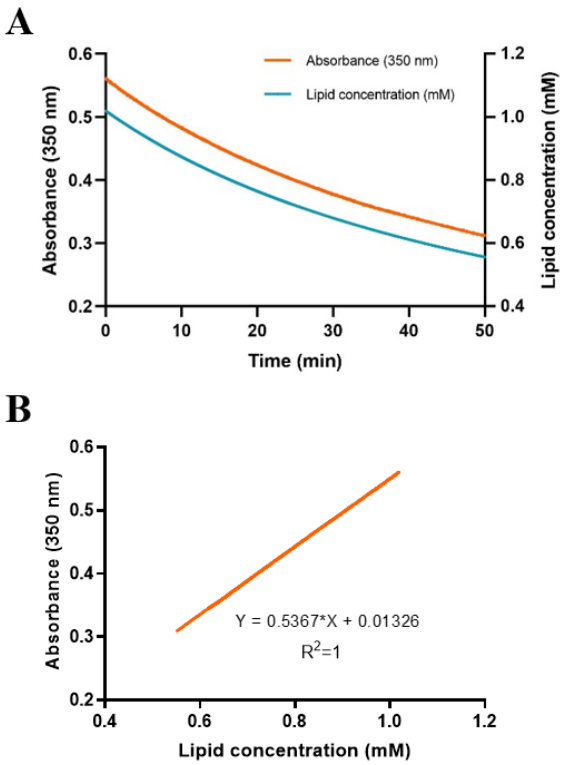

Fig. 11. The lipid concentration and corresponding absorbance of the liposomal dispersion as a function of time (A), and the corresponding absorbance with respect to lipid concentration (B).

Subsequently, to investigate the stability of liposomes in presence of CDs, SUVs consisting of HEPC, cholesterol and DSPE-PEG_{2000} (60:35:5 mol ratio) were prepared by extrusion with 135 nm diameter and diluted to 0.5 mM, 0.75 mM and 1 mM as the starting concentration for turbidity measurements (Fig. 12). γ-CD solution was gradually injected into the SUVs dispersion, leading to slow decrease of the optical density (OD). For example, the initial OD of 0.5 mM SUVs was 0.3, decreasing to 0.15 when the γ-CD concentration reached 50 mM. In contrast to the typical profile

mentioned above, no characteristic points were observed on the curve of γ-CD, indicating that γ-CD did not disrupt the liposomes and the decrease of turbidity was entirely due to the dilution factor. Moreover, a higher initial concentration of liposomes demonstrated a higher level of turbidity, which is in agreement with the proportionality of absorbance illustrated in Fig. 11.

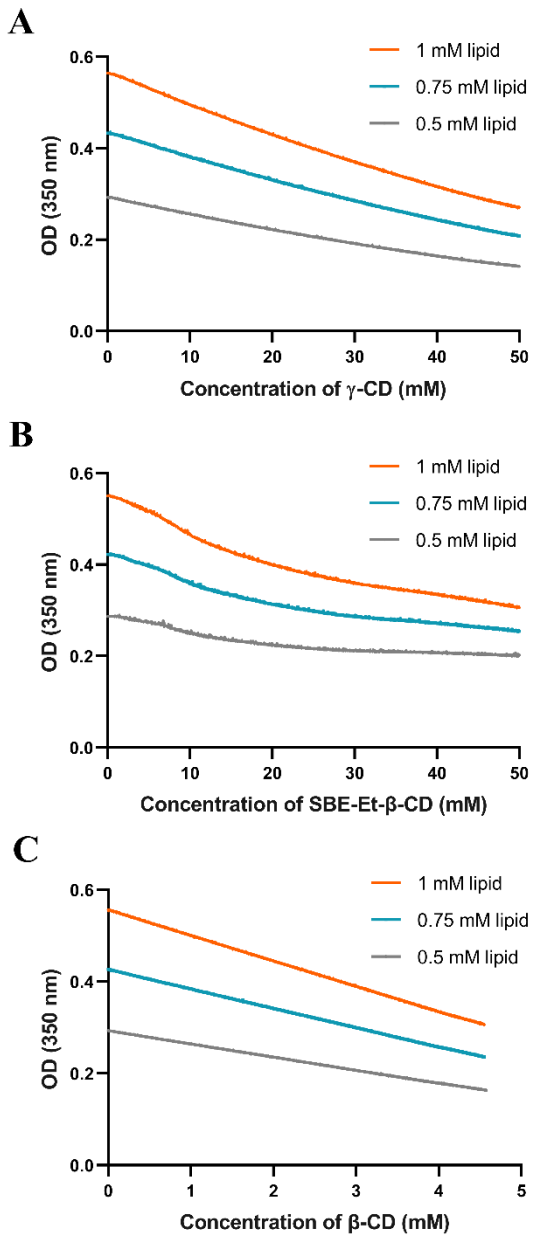

Fig. 12. The OD of SUVs (with cholesterol) dispersion with addition of γ-CD (A), SBE-Et-β-CD (B) and β-CD (C).

In contrast, the smooth decreasing curve showed distortion with the addition of SBE-Et-β-CD into the same SUVs suspension, at an initial concentration between 0.5 mM and 1 mM, revealing that the SUVs became unstable and underwent a vesicle-micelle transition in presence of SBE-Et-β-CD (Fig. 12B). The disruptive capability of SBE-Et-β-CD observed in the turbidity experiment is in good agreement with the results acquired by DSC, confirming that SBE-Et-β-CD is an inappropriate candidate for the DCL system. A similar experiment was performed with β-CD, but the final CD concentration was 5 mM because of its low solubility in water (Fig. 12C).

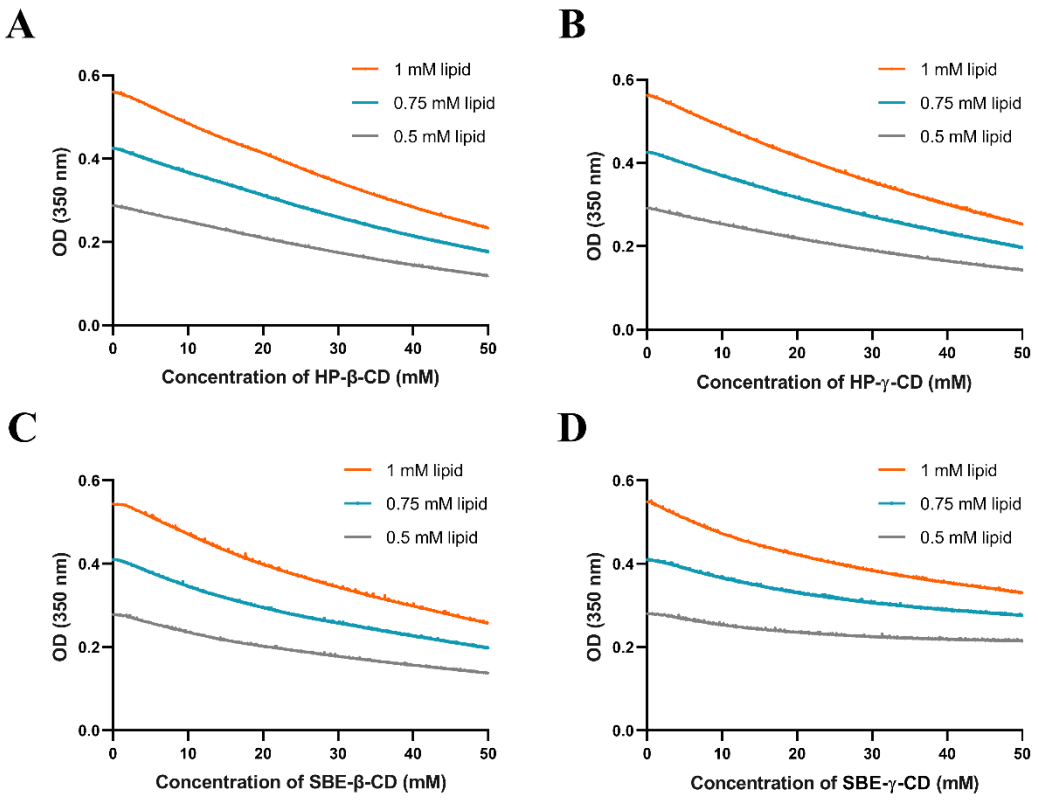

Fig. 13. The OD of SUVs (with cholesterol) dispersion with addition of HP-β-CD (A), HP-γ-CD (B), SBE-β-CD (C) and SBE-γ-CD (D).

HP-β-CD, HP-γ-CD and SBE-β-CD were also evaluated and none of these CDs showed negative effect on the integrity of SUVs, with highly similar decreasing profiles (Fig. 13A, B and C). However, in the case of SBE-γ-CD, the slope of the turbidity curve tended to be flattened, especially for 0.5 mM SUVs (Fig. 13D). The reduction of the

downward trend indicates that a small amount of aggregation of the liposomes occurred during the addition of SBE-γ-CD, since larger liposomes would scatter more light. Apparently, SUVs at a lower initial concentration are more susceptible to this effect, compared with those starting at 0.75 mM or 1 mM.

3.3.2.2 Effect of CDs on the stability of SUVs without cholesterol

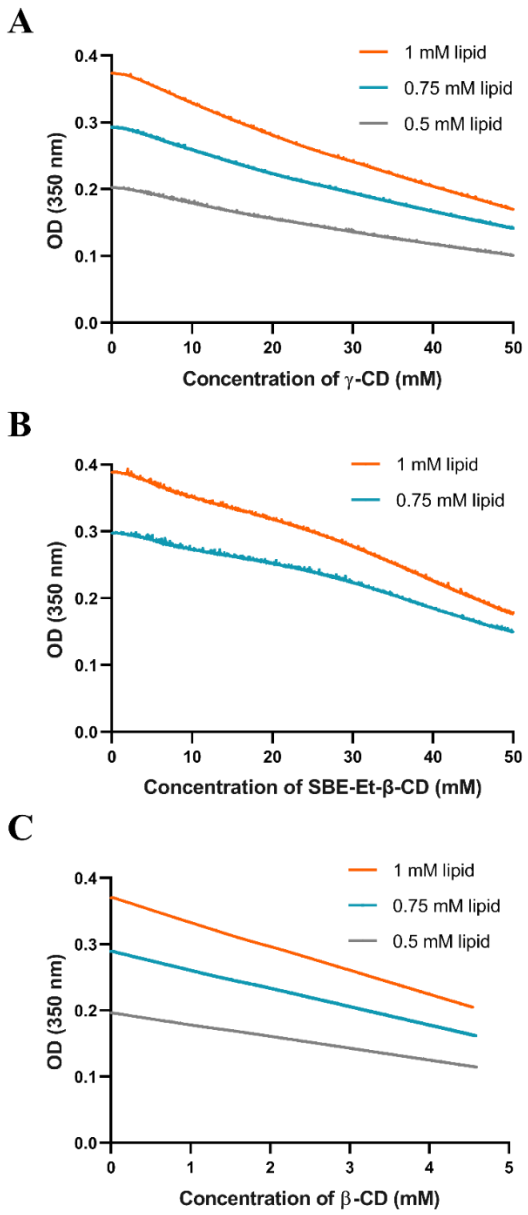

Fig. 14. The OD of SUVs (without cholesterol) dispersion with addition of γ-CD (A), SBE-Et-β-CD (B) and β-CD (C).

SUVs consisting of HEPC and DSPE-PEG$_{2000}$ (95:5 mol ratio) were also studied, in order to investigate the role of cholesterol in the integrity of SUVs (Fig. 14). As for the turbidity experiment performed above, liposomes with starting concentrations of 0.5 mM, 0.75 mM and 1 mM were prepared, with the addition of γ-CD at the same speed. The turbidity decreased gradually with similar trends to those of SUVs with cholesterol, indicating that the liposomes remained stable during the process even without cholesterol.

However, when SBE-Et-β-CD was added, the absorbance curve clearly revealed that it caused instability for both concentrations of liposomes (0.75 mM and 1 mM). Compared with SUVs containing cholesterol, liposomes without cholesterol exhibited lower stability, which is in agreement with the literature and demonstrated the role of cholesterol in enhancing the stability of formulations (Kohli et al. 2014).

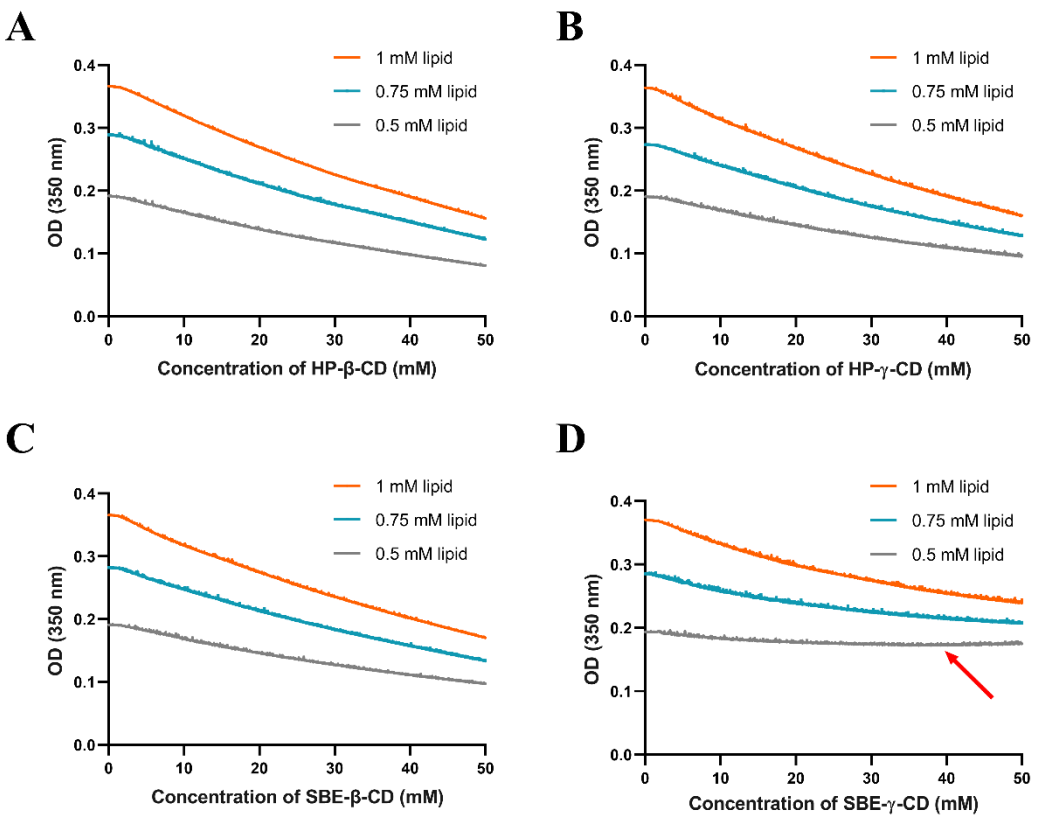

Fig. 15. The OD of SUVs (without cholesterol) dispersion with addition of HP-β-CD (A), HP-γ-CD (B), SBE-β-CD (C) and SBE-γ-CD (D).

Furthermore, the effect of β-CD was investigated and no damaging phenomenon was observed for SUVs without cholesterol (Fig. 15). The stability of SUVs in presence of HP-β-CD, HP-γ-CD, SBE-β-CD and SBE-γ-CD was also assessed. In all cases, SUVs remained intact, except with SBE-γ-CD. When the SBE-γ-CD solution was injected into 0.5 mM SUVs, the turbidity underwent a slight increase, implying an aggregation of liposomes. Therefore, SBE-γ-CD may not be a suitable lipid to prepare the DCL system when there is a high CD/lipid ratio.

3.3.3 Interaction between CPZ and lipid bilayers

To better understand the stability of the DCL system, the interaction between CPZ and phospholipid is also a critical issue to be investigated. The encapsulation efficiency of CPZ is an important parameter of the liposomal formulation; however, considering the amphiphilic property of CPZ, a large amount of drug inserted into the liposomal membrane may increase the permeability of the system and reduce its circulation time after intravenous administration. Therefore, the interaction of CPZ with PSPC model membranes was investigated by DSC as for CDs above.

Fig. 16 clearly shows that the main transition of PSPC (onset Tm = 49.5°C and ΔH = 55.18 J/g) was reduced in amplitude and tended to shift to lower temperatures with increasing molar ratios of CPZ. This could be explained by the amphipathic properties of CPZ, which allow it to penetrate into the MLVs bilayer even at a low CPZ/PSPC molar ratio. When the molar ratio reached 10%, two peaks appeared on the thermogram and the peak at lower temperature increased in size and shifted towards lower temperature. No saturation was observed even at a CPZ/PSPC molar ratio as high as 45%.

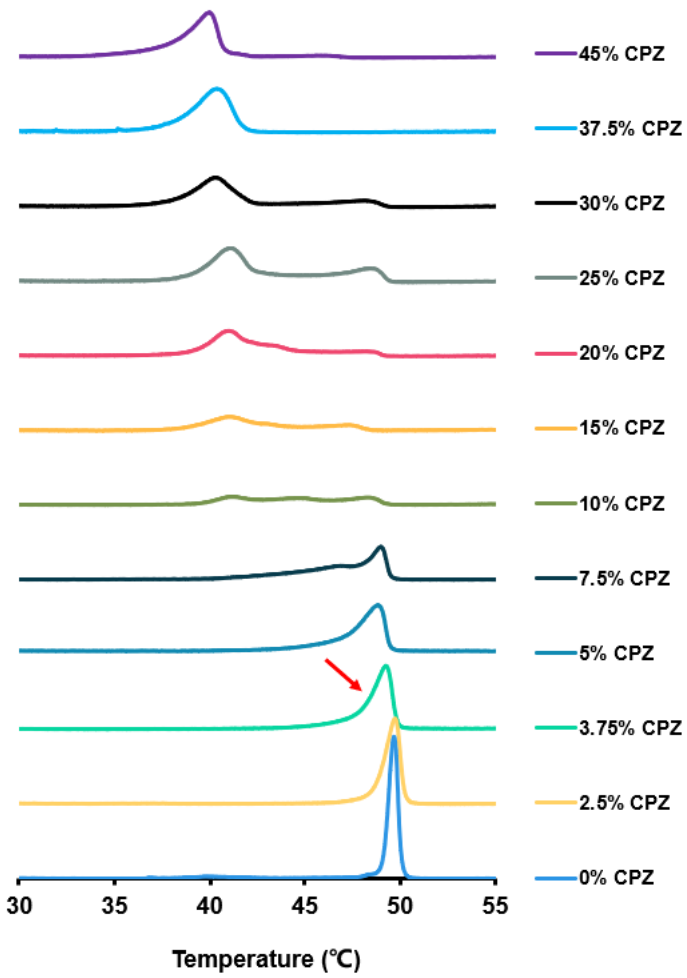

Fig. 16. Effect of CPZ on the PSPC thermotropic behavior with increasing mole percentage.

A similar study was carried out by Banerjee et al to investigate the interaction between CPZ and DPPC (Banerjee et al. 1999). They demonstrated the evolution of the calorimetric profile for DPPC MLV as a function of the amount of CPZ from 2% to 30%. As in our study, the main transition peak of DPPC was found to decrease and gradually become broader and flatter. At pH 4.5, a saturation of the transition temperature shift was obtained when 60% of CPZ was added.

Although 45% of CPZ does not saturate the PSPC membrane, the stability of liposomes is a priority for the development of DCL system, from the view of pharmacodynamics and storage. Therefore, considering the integrity of the main transition peak of PSPC, 3.75 mol% of CPZ is a suitable ratio for the preparation of liposomal formulations in subsequent work.

3.4 Conclusion

The calorimetric investigation by DSC revealed that no interaction occurred between PSPC MLVs and the CD candidates (β-CD, γ-CD, SGM, HP-β-CD, HP-γ-CD, SBE-β-CD and SBE-γ-CD), except for SBE-Et-β-CD. The unchanged lamellar distance and hydrocarbon chain packing determined by X-ray scattering further confirmed the limited effect of CD on PSPC bilayers, especially at low CD concentrations. Moreover, HEPC SUVs with and without cholesterol showed good stability in presence of low concentration of CDs, which is consistent with the results obtained with PSPC MLVs and provides evidence for the feasibility of DCL formulation. Additionally, a study of the interaction between CPZ and PSPC bilayers determined that 3.75 mol% of CPZ is a safe ratio for the stability of the DCL system, considering the amphiphilic property of CPZ.

References

Andrieux K, Forte L, Lesieur S, Paternostre M, Ollivon M, Grabielle-Madelmont C. Solubilisation of dipalmitoylphosphatidylcholine bilayers by sodium taurocholate: a model to study the stability of liposomes in the gastrointestinal tract and their mechanism of interaction with a model bile salt. European Journal of Pharmaceutics and Biopharmaceutics. 2009, 71(2): 346-55.

Banerjee S, Bennouna M, Ferreira-Marques J, Ruysschaert JM, Caspers J. Lipid–drug interaction and colligative properties in phospholipid vesicles. Journal of Colloid and Interface Science. 1999, 219(1):168-77.

Boulmedarat L, Piel G, Bochot A, Lesieur S, Delattre L, Fattal E. Cyclodextrin-mediated drug release from liposomes dispersed within a bioadhesive gel. Pharmaceutical Research. 2005, 22(6):962-71.

Cohen BE, Bangham AD. Diffusion of small non-electrolytes across liposome membranes. Nature. 1972, 236(5343):173-4.

Chellam JA and Mandal AB. Influence of Cyclodextrins on the Physical Properties of Collagen. International Journal of Pharma and Bio Sciences. 2013, 4 (4): 795–806.

Chen SC, Sturtevant JM. Thermotropic behavior of bilayers formed from mixed-chain phosphatidylcholines. Biochemistry. 1981, 20(4):713-8.

Cunningham BA, Brown AD, Wolfe DH, Williams WP, Brain A. Ripple phase formation in phosphatidylcholine: Effect of acyl chain relative length, position, and unsaturation. Physical Review E. 1998, 58(3): 3662.

Fatouros DG, Piperoudi S, Gortzi O, Ioannou PV, Frederik P, Antimisiaris SG. Physical stability of sonicated arsonoliposomes: effect of calcium ions. Journal of Pharmaceutical Sciences. 2005, 94(1): 46-55.

Goto M, Kusube M, Tamai N, Matsuki H, Kaneshina S. Effect of hydrostatic pressure on the bilayer phase behavior of symmetric and asymmetric phospholipids with the same total chain length. Biochimica et Biophysica Acta (BBA)-Biomembranes. 2008, 1778(4):1067-78.

Hait WN, Grais L, Benz C, Cadman EC. Inhibition of growth of leukemic cells by inhibitors of calmodulin: phenothiazines and melittin. Cancer Chemotherapy and Pharmacology. 1985, 14(3):202-5.

Huang Z, London E. Effect of cyclodextrin and membrane lipid structure upon cyclodextrin–lipid interaction. Langmuir. 2013, 29(47):14631-8.

Jørgensen K. Calorimetric detection of a sub-main transition in long-chain phosphatidylcholine lipid bilayers. Biochimica et Biophysica Acta (BBA)-Biomembranes. 1995, 1240(2):111-4.

Kohli AG, Kierstead PH, Venditto VJ, Walsh CL, Szoka FC. Designer lipids for drug delivery: from heads to tails. Journal of Controlled Release. 2014, 190:274-87.

Lin HN, Wang ZQ, Huang CH. Differential scanning calorimetry study of mixed-chain phosphatidylcholines with a common molecular weight identical with diheptadecanoylphosphatidylcholine. Biochemistry. 1990, 29(30):7063-72.

Mattai J, Sripada PK, Shipley GG. Mixed-chain phosphatidylcholine bilayers: structure and properties. Biochemistry. 1987, 26(12):3287-97.

Nishijo J, Mizuno H. Interactions of cyclodextrins with DPPC liposomes. Differential scanning calorimetry studies. Chemical and Pharmaceutical Bulletin. 1998, 46(1):120-4.

Nishijo J, Shiota S, Mazima K, Inoue Y, Mizuno H, Yoshida J. Interactions of cyclodextrins with dipalmitoyl, distearoyl, and dimyristoyl phosphatidyl choline liposomes. A study by leakage of carboxyfluorescein in inner aqueous phase of unilamellar liposomes. Chemical and Pharmaceutical Bulletin. 2000, 48(1):48-52.

Ohvo-Rekilä H, Ramstedt B, Leppimäki P, Slotte JP. Cholesterol interactions with phospholipids in membranes. Progress in Lipid Research. 2002, 41(1):66-97.

Piel G, Piette M, Barillaro V, Castagne D, Evrard B, Delattre L. Study of the relationship between lipid binding properties of cyclodextrins and their effect on the integrity of liposomes. International Journal of Pharmaceutics. 2007, 338(1-2):35-42.

Pignatello R, Musumeci T, Basile L, Carbone C, Puglisi G. Biomembrane models and drug-biomembrane interaction studies: Involvement in drug design and development. Journal of Pharmacy and Bioallied Sciences. 2011, 3(1):4.

Pressl K, Jørgensen K, Laggner P. Characterization of the sub-main-transition in distearoylphosphatidylcholine studied by simultaneous small-and wide-angle X-ray diffraction. Biochimica et Biophysica Acta (BBA)-Biomembranes. 1997, 1325(1):1-7.

Ramaldes GA, Fattal E, Puisieux F, Ollivon M. Solubilization kinetics of phospholipid vesicles by sodium taurocholate. Colloids and Surfaces B: Biointerfaces. 1996, 6(6):363-71.

Ruocco MJ, Shipley GG. Characterization of the sub-transition of hydrated dipalmitoylphosphatidylcholine bilayers. Kinetic, hydration and structural study. Biochimica et Biophysica Acta (BBA)-Biomembranes. 1982, 691(2):309-20.

Stümpel J, Eibl H, Nicksch A. X-ray analysis and calorimetry on phosphatidylcholine model membranes. The influence of length and position of acyl chains upon structure and phase behaviour. Biochimica et Biophysica Acta (BBA)-Biomembranes. 1983, 727(2):246-54.

Sun HY, Wu FG, Li ZH, Deng G, Zhou Y, Yu ZW. Phase behavior of a binary lipid system containing long-and short-chain phosphatidylcholines. RSC Advances. 2017, 7(10):5715-24.

Trandum C, Westh P, Jørgensen K. Slow relaxation of the sub-main transition in multilamellar phosphatidylcholine vesicles. Biochimica et Biophysica Acta (BBA)-Biomembranes. 1999, 1421(2):207-12.

Wang A, Miller CC, Szostak JW. Interpreting turbidity measurements for vesicle studies. BioRxiv. 2018, 348904.

Wang L, Quan C, Liu B, Wang J, Xiong W, Zhao P, Fan S. Functional reconstitution of staphylococcus aureus truncated agrc histidine kinase in a model membrane system. PloS One. 2013, 8(11):e80400.

Chapter 4

Formulation and biological evaluation of CPZ-in-CD-in-liposomes

4.1 Introduction

In the treatment for acute myeloid leukemia (AML), the standard "7+3 regimen" (cytarabine for 7 days with daunorubicin or idarubicin for 3 days) is the most commonly used clinical chemotherapy. However, the severe side effects of treatment and the limited solutions for older patients have motivated researchers to develop novel agents for this disease. At present, several small molecules are undergoing investigation, including clofarabine, sorafenib, midostaurin and crenolanib. Chlorpromazine (CPZ) is widely used as an antipsychotic that is effective in treating schizophrenia and it is well tolerated. Although most of the medical applications of CPZ are focused on the treatment of psychological disorders, Hait et al reported a study in 1985 that investigated the effect of CPZ and chlorpromazine-sulfoxide on the growth of murine leukemic lymphocytes (L1210 and L5178Y) and human promyelocytic leukemic granulocytes (HL-60) (Hait et al. 1985). CPZ was found to show higher cytotoxicity against leukemic cell lines than its sulfoxide derivative, with IC_{50} values of 8 μM and 100 μM respectively on the HL-60 cell line. This result suggested that CPZ could be repurposed as a novel way to treat AML.

Nevertheless, the antipsychotic activity of CPZ depends on its ability to pass through the blood-brain barrier (BBB) and concentrate in the central nervous system. Therefore, a new strategy needs to be developed for repurposing, to prevent CPZ from accumulating in the brain but deliver it to the target site, the bone marrow. Liposomes have been widely used as an efficient nanometric drug delivery system over the past 50 years since their first discovery in 1965 (Bangham et al. 1965), especially since the 1980s when traditional liposomes were first used in a clinical setting (Gabizon et al. 1982). Numerous agents, including hydrophobic, hydrophilic and amphiphilic molecules, can be encapsulated in the lipid vesicles and further transported into the circulatory system after different routes of administration.

In the present study, the hypothesis was that entrapping CPZ in liposomes could efficiently avoid passage through the BBB and prolong the circulation time in plasma,

contributing to the accumulation and uptake of CPZ in the bone marrow. Moreover, the liposomal formulation provides the possibility of active targeting for the drug, by coating the surface of liposomes with appropriate monoclonal antibodies or fragments. However, considering the amphiphilic property of CPZ, drug leakage or rapid release may occur due to its tendency to locate within the phospholipid bilayer. Therefore, a versatile drug delivery strategy, the drug-in-CDs-in-liposomes (DCL) system will be employed to obtain the liposomal formulation. This concept was first proposed by McCormack and Gregoriadis in 1994 and has applied in virous liposomal carrier cases (McCormack and Gregoriadis 1994). The DCL system involves 3 interrelated ingredients: CDs, CPZ and phospholipids, involving complicated interactions between CD/CPZ, CD/lipid and CPZ/lipid.

In preliminary work, we performed comprehensive investigations on CD/CPZ inclusion complexes and as a result selected three cyclodextrins: HP-γ-CD, SBE-β-CD and Sugammadex (SGM) that showed the highest complexation ratios with CPZ. The high formation constant of these complexes indicates a strong capability of the CD to entrap CPZ within its internal cavity, thus drug leakage or rapid release could be avoided. However, it is also important to determine the influence of CDs on lipids. Therefore, in a previous study, the effect of various CDs on the integrity of model liposomes was studied. Most CD types showed no influence on the stability of liposomes, allowing the preparation of a DCL system and its subsequent biological evaluation.

Several methods can be used to prepare drug-loaded liposomes, including thin-film hydration and ethanol injection. Both these methods are easy to perform, but the efficiency of drug loading relies heavily on the physicochemical properties of the lipids, CD and drug. Since the CD/CPZ complex is hydrophilic, it will not be efficiently incorporated using the methods mentioned above. Therefore, a method more appropriate for encapsulation of hydrophilic molecules, dehydration-rehydration vesicles (DRV), has been employed. The DRV method was first developed by Kirby and Gregoriadis in 1984 (Kirby and Gregoriadis 1984), and has been widely used to

prepare liposomal formulations containing various substances, in particular, large hydrophilic molecules like proteins and nucleic acids. This method has already been applied to CD complexes by Antimisiaris et al (Antimisiaris et al. 2017).

In this work, we describe the formulation of liposomes by the DRV method and its optimization, followed by characterization of the resulting DCL system, including the vesicle diameter, encapsulation efficiency (EE) of CPZ and phospholipid concentration in the final formulation. Furthermore, the cytotoxicity of CPZ, CDs, empty liposomes and the DCL systems is evaluated against a panel of leukemia cell lines.

4.2 Materials and methods

4.2.1 Materials

HP-γ-CD (Cavasol® W8HP Pharma) was a gift from Ashland Global Specialty Chemicals Inc., SBE-β-CD (Captisol®) was a gift from Ligand Pharmaceuticals Inc. and Sugammadex (Bridion®) was kindly provided by Dr. Luc de Chaisemartin from Bichat Hospital. Chlorpromazine hydrochloride, sodium chloride and ammonium sulfate were purchased from Sigma-Aldrich. Milli-Q water was obtained by a Millipore® purification system (Millipore, Germany).

Hydrogenated Egg L-α-phosphatidylcholine (HEPC), cholesterol, 1,2-distearoyl-sn-glycero-3-phosphoethanolamine-N-[methoxy(polyethylene glycol)-2000] ammonium salt (DSPE-PEG_{2000}), 1,2-dioleoyl-sn-glycero-3-phosphoethanolamine-N-(lissamine rhodamine B sulfonyl) ammonium salt (Liss Rhod PE) were all supplied by Avanti Polar Lipid, Inc. (Albaster, AL, USA).

4.2.2 Methods

4.2.2.1 SUV preparation

Liposomes composed of HEPC, cholesterol and DSPE-PEG_{2000} (65:30:5, molar ratio) were obtained by the film hydration method. Specifically, the components were dissolved in a mixture of chloroform and methanol (2:1, v/v) and then organic solvents were evaporated at room temperature under a gentle stream of nitrogen, followed by drying under a vacuum overnight in order to completely remove residual organic solvents.. An appropriate volume of filtered (2 passages through 0.2 μm pore size) buffer (10 mM HEPES, 145 mM sodium chloride, pH 7.4) was added to the film to obtain a total lipid concentration of 30 mM. The lipid suspension subsequently underwent 10 repeats of 1 min heating at 62 °C and 1 min vortexing. SUVs were yielded by extrusion (Lipex^{TM}, Northern Lipids, Canada) through polycarbonate membranes (1 passage through 0.4 μm pore size, 2 passages through 0.2 μm pore size, 10 passages through 0.1 μm pore size) at 62 °C.

Fluorescent liposomes composed of HEPC, cholesterol, DSPE-PEG_{2000} and rhodamine B PE (65:30:5:0.5, molar ratio) were prepared by the same method as above.

4.2.2.2 DRV preparation

DRV were prepared as previously described (Kirby and Gregoriadis 1984). 2 mL of empty SUVs (30 mM) were first obtained by the extrusion method, an equal volume of CPZ solution prepared by Milli-Q water (4 mM) was then added and the mixture was vortexed vigorously for 3 min. The mixture was frozen at -20 °C for 3h, followed by overnight lyophilization (Cosmos, Cryotec). For the rehydration, 0.2 mL of pre-heated (at 62 °C) Milli-Q water was added to the freeze-dried lipid pellet that was then heated at 62 °C and vortexed for several cycles until total hydration. After leaving the MLV dispersion at room temperature for 30 min, 1.8 mL of 10 mM HEPES buffer (pH 7.4) was added and the mixture was kept at 62 °C for 50 min. To further homogenize the liposomes (optimized DRV method), an additional extrusion step was

performed with two passages through a 0.2 μm polycarbonate membrane. In the ammonium sulfate gradient DRV preparation protocol, Milli-Q water was replaced by the same volume of 300 mM ammonium sulfate in the re-hydration step while the other procedures remain unchanged. These procedures are illustrated in Figure 1 (Fig. 1).

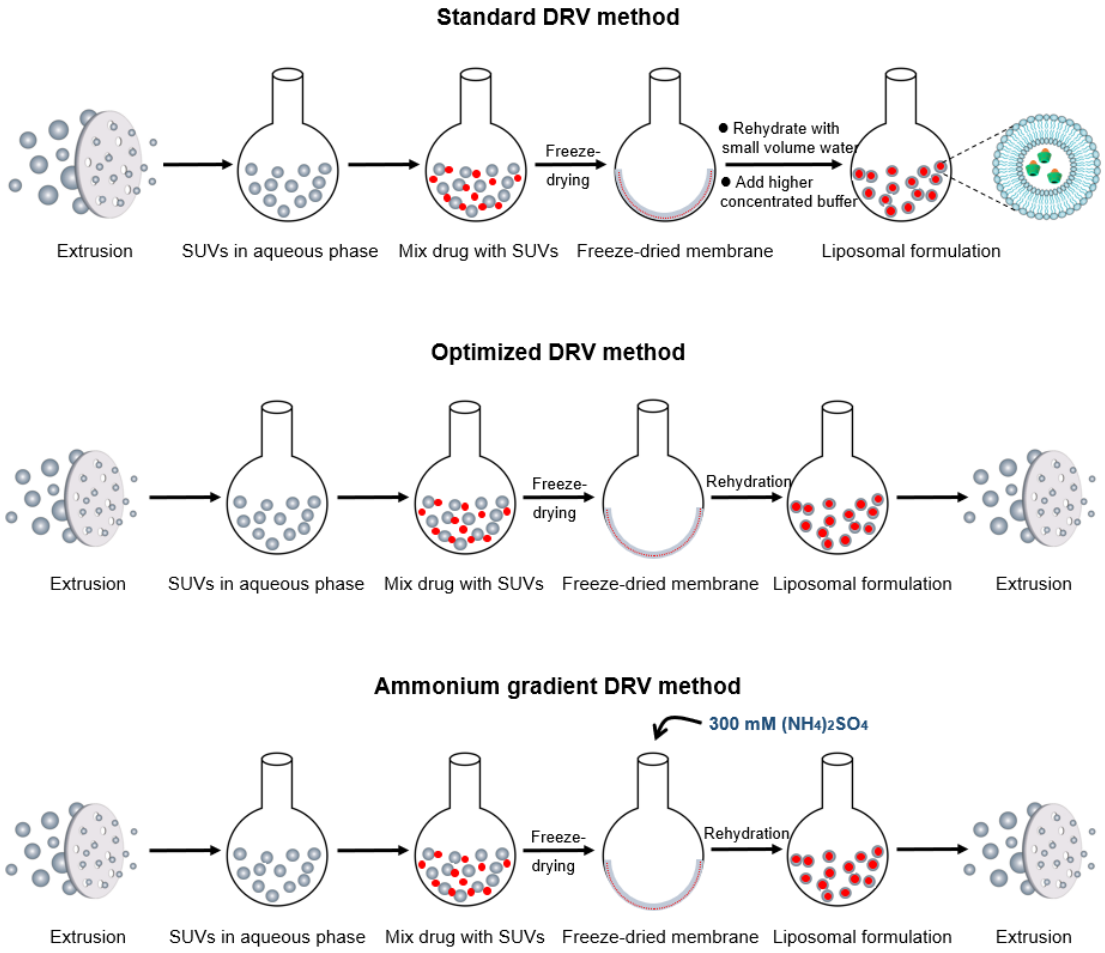

Fig. 1. Schematic representation of the standard DRV method, optimized DRV method and ammonium sulphate gradient DRV method.

To prepare the DRV containing CD/CPZ complexes, an equimolar solution containing 4 mM of CDs and 4 mM of CPZ was first obtained and then mixed well with the same volume of empty SUVs. Thereafter, freeze-drying, re-hydration and re-extrusion procedures were performed as above.

Non-encapsulated CPZ by was removed by ultracentrifugation in a Beckman Optima L-90K ultracentrifuge equipped with a Type 70:1 Ti rotor at 40,000 rpm (146682 × g) at 4 ℃ for 6 h. The DRV pellet was resuspended with 1.5 mL HEPES buffer.

4.2.2.3 Size measurements

Mean hydrodynamics diameters of the liposome preparations were obtained by dynamic light scattering using a Zetasizer Nano ZS90 (Malvern Instruments Corp., Worcestershire, UK). 40 μL sample was diluted into 1.6 mL buffer (10 mM HEPES, 145 mM sodium chloride, pH 7.4) for the measurements at 25 ℃, at a detection angle of 90°. Size distributions by intensity were recorded and the polydispersity index (PdI) was also acquired as an indication of the size distribution.

4.2.2.4 Quantification of CPZ by HPLC

HPLC analysis of CPZ concentration was performed using a Waters 717 Plus Autosampler HPLC system equipped with Waters 2487 Dual λ Absorbance Detector at wavelength of 254 nm and 309 nm. A C18 chromatographic column (Waters XTerra®, 5μm, 3.0×150 mm) was used for separation. The mobile phase was comprised of a mixture of acetonitrile, water and 0.1 mM ammonium bicarbonate pH 7 (7:2:1, v:v:v) and flow rate was set at 0.7 mL/min. The injection volume was 10 μL. A calibration curve was prepared using CPZ in mobile phase at concentrations between 5 μg/mL and 100 μg/mL.

4.2.2.5 Determination of the encapsulation efficiency of CPZ

The encapsulation efficiency (EE) of CPZ was determined after removing the unencapsulated CPZ by ultracentrifugation as described above. 0.1 mL of the dispersed DRV pellet was mixed with 0.4 mL HPLC mobile phase solution and HPLC was carried out as above. The CPZ was calculated from the calibration curve and the EE was obtained by the following equation:

$$EE\ (\%) = Area_{DRV} / Area_{initial\ CPZ} \times 100 \quad (1)$$

4.2.2.6 Phospholipid assay

The phospholipid concentration in the liposome preparations was estimated by measuring phosphatidylcholine using a commercial kit (Phospholipids Colorimetric Enzymatic Method, BIOLABO, France) according to the manufacturer's instructions. The reaction scheme of enzymatic colorimetric method is as follows:

$$\text{Phospholipid} + H_2O \xrightarrow{\text{Phospholipase D}} \text{Choline + phosphatidic acid + lysophophatidic acid + N acylsphingosyl phosphate}$$

$$\text{Choline} + 2O_2 \xrightarrow{\text{Choline Oxidase}} \text{Betaine} + 2H_2O_2$$

$$2H_2O_2 + \text{Pheol} + \text{4AAP} \xrightarrow{\text{Peroxidase}} \text{Quinoneimine} + 4H_2O$$

Concretely, 1 mL of the reagent was pipetted into 1.5 mL Eppendorf tubes for blank, standard and samples to be assayed, followed by addition of 10 μL Milli-Q water, standard phospholipid solution and sample, respectively. After vigorously mixing, the tubes were incubated at 37 °C for 10 min. The absorbance was recorded at 500 nm against the blank with Perkin-Elmer Lambda 2 double beam spectrophotometer (Perkin-Elmer, Courtaboeuf, France). The result was calculated according to the following equation:

$$\text{Concentration}_{Sample} = \text{Absorbance}_{Sample} / \text{Absorbance}_{Standard} \times \text{Concentration}_{Standard} \quad (2)$$

4.2.2.7 Cell culture

Four human leukemic cells lines and a rat kidney fibroblast cell line (NRK) were used to evaluate the cytotoxicity of the different formulations. The human promyelocytic leukemia cell line HL-60 was obtained from Dr. Brigitte Bauvois INSERM U872, Paris. NRK, MOLM13 (AML), OCI-AML (AML) and MV4-11 (myelomonocytic leukemia) cell lines were provided by Lars Herfindal (University of Bergen, Norway). HL-60, MOLM13 and OCI-AML were cultured in RPMI 1640 medium (Sigma-Aldrich), while MV4-11 cells were cultured in IMDM medium (Sigma-Aldrich) and NRK cells in DMEM medium (Sigma-Aldrich). All media were

supplemented with 10% fetal bovine serum (Gibco® by Life Technologies™), 1% penicillin streptomycin (Sigma-Aldrich) and 1% sodium pyruvate (Sigma-Aldrich). Cells were maintained in humidified incubator at 37 °C with 5% CO_2.

Mild trypsin treatment (0.33 mg/mL trypsin for 5 min at 37 °C) was performed when NRK cells reached 80% confluence, followed by centrifugation at 160g for 4 min and reseeding in fresh medium (Ibrahim et al. 2019).

4.2.2.8 Cytotoxicity evaluation

The cytotoxicity against HL-60 was evaluated by MTS metabolism. Briefly, 25000 cells in 50 µL medium per well were seeded in 96-well plates (TPP®, Swiss) and incubated in a humidified atmosphere with 5% CO_2 at 37 °C. 4 h later, 50 µL medium containing different concentration of CPZ, CDs, empty liposomes, liposomes containing CPZ and liposomes containing CD/CPZ complexes were added. The plates were incubated for 24 h, 48 h or 72 h. Cell viability was assessed by CellTiter 96® Aqueous One Solution Cell Proliferation Assay (Promega, France). Briefly, 25 µL of MTS reagent was added to each well and the plates were incubated for a further 2 or 4 h, after which the optical density (OD) was measured with a high-pass filter at 490 nm with ELISA plate reader (LT-5000 MS, Labtech).

The cytotoxicity towards MOLM13, OCI-AML and MV4-11 was assessed by a similar method involving the metabolism of WST-1. 50 µL medium containing different concentration of drugs was first added in the wells of 96-well plate, followed by the seeding of cells in 50 µL medium (35000 cells per well for 24 h incubation and 10000 cells for 72 h). After incubating the plate for 24 h or 72 h, 10 µL WST-1 reagent was added to each well and the plate was incubated for another 2 h. The OD was measured by plate reader (TECAN Infinite M200 Pro) at 450 nm.

For the NRK cells, 5000 cells in 100 µL medium per well were seeded in 96-well plates and incubated at 37 °C for 24 h. Different concentrations of drugs diluted in the medium was added to the cells and afterwards the same WST-1 procedures were

conducted. For the washout experiment, 100 μL of NRK cell suspension (10000 cells/mL) per well was seeded in 96-well plates and incubated at 37 °C for 24 h before treatment. After exposing the cells to different liposomal formulations for 24 h, the cells were washed twice with PBS buffer and fresh medium (100 μL/well) was added. Cells were incubated for another 48 h and the viability was assayed by WST-1.

In all cases, wells containing the different dilutions of the substances to be tested but without cells were used as blanks to correct for any interference due to the absorbance of the samples.

4.2.2.9 Flow cytometry

500 μL MOLM13 cell suspension (350000 cells/mL) per well was seeded in 48-well plates, followed by addition of fluorescent liposomes at defined concentrations and timepoints. The plate was incubated at 37 °C and the experiment was stopped by washing with PBS buffer for twice. Cells were kept in ice and dark until measured by flow cytometry with FACS Accuri C6 (BD Biosciences, San Jose, CA, US). The laser wavelength was 488 nm with a 585/40 nm filter and the fluid flow rate was 66 μL/min.

4.3 Results and discussion

4.3.1 DRV preparation and characterization

4.3.1.1 DRV prepared by the standard method

Preliminary investigations of the interactions between CPZ and phospholipids by differential scanning calorimetry (DSC) indicated that a reasonable molar ratio of CPZ to prepare a liposomal formulation with maximal encapsulation in the aqueous core without disrupting the bilayer is 3.75 %. Thus 1.1 mM of CPZ was used with a total lipid concentration of 30 mM.

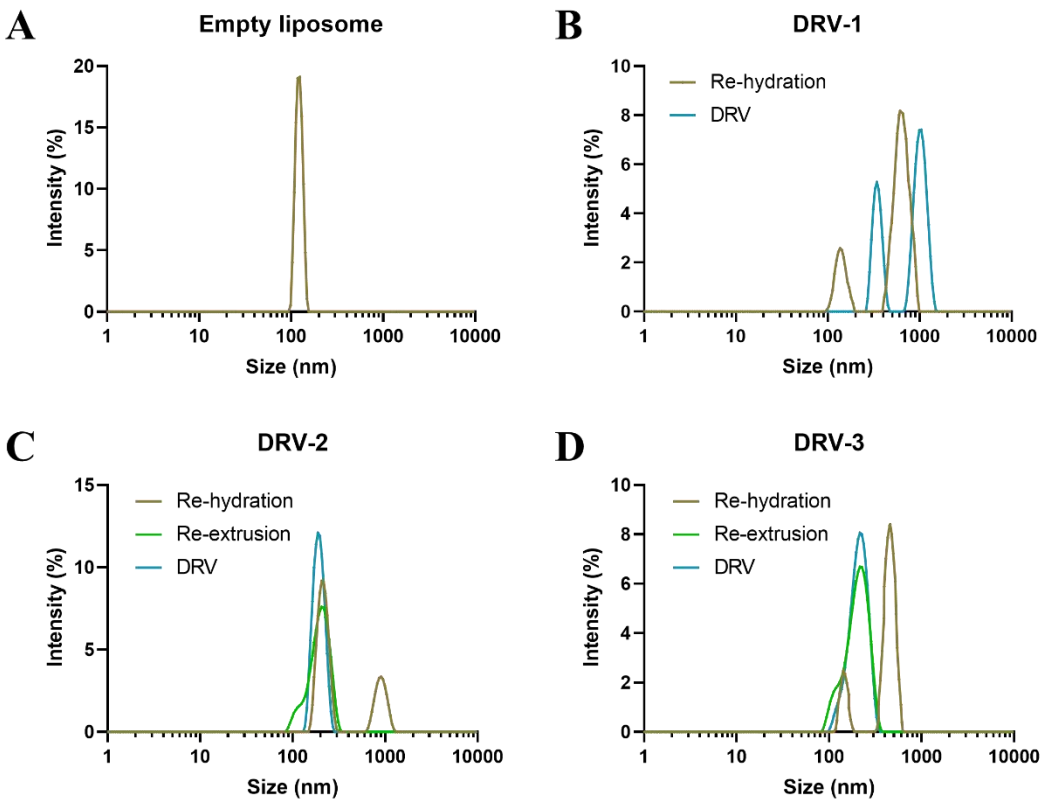

Fig. 3. Dynamic light scattering profile of empty liposomes (A), DRV prepared by standard method with 1.1 mM CPZ (DRV-1, B), DRV prepared by optimized method with 1.1 mM CPZ (DRV-2, C) and DRV prepared by optimized method with 5.4 mM CPZ (DRV-3, D).

Firstly, empty liposomes (HEPC:Chol:DSPE-PEG$_{2000}$, 65:30:5) were obtained by extrusion with a diameter of 122 nm (Fig. 3A). DRV-1 was prepared by the standard method. After rehydration, a distribution with 2 peaks was observed, with diameters of 134 nm and 664 nm, respectively (Fig. 3B). After removing the unencapsulated CPZ by ultracentrifugation, the main peak of the distribution shifted to 1026 nm. Although the EE of CPZ was high (28.3%, Table 1), this diameter was not ideal for intravenous administration. To obtain smaller liposomes for *in-vivo* application, a re-extrusion procedure (two passages through 0.2 μm) was added after the rehydration step. The optimized protocol yielded DRV-2, whose average size decreased to 188 nm as a result of re-extrusion and expanded slightly to 193 nm after ultracentrifugation (Fig. 3C). For DRV-2, the diameter fulfilled the requirements for intravenous injection but another drawback appeared, the low EE (9.8%), which is an important parameter for a drug

delivery system. The low EE may not only reduce the therapeutic effect due to insufficient drug reaching the target tissue but also increase the possibility of side effects caused by a higher dose of the formulation. Therefore, a higher concentration of CPZ was used in an attempt to improve the EE.

Thus, 5.4 mM CPZ was used to prepare DRV-3. The diameters of DRV-3 after re-extrusion and ultracentrifugation were 189 nm and 208 nm, respectively (Fig. 3D). Moreover, the EE rose to 18.3%, with an increase of 8.5% compared with DRV-2 (Table 1), suggesting that adopting a higher concentration of CPZ could be an efficient way to increase the EE, despite the risk of CPZ interacting with the lipid bilayer and destabilizing the liposomes.

Table 1 Properties of DRV-1, DRV-2 and DRV-3

	DRV-1		DRV-2		DRV-3	
	Size (nm)	PdI	Size (nm)	PdI	Size (nm)	PdI
Re-extrusion size	-	-	188	0.094	189	0.078
DRV size	1026	0.308	193	0.070	208	0.084
CPZ EE (%)	28.3		9.8		18.3	
C_{CPZ} (μM)	311		529		988	

Abbreviations: EE, encapsulation efficiency; C_{CPZ}, concentration of CPZ in DRV.

4.3.1.2 DRV prepared by the ammonium sulfate gradient method

Fixing the concentration of CPZ at 5.4 mM, DRV containing SBE-β-CD/CPZ complexes (DRV-4) was prepared but a low EE was obtained (9.9%) (Fig. 4A), indicating that the complexes are not as efficiently encapsulated as the free drug. Different results have been obtained when comparing the EE of free drug and CD-associated drug. A higher EE for HP-γ-CD/curcumin MLVs (50%) was found compared with curcumin MLVs (Dhule et al. 2012). On the contrary, the EE of HP-β-CD/nifedipine liposomes (21.9%) was lower than those without HP-β-CD (56.2%)

(Skalko 1996). No difference was found between γ-CD/doxorubicin-PEGylated liposomes (91.1%) and doxorubicin-PEGylated liposomes (96.4%) (Hagiwara et al. 2006). Moreover, the type of CD also has an impact on the EE. For example, Maestrelli et al reported that the EE of HP-β-CD/ketoprofen MLVs (33.8%) is higher than that of β-CD/ketoprofen (26.8%) (Maestrelli et al. 2005). Despite a number of related studies, the mechanism of how CDs affect the EE of DCL system remains unclear.

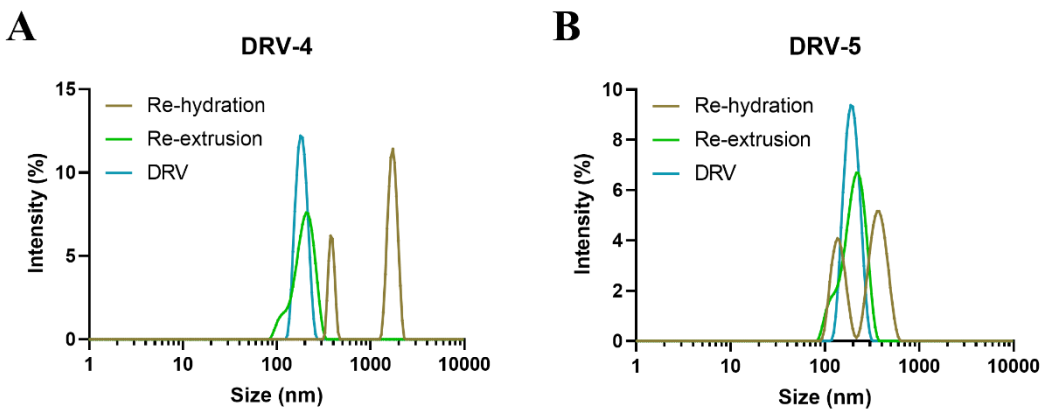

Fig. 4. Dynamic light scattering profile of DRV prepared by the optimized method with SBE-β-CD/CPZ complexes (DRV-4, A) and DRV prepared by the ammonium sulphate gradient DRV method with CPZ (DRV-5, B).

Since the EE of SBE-β-CD/CPZ was reduced compared with the free drug, to further optimize the encapsulation, an active loading strategy with an ammonium sulfate gradient was combined with the standard DRV method. The ammonium sulfate gradient method was first reported by Gabizon in 1989 (Gabizon et al. 1989). Relying on the transmembrane gradient of ammonium sulfate, this method is efficient at entrapping small molecules, especially amphipathic ones, in liposomes. It is worthwhile to note that the first PEGylated liposomal doxorubicin (Doxil®) approved by FDA in 1995 was produced by ammonium sulfate gradient method. By adopting this strategy in CPZ encapsulation, the EE increased to 27.4% (DRV-5) compared to the standard DRV protocol (18.3%) (Fig. 4B). Since Hait reported the IC_{50} of CPZ for HL-60 cell

line was 8 μM (Hait et al. 1985), the final concentration of CPZ in DRV-5 (1479 μM) is sufficient for the *in-vitro* evaluation.

Table 2 Properties of DRV-4 and DRV-5

	DRV-4		DRV-5	
	Size (nm)	PdI	Size (nm)	PdI
Re-extrusion size	188	0.094	183	0.073
DRV size	189	0.088	197	0.119
C_{PS} in DRV (mM)	15.2		13.9	
CPZ EE (%)	9.93		27.4	
C_{CPZ} (μM)	534		1479	

Abbreviations: EE, encapsulation efficiency; C_{CPZ}, concentration of CPZ in DRV.

4.3.1.3 DCL liposomal formulation

The ammonium sulfate gradient DRV method proved to be an efficient strategy to prepare the DCL liposomal formulation. According to preceding comprehensive investigations on the physicochemical properties and interaction with CPZ and phospholipid, HP-γ-CD, SBE-β-CD and SGM were selected for the preparation of the DCL system because of their high association capacity with CPZ revealed by ITC, which could reduce the possibility of drug leakage and contribute to delayed release during the long circulation time after intravenous administration.

Consequently, DRV containing CPZ alone, HP-γ-CD/CPZ, SBE-β-CD/CPZ and SGM/CPZ were obtained by the ammonium sulfate gradient method. Despite the variation of size distribution after re-hydration, these 4 types of DRV showed a slight increase in the vesicle diameter of the final DRV (202 nm, 206 nm, 217 nm and 260 nm, respectively) (Fig. 5), implying that CDs have an influence on the diameter of DCL formulation in the order SGM > SBE-β-CD > HP-γ-CD.

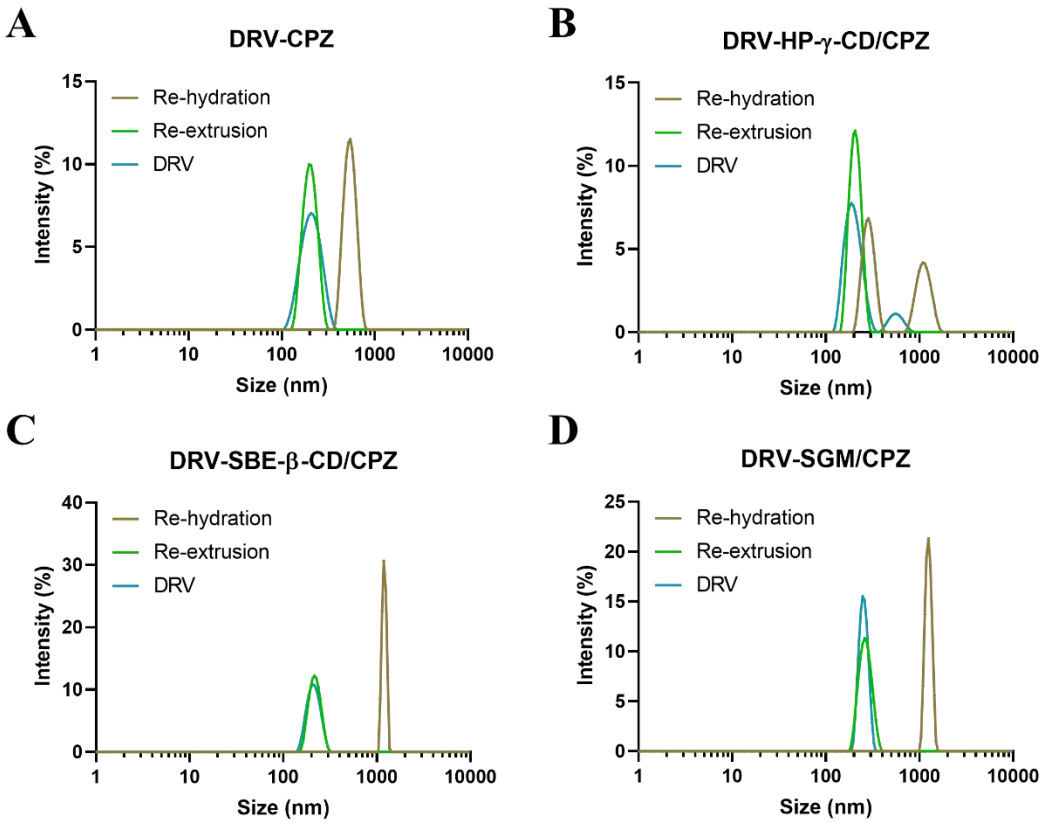

Fig. 5. Dynamic light scattering profile of DRV-CPZ (A), DRV-HP-γ-CD/CPZ (B), DRV-SBE-β-CD/CPZ (C) and DRV-SGM/CPZ (D).

The impact of CDs on the diameter of DCL was also studied by other researchers. Liposomes encapsulating CD/ketoprofen complexes were prepared by Maestrelli et al. The diameter of MLVs containing ketoprofen (1.52 μm ± 0.05) is similar to that of empty ones (1.58 μm ± 0.08), while the size increased significantly in the presence of β-CD (3.05 μm ± 0.07) and HP-β-CD (3.16 μm ± 0.10) (Maestrelli et al. 2005). Piel et al prepared MLVs entrapping betamethasone complexed with a series of CD derivatives (HP-β-CD, HP-γ-CD, Rameb, Crysmeb) at 10 mM and 40 mM, demonstrating a similar vesicle size for liposomes with and without CDs (Piel et al. 2006). Similarly, no obvious difference was observed in HP-β-CD/nifedipine SUVs (155 nm) and nifedipine SUVs (153 nm) (Skalko 1996). In fact, to the best of our knowledge, CDs show no significant effect on the diameter of DCL system with respect to the empty liposomes in most cases (Gharib et al. 2015).

Furthermore, an obvious decrease of the EE was observed for the DRV containing CD/CPZ complexes (18.3%, 15.6% and 18.2% in presence of HP-γ-CD, SBE-β-CD and SGM, respectively) compared to the DRV entrapping CPZ alone (29.5%) (Table 3). In the ammonium sulfate gradient method, the unionized form of CPZ can cross the lipid membrane easily and subsequently undergoes ionization in intraliposomal solution and becomes "locked" inside. However, when forming inclusion complexes with CDs, only a small amount of CPZ can pass through the liposomal membrane freely, thus leading to a low EE in DCL system.

In fact, the effect of CDs on the EE of DCL system varies in different situations. According the study of Piel et al, the EE of betamethasone showed obvious differences between CD types (Piel et al. 2006). The dependence of drug EE on the CD concentration in a DCL system was investigated by Maestrelli et al, who reported that the EE of ketoprofen could reach to the peak value at 10 mM with the increase of HP-β-CD/ketoprofen complexes concentration and then declined at lower concentration. The decrease of EE was explained by the destabilizing effect of CD at high concentration (Maestrelli et al. 2006), while the CDs in our DCL system showed no destabilizing effect. Despite the variety of CDs, HP-β-CD has been used to achieve higher EE in many cases, due to its high aqueous solubility (Gharib et al. 2015).

Table 3 Properties of DRV-CPZ, DRV-HP-γ-CD/CPZ, DRV-SBE-β-CD/CPZ and DRV-SGM/CPZ

	DRV-CPZ		DRV-HP-γ-CD/CPZ		DRV-SBE-β-CD/CPZ		DRV-SGM/CPZ	
	Size	PdI	Size	PdI	Size	PdI	Size	PdI
Re-extrusion size	195	0.080	207	0.058	216	0.041	257	0.019
DRV size	202	0.069	206	0.089	216	0.100	256	0.038
C_{PS} in DRV (mM)	15.7		15.4		16.6		16.3	
CPZ EE (%)	29.5		18.3		15.6		18.2	
C_{CPZ} (μM)	1180		732		624		728	

Abbreviations: EE, encapsulation efficiency; C_{CPZ}, concentration of CPZ in DRV.

4.3.2 *In-vitro* evaluation of DCL

4.3.2.1 Cytotoxicity of CPZ

First of all, to confirm that the drug could have an effect on leukemic cells, we studied the cytotoxicity of CPZ towards the HL-60 cell line after 24 h, 48 h and 72 h incubation (Fig. 6). A clear concentration-dependent decrease of cell viability was observed at each time point, demonstrating that CPZ is capable of inhibiting the growth of the cells. Furthermore, CPZ showed a time-dependent effect. The concentration inhibiting 50% cell viability (IC_{50}) of CPZ decreased from 27.3 μM after 24 h incubation, to 21.9 μM and 18.2 μM in the case of 48 h and 72 h incubation, respectively. This value is higher than that of 8 μM reported by Hait et al using the same cell line (Hait et al. 1985). Nevertheless, the result justifies the further application of CPZ for AML treatment. To simplify the *in-vitro* assessment and compare the results directly, we selected the 48 h incubation time for the subsequent study with HL60 cells.

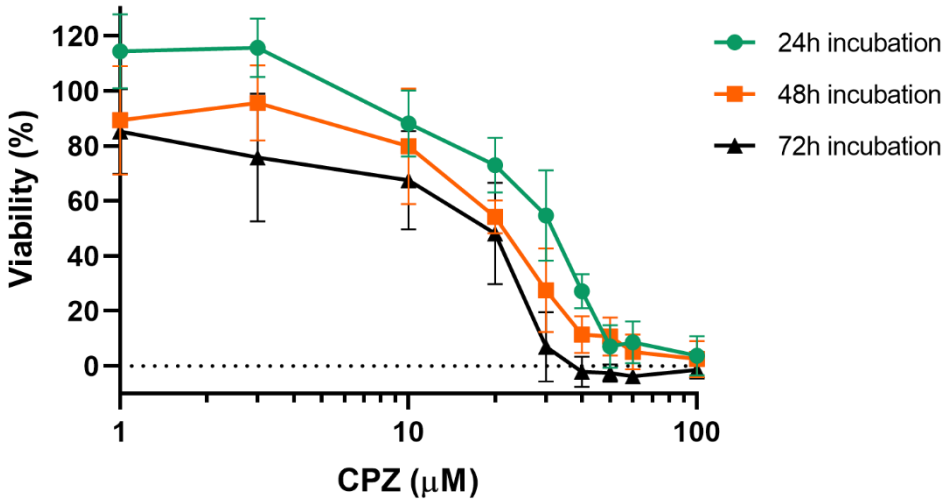

Fig. 6. Effect of CPZ on the viability of HL-60 cells. The results are mean ± SD of six wells measured by MTS.

4.3.2.2 Cytotoxicity of empty liposomes and CDs

The cytotoxicity of empty liposomes was also evaluated. Fig. 7A shows that the cell viability increased slightly with the liposomal concentration, since 125% of control viability as determined by MTS reduction was observed when the cells were incubated with 1600 μM liposomes for 48 h, indicating that the liposomes could facilitate the growth of HL-60.

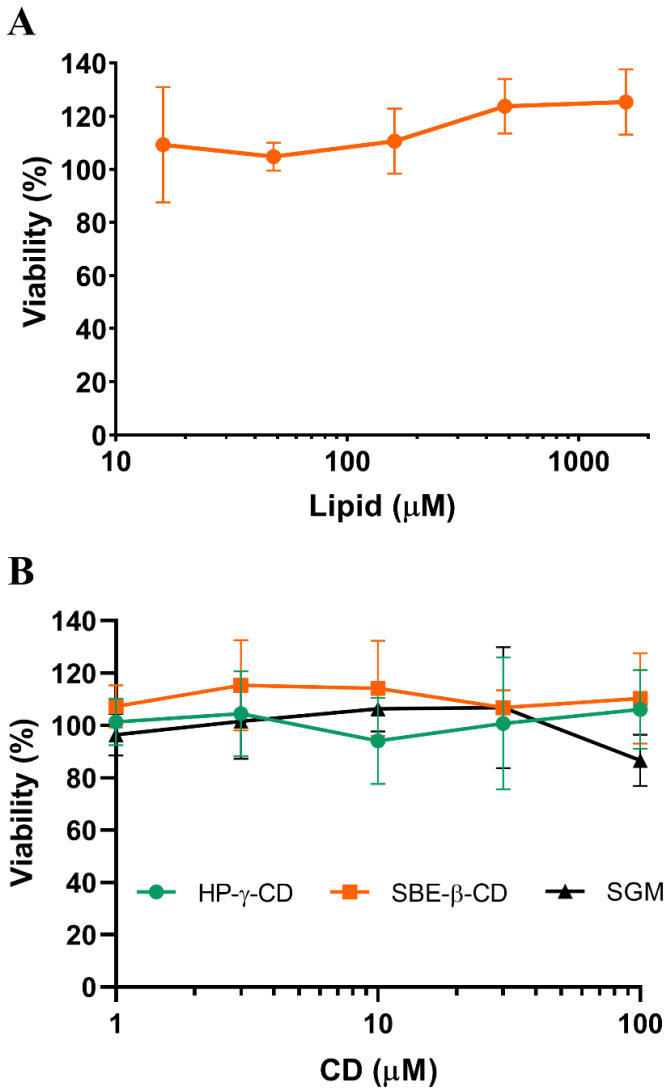

Fig. 7. Effect of empty liposomes (A) and CDs (B) on the viability of HL-60 cells. The results are mean ± SD of four wells measured by MTS.

Though there is no clear mechanism about the effect of liposomes on AML cell lines, a possible hypothesis is that an enhancement of de novo synthesis of fatty acids is necessary for membrane synthesis and therefore for cell proliferation in many tumors, with a symptom of enhanced lipogenesis (Stefanko et al. 2017; Loew et al. 2019). In the microenvironment of bone marrow, fatty acids are accumulated, indicating an increased lipid catabolism of the AML cells. In fact, global proteomic and lipidomic approaches have demonstrated an increase of lipid metabolism concerning phosphatidylinositol, sphingolipids, free cholesterol and monounsaturated fatty acids in leukemic cells (Stuani et al. 2018). Thus, the incubation of HL-60 cells with empty liposomes could stimulate the cell proliferation. The absence of any toxic effects of empty liposomes facilitates the interpretation of results obtained with encapsulated CPZ.

It was also important to check the cytotoxicity of the CDs used: HP-γ-CD, SBE-β-CD and SGM, against HL-60 (Fig. 7B). No significant cytotoxicity was observed for any of the three CDs. These findings are in accordance with many other observations of the safety of CDs for pharmaceutical applications (Loftsson et al. 2005). Generally, CDs present no cytotoxicity at the concentrations used in pharmaceutical preparations. For example, the IC_{50} of HP-β-CD and ionic β-CDs was found to be higher than 200 mM against Caco-2 cells (Kiss et al. 2010). Although the methylated-β-CD derivatives are more toxic, most of them have an IC_{50} higher than 50 mM. In fact, CD complexation can reduce the toxicity of the drug: chlorzoxazone in complex form with β-CD and HP-β-CD showed less toxic to normal liver cells than its free form (Tang et al. 2015). As far as *in-vivo* toxicity is concerned, the LD_{50} doses of intravenously administered CD are quite high: 1.0 g per kg, 0.79 g per kg and 4.0 g per kg for α-, β- and γ-CD respectively (Davis and Brewster 2004).

4.3.2.3 Cytotoxicity of DCL

Fig. 8 shows the cytotoxicity of DRV containing CPZ and the different CD/CPZ complexes (Fig. 8). Since the EE varied among the 4 DRVs, different dilutions were done to adjust the CPZ concentration to the same level. Free CPZ and the simple

liposomal form (CPZ DRV) showed very similar IC_{50} values of 12.8 μM and 13.3 μM, respectively. The slightly lower value for CPZ DRV could be attributed to the promoting effect of empty liposomes compensating for the effect of CPZ or that encapsulation rendered the CPZ less available to the cells. For the CD DRVs, low concentrations showed slightly increased viability, compared with the control, and the IC_{50} values varied depending on the CD type. The IC_{50} for HP-γ-CD DRV was 21.1 μM, slightly higher than that of CPZ DRV. In the case of SBE-β-CD DRV, a higher IC_{50} was obtained at 33.4 μM. This suggests that CPZ is more strongly retained in the CD and not able to exert its effect on the cells. Interestingly, no cytotoxicity was exhibited by SGM DRV, even at a concentration of 100 μM CPZ, indicating that SGM entrapped CPZ tightly within its hydrophobic cavity and the inclusion complexes efficiently restricted the release of CPZ. These findings are in accord with the results acquired in the ITC experiment in which SGM had the highest complex formation constant with CPZ.

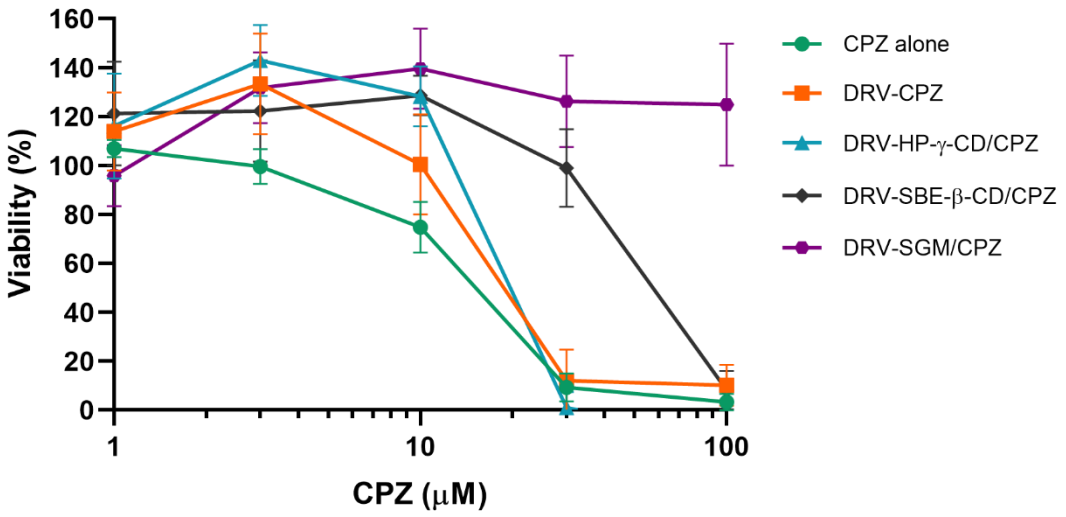

Fig. 8. Effect of CPZ and DRVs on the viability of HL-60 cells. The results are mean ± SD of four wells measured by MTS.

In brief, the 3 DCL formulations of CPZ showed reduced activity compared with CPZ alone, which would indicate that the drug was sequestered within the CD to a greater or lesser extent, which could provide delayed release properties and be an advantage to maintain an effective concentration of CPZ for a longer time after intravenous administration. A similar phenomenon was observed by Chen et al, who found the hydrophobic drug, indomethacin, was released rapidly from the lipid bilayers, whereas for liposomes containing CD/indomethacin complexes, a slower drug release was observed (Chen et al. 2007). According to the authors, two routes of drug release from the DCL system can be envisaged: a) the CD/drug complexes can be released from the liposomes intact by passing through the lipid bilayers; b) free drug is released from the interior aqueous phase of liposomes as equilibrium is established between CD and drug. Therefore, in both situations, the speed of drug release will be affected by the CD. Furthermore, the type of CD also plays an important role in the drug release for DCL system, due to their different complexation capabilities. Piel et al reported a decreasing order of the release rate of betamethasone from DCL formulations: Crysmeb > HP-γ-CD > Rame b> γ-CD > HP-β-CD (Piel et al. 2006). In addition, the drug release is also related to the type of liposomes. For example, the release of ketoprofen could be observed in increasing order： LUV containing HP-β-CD/ketoprofen < MLV containing HP-β-CD/ketoprofen < SUV containing HP-β-CD/ketoprofen, which can be explained by the smaller size of SUV and higher viscosity of LUV (Maestrelli et al. 2006; Gharib et al. 2015).

4.3.2.4 Cytotoxicity evaluation of DCL on a panel of cell lines

After the promising initial results of cytotoxicity against the HL-60 cell line, the effect of the DCL system containing CPZ was evaluated against four further cell lines: the rat kidney fibroblast line (NRK) as an example of non cancerous cells and 3 AML cell lines (MOLM13, MV4-11 and OCI-AML). The properties of the preparations used in this part of the study are listed in Table 4. As before, DRV containing CPZ, HP-γ-

CD/CPZ, SBE-β-CD/CPZ and SGM/CPZ were obtained by the ammonium sulfate gradient method, with diameters of 201 nm, 189 nm, 212 nm and 225 nm, respectively. The EE decreased from 28.9% in DRV with CPZ to approximately 12% in presence of CDs (Table 4).

Table 4 Properties of formulations for *in-vitro* evaluation of cytotoxicity

	DRV-CPZ		DRV-HP-γ-CD/CPZ		DRV-SBE-β-CD/CPZ		DRV-SGM/CPZ	
	Size	PdI	Size	PdI	Size	PdI	Size	PdI
Re-extrusion size	189	0.078	184	0.049	205	0.060	230	0.013
DRV size	201	0.002	189	0.070	212	0.062	225	0.085
C_{PS} in DRV (mM)	12.1		14.1		15.6		16.0	
CPZ EE (%)	28.9		12.6		12.8		11.5	
C_{CPZ} (μM)	1156		504		512		460	

Abbreviations: C_{PS}, concentration of phospholipids; EE, encapsulation efficiency; C_{CPZ}, concentration of CPZ in DRV.

The viability of NRK cells after 24 h of exposure to the different formulations is shown in Fig. 9A. These “normal” cells are less sensitive to CPZ than HL-60 cells. For NRK cells, the CPZ DRV and HP-γ-CD DRV showed a higher inhibiting effect than CPZ alone. This difference may be due to a difference in drug release or cellular uptake mechanism in the interaction between liposomes and NRK cells. However, a similar reduced effect of CPZ was observed in the case of SBE-β-CD DRV as well as no cytotoxicity and a slight growth-promoting effect of SGM DRV was observed.

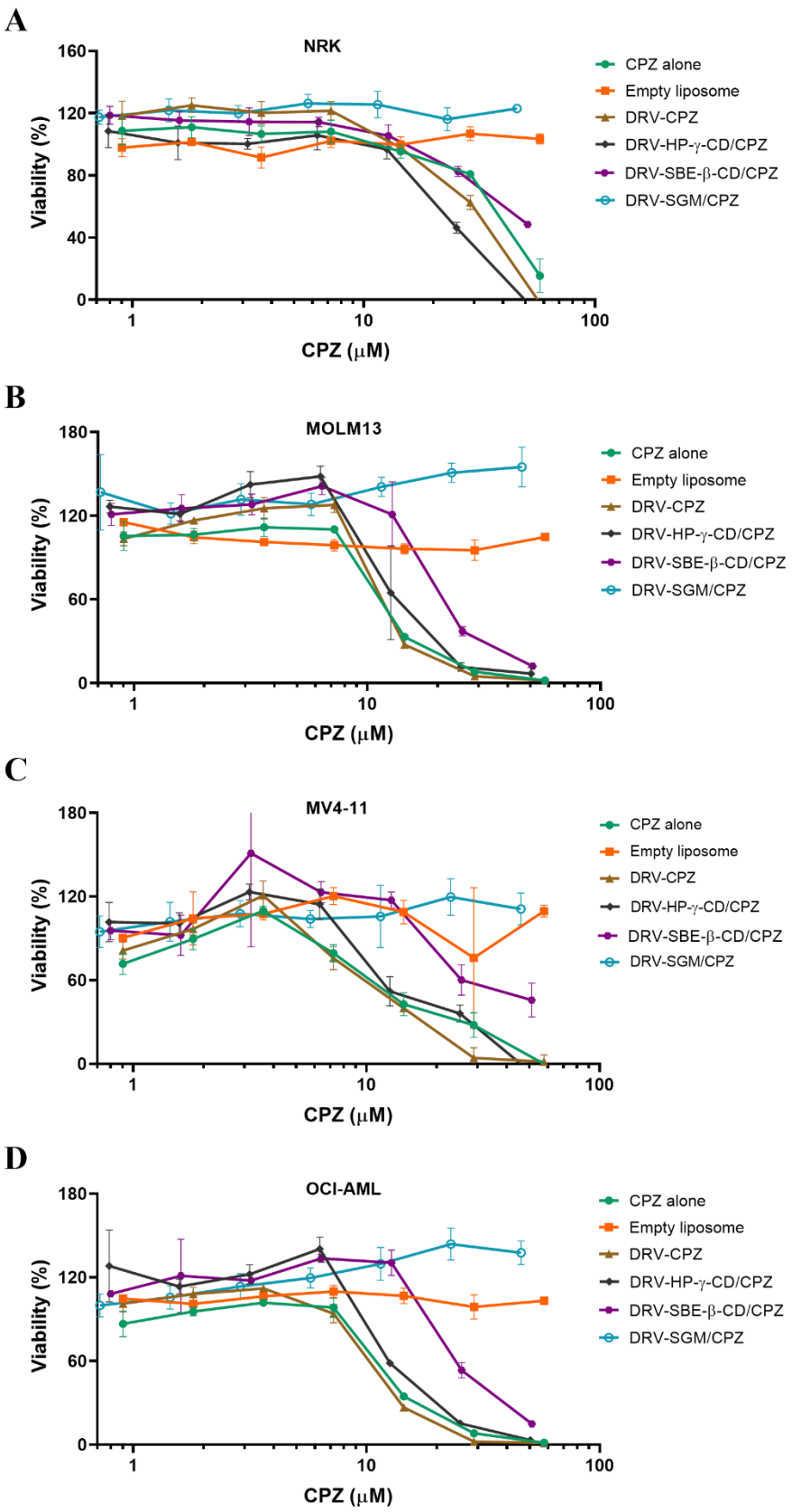

Fig. 9. Effect of CPZ, empty liposomes and DRVs on the viability of NRK cells (A), MOLM13 cells (B), MV4-11 cells (C), and OCI-AML cells (D) after 24 h incubation. The results are mean ± SD of three wells measured by WST-1.

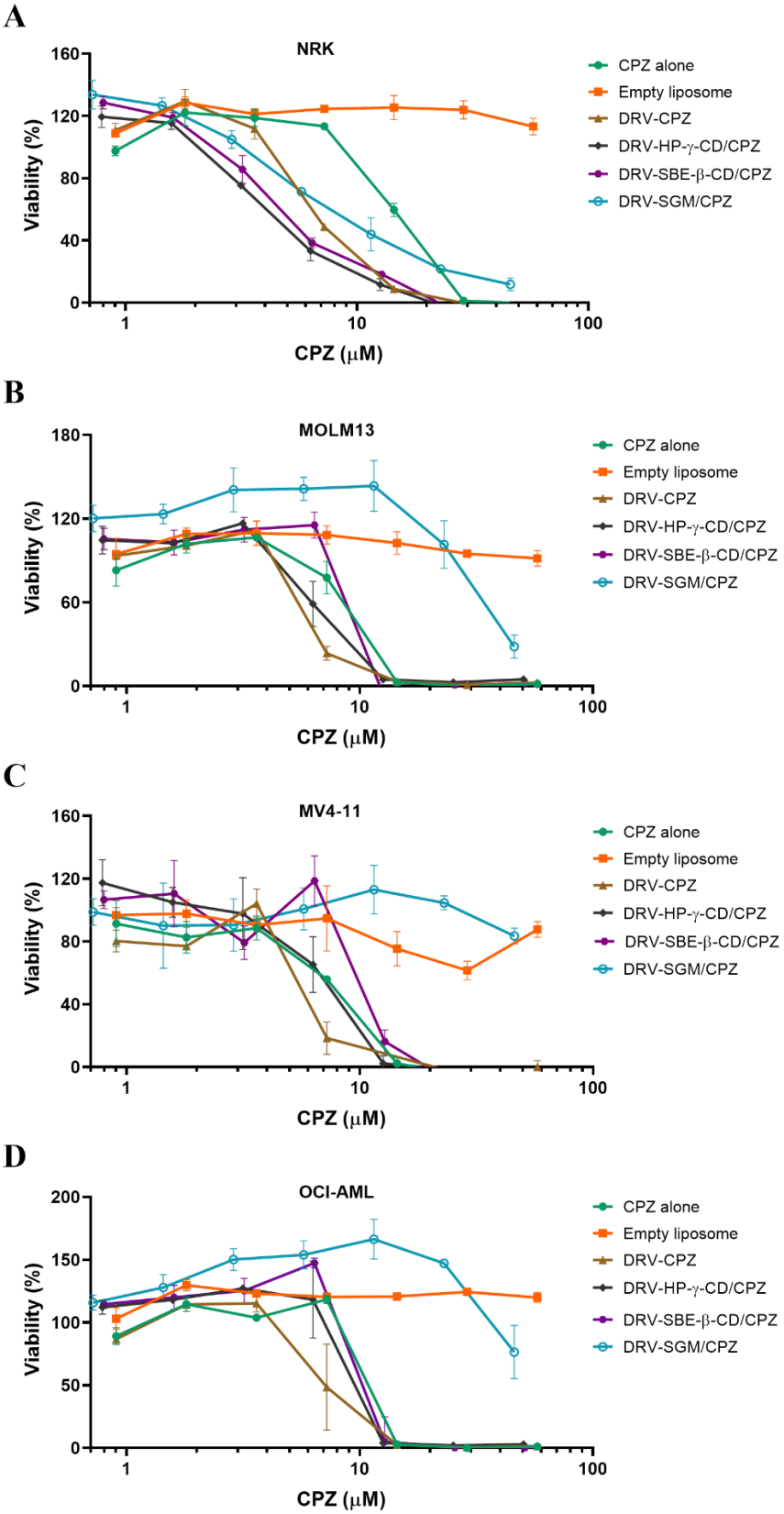

Fig. 10. Effect of CPZ, empty liposomes and DRVs on the viability of NRK cells (A), MOLM13 cells (B), MV4-11 cells (C), and OCI-AML cells (D) after 72 h incubation. The results are mean ± SD of three wells measured by WST-1.

Three AML cell lines, MOLM13, MV4-11 and OCI-AML, were also investigated (Fig. 9B, C, D). In general, the results were similar to those observed with HL-60. Specifically, compared to the free form of CPZ, the liposomal form exhibited reduced cytotoxicity. For example, in the case of MOLM13, the IC_{50} of CPZ alone was 12.5 μM, while it was 13.8 μM and 20.5 μM for HP-γ-CD DRV and SBE-β-CD DRV, respectively. CPZ DRV showed similar cytotoxicity to CPZ alone, and a growth-promoting effect was also found with SGM DRV, with 154% of viability when the cells were incubated with liposomes containing 46 μM CPZ. Similar results were obtained with the MV4-11 and OCI-AML cell lines, confirming the therapeutic potential of CPZ DCL system for AML treatment and the variations between the different CDs.

To further investigate the hypothesis that the DCL system allows delayed release of CPZ, experiments were performed with an incubation time of 72 h. Even with this longer incubation time, the empty liposomes were not cytotoxic and had a slight growth-promoting effect on all four cell lines. However, there were some differences in the cytotoxicity of CPZ (free or liposomal form) compared with the 24 h incubation (Fig. 10). For example, the cytotoxicity of CPZ-loaded liposomes towards AML cells was obviously increased after the longer incubation time. Additionally, in terms of NRK cells, all the liposomal forms of CPZ, CPZ DRV, HP-γ-CD DRV, SBE-β-CD DRV and SGM DRV, showed a stronger inhibiting effect than CPZ alone.

According to Torchilin, there are several modes of interaction between liposomes and cells (Torchilin 2005). The liposomes could release the drug into the extracellular matrix after which it would enter the cell as free drug or fuse with the cell membrane and discharge drug into the cell cytoplasm. However, the most common route for the liposome-cell interaction is endocytosis. Therefore, for NRK cell line, the higher cytotoxicity of CPZ in the liposomal form could be explained by the latter two mechanisms, fusion or endocytosis, allowing a better accumulation of drug than when the drug is given in the free form. Another consideration could be drug stability in the culture medium during the longer incubation. Encapsulation in liposomes could protect the drug and allow effective concentrations to be maintained for longer.

Another observation after the 72 h incubation is the cytotoxicity due to SGM DRV, in contrast to the effects at 24 h. This confirms the complexation capability of SGM that could be an advantage for avoiding rapid release of CPZ in the plasma, a more challenging physiological environment for liposomes than cell culture medium.

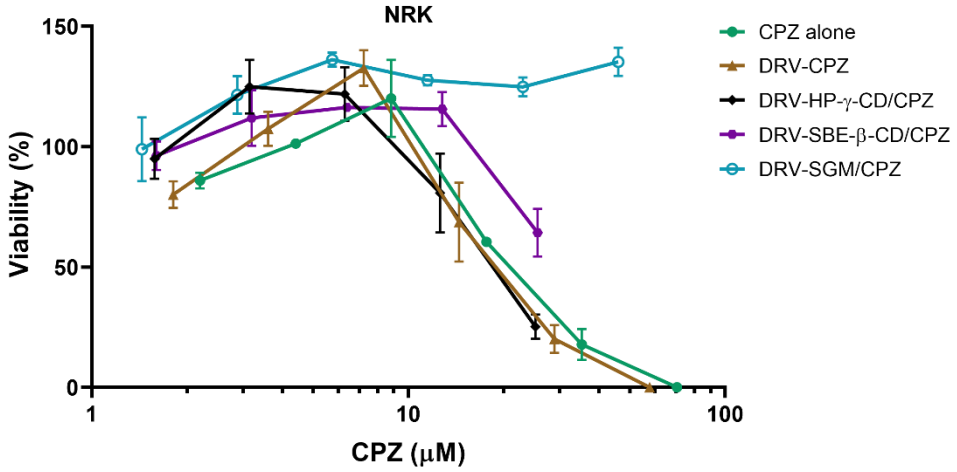

Fig. 11. Effect of CPZ and DRVs on the viability of NRK cells, with 24 h incubation with drugs plus 48 h incubation with fresh medium. The results are mean ± SD of two wells measured by WST-1.

Compared to the AML cell lines, we observed a significant increase of the cytotoxicity of DRV containing CPZ after 72 h incubation with NRK cells, compared with 24 h. There are several hypothesis for this difference: a) for NRK cells, a sufficient uptake of DRV occurs at earlier stage but the intracellular release or taking effect of CPZ needs a longer time; b) the uptake rate of DRV for NRK cells is slower than that for AML cells; c) NRK cells need a higher dose of CPZ to show cytotoxic effect than the AML cells. In an attempt to distinguish between these hypotheses, a washout experiment was carried out. Concretely, after 24 h exposure to liposomal formulations, the NRK cells were washed and fresh medium was added, followed by another 48-h incubation. Figure 11 shows that, for all the formulations, a similar inhibiting effect to that obtained after a simple 24 h incubation was observed. This result suggests that one of the last two hypotheses (b or c) applies, thereby providing promising evidence that CPZ and its liposomal formulations are selective towards AML cells.

4.3.2.5 Cellular uptake of the DCL system

In addition, the cellular uptake of liposomes by one of the AML lines was investigated by flow cytometry. The properties of the fluorescent DRV preparations are shown in Table 5. Their fluorescence intensity was determined for various dilutions in a microplate reader. As shown in Fig. 12A, the fluorescence intensity was concentration-dependent manner for all the liposomal formulations, but the slopes were different. Despite a similar content of the fluorescent label, rhodamine B PE in all formulations, empty liposomes demonstrated significantly higher fluorescence intensity than other DRV. A probable explanation of this phenomenon is fluorescence quenching by CPZ. Jiang et al observed that the fluorescence of rhodamine B PE in POPC liposomes was quenched in a concentration-dependent way for 0.1mM to 10 mM CPZ (Jiang et al. 2017). It is perhaps noteworthy that less quenching was observed with DRV containing SGM, which has the strongest affinity for CPZ. This could indicate that in these DRV the CPZ remains better associated with the CD and is less available to interact with the lipids in the liposome membrane.

Table 5 Properties of fluorescent liposomal formulations

	DRV-CPZ		DRV-HP-γ-CD/CPZ		DRV-SBE-β-CD/CPZ		DRV-SGM/CPZ	
	Size	PdI	Size	PdI	Size	PdI	Size	PdI
Re-extrusion size	199	0.051	191	0.040	193	0.070	207	0.002
DRV size	206	0.071	195	0.086	210	0.041	213	0.111
C_{PS} in DRV (mM)	19.3		19.9		18.7		19.7	
CPZ EE (%)	35.3		21.6		14.5		13.0	
C_{CPZ} (μM)	1411		862		579		519	

Abbreviations: C_{PS}, concentration of phospholipids; EE, encapsulation efficiency; C_{CPZ}, concentration of CPZ in DRV.

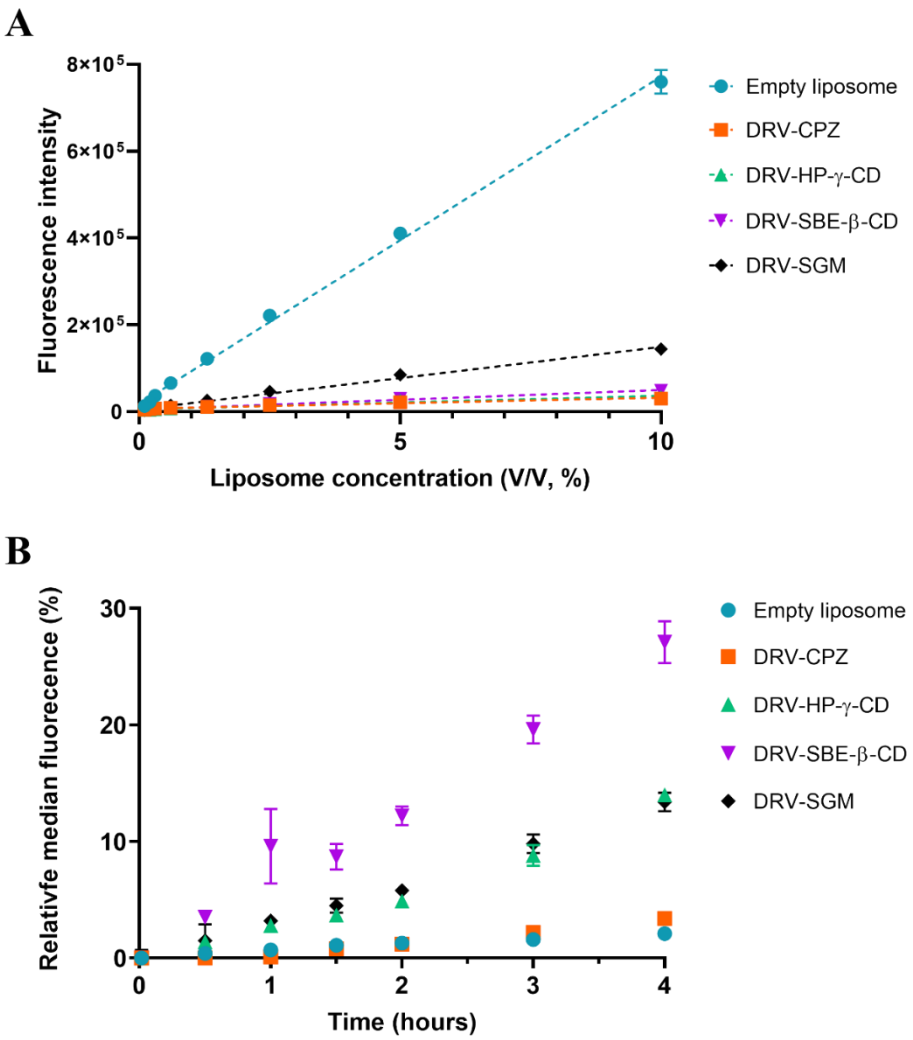

Fig. 12. Calibration curve of fluorescent liposomes (A) and cellular uptake in MOLM13 cells determined by flow cytometry (B). The results are mean ± SD of three repeats.

Subsequently, uptake by MOLM13 cells was investigated by incubating with 2% (v/v) of fluorescent liposomes. For all the samples, the relative median fluorescence, namely the amount of fluorescence associated with the cells, increased with time, indicating that liposomes accumulated gradually in the cells and that the process was not saturated at 4 h (Fig. 12B). After 4 h of contact, the liposomes were taken up by MOLM13 cells in the order: SBE-β-CD DRV > HP-γ-CD DRV > SGM DRV > CPZ DRV > empty liposomes, with a relative uptake of 27.1%, 14.0%, 13.4%, 3.4% and 2.1%, respectively. This seems to indicate that liposomes containing CDs were more

easily absorbed compared with those without CDs. One hypothesis could be the interaction between CDs and the PEG on the surface of the liposomes, which would impair the “stealth” effect of DCL system but improve the possibility of liposome-cell contact, leading to uptake. It would be useful to perform zeta potential measurements or studies of the complement-activating properties (Coty et al. 2017) of the DRV to have a better idea of the nature of their surface.

Another explanation could lie in the cholesterol-extracting effect of CDs, which has been reported by Kiss et al (Kiss et al. 2010). This could modify the interaction between liposomes and the cell membrane, inducing an alteration of fusion or endocytosis. However, this effect is mainly seen with β-CD, in particular methyl β-CD. Furthermore, our previous studies on the stability of SUV in the presence of CD indicated that the three CDs chosen to prepare DRV did not interact with cholesterol-containing membranes.

CPZ itself is known to be an inhibitor of clathrin-mediated endocytosis, acting at concentration similar to those employed in this study (10-100 μM) (Wang et al. 1993). Therefore, if the drug had been able to leak from the DRV it could have reduced the liposome uptake, and this effect might have been more prominent with DRV-CPZ because the drug was retained less well in the absence of CDs.

Furthermore, the uptake results do not correlate well with the cytotoxicity evaluation above. The observed cytotoxic activity was, in decreasing order: CPZ DRV > HP-γ-CD DRV > SBE-β-CD DRV > SGM DRV. That is, CPZ DRV demonstrated the lowest uptake rate but the highest cytotoxicity among the four DRVs. It could be explained by the strong CPZ-entrapping capability of CDs as revealed by previous ITC study, meaning that even if the formulations entered the cells, they did not release the drug. However, given the effect of CPZ on rhodamine fluorescence, it is quite difficult to interpret the results, because if the encapsulated CPZ were to be released either outside or inside the cell, the fluorescence of the liposome could cease to be quenched and no longer correspond to the calibration curve.

As mentioned above, the CDs help to retain drugs in the DCL system. However, from another point of view, a strong restraining force may block the release of the agent and impair the final therapeutic effect. Therefore, a balance should be found between delayed release and effective drug concentration.

4.4 Conclusion

In this work, a liposomal formulation of CPZ with sufficient encapsulation and suitable size for IV administration was obtained by the ammonium sulfate gradient DRV method. An *in-vitro* evaluation confirmed the inhibiting effect of CPZ on human leukemia cell lines (HL-60, MOLM13, MV4-11 and OCI-AML), while empty liposomes and CDs alone had no significant cytotoxicity. CPZ in the liposomal forms demonstrate a tendency for delayed release, in the order: DRV-SGM/CPZ > DRV-SBE-β-CD/CPZ > DRV-HP-γ-CD/CPZ > DRV-CPZ, implying that the CD/CPZ inclusion complexes can persist within the inner water phase of liposomes and further restrict the release of CPZ. However, the excessively strong entrapping capability of SGM may impair the therapeutic aim of the drug delivery system to a certain extent. In addition, CPZ and its liposomal formulations revealed selectivity towards AML cells, and liposomes containing CDs appeared to be taken up more avidly by MOLM13 cells than those without CDs.

References

Antimisiaris SG. Preparation of DRV liposomes. In Liposomes. 2017 (pp. 23-47). Humana Press, New York, NY.

Bangham AD, Standish MM, Watkins JC. Diffusion of univalent ions across the lamellae of swollen phospholipids. Journal of Molecular Biology. 1965, 13(1): 238-52.

Chen H, Gao J, Wang F, Liang W. Preparation, characterization and pharmacokinetics of liposomes-encapsulated cyclodextrins inclusion complexes for hydrophobic drugs. Drug Delivery. 2007, 14(4):201-8.

Coty JB, Oliveira EE, Vauthier C. Tuning complement activation and pathway through controlled molecular architecture of dextran chains in nanoparticle corona. International Journal of Pharmaceutics. 2017, 532(2):769-78.

Gabizon A, Dagan A, Goren D, Barenholz Y, Fuks Z. Liposomes as in vivo carriers of adriamycin: reduced cardiac uptake and preserved antitumor activity in mice. Cancer Research. 1982, 42(11):4734-9.

Davis ME, Brewster ME. Cyclodextrin-based pharmaceutics: past, present and future. Nature Reviews Drug Discovery. 2004, 3(12):1023.

Dhule SS, Penfornis P, Frazier T, Walker R, Feldman J, Tan G, He J, Alb A, John V, Pochampally R. Curcumin-loaded γ-cyclodextrin liposomal nanoparticles as delivery vehicles for osteosarcoma. Nanomedicine: Nanotechnology, Biology and Medicine. 2012, 8(4):440-51.

Gabizon A, Shiota R, Papahadjopoulos D. Pharmacokinetics and tissue distribution of doxorubicin encapsulated in stable liposomes with long circulation times. JNCI: Journal of the National Cancer Institute. 1989, 81(19):1484-8.

Gharib R, Greige-Gerges H, Fourmentin S, Charcosset C, Auezova L. Liposomes incorporating cyclodextrin–drug inclusion complexes: Current state of knowledge. Carbohydrate Polymers. 2015, 129:175-86.

Hagiwara Y, Arima H, Hirayama F, Uekama K. Prolonged retention of doxorubicin in tumor cells by encapsulation of γ-cyclodextrin complex in pegylated liposomes. Journal of Inclusion Phenomena and Macrocyclic Chemistry. 2006, 56(1-2):65-8.

Hait WN, Grais L, Benz C, Cadman EC. Inhibition of growth of leukemic cells by inhibitors of calmodulin: phenothiazines and melittin. Cancer Chemotherapy And Pharmacology. 1985, 14(3):202-5.

Ibrhaahim AH, Herfindal L, Rathe B, Andersen HL, da Silva Almeida JR, Fossen T. A novel poly-oxygenated flavone glucoside from aerial parts of the Brazilian plant *Neoglaziovia variegata* (Bromeliaceae). Heliyon. 2019, 5(3):e01369.

Jiang YW, Gao G, Chen Z, Wu FG. Fluorescence studies on the interaction between chlorpromazine and model cell membranes. New Journal of Chemistry. 2017,

41(10):4048-57.

Kirby C, Gregoriadis G. Dehydration-rehydration vesicles: a simple method for high yield drug entrapment in liposomes. Nature Biotechnology. 1984 Nov;2(11):979.

Kiss T, Fenyvesi F, Bacskay I, Varadi J, Fenyvesi E, Ivanyi R, Szente L, Tosaki A, Vecsernyes M. Evaluation of the cytotoxicity of β-cyclodextrin derivatives: Evidence for the role of cholesterol extraction. European journal of Pharmaceutical Sciences. 2010, 40(4):376-80.

Loew A, Köhnke T, Rehbeil E, Pietzner A, Weylandt KH. A role for lipid mediators in acute myeloid leukemia. International Journal of Molecular Sciences. 2019, 20(10):2425.

Loftsson T, Jarho P, Masson M, Järvinen T. Cyclodextrins in drug delivery. Expert Opinion on Drug Delivery. 2005, 2(2):335-51.

Maestrelli F, González-Rodríguez ML, Rabasco AM, Mura P. Effect of preparation technique on the properties of liposomes encapsulating ketoprofen–cyclodextrin complexes aimed for transdermal delivery. International Journal of Pharmaceutics. 2006, 312(1-2):53-60.

Maestrelli F, González-Rodríguez ML, Rabasco AM, Mura P. Preparation and characterisation of liposomes encapsulating ketoprofen–cyclodextrin complexes for transdermal drug delivery. International Journal of Pharmaceutics. 2005, 298(1):55-67.

McCormack B, Gregoriadis G. Drugs-in-cyclodextrins-in liposomes: a novel concept in drug delivery. International Journal of Pharmaceutics. 1994, 112(3):249-58.

Piel G, Piette M, Barillaro V, Castagne D, Evrard B, Delattre L. Betamethasone-in-cyclodextrin-in-liposome: the effect of cyclodextrins on encapsulation efficiency and release kinetics. International Journal of Pharmaceutics. 2006, 312(1-2):75-82.

Skalko N, Brandl M, Becirevic-Lacan M, Filipovic-Grcic J, Jalsenjak I. Liposomes with nifedipine and nifedipine-cyclodextrin complex: calorimetrical and plasma stability comparison. European Journal of Pharmaceutical Sciences. 1996, 4(6):359-66.

Stefanko A, Thiede C, Ehninger G, Simons K, Grzybek M. Lipidomic approach for stratification of acute myeloid leukemia patients. PloS One. 2017, 12(2):e0168781.

Stuani L, Riols F, Millard P, Sabatier M, Batut A, Saland E, Viars F, Tonini L, Zaghdoudi S, Linares L, Portais JC. Stable isotope labeling highlights enhanced fatty acid and lipid metabolism in human acute myeloid leukemia. International Journal of Molecular Sciences. 2018, 19(11):p3325.

Tang P, Li S, Wang L, Yang H, Yan J, Li H. Inclusion complexes of chlorzoxazone with β-and hydroxypropyl-β-cyclodextrin: characterization, dissolution, and cytotoxicity. Carbohydrate Polymers. 2015, 131:297-305.

Torchilin VP. Recent advances with liposomes as pharmaceutical carriers. Nature Reviews Drug discovery. 2005, 4(2):145.

Wang LH, Rothberg KG, Anderson RG. Mis-assembly of clathrin lattices on endosomes reveals a regulatory switch for coated pit formation. The Journal of Cell Biology. 1993, 123(5):1107-17.

General discussion

As a typical antipsychotic, CPZ was reported to have inhibiting effect on the human promyelocytic leukemic granulocytes (HL-60) (Hait et al. 1985). To repurpose CPZ for the treatment of AML, its passage through the BBB should be prevented, since the main therapeutic target for AML is the bone marrow (BM). Therefore, liposomes were used as a drug carrier for CPZ because they do not normally penetrate the BBB. Moreover, a "stealth" effect of the formulation could be achieved by coating the liposomal surface with PEG.

To further avoid the drug leakage caused by the amphiphilic property of CPZ, an efficient drug delivery system, drug-in-CDs-in-liposomes (DCL) was adopted. The concept of DCL was first proposed by McCormack and Gregoriadis in 1994 and has been widely used to delivery numerous drugs (McCormack and Gregoriadis 1994). As previously discussed, the DCL system is a complicated assembly composed by 3 relatively independent and interrelated ingredients: CD, CPZ and phospholipids, resulting in interactions between CD/CPZ, CD/phospholipids and CPZ/phospholipids. The first question to be answered is which of the wide range of CDs available for pharmaceutical uses (α-CD, β-CD, γ-CD, HP-β-CD, HP-γ-CD, SBE-β-CD, SBE-γ-CD, SBE-Et-β-CD and SGM). Therefore, in the preliminary experimental stage, we carried out an in-depth study on the 3 types of interactions with several physicochemical methods.

The ITC investigation revealed that the formation of CD/CPZ complexes varies in different kinds of CDs. α-CD and most of the β CDs form 1:1 complexes with CPZ, while the γ CDs mainly form a mixture of 1:1 and 1:2, except SGM, which can directly form 1:2 complexes with a high formation constant ($k_{1:2} = 6.36\times10^9 \pm 2.53\times10^8$). ^{1}H NMR has also confirmed the stoichiometry of SGM/CPZ complexes (1:2). As mentioned previously, a dynamic equilibrium could be established between the CD/drug complexes and free molecules of CD and drug in the aqueous medium. This process could be influenced by several factors, such as the size of cavity of CD, the hydrophobic properties and ion pairing of the host and guest molecules. In fact, this

equilibrium is a balance of driving forces, involving van der Waals interactions, hydrophobic interactions and electrostatic interactions (Jambhekar and Breen 2016). Concerning the therapeutic aim of CPZ, the drug release from the complexes should be considered. Since we require sufficient release of CPZ in the BM after long circulation in the plasma, a balance needs to be found between the binding and release of CPZ from the complexes. For example, the high complexation constant of SGM might become a drawback if CPZ cannot escape easily from the complex at the target site. Indeed, our *in-vitro* evaluation has demonstrated that the liposomes containing SGM/CPZ did not show cytotoxicity towards the AML cells after 24 h incubation whereas those with other CD/CPZ did. However, it will be discussed in more detail in a later part.

We observed decreased photostability of CPZ in presence of all the CD candidates. Generally, CDs show a protective effect towards the photodegradation of included guests. For example, tretinoin/β-CD complexes demonstrated an obvious increase in drug stability compared with free tretinoin (Caddeo et al. 2007). However, in a comprehensive investigation on the photostability of parathion and paraoxon with a series of CDs, either a photoprotective or an accelerating effect was observed. The authors explained this by the difference in distance between the catalytic sites of the host cavities and the reaction centers of the included pesticide molecules (Kamiya and Nakamura 1995). An interesting study was conducted by Wang et al, who found that the enhanced degradation of bisphenol Z (1,1-bis(4-hydroxyphenyl) cyclohexane (BPCH) in the presence of β-CD could be attributed to direct photolysis and photooxidation, by analyzing the photodegradation products of BPCH (Wang et al. 2007). Therefore, we may get a better insight of the photodegradation mechanism of CPZ by performing on LC-MS study on the solution after photodegradation.

Secondly, we studied the interaction between CD/phospholipids, both MLVs and SUVs. We designed our liposomal formulation with a composition of HEPC, cholesterol and DSPE-PEG_{2000} (65:30:5, molar% respectively), based on the encouraging work conducted previously in our laboratory (Sauvage et al. 2016)(Sauvage et al. 2018). PSPC was used as a model phospholipid since it is the main

species present in HEPC. The thermotropic behavior of PSPC in presence of CDs investigated by DSC demonstrated that there is no interaction between PSPC MLVs and most of the CDs, except SBE-Et-β-CD above 25 mM. A similar phenomenon was observed by Nishijo and Mizuno, who found that CDs exerted different effects on the thermotropic properties of DPPC. The different types of interaction were elucidated by the authors, showing that heptakis (2,6-di-O-methyl)-β-cyclodextrin could subtract DPPC molecules from the lipid bilayer and form soluble complexes, α-CD forms insoluble complexes also by lipid subtraction, while heptakis (2,3,6-tri-O-methyl)-β-cyclodextrin could penetrate into the matrix of liposomes (Nishijo and Mizuno et al. 1998). These three modes of interaction provide us with clues to explore the exact interaction mechanism between SBE-Et-β-CD and PSPC in the future, by measuring the concentration of CD and lipid in the supernatant as described in the literature.

SAXS experiments were carried out to gain an insight into the impact of CDs on the lipid lamellar organization. The lamellar distance of pure PSPC at different phases showed good agreement with other researchers' work. In the $P_{\beta'}$ and L_{α} state, lamellar expansion could be observed when PSPC was in the presence of higher concentrations (25 mM) of SBE-β-CD, SBE-γ-CD, SGM and especially SBE-Et-β-CD. While at lower temperature, 25°C at $L_{\beta'}$ phase, the lamellar distance remained unchanged, indicating that no interaction between CDs and PSPC occurred in this state. Therefore, the CDs wouldn't disrupt PSPC liposomes in the $L_{\beta'}$ phase. According the DSC study, the Tp-onset (onset of pre-transition) was 38.7°C, suggesting that under physiological conditions, *in-vitro* or *in-vivo*, the PSPC bilayers would remain intact.

Moreover, the influence of CDs on the hydrocarbon chain packing of PSPC was studied by WAXS. In contrast to the observations made by SAXS, the packing state of PSPC acyl chains was found to be barely disturbed by the addition of CDs, even for 50 mM SBE-Et-β-CD. Since the lamellar distance revealed by SAXS consists of two phases: the aqueous phase and the lipid phase, it could be concluded that the interaction between CDs and PSPC occurred mainly near the polar head but not in the alkyl chain region of the lipid lamellae.

The situation will become more complicated in the case of SUVs, since they consist of HEPC, cholesterol and DSPE-PEG$_{2000}$. The previously mentioned DSC or X-ray method cannot provide clear information about the multicomponent mixture chosen to prepare formulations for the biological experiments. Therefore, turbidimetry, a simple but effective technique, was used to investigate the stability of SUVs (HEPC:cholesterol:DSPE-PEG$_{2000}$, 65:30:5) in the presence of CDs. It was observed that SUVs showed good integrity in presence of all CDs tested except SBE-Et-β-CD, which is in accordance with the DSC results on PSPC membranes. It reconfirms the feasibility of using these CD candidates in the preparation of the DCL formulation. Additionally, the role of cholesterol in the stability of liposomes were studied, by investigating the behavior of SUVs (HEPC:DSPE-PEG$_{2000}$, 95:5) under the same conditions. Similar results were obtained to those observed with SUVs containing cholesterol. Although these findings cannot reveal the exact function of cholesterol in HEPC SUVs, the use of cholesterol as a stabilizer in liposomal formulations has been widely reported (Briuglia et al. 2015)(Papahadjopoulos et al. 1973)(Kaddah et al. 2018). Therefore, since it did not increase the susceptibility of liposomes to destabilization by CDs, cholesterol was retained in the composition of SUVs.

Another question needs to be answered is that of the interaction between CPZ and lipid bilayers. Due to the amphiphilic nature of CPZ, interaction was observed from a low CPZ/PSPC molar ratio. Finally, 3.75 mol% was determined as the suitable percentage for the liposomal preparation, although the PSPC membranes were not saturated with 45 mol% of CPZ. It should be noted that that CDs would be expected to form inclusion complexes with CPZ in the DCL system, and because of this a higher percentage of CPZ could be used. However, considering that the formulation is designed to be long-circulating, a relatively conservative choice would be prudent.

After a comprehensive investigation of the interaction between CD/CPZ and CD/lipids, liposomes (HEPC:Chol:DSPE-PEG$_{2000}$, 65:30:5) were prepared by the dehydration-rehydration vesicles (DRV) method, a strategy proposed by Kirby and Gregoriadis in 1984 (Kirby and Gregoriadis 1984). However, the low EE of CPZ led

us to combine the DRV method with an active loading strategy, ammonium sulfate gradient, which was developed by Gabizon in 1989 (Gabizon et al. 1989). According to the ITC study, HP-γ-CD, SBE-β-CD and SGM were selected for the preparation of DCL system, because of their higher formation constants with CPZ. However, after obtaining liposomes via the ammonium sulfate gradient DRV method, we observed an obvious decrease of EE in DRV containing CD/CPZ complexes compared with the DRV with CPZ alone. According to the mechanism of ammonium sulfate gradient method (Yingchoncharoen et al. 2016), the "locking" would become less effective for CD/CPZ inclusion complexes since part of CPZ cannot be ionized, thus leading to lower EE. A similar phenomenon was reported by Skalko, who found the EE of HP-β-CD/nifedipine liposomes (21.9%) was lower than those without HP-β-CD (56.2%) (Skalko 1996). According to Maestrelli, the type of CD has an effect on the EE of DCL system. For example, the HP-β-CD/ketoprofen MLVs (33.8%) is higher than that of β-CD/ketoprofen (26.8) (Maestrelli et al. 2005).

Although the stability of liposomes has been verified by DSC and turbidimetry, the situation in the DCL system is different. Therefore, in future experiments, it is also necessary to investigate the stability of the DCL liposomal formulation. Several methods could be employed for this. For example, the evolution of the diameter of the DRV after incubation in HEPES buffer for different periods could be determined by DLS. Another parameter related to the liposomal integrity that is important for the performance of the formulation is the release of CPZ during the storage, which could be studied by assaying the concentration of CPZ remaining after different intervals of dialysis.

Furthermore, in terms of the physicochemical studies of the DCL system, the photodegradation of CPZ should also be investigated. We have observed the facilitating effect of CDs on this process in the case of CD/CPZ complexes, while the situation remains unclear when CPZ is encapsulated in liposomes as the free or complex form. It is possible that liposomes might be able to provide a protective screen against light to some extent, thus less photodegradation of CPZ would be observed. However, we

need to conduct experiments to clarify this aspect.

An *in-vitro* evaluation of the DCL system was performed. Firstly, the cytotoxicity of CPZ was studied against HL-60 cells and IC_{50} of 21.9 μM was obtained, which is slightly higher than that (8 μM) reported by Hait (Hait et al. 1985). The CDs showed no cytotoxicity while empty liposomes exhibited a growth-promoting effect towards the HL-60 cells. A hypothesis to explain this facilitation of growth is the necessity of *de novo* synthesis of fatty acids for membrane synthesis, especially for tumor cell proliferation (Stefanko et al. 2017). Stuani et al provided some evidence for this hypothesis, by carrying out global proteomic and lipidomic approaches that have showed an increase of lipid metabolism concerning phosphatidylinositol, sphingolipids, free cholesterol and monounsaturated fatty acids in leukemic cells (Stuani et al. 2018).

Reduced cytotoxicity activity was observed in the DRV containing CD/CPZ complexes compared with CPZ DRV. It could be explained by the complexation of CPZ by CD, as already shown by the results in ITC, and provides the possibility of delayed release. However, the complexation capability of SGM might be too high to release CPZ efficiently, since no cytotoxicity was observed with the SGM DRV. The effect of CD type on the drug release from DCL was also reported by Piel et al (Piel et al. 2006). Moreover, the type of liposomes also influences the release kinetics of DCL. SUVs containing HP-β-CD/ketoprofen showed a faster drug release rate than its MLV and LUV form, due to their smaller size (Maestrelli et al. 2006). Therefore, if the release kinetics of our liposomal formulations need to be tuned for *in-vivo* use, it would be possible to modify the release of CPZ by changing the DRV diameter.

It was also necessary to evaluate the cytotoxic effect of DRV against non-malignant cells and for this the NRK cell line was chosen, beginning with a 24-h incubation. Compared with HL-60, the DRV showed a different order of activity against the “normal” cells, indicating a different route of interaction between liposomes and NRK cells. However, when other leukemic cell lines were tested, MOLM13, MV4-11 and OCI-AML, the DRV activity was similar with that obtained with HL-60. To study the possibility of delayed release from the DCL system, we performed a longer contact

time, 72 h. An obvious difference was that SGM DRV started to show cytotoxicity against the four cell lines, with a high IC_{50}. This provides evidence that it would be possible to avoid release of drug from our DCL liposomal formulation in the circulation system, and delay it until the accumulation or cellular uptake of liposomes in the bone marrow. However, as discussed, a high complexation affinity could prevent drug release in or around the target cells or even make the DCL system as a fatty acid supplier, as the empty liposomes did, which would promote the growth of tumor cells.

The DRV showed a significant increase of the cytotoxicity towards NRK cells when the incubation time was prolonged to 72 h. From the results of the washout experiment, we can propose two hypotheses for this finding: 1) NRK cells take up DRV slower than the AML cells; 2) a higher dose of CPZ is needed for NRK cells to show a toxic effect than the AML cells. Both of these hypotheses suggest that CPZ and its liposomal formulations are selective towards AML cells, which is promising for the further *in-vivo* application of our DCL system.

Finally, the cellular uptake was studied with fluorescent liposomes loaded with rhodamine B PE. Empty liposomes showed a much stronger fluorescence intensity than those containing CPZ, which could be explained by the fluorescence quenching property of CPZ (Jiang et al. 2017). For MOLM13 cells, liposomes containing CDs were more easily taken up than those without CDs. This phenomenon could be explained by several hypotheses. One is the interaction between CDs and the PEG grafted on the liposomes, which could weaken their “stealth” effect. In this respect, investigation on the zeta potential or the complement-activating properties (Coty et al. 2017) of the DRV would provide more information. Other hypotheses such as the cholesterol-extracting effect of CDs or the role of CPZ in clathrin-mediated endocytosis have also been discussed in detail in Chapter 4.

A promising perspective in this project is the active targeting of the DCL system. In the past decade, targeted monoclonal antibodies have facilitated chemotherapy for cancers. As an exclusive surface marker for leukemic stem cells, CD33 antigen could be used to optimize our DCL system in the future. In fact, this has been investigated by

several researchers (Rothdiener et al. 2010)(Simard and Leroux 2010). For example, Li et al reported CD33-targeted lipid nanoparticles loaded with GTI-2040, an antisense oligonucleotide, for AML treatment. They used anti-CD33 scFv as the targeting ligand and the system showed a significant uptake and a 15-fold reduction in the IC_{50} of antileukemic drug Ara-C against Kasumi-1 cells(Li et al. 2015). Another potential surface marker that could be considered for the targeting of our system is CD123. An immunoliposome piloted by CD123 antibody has been obtained by Wang and his colleagues to target to AML cells, with positive results both *in-vitro* and *in-vivo* (Wang et al. 2017). Therefore, these related studies provide us with sufficient choices and promising possibilities of achieving a CPZ-loaded liposomal formulation for the treatment of AML.

References

Briuglia, M. L., Rotella, C., McFarlane, A., & Lamprou, D. A. (2015). Influence of cholesterol on liposome stability and on in vitro drug release. Drug Delivery and Translational Research, 5(3), 231–242.

Caddeo, C., Manconi, M., Valenti, D., Pini, E., & Sinico, C. (2007). Photostability and solubility improvement of β-cyclodextrin-included tretinoin. Journal of Inclusion Phenomena and Macrocyclic Chemistry, 59(3–4), 293–300.

Coty, J. B., Eleamen Oliveira, E., & Vauthier, C. (2017). Tuning complement activation and pathway through controlled molecular architecture of dextran chains in nanoparticle corona. International Journal of Pharmaceutics, 532(2), 769–778.

Gabizon, A., Shioia, R., & Papahadjopoulos, D. (1989). Pharmacokinetics and tissue distribution of doxorubicin encapsulated in stable liposomes with long circulation times. Journal of the National Cancer Institute, 81(19), 1484-1488.

Gharib, R., Greige-Gerges, H., Fourmentin, S., Charcosset, C., & Auezova, L. (2015). Liposomes incorporating cyclodextrin-drug inclusion complexes: Current state of knowledge. Carbohydrate Polymers, 129, 175–186.

Hait, W. N., Grais, L., Benz, C., & Cadman, E. C. (1985). Inhibition of growth of leukemic cells by inhibitors of calmodulin. Cancer Chemotherapy and Pharmacology, 14(3), 202-205.

Jambhekar, S. S., & Breen, P. (2016). Cyclodextrins in pharmaceutical formulations II: Solubilization, binding constant, and complexation efficiency. Drug Discovery Today, 21(2), 363–368.

Jiang, Y. W., Gao, G., Chen, Z., & Wu, F. G. (2017). Fluorescence studies on the interaction between chlorpromazine and model cell membranes. New Journal of Chemistry, 41(10), 4048–4057.

Kaddah, S., Khreich, N., Kaddah, F., Charcosset, C., & Greige-Gerges, H. (2018). Cholesterol modulates the liposome membrane fluidity and permeability for a hydrophilic molecule. Food and Chemical Toxicology, 113(January), 40–48.

Kamiya, M., & Nakamura, K. (1995). Cyclodextrin inclusion effects on photodegradation rates of organophosphorus pesticides. Environment International, 21(3), 299–304.

Kirby, C., & Gregoriadis, G. (1984). Dehydration-Rehydration Vesicles: A simple method for high yield drug entrapment in liposomes. Nature Biotechnology, 2(11), 979.

Li, H., Xu, S., Quan, J., Yung, B. C., Pang, J., Zhou, C., … Lee, R. J. (2015). CD33-Targeted lipid nanoparticles (aCD33LNs) for therapeutic delivery of GTI-2040 to acute myelogenous leukemia. Molecular Pharmaceutics, 12(6), 2010–2018.

Loew, A., Köhnke, T., Rehbeil, E., Pietzner, A., & Weylandt, K. H. (2019). A role for

lipid mediators in acute myeloid leukemia. International Journal of Molecular Sciences, 20(10), 2425.

Maestrelli, F., Lu, M., Maria, A., & Mura, P. (2005). Preparation and characterisation of liposomes encapsulating ketoprofen – cyclodextrin complexes for transdermal drug delivery. International Journal of Pharmaceutics, 298(1), 55-67.

Maestrelli, F., González-Rodríguez, M. L., Rabasco, A. M., & Mura, P. (2006). Effect of preparation technique on the properties of liposomes encapsulating ketoprofen-cyclodextrin complexes aimed for transdermal delivery. International Journal of Pharmaceutics, 312(1–2), 53–60.

McCormack, B., & Gregoriadis, G. (1994). Drugs-in-cyclodextrins-in liposomes: a novel concept in drug delivery. International Journal of Pharmaceutics, 112, 249–258.

Nishijo, J., & Mizuno, H. (1998). Interactions of cyclodextrins with DPPC liposomes. Differential scanning calorimetry studies. Chemical and Pharmaceutical Bulletin, 46(1), 120-124.

Papahadjopoulos, D., Jacobson, K., Nir, S., & Isac, I. (1973). Phase transitions in phospholipid vesicles Fluorescence polarization and permeability measurements concerning the effect of temperature and cholesterol. BBA - Biomembranes, 311(3), 330–348.

Piel, G., Piette, M., Barillaro, V., Castagne, D., Evrard, B., & Delattre, L. (2006). Betamethasone-in-cyclodextrin-in-liposome: The effect of cyclodextrins on encapsulation efficiency and release kinetics. International Journal of Pharmaceutics, 312(1–2), 75–82.

Rothdiener, M., Müller, D., Castro, P. G., Scholz, A., Schwemmlein, M., Fey, G., … Kontermann, R. E. (2010). Targeted delivery of SiRNA to CD33-positive tumor cells with liposomal carrier systems. Journal of Controlled Release, 144(2), 251–258.

Sauvage, F., Fattal, E., Al-Shaer, W., Denis, S., Brotin, E., Denoyelle, C., Blanc-Fournier, C., Toussaint, B., Messaoudi, S., Alami, M. and Barratt, G. (2018). Antitumor activity of nanoliposomes encapsulating the novobiocin analog 6BrCaQ in a triple-negative breast cancer model in mice. Cancer Letters, 432(June), 103–111.

Sauvage, F., Franzè, S., Bruneau, A., Alami, M., Denis, S., Nicolas, V., Lesieur, S., Legrand, F.X., Barratt, G., Messaoudi, S. and Vergnaud-Gauduchon, J. (2016). Formulation and in vitro efficacy of liposomes containing the Hsp90 inhibitor 6BrCaQ in prostate cancer cells. International Journal of Pharmaceutics, 499(1–2), 101–109.

Simard, P., & Leroux, J. C. (2010). In vivo evaluation of pH-sensitive polymer-based immunoliposomes targeting the CD33 antigen. Molecular Pharmaceutics, 7(4), 1099–1107.

Skalko. (1996). Liposomes with nifedipine and nifedipine-cyclodextrin complex: calorimetrical and plasma stability comparison. European Journal of Pharmaceutical Sciences, 4, 359–366.

Stefanko, A., Thiede, C., Ehninger, G., Simons, K., & Grzybek, M. (2017). Lipidomic approach for stratification of acute myeloid leukemia patients. PLoS ONE, 12(2), 1–12.

Stuani, L., Riols, F., Millard, P., Sabatier, M., Batut, A., Saland, E., … Bertrand-Michel, J. (2018). Stable isotope labeling highlights enhanced fatty acid and lipid metabolism in human acute myeloid leukemia. International Journal of Molecular Sciences, 19(11). 3325

Wang, G., Qi, P., Xue, X., Wu, F., & Deng, N. (2007). Photodegradation of bisphenol Z by UV irradiation in the presence of β-cyclodextrin. Chemosphere, 67(4), 762–769.

Wang, Y., Liu, F., Wang, Q., Xiang, H., Jin, H., Li, H., & Mao, S. (2017). A novel immunoliposome mediated by CD123 antibody targeting to acute myeloid leukemia cells. International Journal of Pharmaceutics, 529(1–2), 531–542.

Yingchoncharoen, P., Kalinowski, D. S., & Richardson, D. R. (2016). Lipid-based drug delivery systems in cancer therapy: what is available and what is yet to come. Pharmacological Reviews, 68(3), 701–787.

Titre: Mise au point des liposomes innovants avec double encapsulation des principes actifs pour le traitement des leucémies myéloïdes aigües

Mots clés: leucémie myelôide aigüe, liposome, cyclodextrine, chlorpromazine, vectorisation, libération contrôlée

Résumé: La leucémie myéloïde aigue (AML) reste difficile à traiter en particulier chez les personnes âgées. La chlorpromazine (CPZ), un anti-schizophrénique, pourrait être efficace contre ce cancer mais doit être délivrée aux cellules malignes de la moelle osseuse sans lui permettre d'atteindre le cerveau où il peut y avoir des effets secondaires. Nous avons mis au point un système d'administration de médicaments dans lequel la CPZ est d'abord incluse dans une cyclodextrine (CD), une molécule-cage à base de glucose, et le complexe est ensuite inclus dans des liposomes, vésicules constituées d'une paroi similaire à celle de la membrane cellulaire. Ces liposomes circulent dans le sang après injection intraveineuse mais ne peuvent pas pénétrer dans le cerveau. La formulation a été optimisée pour donner une bonne encapsulation de la CPZ dans les liposomes tout en conservant leur stabilité. L'activité des liposomes a été évaluée sur des cellules AML et une libération contrôlée a ainsi été observée.

Title: Innovative liposomes with double encapsulation properties for the treatment of acute myeloid leukemia

Keywords: Acute myeloid leukemia, liposome, cyclodextrin, chlorpromazine, drug delivery, controlled release

Abstract: Acute myeloid leukemia (AML) remains difficult to treat, especially in older people. Chlorpromazine (CPZ), a drug used to treat schizophrenia, could be effective against this cancer but is necessary to deliver it to the malignant cells in the bone marrow without allowing it to reach the brain where it could have side effects. We have designed a drug delivery strategy to achieve this. CPZ is first included with a cyclodextrin (CD), a cage-like molecule made of glucose units, and the complex is then included with liposomes, vesicles made of lipids similar to those found in cell membranes. These liposomes will be able to circulate in the blood after intravenous injection but cannot penetrate into the brain. The formulation was optimized to select the best CDs for including CPZ and giving good encapsulation in liposomes without destabilizing their structure. The activity of the CPZ-in-CD-in liposomes was evaluated against AML cells and shown to have potential for controlled release.